The role of guard cell chloroplasts in stomatal function and coordinating stomatal and mesophyll responses

Kucheli Batta

A thesis submitted for the degree of Doctor of Philosophy

School of Biological Sciences

University of Essex

April 2018

SUMMARY

Guard cells controls the stomata through which exchange of gas takes place by balancing between CO_2 uptake for photosynthesis and water loss through transpiration leading to ultimate plant water use efficiency (WUE). Climate change is predicted to lead to greater temperatures and reduced water availability resulting in adverse effect on plant productivity. Sustainable agriculture will therefore require a major reduction in plant water use hence stomata have become potential target for manipulation. Understanding the signal mechanisms of stomata in response to these changing environmental conditions is therefore critically important. In order to facilitate an understanding of stomatal regulation and how it is influenced by the surrounding mesophyll cells, we have used two approaches to find a possible coordination that links mesophyll and guard cell metabolism through the use of stomatal physiology and genetic engineering. The first approach used a novel epidermal mesophyll transfer experiment to monitor stomatal responses to dynamic environmental changes with and without the mesophyll present. The second approach used new molecular tools and techniques to manipulate chloroplast metabolism specifically in the guard cells to elucidate mesophyll-derived signals that coordinate mesophyll CO_2 demands with stomatal behaviour towards crop improvement. The results presented have shown guard cells plays a role in stomatal function even though the degree of responsiveness is slower than when the mesophyll is present. Furthermore, the molecular approach demonstrated using Arabidopsis plants overexpressing Rieske and SBPase resulted in substantial and significant impacts on plant development coupled with increases in photosynthetic efficiency of photosystem II in the early stages of seedling development. The result obtained proves more opportunities await the exploitation of guard cells metabolism towards the improvement of plants.

ABBREVIATIONS

ATP	Adenosine -5-triphosphate
BASTA	Glofusinate ammonium herbicide
bp	Base pair
CAM	Crassulacean acid metabolism
cDNA	Complementary DNA
C_i	Intercellular CO_2 concentration
DNA	Deoxyribonucleic acid
EDTA	Ethylenediaminetetraacetic Acid Tetrasodium Salt
ETC	Electron transport chain
Kn	Kanamycin
LB	Luria Broth
MS	Murashige and Skoog basal media
NAD	Nicotinamide adenine dinucleotide
NADP	Nicotinamide adenine dinucleotide phosphate
PCR	Polymerase chain reaction
PEPc,	Phosphoenolpyruvate carboxylase
PPDK	Pyruvate orthophosphate dikinase
qRT-PCR	Quantitative reverse transcriptase polymerase chain reaction
RNA	Ribonucleic acid
Rubisco	Ribulose-1,5-bisphosphate carboxylase/oxygenase
RuBP	Ribulose-1,5-bisphosphate
RT-PCR	Reverse transcriptase polymerase chain reaction
WT	Wild type

ACKNOWLEDGEMENTS

First and foremost, am most grateful to my Father, God Almighty for His love which has strengthened and assured me all through my studies. To my man of God, Rev. Dr Chris Oyakhilome whose teachings have made me subdue all the challenges faced. What a blessing you are to me Sir. To my precious family especially my mum and siblings for their continual support and prayers. My amiable, hardworking and accessible supervisor, Prof. Lawson. Thank you for always being available and helpful. To my one and only board member, Dr Mattew Jones. am blessed to have you as my board member and for all the support you have shown me. To Prof. Christine Raines, your smiles always means a lot to me Ma, thank you for your kind nature. To Phil Davey for your energetic disposition and readily available whenever needed and help rendered towards the gas exchange. To Silvere also for your immense help and all the guys in lab 6.23 for help rendered one way or the other. You guys are the best. To my dearest Patty of whom I have often referred to as my second supervisor. Thank you for all the help rendered towards the molecular stuff. Sue for her tender cares towards the plants. To the head of School Prof. Phil Mullineux for the great work you are doing in moving the school forward and all the staff particularly the plant group. I have thoroughly enjoyed the times I had with you. To dearest Emma for being so efficient and of great help whenever needed. To my beloveth daddy here in the Uk, Daddy Alan Harvey. Thank you for being so different and there at my crucial time. Last but not the least, the University of Essex community for the peace and great time I have had. Above all, the Holy Spirit of God who has been my advantage of whom this work is dedicated to. Thank you and God bless you all.

TABLE OF CONTENTS

LIST OF FIGURES

LIST OF TABLES

CHAPTER 1: INTRODUCTION

Climate change is predicted to lead to greater temperatures and reduced water availability as a result of increasing global CO_2 concentration, which is anticipated to double by the end of this century (Keeling et al., 2010, Keenan et al., 2014). Global surface temperature is predicted to rise by 2.6–4.8°C by the end of this century according to IPCC, 2013. The increase in temperature will lead to increases in evaporative demand which in turn will decreases soil moisture and subsequently results in reduced water availability for plants leading to a decline in plant productivity (Anderegg et al., 2013, Park Williams et al., 2012). Reduced water availability severely damages crops and results in major yield losses (Zhu and Assmann, 2017) and has been shown to cause more yield losses than any other single biotic or abiotic factor globally (Boyer, 1982). Sustainable agriculture will require a major reduction in plant water use in many areas as fresh water available for crops will decrease due to climate change and the predicted increase in global water usage due to increasing global population (World Water Organization, 2010). Additionally severe drought plays a critical role in carbon cycling with the loss of carbon sinks resulting from widespread crop mortality in all vegetation types across all continents observed in the past few decades (Ciais et al., 2005, Anderegg et al., 2012, Reichstein et al., 2013, Allen et al., 2010). Therefore, in order to maintain crop productivity to feed the growing population, it is necessary to develop new crop varieties or identify potential targets for manipulating plants for improved water use and productivity. A key target is to produce future crop plants that have the ability to maintain productivity if not increase productivity amidst all these predicted changes in climatic conditions (Jezek and Blatt, 2017, Lawson et al., 2011). Stomata and their behaviour have affected global fluxes of CO_2 and H_2O, with an estimated 300 x 10^{15} g of CO_2 and 35 x 10^{18} g of H_2O vapour passing through stomata of leaves every year (Hetherington and

Woodward, 2003a). As stomatal conductance determines the flux of gases between the inside of the leaf and the external atmosphere and therefore greatly influence photosynthetic carbon assimilation and water use, stomata are potential unexploited targets. Understanding the structure, function and signalling mechanism in stomata in response to these changing environmental conditions is therefore critically important if we are to manipulate the processes (Buckley, 2005, Hetherington and Woodward, 2003b, Bergmann and Sack, 2007). Figure 1.1 below shows the guard cells that controls stomatal size and the targeted enzymes manipulated in the chloroplast of the guard cells. Uses of these enzymes are described in further chapter.

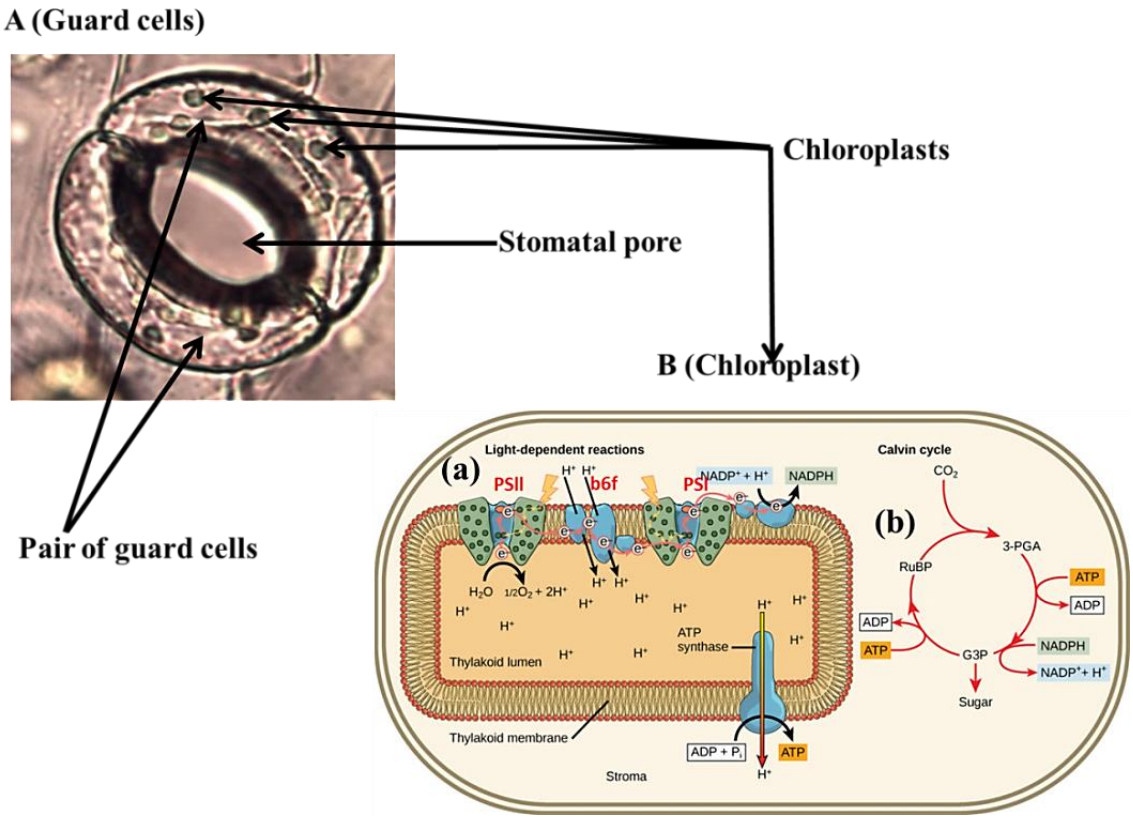

Figure 1. 1.Guard cell as a potential tool for manipulation. (A) guard cells from an epidermal peel showing chloroplasts which are the site of photosynthesis and the stomata through which exchange of gas takes place. The guard cells control the stomatal pore i.e the opening and closing of the stomata. (B) Schematic diagram of a single chloroplast illustrating (a) the thylakoid membrane where electron transport chain takes place. The cytochrome b_6f between the PSII and PSI shuttles electron which is used for the synthesis of NADPH and ATP as energy for fuelling the Calvin cycle. (b) Calvin Cycle found in the stroma of the chloroplast where sedoheptulose-1, 7-bisphosphatase (SBPase) a key component in the regeneration of RuBP in the Calvin cycle functions.

Stomata has therefore attracted the attention of scientists for almost three centuries (Meidner and Willmer, 1993), and a great deal of knowledge related to the structure, development, and physiology of stomata have so been acquired (Bergmann and Sack, 2007, Buckley, 2005, Berry et al., 2010) nevertheless, there are still many unanswered questions regarding signalling pathways, osmoregulation and the co-ordination between stomatal behaviour and mesophyll photosynthesis. For an optimal plant productivity and water use efficiency (defined at the leaf level as the ratio of carbon gained relative to

water lost) stomata must open and close to environmental stimuli and internal signal to balance CO_2 uptake for photosynthesis (*A*) with water lost through transpiration (*E*) for optimal plant productivity and plant water use efficiency (WUE = *A*/E (Lawson & Blatt, 2014). A strong correlation between mesophyll photosynthesis (*A)* and stomatal conductance (g_s) has often been observed (Messinger et al., 2006, Wong et al., 1979); however, the underlying mechanisms or possible signals that promote this relationship are not entirely understood and are currently being studied (Lawson and Blatt, 2014, Lawson et al., 2014c, Lawson and Weyers, 1999, Terashima et al., 2016). Although the strong relationship between *A* and g_s is conserved, it is not always constant (Lawson and Blatt, 2014) and under fluctuating environmental conditions, stomatal responses to changing conditions are often slower than those of the photosynthetic responses (Barradas and Jones, 1996, Lawson and Blatt, 2014a) leading to a disconnect between *A* and g_s that impacts on productivity and water use efficiency (WUE). In order to balance between carbon supply and the ability to optimise or sustain plant growth in an ever fluctuating environment, a full understanding of these responses requires as well new approaches that integrate both molecular and physiological approaches (Lawson and Blatt, 2014a, Smith and Stitt, 2007). Boyer (1982) has long emphasized that genetic potentials for yield lies unrealized and the need for better adaptation of plants to climatic factors in which the plants are grown are still enormous.

In view of this, the epidermal peel experiments provides a way to assess stomatal responses in the epidermis relative to intact leaves in order to find a possible mechanism coordinating stomata with mesophyll resulting in both improvement of WUE and plant productivity. Similarly, manipulating the guard cells aims to elucidate the role of guard cell chloroplasts on stomatal function through the production of transgenic plants with altered expression of the Calvin cycle enzyme Sedoheptulose-1,7-bisphosphatase

(SBPase) a key component in the regeneration of RuBP in the Calvin cycle and cytochrome b_6f (Rieske), a key component of the electron transport used towards ATP production. The effect of these manipulations will be evaluated and assessed physiologically towards possible improvement of plant productivity (Lawson and Weyers, 1999).

1.1. Stomatal regulation of gas exchange

The external surfaces of most herbaceous and woody plants are covered with a waxy cuticle layer impermeable to water vapour and CO_2 therefore all gaseous exchange between the external environment and the internal leaf must pass through stomatal pores (Berry et al., 2010, Shtein et al., 2017, Edwards et al., 1998, Hetherington and Woodward, 2003a). Stomata (singular, stoma) are minute adjustable pores found in large numbers on surfaces of most aerial parts (stems, leaves, flowers and fruits) of higher plants but not on aerial roots (Tichá, 1982). Apart from the central role of stomata in regulating gas exchange between the inside of the leaf and the external environment (Cowan and Troughton, 1971), stomatal behaviour also influences transpiration, leaf cooling and metabolites fluxes (Brownlee, 2001, Lake et al., 2001, Jia and Zhang, 2008) as well as acting as a barrier to harmful substances/pollutants such as ozone and pathogens (Meidner and Mansfield, 1968, Mansfield and Majernik, 1970). Stomata in most plants can be found both on the upper (adaxial) and lower (abaxial) surfaces and are called amphistomaceous however, stomata are usually more abundant on the abaxial surface (Tichá, 1982). In some species especially trees, stomata are only found on the lower surface (i.e. the leaf is hypostomatous), while in aquatic plants, they are only found on the upper surfaces (and the leaf is termed epistomaceous). Stomata vary widely in density and size and consist of a pore bordered by a pair of cells called the guard cells. In

some species specialised adjacent epidermal cells termed subsidiary cells surround the guard cell and all together make up the stomatal complex (Willmer and Fricker, 1996). Subsidiary cells play a role in guard cell functioning by reinforcing or protecting the stomatal cells given that plant cells are relatively rigid due to the cellulose cell walls. Because the stomata must expand and contract, subsidiary cells afford a cushioning effect for the adjoining rigid cells from the stomatal expansions and contractions (Ferry, 2008). Most importantly, subsidiary cells greatly assist in regulating stomatal behaviour. Franks and Farquhar (2007) showed that maximum stomatal aperture (and therefore g_s) could not be obtained in some species of wheat without a substantial reduction in subsidiary cell turgor pressure and a reduction in the mechanical advantage of the subsidiary cells to close stomata. These findings illustrated that rapid stomatal movement in species with dumb-bell shaped guard cells is facilitated by a "see-sawing" of turgor pressure between subsidiary and guard cells during stomatal opening. This work highlight the importance of the mechanical properties of stomata in their performance for regulations of gas-exchange regulation, however relatively little is known about these properties vary across different species (Franks and Farquhar, 2007). Recently an experiment supported this hypothesis by showcasing the role of subsidiary cells in stomatal behaviour in grasses was published in Science (Raissig et al., 2017). In this study a transcriptions factor was manipulated that resulted in *Brachypodium* plants without subsidiary cells. Stomata in these plants had reduced stomatal aperture and lower fresh weight (Raissig et al., 2017). Thus, it was suggested that the manipulation of subsidiary cell formation and function in crops may be an effective approach to enhance plant performance.

Both the rapidity of stomatal function and the magnitude of the g_s are important for plant productivity and plant water use and therefore understanding the mechanisms and signalling processes and pathways that underlie stomatal responses to changing

environmental condition is essential if these are to be targets for manipulation to optimised co-ordination between mesophyll demands for CO_2 and water loss.

1.2 Stomatal response to environmental factors and internal cues

Stomata have a complex signal transduction networks which enables them to respond to endogenous and environmental signals promoting opening and closing of the stomatal pore within time scales of seconds to hours (Assmann and Wang, 2001, Assmann and Jegla, 2016).

The balance between CO_2 uptake and transpiration rate depends on stomatal responses to these factors and is important for synchronizing stomatal behaviour relative to mesophyll demands for CO_2. Stomatal behaviour is influenced by variables such as light, [CO_2], humidity, pathogens, abscisic acid (ABA) and temperature (Vavasseur and Raghavendra, 2005, Kim et al., 2004).

Stomata in leaves respond rapidly and reversibly to both light and intercellular CO_2 concentration (C_i) (Fujita et al., 2013). However as stated above, these responses vary in magnitude among and within species under different growth conditions (Doi et al., 2015, Talbott and Zeiger, 1998, Talbott and Zeiger, 1996). Stomatal responses will therefore be focused on light and intercellular CO_2 because of their importance to photosynthesis.

1.2.1 Stomatal responses to light

Stomata respond to light through the activation of pigments and photoreceptors. This happens through the absorption of light by these pigments in the guard cell chloroplasts resulting in proton extrusion thereby activating a specific plasma membrane proton pump and causing membrane hyperpolarization. This leads to ion transport K^+ influx and

subsequent swelling of the guard cells resulting in stomatal opening (Shimazaki and Zeiger, 1985).

The spectral quality of light modulates the mechanisms of osmotic accumulation in guard cells and include potassium uptake, photosynthetic sugar production, and starch breakdown (Talbott and Zeiger, 1993). Suetsugu et al. (2014) demonstrated that guard cell chloroplasts provide ATP and/or reducing equivalents that mediate blue light-dependent stomatal opening and hence suggested that they indirectly monitor photosynthetic CO_2 fixation in mesophyll chloroplasts by absorbing light in the epidermis. Recently, Horrer et al. (2016) provided a direct link of stomatal response to blue light and starch degradation mediated by the action of β-amylase 1 (BAM1) and α-amylase 3 (AMY3)-enzymes. These enzymes under normal circumstances do not require starch breakdown in the night of other leaf tissues. The pathway was found to be under the control of the phototropin-dependent blue-light signalling and correlated with the plasma membrane H^+- ATPase activity.

1.2.2 Stomatal response to [CO_2]

Stomatal conductance is also mediated by the CO_2 concentration inside the leaf (internal CO_2 concentration, C_i (Mott 1988) which is also determined by the photosynthetic rate. As a result, increased photosynthetic activities decrease C_i to which stomata respond by opening (Assmann and Shimazaki, 1999, Mott, 1988). Stomatal opening is stimulated when the internal CO_2 concentrations decreases for example, with increasing *A*, whilst increasing C_i induces stomatal closure (Mansfield et al., 1990, Assmann and Shimazaki, 1999). The stomatal response to C_i has often been assumed to be the mechanism that co-ordinates *A* and g_s in order to balance CO_2 uptake to optimising mesophyll carbon demands without unnecessarily losing excess water (Lawson, 2009, Lawson and Blatt, 2014, Mott, 1988). It is assumed that stomata respond to a constant ratio of atmospheric

CO_2 to C_i of about ⅔ atmospheric CO_2 (Mott, 1988). However several studies have argued that changes in C_i are often too small to account for the changes in stomatal aperture. This is supported by reports of stomatal responses to PPFD when C_i is held constant (Lawson et al., 2008, Messinger et al., 2006, Wang and Song, 2008). The challenge however is whether this signal is sensed directly by guard cells and/or by the mesophyll (Assmann and Shimazaki, 1999, Lawson et al., 2011) or whether a combination of the two contributes to the response. Recently, Jakobson et al. (2016) demonstrated the deletion of mitogen-activated protein (map) kinase 12 (MPK12) showed a lack of CO_2 insensitivity in plant suggesting a new function for plant MPKs as protein kinase inhibitors and a mechanism through which guard cell CO_2 signaling controls plant water management.

Hiyama et al. (2017) demonstrated the involvement of two kinases; (convergence of blue light and CO_2 1 and 2 (CBC1/CBC2) which function in the signalling pathways of phototropins and high leaf temperature1 (HT1). CBC1/CBC2 interacted with and are phosphorylated by HT1. Hence, they proposed that CBCs mediates stomatal aperture through the integration of signals from blue light and CO_2 which also acts as a convergence site for signals from blue light and low CO_2.

Genetic mutants especially in *Arabidopsis* have identified and characterized signal transduction mechanisms and those with impaired stomatal response to [CO_2] have already begun to reveal the mechanisms that mediate CO_2 regulation of stomatal conductance. It cannot be emphasised enough that the involvement of guard cell photosynthesis demands genetic analyses by guard cell-specific impairment of photosynthesis, Lawson (2009).

1.3 Guard cell osmoregulation

Guard cells are highly specialised and complex structures possessing complex signal transduction networks, membrane ion transport capability and modified metabolic pathways (Assmann and Wang, 2001). As stated previously, stomatal aperture is controlled by reversible changes in the concentration of osmolytes in guard cells which is regulated by the ongoing metabolism of the surrounding guard cells influenced both by endogenous and environmental signals (Daloso et al., 2016). Stomatal opening is achieved when the accumulation of osmotica lowers the water potential promoting the inflow of water into the guard cell vacuoles which leads to the swelling of guard cells thereby opening the stomatal pore. Similarly in the same way but in opposite direction, stomatal closure occurs when guard cells release ions into the cell wall and the consequent efflux of water leading to reduction in volume. These dynamic changes in volume and structure results in stomatal movements (Andres et al., 2014, Berry et al., 2010, Gao et al., 2015).

There have been many decades of research that have focused on guard cell osmoregulation and many pathways put forward with evidence for all of these. The key osmotically active solutes inorganic ions such as Potassium (K^+) and Chloride (Cl^-) with malate^{2-} and sucrose function as the main organic solutes. Where and how these osmotically active solutes are generated and taken up into the guard cells has also been subject of intense debate, with K^+ and Cl^- assumed to be taken up from the apoplast, whilst sucrose and malate^{2-} could be imported from the mesophyll or synthesized internally in the guard cells themselves, from starch degradation or guard cell CO_2 fixation (Roelfsema and Hedrich, 2005, Horrer et al., 2016, Lawson et al., Vavasseur and Raghavendra, 2005, Lawson, 2009). As stated earlier, a deeper and better understanding of the mechanisms of signal transduction pathway could provide targets

for manipulation. Although there are still may gaps in our knowledge regarding stomatal regulation, as well as sensory and signalling mechanisms of guard cells, there is considerable information available on stomatal responses to various environmental stimuli, guard cell osmoregulation and mechanisms of movement. Below a historical account of the various osmoregulatory pathways and solutes involved stomatal regulation is provided which not only demonstrates the wealth of information but also hints at extreme plasticiy in guard cell function.

1.3.1 Starch-sugar theory

In the early 20th century, researchers supported the hypothesis that sucrose was the only osmolyte required for stomatal opening which was produced by starch breakdown in the guard cells (Lloyd, 1908). The starch-sugar hypothesis is based on the fact that in the dark inactive starch is accumulated and stored in the guard cells which is subsequently converted to active sugar during the day in the light (Lloyd, 1908). This was first observed by the fact that open stomata in the light period had less starch than closed stomata at night time. The sugars produced from starch breakdown increases the osmotic potential of guard cells which results in water uptake and increase turgor pressure of the guard cells thereby opening stomata. However, the disappearance of starch in the guard cells has also been linked to contribute to the development of carbon skeleton needed for the synthesis of organic anions such as malate, to act as counter ions to K^+ uptake to support stomatal opening (Outlaw and Lowry, 1977). Although, in 1960, the starch-sugar hypothesis was replaced by the K^+-malate theory along with the counter ions $malate^{2-}$ and/or Cl^- (Allaway, 1973, Schnabl, 1980), the sucrose paradox was revisited when Macrobbie and co-workers showed that K^+ and counter ions could not provide all the osmoticum for stomatal opening (MacRobbie, 1987). Additionally, the reported decline in K^+ ion concentration during stomatal opening along with a simultaneous

increase in sucrose concentration later in the day led to the suggestion that K^+ is important for stomatal opening early in the day and replaced by sucrose later on in the day (Schroeder et al., 2001, Talbott and Zeiger, 1993). These findings demonstrates that osmoregulation in guard cells depends on at least two different osmoregulatory pathways, K^+ transport and sucrose metabolism that occurs at different times of the day (Talbott and Zeiger, 1993).

1.3.2 Potassium chloride-malate theory

The Potassium-malate theory replaced the starch-sugar theory in 1960 (Imamura, 1943, Fischer and Hsiao, 1968, Raschke, 1975). This became the accepted and main guard cell osmoregulatory pathway and is still often considered the exclusive mechanism for regulating stomatal aperture. Starch breakdown has long been associated with the synthesis of malate (Ogawa et al., 1978). As a result of high accumulation of starch and PEP carboxylase in guard cells, this led to the suggestion by many that this is the only or major pathway of CO_2 fixation in guard cells (Ogawa et al., 1978). The importance of malate in guard cell osmoregulation has been demonstrated by blue light induced stomatal opening which resulted in severe impairment of *A. thaliana* phosphoglucomutase mutant, as a result of negligible starch accumulation in guard cell chloroplasts (Lasceve et al., 1997). Addition of chloride (Cl^-) in the medium rescues the stomatal aperture of the mutant compared with wild-type plants suggesting that starch degradation in guard cells provides carbon for the accumulation of a counter-ion to potassium, probably $malate^{2-}$ (Lasceve et al., 1997). This has further been supported by the recent work of Horrer et al. (2016) which estimates that half of the starch degraded in guard cells is sufficient to provide carbon for rapid malate synthesis under blue light. Additional support for the involvement or importance of PEPc in stomatal opening has also come from the work of (Cousins et al., 2007) who conducted an experiment on PEPc

deficient mutant of *Amaranthus edulis* and reported reduced rates of stomatal opening and g_s compared with the wild types**.**

Despite all these recent findings and the undisputed importance of K^+ and its counter ions uptake in stomatal opening, studies still showed it cannot solely account for the increase in osmotic pressure necessary for stomatal aperture which was based on the findings of Tallman and Zeiger (1988a) who suggested and demonstrated that the general assumption of K^+ and its counter ions as the universal osmoticum was not the case for osmoregulatory stomatal opening but rather, their data showed that sugars arising from photosynthesis and from starch degradation were additional osmotica. Similar results were also demonstrated in *Vicia faba* guard cells that took up approximately 2 pmol of K^+ during stomatal opening which is less than the 4.5 MPa expected to fully open stomata even if it was still balanced by the accumulation of similar amounts of counter ions (Cl^- and/or malate^{2-}),(Chen et al., 2012, Fischer, 1968b).

Apart from malate being the predominant anion in plants during stomatal responses, there are evidences that support roles played by other carboxylates. Pyruvate is one of such which has been involved in metabolic pathways. Pyruvate has long been implicated in the regulation of stomatal function where it showed its effect as a negative regulator of ABA by an induced inhibition of stomatal opening in the light (Raghavendra et al, 1976). Recently, a putative pyruvate carrier (NRGA1), was identified to negatively regulates ABA-induced signalling in guard cell and a disruption of this resulted in an increased in ABA sensitivity in stomatal movements (Li et al., 2014).

Nonetheless, sucrose was again put forward as the most likely additional solute to support stomatal opening (MacRobbie, 1987, Tallman and Zeiger, 1988b).

1.4 Guard cell chloroplasts

Photosynthesis takes place primarily in the mesophyll tissue as epidermal cells generally lack chloroplasts. However, guard cells, which developed from protodermal cells, also contain photosynthetically active chloroplasts in most but not all species (Outlaw et al., 1981, Zeiger et al., 1981, Shimazaki et al., 1982, Zemel and Gepstein, 1985, Gotow et al., 1988b). The number of chloroplasts in each guard cell depends on the species (Wilmer and Fricker, 1996, Lawson et al., 2003c). Majority of species contain between 10-15 chloroplasts per guard cell (Humble and Raschke, 1971) compared with 30-70 in a palisade mesophyll cell, however in some species like the *Selaginella*, the number of chloroplasts per guard cell is only 3-6 (Allaway and Milthorpe, 2012) whilst in some species, up to 100 can be found e.g *Polypodium vulgar* (Stevens and Martin, 1978). However, guard cells of *Paphiopedium* spp completely lacks chloroplasts but still maintains functional stomata (Nelson and Mayo, 1975) suggesting that they may not be essential for stomatal function. Guard cell chloroplasts are smaller and have less granum hence could be said to be less developed than the mesophyll cells. Guard cell chloroplasts have a reduced thylakoid network and chlorophyll contents compared to the mesophyll (Shimazaki and Okayama, 1990) and have functional photosystems I and II, electron transport, oxygen evolution and photophosphorylation (Gotow, 1998, Lawson et al., 2002).

Calvin cycle activity has been demonstrated in guard cells, although the activity of ribulose bisphosphate oxygenase carboxylase (Rubisco) has been reported to be lower compared with mesophyll. The role of guard cell chloroplasts and the amount and importance of guard cell photosynthesis is a controversial topic with different reports in different species and from different laboratories. This could be due to the complex and functional plasticity of guard cell osmoregulation and signalling pathways coupled with

the possible multiple roles for which may vary depending on conditions or time of the day (Zeiger et al., 2002). Therefore elucidating the role of the guard cell chloroplasts and guard cell photosynthesis presents a serious challenge for researchers in the field.

The following roles have been proposed for guard cell chloroplasts.

1. Electron transport in guard cells are capable of producing ATP used in osmoregulation (Schwartz and Zeiger, 1984, Shimazaki and Zeiger, 1985, Daloso et al., 2015).

2. Photosynthetic carbon assimilation within guard cells produces osmotically active sugars (Madhavan and Smith, 1982, Zemel and Gepstein, 1985, Shimazaki and Zeiger, 1985, Gotow et al., 1988b)

3. Chloroplasts are involved in blue-light signalling and response (Frechilla et al., 2004, Zeiger and Zhu, 1998).

4. Starch stored in the chloroplasts (either produced from carbon assimilation in the guard cell chloroplasts, or imported from the mesophyll) is available to synthesize malate as a counter ion to K^+or is degraded into sucrose.

1.4.1 Electron transport in guard cells

Studies have provided evidence for linear electron transport, photophosphorylation in the guard cells and that the rates of these processes are dependent on CO_2 concentrations (Hipkins et al., 1983, Shimazaki and Zeiger, 1985, Willmer and Fricker, 1996, Tsionsky et al., 1997). Furthermore, a role of guard cell photosynthetic electron transport in red light-induced stomatal opening has been proposed (Olsen et al., 2002, Suetsugu et al., 2014a). The quantum efficiency for PSII photochemistry in guard cells has been shown to the rate of 70 to 80% that of mesophyll cells when subjected to a wide range of light levels suggesting a similarity of operation in mechanisms in both guard and mesophyll

cell (Baker et al., 2001, Lawson et al., 2002). The pigment composition of guard cells is similar to that of the mesophyll cells and the rates of cyclic electron flow observed in guard cell protoplasts of *V. faba* supported by high PSI activity compared with the mesophyll (Lurie, 1977) which leads to enhance ATP production. Such electron transport rate could provide sufficient energy to drive ions for stomatal opening in the absence of CO_2 fixation. This however did not agree with the work of Shimazaki and Zeiger (1985) who did not observe a high PSl activity in guard cells of *Vicia fab.* Using the high-resolution chlorophyll fluorescence imaging , (Lawson et al., 2002, Lawson et al., 2003a) found that Rubisco acts as a major sink for the products of electron transport suggesting that guard cell electron transport can be mediated by [CO_2] and that Calvin Cycle activity do take place in the guard cell (Melis and Zeiger, 1982a) which, eliminates photorespiration by CO_2-concentrating mechanism in the guard cells. However, PSII photochemistry responded to changes in oxygen concentration in guard cells, suggesting that Rubisco activity was a sink for the end products of electron transport in *A. caudatus* in guard cells but not in mesophyll cells (Ueno, 2001).

A sink for the products of electron transport in photosynthesis is evident under red light However blue light- induced stomatal opening is thought to not be dependent on the products of guard cell electron transport (Schwartz and Zeiger, 1984).

1.4.2 Photosynthetic CO_2 fixation in guard cell

There have been several conflicting reports in the literature concerning the capacity of photosynthetic carbon reduction in guard cell chloroplasts and its importance in stomatal function (Shimazaki et al., 1989; Outlaw, 1989; reviewed by Lawson 2009). Early studies provided little evidence of Calvin cycle activity in guard cells and demonstrated that CO_2 is incorporated as malate (Raschke and Dittrich, 1977). Evidence for a lack of Calvin cycle activity was provided by Raschke and Dittrich (1977), who showed that radioactive

3-PGA/Rubisco activity was present in epidermal peels of the same tissues when they were exposed to $^{14}CO_2$. Subsequent experiments demonstrated that guard cell chloroplasts lacked ribulose-1,5-bisphosphate carboxylase (RuBPC) and ribulose-5-phosphate kinase (Ru5PK) activity (Outlaw and Manchester, 1979) and other key enzymes (Outlaw and Manchester, 1979, Schnabl, 1981) for the photosynthetic carbon reduction pathway. These findings concluded that there was insignificant Rubisco activity, confirming the conclusion of Hampp et al. (1982) that photo-reduction of CO_2 by guard cells was absent.

Despite the above findings of lack of carbon fixation in the guard cell chloroplasts, studies in the last two-three decades have shown that photosynthetic carbon fixation takes place in the guard cells. For instance, studies have shown that guard cells contain Rubisco (Madhavan and Smith, 1982, Zemel and Gepstein, 1985) and several other key Calvin cycle enzymes (Shimazaki and Zeiger, 1985, Gotow, 1998). Chlorophyll florescence measurements in guard cells of intact leaves (Lawson et al 2001; 2002) and epidermal peels have shown distinct features associated with Calvin cycle activity (Melis and Zeiger, 1982b). The demonstration of photorespiration and CO_2 fixation in single guard cells by chlorophyll fluorescence kinetics measurement (Cardon and Berry, 1992), the dichlorophenyl dimethyl urea (DCMU) sensitivity of sucrose accumulation in guard cells from sonicated epidermal peels incubated under red light (Poffenroth et al., 1992b) indicated the ability of the guard cell chloroplasts to fix carbon. Zeiger et al, (2002) also detected significant Calvin cycle activity and demonstrated that it was osmotically important without the breakdown of starch (Talbott and Zeiger, 1993, Tallman and Zeiger, 1988a) for stomatal function. Carbon dioxide uptake into 3-PGA and ribulose 1,5-bisphosphate along with evidence for guard cell production of sucrose during red light-induced stomatal opening in *V. faba*, where no starch breakdown was observed and sugar

import was ruled out as a result of the use of epidermal peels (Gotow et al., 1988a, Poffenroth et al., 1992a, Talbott and Zeiger, 1993, Tallman and Zeiger, 1988a). Significant reduction in photosynthetic efficiency in guard cells of antisense SBPase tobacco plants suggested that the Calvin cycle was the major sink for the end products of electron transport (Lawson et al., 2008b)

Despite the evidence outlined above many other reports have suggested that the rates are too low for any functional significance (Outlaw, 1989; Outlaw et al., 1982) with the contribution to osmotic requirements for stomatal opening only about 2% (Reckmann et al., 1990) but a later report by Poffenroth et al. (1992a) reported this figure to be about 40%.

However, in the last few decades, more evidence for guard cells carbon reduction has been published. For instance, tobacco plants with reduced levels of Rubisco had been found with substantially low photosynthetic capacity and with stomatal responses to light and changing [CO_2] similar to those of the wild type (Baroli et al., 2008b, von Caemmerer et al., 2004). Additionally, Wang et al. (2014a) Arabidopsis plants lacking guard cell chloroplasts were 30% to 40% smaller than that of plants with guard cell chloroplasts and suggested that this was likely due to reduced phosphorylation levels in the guard cells.

The recent work of Daloso et al., (2015) using transgenic tobacco showed that guard cells are able to fix CO_2 via both Rubisco and phosphoenolpyruvate carboxylase (PEPc) where stomatal opening occurred without exogenous application of K^+ or sucrose and with no evidence of starch breakdown, suggesting that guard cells fix carbon via photosynthesis. The study further suggested that both enzymes play roles in guard cell metabolism but their roles may be dependent on time or environmental factors. Further evidence for PEPc

in stomatal function came from studies on transgenic C_3 potato. Over expression of PEPc resulting in an increase in the rate of stomatal opening,whereas antisense PEPc expression reduced stomatal opening rates respectively (Gehlen et al., 1996).

A source for guard cell sucrose has also shown to result from gluconeogenesis and high expression of gluconeogenesis-related genes such as PEPc, phosphoenolpyruvate carboxykinase (PCK) and cytosolic malate dehydrogenase have been demonstrated in guard cells which suggested the likelihood of sucrose being produced via gluconeogenesis after CO_2 fixation by PEPc and OAA decarboxylation by PCK (Eastmond et al., 2015). This is in agreement of PEPc as an alternative for carbon fixation in the absence of carbon fixation by Rubisco in guard cell (Willmer and Ditrich 1974, Raschke and Dittrich, 1977, Outlaw 1990). Antunes et al. (2012a) in his study also supported the hypothesis that alterations in partitioning of sucrose between storage and breakdown may affect stomatal function. In agreement with this hypothesis, solanum tuberosum plants expressing an antisense construct targeted against sucrose synthase 3 (SuSy3) had a lower stomatal conductance compared with WT controls. The decrease in g_s resulted in a slight reduction in CO_2 fixation and increase in WUE. On the other hand, plants with increased guard cell acid invertase activity caused by the introduction of the SUC2 gene had a greater stomatal conductance, increased CO_2 fixation and decreased WUE. These results highlighted the important role that sucrose plays in guard cell function and indicates the feasibility of enhancing plant WUE through the manipulation of guard cell sucrose metabolism.

Similarly, Daloso et al. (2016a) characterised the function of isoform 3 of sucrose synthase (SUS3) in transgenic Nicotiana tabacum plants overexpressing SUS3 under the control of the guard cell specific promoter, KST1 and investigated the changes in guard cell metabolism during the dark to light transition. Overexpression of guard cell-specific

SUS3 led to increased SUS activity, greater stomatal aperture, stomatal conductance, transpiration rate, net photosynthetic rate and growth. These results suggested that sucrose breakdown provide substrate for the provision of organic acids towards stomatal function and further suggested that the manipulation of guard cell metabolism may represent potential for an effective plant growth improvement.

Genetic manipulation of guard cell sucrose metabolism has contributed important evidence for the role of sucrose, starch and triacylglycerols in stomatal movements (Daloso et al., 2015; Horrer et al., 2016; McLachlan et al., 2016).

Light-stimulated increases in PEPc activity have been demonstrated with enhanced malate accumulation and increased NADP or NAD-dependent MDH activity, which facilitates the reduction of OAA to malate (Rao and Anderson, 1983, Scheibe et al., 1990).

A recent study of gene expression in guard cells of C_3 and C_4 species revealed low expression of C_4 genes in C_3 guard cells suggesting limited carbon fixation via PEPc. Additionally, the gene expression of C_4 plants showed similar gene expression patterns to those of C_4 mesophyll cells, indicating a role for C_4 genes in guard cell regulation in C_4 plants (Aubry et al., 2016).

All the above have demonstrated that guard cell photosynthesis exists and either supplies the energy for the proton pumps and/or produces solutes that contributes to guard cell osmoregulation of stomatal behaviour, however more further studies using recent advances in molecular technology, such as cell-specific promoters are highly needed to fully elucidate the role of guard cell photosynthesis in stomatal function (Lawson, 2009; Lawson and Blatt, 2014).

1.4.3 Guard cell chloroplasts in blue-light signalling:

Blue light exerts the most pronounced effect on stomatal opening as it stimulates potassium and chloride uptake with starch hydrolysis producing malate (Tallman and Zeiger, 1988a, Talbott and Zeiger, 1993, Horrer et al., 2016).The process of stomatal opening in response to blue light occurs when the blue light receptors (phototropins 1 & 2) activate plasma membrane H^+-ATPases (Kinoshita et al., 2001). Activated H^+-ATPase induces hyperpolarization of the plasma membrane thereby leading to K^+ uptake via the K^+_{in} channels, (Kinoshita and Shimazaki, 2002).

Suetsugu et al. (2014b) demonstrated that the end products of electron transport (ATP and NADPH) in guard cells are essential for blue light responses which showed by the application of DSMU inhibited red light-enhanced and blue light-induced opening of Arabidopsis stomata but did not affect H^+-ATPase in response to blue light but both red light and blue light-dependent stomatal opening were inhibited in intact leaves. However, blue light responses is not universal though as some species lack the blue light induced opening *Adiantum caillus-veneris* despite having a functional plasma membrane H^+-ATPase and phototropins does not open in blue light (Doi et al., 2006).

1.5 Co-ordination between guard and mesophyll cells

For optimal plant growth, stomata must be able to balance between supply of CO_2 for photosynthesis and the plant's need to remain hydrated for maximum growth (Wong, 1979, Farquhar et al., 1978) which are generally observed in steady-state. However, in the fluctuating environment, photosynthetic responses are an order of magnitude slower which means that A and g_s are not always co-ordinated (Pearcy, 1990, Pearcy and Way, 2012). In C3 plants for instance, the photosynthetic rate can adjust in seconds to increasing irradiance but the slow response in stomata can restrict CO_2 diffusion and

negatively impact on photosynthesis (Barradas and Jones, 1996, Tinoco-Ojanguren and Pearcy, 1993, Lawson et al., 2012). Plants therefore experience short and long term fluctuations in PPFD to which A and g_s respond. The temporal disconnect between the stomatal conductance (g_s) and carbon assimilation (A) means that carbon gain relative to water loss is far from optimal (Lawson & Blatt, 2014). Stomatal limitation can limit up to 20%, which can impact substantially on crop yields (Farquhar and Sharkey, 1982, Jones, 1998). Amplitude and rapidity of stomatal movements are therefore potential targets to look out for when improving A and g_s. The relationship between A and g_s is shown on Fig 1.1 where dark adapted plants subjected to a step change in light exhibited nonsynchronous effect of A and g_s leading to loss in carbon and water gain (Lawson and Blatt, 2014).

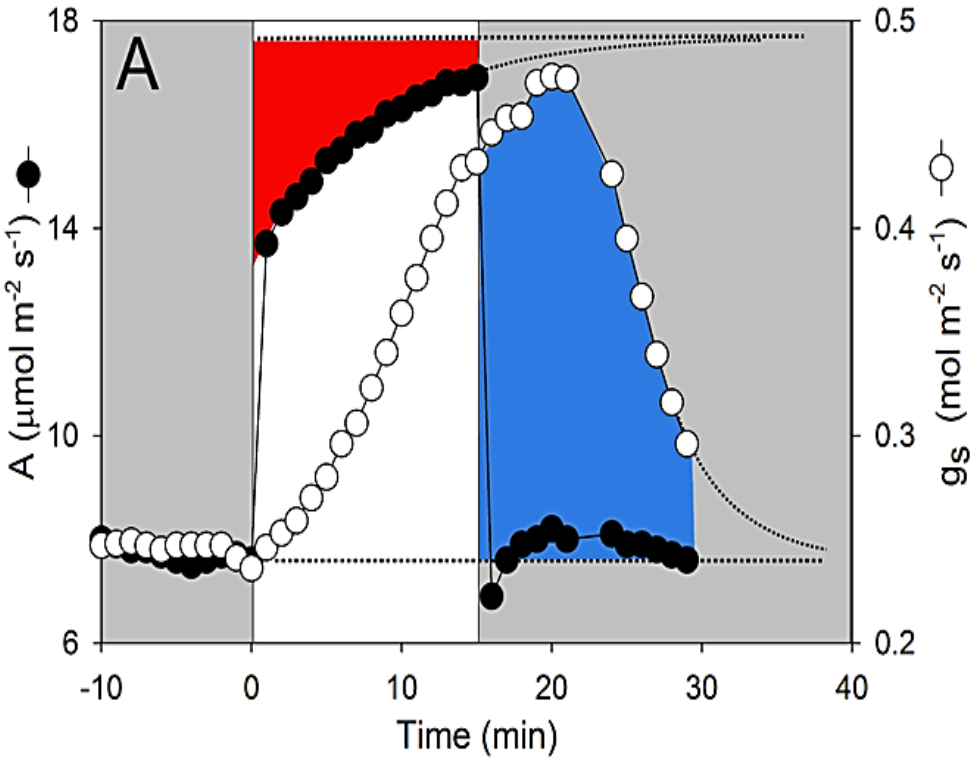

Figure 1. 2. Relationship between carbon assimilation *(A)* and stomatal conductance *(g_s)* subjected to 100 µmol $m^{-2}s^{-1}$ and 1000 µmol $m^{-2}s^{-1}$ of light. Leaves were first equilibrated at a PPFD of 100 µmol m^{-2} s^{-1}until both *A* and g_s reached steady state (first shaded part). Once steady state was achieved, PPFD was increased to 1000 µmol m^{-2} s^{-1} for 1 hour showing complete disconnect of *A* and g_s where g_s response was slower than *A*. On returning to the initial light of 100µmol m^{-2} s^{-1}, *A* immediately decreased while again g_s took time to reach steady stage showing great difference and lack of coordination leading to drastic effect on photosynthetic carbon assimilation and WUE. The red shaded part indicates carbon loss while the blue shaded part indicates water loss (Lawson and Blatt, 2014).

It is generally assumed that the internal CO_2 concentration inside the leaf (C_i) enables stomatal behaviour to be coordinated with mesophyll photosynthetic rates (Mott, 1988). As photosynthesis increases, C_i is lowered which results in stomatal opening however when photosynthesis decreases C_i increases leading to stomatal closure.

However, it is now believed that the large changes observed in g_s could not be accredited to C_i alone (Farquhar et al., 1978, Morison and Jarvis, 1983, Raschke and Schnabl, 1978). Several studies have also demonstrated changes in stomatal conductance (g_s) in response

to light, even when C_i was held constant (Lawson et al., 2008b, Matrosova et al., 2015, Wang et al., 2008). This supported previous work that suggested a signal is transferred from the mesophyll to guard cells (Lee and Bowling, 1992, Mott, 2009, Mott et al., 2014, Mott et al., 2008b). Health and Russell in 1954 suggested that a chemical or signal transmitted from the mesophyll was responsible for guard and mesophyll cells coordination. Fig. 1.3 below shows possible mesophyll-driven signals that connect stomata with the mesophyll.

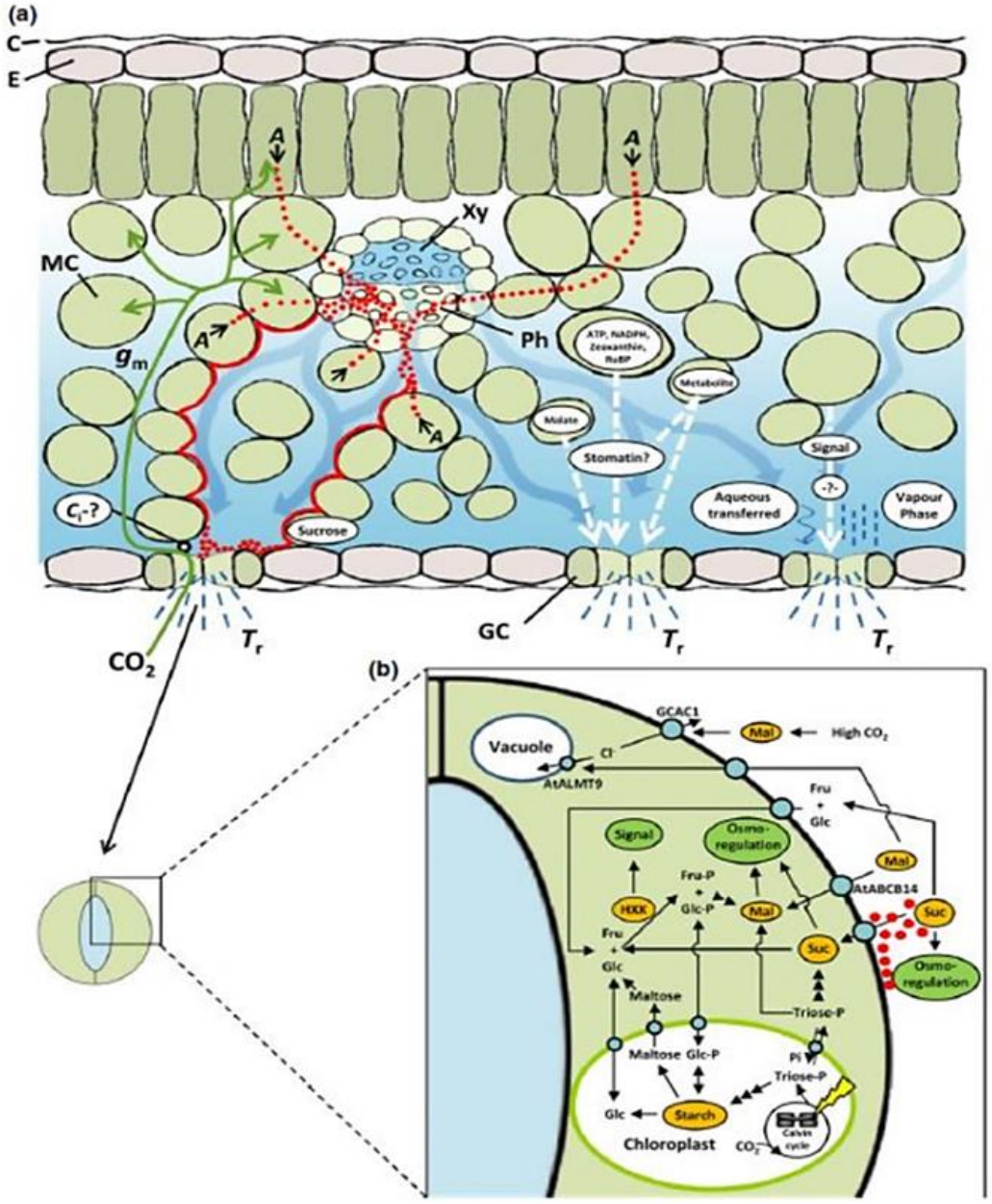

Figure 1. 3 Schematic diagram of a leaf cross section showing possible mechanisms that connect mesophyll and guard cells that affect stomatal behaviour (a). CO_2 absorbed from the atmosphere through the stomatal pore diffuses towards the mesophyll cells (green line), where it is used for photosynthesis (*A*). Sucrose (Suc - represented by red dots) moves from the mesophyll cells (MC) toward the phloem (Ph). Water (blue arrows) coming out of the xylem (Xy) move toward the guard cells and evaporate (T_r) to the atmosphere. Some of the apoplastic Suc (red line) is carried by the transpiration stream toward the guard cells (GC) and accumulates at the GC.The diagram includes additional potential effectors (such as Ci, metabolites and aqueous- versus vopour-carried signals). (b) Schematic diagram of the primary metabolism in GC and the potential effects. Suc may accumulate at the GC cell wall (red dots), and may have an extracellular osmotic effect. Suc may enter the GC via Suc transporters (blue circle) or might be cleaved in the apoplast into glucose (Glc) and fructose (Fru) that also enter GC via hexose specific transporter (blue circle). In the cytosol, Suc may have an osmotic effect. Photosynthesis

in GC yields triose-phosphates (triose-P) which may be converted to starch within the chloroplast or exported to the cytoplasm, where it might be converted to Suc or malate. Starch degradation may also contribute to Suc and malate accumulation. The cytosolic Glc and Fru obtained from Suc cleavage or from starch degradation must be phosphorylated into Glc-P and Fru-P to be further metabolized. Phosphorylation of Glc and Fru by hexokinases (HXK) may generate a signal that closes stomata.C–cuticle; E–epidermis; MC – mesophyll cell; GC – guard cell; *A*– photosynthesis; Xy– xylem; Ph–phloem; g_m–mesophyll conductance to CO_2; C_i–substomatalCO_2 concentration; T_r – transpiration; ATP– adenosine triphosphate; NADPH–Nicotinamide adenine dinucleotide phosphate; RuBP– Ribulose 1, 5-bisphosphate; Glc-P–glucose phosphate; HXK – hexokinase; Suc–sucrose; Triose-P–triose phosphate; White circles and white arrows represent mesophyll- driven signals affecting stomatal movement; Red dots and lines represent sucrose paths; Blue faded arrows represent the flow of water from xylem toward the stomata; Green arrow represent CO_2 movement; Blue circles represent transporters; Green circles represent the effect on stomatal aperture. Copied from Lawson et al., 2014.

Recently, Matrosova et al. (2015) found the role of C_i in stomatal responses to red light using Arabidopsis mutants. Mutants with impaired low CO_2-induced stomatal opening was shown to be essential for red light stomatal opening, which has shown that photosynthetic reductions in C_i contribute to stomatal opening in response to light. On the other hand, mutants which typically exhibit slow stomatal responses to [CO_2], responded more strongly to red light than to low [CO_2], suggesting that other processes other than low C_i are involved in red light-induced stomatal opening (Matrosova et al., 2015). This study concluded that red light responses can be mediated both by independent and dependent reduction in C_i concentration.

Mott et al. (2008b) demonstrated that stomata in epidermal strips responded much less to changes in light and [CO_2] than epidermal strips that where placed back onto mesophylls. These experiments formed the basis of their suggestion that there is a signal transduction pathway from the mesophyll to the guard cell which aid stomatal opening. The metabolite or signal was suggested to be a product of photosynthesis which balances photosynthetic

limitation between Rubisco and electron transport (Wong et al., 1979, Messinger et al., 2006).

Nelson and Mayo (1975) observed that stomata or guard cells devoid of chloroplasts open normally in the light which suggested that chlorophyll of mesophyll are sensitive to red light hence the transfer of signal from the mesophyll to guard cells. Support for a mesophyll-driven signal also came from the inability of the stomata to respond to red light in peels (Lee and Bowling, 1992) or slower responses than in mesophyll (Roelfsema et al., 2002, Olsen et al., 2002). Apoplast transfer of mesophyll signals has resulted in stomatal opening and shown to be dependent on photosynthesis (Fujita et al., 2013b). This substance was named to be sucrose by Lu et al. (1997a) who summarised their findings as follows (a) multiple sucrose pools in mesophyll cells, (b) a localized mesophyll-apoplast region that exchanges with phloem and stomata, and (c) mesophyll-derived suc in guard-cell walls sufficient to diminish stomatal opening. Hence, they concluded that multiple physiological factors are integrated in the attenuation of stomatal aperture size by this previously unrecognized mechanism.

Furthermore, attempts to understand the link between mesophyll and guard cell metabolism have been employed through the use of genetic engineering combined with stomatal physiology and mesophyll function (Nilson and Assmann, 2007). Through the advancement of biotechnology, it is now relatively straight forward to employ cell-specific or tissue specific transcriptomic assays which enables specific and individual cell mechanisms to be studied facilitating a complete understanding of stomatal regulation and how it is influenced by the surrounding mesophyll cells. This represents an important step towards finding mechanisms to produce plants with greater water use efficiency (Yang et al., 2005, Gago et al., 2016, Lawson et al., 2014b) . Examples of such

manipulation are numerous among which is the use of tobacco antisense SBPase plant. Lawson et al. (2008a) demonstrated the relationship between CO_2 assimilation rate and stomatal conductance under mixed blue/red light and red light alone and found stomatal opening to be fast in transgenics compared to wild type and final stomatal conductance was higher in the antisense plants. The results showed that light-induced opening or high CO_2 mediated closure was not dependent on the photosynthetic capacity but on photosynthetic electron transport or its end products.

Sucrose has long been proposed to be a metabolite connecting between mesophyll and guard cells (Gotow et al., 1988, Reckmann et al., 1990, Poffenroth et al., 1992, Muschak et al., 1999).This has been supported by research on transgenic plants overexpressing hexokinase specifically in guard cells which have been shown to have accelerated stomatal closure (Kelly et al, 2013). These findings suggested that sucrose produced by mesophyll photosynthesis is carried through the apoplast to the guard cells, where an osmotic effect due to overloading of sucrose in the guard cell walls closes the stomata (Kang et al., 2007, Lu et al., 1997, Lu et al., 1995, Outlaw and De Vlieghere-He, 2001). Stomatal conductance in an Arabidopsis mutant with a loss of function of the trafficking protein SYP121 led to greater WUE but reduced CO_2 assimilation that impaired growth (Eisenach et al., 2012). Reduction in sucrose synthese 3 (SuSy3) in *Solanum tuberosum* reduced stomatal conductance leading to an increased WUE but the lower g_s also restricted carbon assimilation (Antunes et al., 2012b). Tanaka et al. (2013) showed that stomagen (EPLF9), increased stomatal density and resulted in an increase in assimilation rate by 30% however transpiration rate increased by 50% which led to a reduction in WUE. However, some manipulation appear to be beneficial for example high WUE was achieved by a 20% reduction in transpiration and g_s without a cost in CO_2 assimilation

rate was reported in Arabidopsis loss of function GT-2LIKE1 (GTL1) mutants (Yoo et al., 2010).

The manipulation of carboxylates metabolism have also been demonstrated of the importance of organic acids in coordinating stomatal behaviour with mesophyll which was recently showcased by studies where higher stomatal conductance were observed in plants with increased accumulation of malate in comparison to the plants lacking a functional AtALMT12 malate channel which has a lower g_s (Medeiros et al., 2016, Gago et al., 2016).

These recent studies have all shown clearly a role for mesophyll regulation of stomatal aperture by importing organic acids from the mesophyll for osmotic adjustments as well as the production of ATP providing the energy required for the proton pumps involved in guard cell osmoregulation. Therefore, the genetic manipulation of metabolites involved in metabolism and photosynthetic enzymes in the guard cells themselves could also lead to changes in stomatal behaviour and potentially improve photosynthesis and water use efficiency in plants (Santelia and Lawson, 2016).

1.6. Advances, tools and techniques for guard cells manipulation towards stomatal function:

Recent developments in technology has opened opportunities to explore guard cell signalling and mechanisms that co-ordinates stomatal responses with mesophyll demands for CO_2 and therefore potentials for regulating WUE and enhancing plant productivity. Models are now available to assess temporal relationship between A and g_s (Vialet-Chabrand et al., 2016) within a limited time. Efficient, simple and fast cloning techniques are available for the design of desired single or multiple genes to be expressed in plants for genetic manipulation of metabolites involved in photosynthetic metabolism which

could lead to changes in stomatal behaviour and potentially improve photosynthesis and water use efficiency in plants.

Specific cell metabolisms in guard and mesophyll cells can now be targeted and the possible coordination between mesophyll metabolites in relation to stomatal functions determined. The development of guard cell specific promoters has made these manipulation of expression of specific gene transcripts possible which provides opportunities to manipulate guard cell specific metabolisms or specific stomatal traits in order to elucidate mesophyll-stomatal interactions. Guard cell specific promoters combined with specific organelle transit peptides allow the elucidation of the roles of specific transcripts involved in electron transport, ion channel function, carbohydrate biosynthesis to be evaluated on a cell by cell basis (Lawson and Blatt, 2014). These tools allow the role of these transcripts in the coordination of guard and mesophyll cells with stomatal interaction to be determined experimentally (Lawson and Blatt, 2014a). For instance, KST1 and MYB60 promoters, which are guard cell specific promoters developed by Müller-Röber et al. (1995) have been used to drive the expression of target genes specifically in guard cells. The use of a specific guard cell promoter has demonstrated an excellent use by Wang et al. (2014) demonstrating an enhanced light-induced stomatal opening, greater photosynthesis and improved growth rate in Arabidopsis over expressing H^+-ATPase amidst others.

Current research efforts towards improvement of plant productivity have focussed on improved photosynthetic carbon assimilation by overexpression and down regulation or antisense technology of photosynthetic enzymes. Prior studies have targeted both the Calvin cycle and electron transport chain enzymes to expressions in order to identify their control on carbon assimilation (Raines, 2003, Lefebvre et al., 2005, Simkin et al., 2017c). It is now possible to demonstrate single or more enzyme transformations which have

shown to enhanced photosynthetic rates in varieties of crops. For instance, increased sedoheptulose-1,7-bisphosphatase activity resulted in tobacco plants with improvements in carbon assimilation by 6–12% (Lefebvre et al., 2005, Lawson et al., 2008b). It is in line with this that we aim to elucidate the role of the guard cells chloroplasts on stomatal function and in coordination with the mesophyll by using both physiological and molecular means.

Aim

To use both physiological and molecular approaches:

- Physiological approach will employ the use of the novel specifically designed environment control chamber (the epidermal-mesophyll transfer experiment) to examine the co-ordinated response between mesophyll photosynthesis and guard cell photosynthesis or to investigate stomatal responses in peel epidermis relative to intact leaves
- To use guard cell specific promoters (Myb60 and KST1) to drive expression specifically in the guard cells in order to produce transgenic plants with manipulation in electron transport chain and Calvin cycle activity.

Objectives

- Characterize stomatal responses in epidermal peels and intact leaves of CAM (*Kalanchoë fedtschenkoi)* and C3 (*Vicia faba)* species.
- Assess co-ordinated responses between stomata and underlying mesophyll using C3 and CAM plants

- Conduct infra-red gas analysis to examine the effect of irradiance and CO_2 concentrations on mesophyll photosynthesis and stomatal conductance in CAM (*Kalanchoë fedtschenkoi)* and C3 (*Vicia faba)* species
- To use guard cell specific promoters (Myb60 and KST1) to produce transgenic plants with manipulation in electron transport chain and Calvin cycle activity in the guard cells.
- To perform stomatal kinetics such as stomatal conductance/assimilation *(A/g_s)* curves, A/q curves, assimilation/ internal CO_2 (A/C_i) curves in order to assess impact on stomata in regard to WUE and plant productivity of the generated transgenic lines.
- To conduct physiological analysis using the chlorophyll fluorescense and High resolution chlorophyll fluorescence imaging to quantify alterations in guard and mesophyll photosynthesis efficiency in transgenic and non-transgenic Arabidopsis (*Arabidopsis thaliana*) and tobacco (*Nicotiana tabacum)* plants to changing environmental conditions including light and CO_2 concentrations.

CHAPTER TWO: MATERIALS AND METHODS

MOLECULAR BIOLOGY TECHNIQUES:

2.1 Primer design

Primers were designed based on the sequences of the genes of interest Sedoheptulose 1,7-bisphosphatase (SBPase) and Cytochrome b_6f complex (Rieske) in Arabidopsis. SBPase and Rieske genes were flanked by BsaI and BpiI restriction sites and using PCR amplification of their coding sequences. Fusion sites overlapping with coding sequences have a start codon with AATG at the 5' ends and GCTT at the 3' end so as to minimize changes to encoded proteins (Weber et al., 2011). Therefore, AATG is included in the forward primer while AAGC is included in the reverse primer. Primers for noncoding modules, fusion site sequences GGAG, TACT, GCTT and CGCT were all positioned in all non-translated sequences but chosen to enable efficient and nonpalindromic cloning. Standardized transcription units of all the level were flanked by these specific fusion sites as described by (Weber et al., 2011). PCR primers were also designed by including the four base pair (CACC) necessary for TOPO directional cloning on the 5' end of the forward primer. This was done in such a way that our gene of interest fused and expressed with the recognition site of the entry vector. Details of primers are shown in the appendix. In addition to the geneious tool used for designing primers, Primer3 (http://biotools.umassmed.edu/bioapps/primer3_www.cgi) and the NCBI tool (http://www.ncbi.nlm.nih.gov/tools/primerblast/index.cgi?ORGANISM=9606&INPUT_SEQUENCE=NM_001618.3&log$=seqview_box_primer) were also utilised.

2.2 Cloning Sedoheptulose-1, 7-bisphosphatase (SBPase) and cytochrome b_6f (Rieske) genes using Golden gate technology

The sequences of the genes of interest SBPase (AT3655800) and Rieske (AT 4G03280 *Arabidopsis thaliana* were retrieved from the TAIR database and primers designed as previously described. The plasmid vectors used for the plant transformation were constructed using the golden gate cloning and the Moclo system (Engler et al., 2008, Weber et al., 2011). The construct design for the sense and antisence plasmid vectors allowed efficient assembly of multiple DNA fragments in a single reaction based on the type IIs restriction enzyme that cut outside of recognition site allowing fragments to be ligated into products lacking the original restriction site and leaving no unwanted sequences in the final constructs (Engler et al., 2008). This made the assembly of constructs of each transcriptional units to be expressed hence multiple desired genes assembled seamlessly in a one-pot one-step cloning reaction. The golden gate assembly enabled promoter (PU), coding sequences (SC) and terminator (T) assembled together seamlessly and expression driven by the highly specific guard cells promoters KST1 (NP001275475) (Müller-Röber et al., 1995a, Kelly et al., 2013, Galbiati et al., 2008) and AtMYB60 (At1g08810) (Cominelli et al., 2005, Rusconi et al., 2013). All DNA fragment of interest from an entry clones were transferred into their expression vector pAGM4723 without any unwanted sequences in the final construct. All sequences of expression vectors were confirmed by sequencing (samples analysed by source bioscience).

2.3 Golden gate DNA assembly protocol

DNA plasmid concentration of each assembly piece was measured and diluted to100 ng/µl using a Nano Drop ® Spectrophotometer ND-1000 (Peqlab, Erlangen). 100 ng of vector backbone and 100 ng of 1 µl of each assembly piece was added to assembly

reaction mixture in a single tube containing 1.5 µl 10x NEB T4 Buffer (Promega 106: 300 mM Tris-HCl pH 7.8, 100 mM MgCl2, 100 mM DTT, 10 mM ATP), buffer 3 (106: 500 mM Tris-HCl pH 7.9, 100 mM MgCl2, 1000 mM NaCl, 10 mM DTT) (New England Biolabs), 0.15 µl 100x BSA (New England Biolabs), 1 µl *Bsa*I (for level 1 assembly) and 1 µl *Bpi*I (for level 2 assembly) all from New England Biolabs, 1 µl NEB T4 ligase (Promega), 1 µl vector backbone (100 ng/µl.) and dH_20 to a total volume of 15 µl. Bearing in mind the use of a high concentration ligase is essential and also *Bsa*I is only 10% active at 37 °C without the addition of BSA. The assembly reaction was performed in a thermocycler (Engler *et al*. 2009) as follows; 3 min at 37 °C, 4 min at 16°C for 25 cycles followed by 5 min at 50°C and 5 min at 80°C for 1 cycle. The assembled construct was transformed into 20 µl of competent *E. coli.*

2.4 Preparation of *E. coli* chemically competent cells ($CaCl_2$ method)

The preparation was done by following the method of Calcagno, (2013). A single colony of *Echerichia coli* (*E.coli*) cells (TOP-10) was used to inoculate 10 ml of luria broth. LB broth composed of (10g Bacto-tryptone, 5g yeast extract, 10g NaCl) and shaken overnight to grow at 37°C. The 10 ml culture was used to inoculate 100ml of LB broth in the ratio (1:100), which had been kept under the same conditions and cells were then collected by centrifugation (10 min at 4°C) and resuspended in 10 ml of ice cold $CaCl_2$ solution (60 mM $CaCl_2$, 15% glycerol, 10 mM Piperazine-1,4-bis (2-ethanesulfonic Acid) (PIPES) pH 7). This was repeated three times and then cells were incubated on ice for 30 min. Finally, the cells were spun down for 5 min at 4°C and the pellet resuspended in 4 mL of $CaCl_2$ solution. The cells were used immediately or aliquoted in microcentrifuge tubes (50–200 µl) which were then stored at -80°C for future use.

2.5 Transformation of *E. coli* competent cells (heat shock)

For the transformation of *E. coli* chemically competent cells, the method described by Sambrook and Russel (2001) was used. 1–2 µl of plasmid DNA (100–200ng/µl) was added to 50-200 µl of $CaCl_2$ competent cells and mixed very gently and incubated on ice for 30 min. The cells were heat-shocked in a water bath at 42°C for 50–90 seconds and placed on ice for 2 min. Immediately after, 500–800 µL of room temperature SOB (2% w/v bacto-tryptone, 0.5% w/v bacto-yeast extract,8.56 mM NaCl, 2.5 mM KCl in H2O) or SOC (SOB + 10 mM MgCl2 or 20 mM MgSO4, 20 mM glucose) medium was added and the cells incubated at 37°C with gentle shaking. The cells were then spun down and resuspended in smaller volume (100-150 µl) which was plated on selective media overnight for colony development and placed at 37°C.

2.6 Polymerase chain reaction (PCR)

PCR reactions were performed in 0.2 ml PCR tubes using 10X DreamTaq 0.5 µl of 20 mM stock per each 25 µL PCR reaction (Thermo Scientific), 1.5 µL of 10 pmol μl^{-1} stock primer solution per each PCR reaction,1–2 µl of DNA and dNTPs 0.5 µl of 10 mM stock per each 25 µl PCR reaction (Thermo Scientific), and the recommended amount of enzyme and buffer with water (see appendix for PCR reaction mix). The volume of the reactions was made up to 15 µL. Cycle conditions were mostly at 35 depending on the size of the fragment to be amplified.

2.7 Agarose gel electrophoresis of nucleic acids

Nucleic acids were separated for analysis using gel electrophoresis. 1% agarose gels were prepared and ran at 100 volts for 40 min (150 ml gels). Tris-borate buffer (TBE: 89 mM Tris, 89 mM Boric acid, 2mM EDTA) or Tris-acetate buffer (TAE: 40 mM Tris ultrapure, 20 mM Acetic acid glacial, 1 mM EDTA.Na2) was used for the preparation of the gels

and as running buffer in the tanks respectively. Safe view nucleic acid (NBS Biologicals) was added to the gel for nucleic acid visualization under UV or blue light respectively.

2.8 Plasmid DNA preparations

High quality/purity plasmid DNA used for sequencing was extracted from *E. coli* cells using Qiagen mini plasmid preparation kit (Thermor scientific) according to the manufacturer's instructions or as follows. From a transformed *E. coli* cell, a single colony from a fresh plate was used to inoculate 10 ml of LB plus antibiotics (50 µg/mL kanamycin) and grown overnight at 37°C. 3–10 ml of the culture were spun down and the cells resuspended thoroughly in 250 µL Buffer P1 containing RNase. After this, 250 µl of Buffer P2 was added and the contents mixed thoroughly by inverting the tube 4–6 times. After this, 350 µl Buffer N3 was added and mixed immediately and thoroughly by inverting the tube again 4–6 times. The lysed cells were then centrifuged for 10 min at maximum speed in a table top microcentrifuge. The supernatant was then recovered and applied to the Qiagen prep spin column by decanting or pipetting. The column was then spun at maximum speed for 45 sec, and the flow-through discarded. The column was then washed by adding 0.5 mL Buffer PB and centrifuged for 30–60s. The column rewashed again by adding 0.75 ml Buffer PE and centrifuging for 30–60s, discarding the flow-through, and centrifuging for an additional 1 min to remove residual wash buffer. The column was transferred into a clean 1.5 ml tube and 50 µl of Buffer EB (10 mM Tris·Cl, pH8.5) or water added to its centre. This was incubated at room temperature for 1 min, and then finally centrifuged for 1 min. Purified Plasmid DNA was stored at -20°C.

2.9 Preparation of *Agrobacterium tumefaciens* competent cells and transformation by electroporation

Preparation of *Agrobacterium tumefaciens* strains, LBA 4404 (for tobacco) and GV3101 (for Arabidopsis) competent cells and transformation using electroporation were accomplished following the protocol described by Sambrook and Russel (2001). A single colony from a fresh plate was inoculated into 10 ml of LB plus antibiotics (50 µg/mL rifampicin for all strains, plus 25 µg/mL gentamicin for GV3101 or 30 µg/mL streptomycin for LBA 4404) and allowed to grow for 48 h at 28°C with vigorous shaking. The stationary culture was quickly chilled on ice and then spun down for 15 min at 4°C and 3000 g. The cells were then suspended in 10 ml of ice cold sterile double distilled water ($_{dd}H_2O$), and centrifuged again for 15 min at 4°C and 3000g. This wash was repeated 4 times, after which the cells were finally resuspended in 200 µl of ice cold sterile 10% glycerol. The competent cells were used straight away or aliquoted in 40 µL aliquots in 1.5 mL tubes and immediately stored at -80°C.

For the transformation of the competent cells, 1–2 µL of plasmid DNA were gently mixed into the tube and this mixture placed into an ice-cold electroporation cuvette. The cells were then electroporated at 2500 V using an EasyJect Prima electroporator (EQUIBIO). The cuvette was then immediately removed and 1ml of ice-cold SOC or LB media added. The culture was put in a new 1.5 mL tube and incubated at 28°C under gentle shaking for approximately 2h. Finally 100–200µL of cells were spread onto LB plates with antibiotics and the transformants allowed to grow at 28°C for 48 hours after which successful colonies were selected.

2.10 Single colony PCR screening of *E. coli* and *Agrobacterium*

Single colony PCR screening of *E. coli* and *Agrobacterium* were carried out where DNA was released by dipping into the PCR mix a tip dipped in the middle of a fresh colony obtained from the transformed *E.coli* or *Agrobacterium* colonies to the PCR reaction. Gel electrophoresis was used to determination fragment sizes afterward.

2.11 Screening of mutants

Arabidopsis and tobacco mutants were identified by PCR screening. The different forward and reverse primers were used for all the genes in the construct. The different forward and reverse primers for coding sequences of genes of interest were as follows. For genes in the construct, pL2B-BAR-(pMYB60)-ASNtSBPase, the forward primer is 5' ACAAGTTGCTTTTCGACGCATT 3' while the reverse primer is 5' GTCTTGGAGCTCAGGTACTTCC 3', for the gene in construct pL2B-BAR-(pKST)ASNtSBPase, the forward primer is 5' ACAAGTTGCTTTTCGACGCATT 3' while the reverse primer is 5' GTCTTGGAGCTCAGGTACTTCC 3', For gene in construct pL2B-BAR-(pKST)AtSBPase, the forward primers is 5' TGTCAAGCACGGACTTGTGT 3' while the reverse primer is 5' TACACACTGCGATACACCGG 3'. For gene in construct pL2B-BAR-(pKST) AtRieske, the forward primer is 5' ATTCCGCTGCAACTACATCG 3' while the reverse primer is 5'ATTCCGCTGCAACTACATCG 3', For the gene in construct pL2B-BAR-(pKST) ASNtRieske, the forward primer is 5' ATGGCTCAAAACTCATCCACCT 3' while the reverse primer is 5' AGTCTGTTTCAACCCATGGGAC 3'. For the gene in construct pL2B-BAR-(pKST)YFP, the forward primer is 5' CTGAGTGGCTCCTTCAACGT 3' while the reverse primer is 5' CCATCCTGGTCGAGCTGGAC 3'. For the gene in the construct pL2B-BAR-

(pMYB60)-ASNtSBPase-(pMYB60)YFP, the forward primer is 5' ACAAGTTGCTTTTCGACGCATT 3' while the reverse primer is 5' TTGGCAGTTGGAGATGTCACAT 3'. For the gene in the construct pL2B-BAR-(pKST) ASNtSBPase-(pKST) YFP, the forward primer is 5' ACAAGTTGCTTTTCGACGCATT 3' while the reverse primer is 5' TTGGCAGTTGGAGATGTCACAT 3'. For the gene in the construct pL2B-BAR-(pKST)AtSBPase-(pKST)YFP, the forward primer is 5' CTTCCACTGGACCTCCCATG 3' while the reverse primer is 5' TACACACTGCGATACACCGG 3'. For the gene in the construct pL2B-BAR-(pKST)AtRieske-(pKST)YFP, the forward primer is 5' ATTCCGCTGCAACTACATCG 3' while the reverse primer is 5' AACGCCCAAGGAAGAGTCGT 3' and finally for construct pL2B-BAR-(pKST)ASNtRieske-(pKST)YFP, the forward primer is 5' ATGGCTCAAAACTCATCCACCT 3' while the reverse primer is 5'AACACAACCAAGGTGAGTACAC 3'.

Arabidopsis stable transformants carrying the transgenes were also screened using antibiotic and/or herbicide. Plants were germinated on agar plates containing 50 μg/mL of kanamycin and 50 μg/mL of glufosinate-ammonium (BASTA; Bayer Crop Science Ltd). For seeds germinated in soil the soil was treated with 0.82 mM of glufosinate-ammonium and were watered with this until selection were obvious and seedling selected plants transplanted into individual pots. The presence of the transgene were reconfirmed by genomic DNA PCR screening. For more detail on the primers and annealing temperatures used and the amplification sizes kindly see Appendix section.

2.12 Plant DNA preparation

Genomic DNA extraction was prepared by grinding a leaf disc of about the size of a lid of a 1.5mL microcentrifuge tube. 200 µL of Extraction Buffer (200 mM Tris-HCl pH7.5, 250 mM NaCl, 25 mM EDTA, 0.5% SDS) was added to it. This was incubated for 2 min at room temperature and then spun down for 5 min at maximum speed in a conventional table top microcentrifuge. The supernatant was carefully recovered into a new tube and precipitated. Thereafter, 150 µl of isopropanol was added and mixed by inverting the tube several times. This was followed by two centrifugations for 10 min each. The supernatant was recovered and allowed to air dry (approximately 15 min). Finally the DNA was resuspended in 50 µl of TE Buffer (10 mM Tris-Cl, pH 7.5, 1 mM EDTA). This DNA was either used immediately or stored at -20°C. (protocol modified from Edwards et al., 1991).

2.13 RNA extraction

Total plant RNA was extracted from Arabidopsis and tobacco leaf samples using the NucleoSpin® RNA Plant Kit (Macherey-Nagel, Germany). Approximately 100 mg of fresh tissue was ground in liquid N_2 using mortar and pestles, and then put in 1.5 mL tubes which was used immediately or stored at -80°C for later use. RNA was then extracted according to the manufacturer's instruction.

2.14 RT-PCR

RNA transcripts were converted to cDNA using RevertAid reverse transcriptase from ThermoScientific. This was carried out following the confirmation of absence of genomic DNA in the RNA samples. The synthesis was performed by adding 1 µL of oligo dTs for each sample, 1 µg of total RNA was diluted to 11µL (RNA- free water) to make a final volume of 12 µL. The sample was heated at 65°C for 10 min and then quickly chilled on

ice for 10 min. The contents of the tube were collected at the bottom by brief centrifugation and the following added 4 μL of 5X reaction buffer, 2 μL dNTPs, 1 μL reverse transcriptase and 1 μL of water making a total volume of 20 μL. The reaction was centrifuged (30 secs) one more time and incubated at 42°C for 60 min followed by inactivation of the enzyme by incubating for 10 min at 70°C. This cDNA was used as template for PCR amplification (semiquantitative RT-PCR or qRT-PCR) immediately or stored at -20°C.

2.15 qRT-PCR

Quantitative reverse transcription PCR (qRT-PCR) reactions were performed using SYBR Green (Bio-line) detection chemistry and run in triplicate on 96-well plates (Greiner, UK) using an iCycler iQ thermocycler (Bio- Rad). Reactions were prepared in a total volume of 15 μL containing the following: 2 μL of cDNA (equivalent to 0.05 μg/μL of RNA), 7.5 μL of SensiFast SYBR taq ready mix (Bio-line) and 0.5 μL of forward and reverse primers each. Blank controls were run in triplicate for each master mix. The cycling conditions were set as follows: initial denaturation step of 95°C for 10 min to activate the polymerase, followed by 45 cycles of denaturation at 95°C for 15 s, annealing at 60°C for 30 s and extension at 72°C for 30 s. The amplification process was followed by a melting curve analysis, ranging from 60°C to 90°C, with temperature increase steps of 0.1°C every 10 s. All other parameters (baseline and threshold cycles (Ct) were automatically determined by the Bio-Rad iQ Software 3.0. The possibility of genomic DNA contamination in the qRT-PCR assays was controlled by means of RT-minus amplification reactions (for each of the RNA samples, a quantity equivalent to the cDNA used in the amplification reactions was amplified by qRT-PCR using each set of primers). The PCR efficiency was determined for each primer pair in its optimal

concentration with the DART-PCR workbook (Peirson et al., 2003), which uses fluorescence data captured during the exponential phase of each amplification reaction. All other analysis of the data collected was done using the relative expression software tool (REST) for group-wise comparison and statistical analysis of relative expression results in real-time PCR version 2009 (Pfaffl et al., 2002).

2.16 qPCR for determination of transgene copy number by iDNA genetics.

After PCR analysis were carried out to confirm the presence of the selective marker bar gene(conferring BASTA resistance) for lines deriving from transformation with the constructs, Quantitative real-time PCR was carried out by iDna genetics in order to estimate copy numbers leading to the yield of homozygous plants by method similar to (Bartlett et al., 2008). Primers from the sequence of the BAR gene (with a FAM reporter) and the internal positive control (IPC, with a VIC reporter) were amplified together in a multiplex reaction (The PCR cycling conditions were 50°C 2 minutes hold, 95°C 10 minutes (enzyme activation), 40 cycles of 95°C 15 seconds, 60°C of 60 seconds. Fluorescence from the FAM and VIC fluorochromes was measured during each 60°C cycle and the Ct values obtained. The difference between the Ct values for the BAR gene and the IPC (the DeltaCt) was used to allocate the assayed samples into groups with the same gene copy number.

PHYSIOLOGICAL AND MOLECULAR GROWTH MEASUREMENTS AND ANALYSIS

2.17 Plant growth

The *in vitro* seedling growth of Arabidopsis and wild-type tobacco plants were surface sterilized and plated on sterile agar medium containing ½ strength Murashige and Skoog incorporated with kanamycin (50 mg/ml) and BASTA (50 mg/ml). Kanamycin/BASTA-

resistant primary transformants with established root systems were transferred to soil (Levington F2, Fisons, Ipswich,UK) and allowed to self-fertilize yielding T1 progeny. Subsequent lines of interest from both Arabidopsis and tobacco were identified by PCR and iDNA technology. Wild-type plants used in this study were a combined group of WT and untransformed null segregants from the SBPase and Rieske lines verified by iDNA.

For experimental study, WT *Arabidopsis thaliana* ecotypes Columbia (Col-0) and transgenics seeds were placed in 4°C for 2 days for stratification (in order to encourage uniform germination) before moving into the growth chambers. The growth chambers conditions were maintained at 22°C at an irradiance of 130 μmol photons m^{-2} s^{-1},under short day (photoperiod of 8 h light/16 h dark, relative humidity (RD) 50% or long day conditions (photoperiod of 16 h light/8 h dark) or in the greenhouse for tobacco. Plants were transferred to individual 5cm pots for Arabidopsis and 8 cm pots for tobacco containing compost. Tobacco plants were cultivated in a controlled greenhouse environment (16 h photoperiod, 25–30/20 °C day/ night, and natural light supplemented with high-pressure sodium light bulbs, giving between 200–350 μmol m^{-2} s^{-1} (low light), 600–1 400 μmol m^{-2} s^{-1} (high light respectively). Plant positions were randomized and trays rotated daily under the light with watering done 3 times a week and an additional nutrient medium (Hoagland and Arnon, 1950) given whenever needed.

2.18 Seed sterilization

Tobacco and Arabidopsis seeds were sterilized following a modified protocol based on those described by Aronsson and Jarvis (2002) and Aronsson and Jarvis (2011). Seeds were surface sterilized by a series of washes of which they were submerged in 70% ethanol for 3 min. Following this, they were rinsed with sterile water and then submerged in 4% bleach + Tween 20 (1 drop in 50 mL) for 15 m and agitating frequently. Finally the

bleach was removed and the seeds were rinsed 3 to 5 times with sterile water. These seeds were placed on sterile filter paper inside the flow hood and allowed to air dry. Seeds were then sown on agar plates immediately or stored in the final rinse water at 4°C for stratification. Tobacco seeds were sown immediately on plates and placed in the growth chamber.

2.19 Arabidopsis plant transformation

The construct plasmids were introduced into wild-type Columbia (Col-0) Arabidopsis (*Arabidopsis thaliana*) by floral dipping using strain of *Agrobacterium tumefaciens* GV3101. The Arabidopsis plant transformation was achieved using the floral dipping method described in Clough Steven and Bent Andrew (2008). Plants were grown in growth chambers approximately 7 weeks in short day length at which time they were flowering. The first bolts were clipped to encourage proliferation of many secondary bolts and plants were dipped 10 days after this, 10 ml cultures of the strains carrying the genes of interest were grown overnight at 37°C in LB with antibiotics (rifampicin 50 μg mL-1, gentamicin 25 μg mL-1, kanamycin 50 μg/ml. These were used the next day to inoculate a 500 mL culture in a 1:100 proportion. These cultures were grown under the same conditions for approximately 24 hours until they reached stationary phase. The bacteria were then spun down (3000 g for 15–20 min) and resuspended in a 5% sucrose solution. Before dipping, 0.05% (500 μL/L) Silwet L-77 was added. Following the addition of silwet the whole inflorescences were dipped in the bacterial suspension for 2 to 3 seconds, with gentle agitation. The plants were then placed in large containers and covered with autoclave bags to maintain high humidity and left in the dark at 18°C for 16 to 24 hours. After this period, the plants were returned to the greenhouse and grown normally. The seed were harvested when dried and the transformants selected using

antibiotics (50 μg ml-1 Kn or herbicide selectable marker (0.82 mM of glufosinate-ammonium). For antibiotic selection, plants were grown on plates containing the antibiotic(s) for 10–15 days or in soil watered with glufosinate-ammonium until selection was carried out.

2.20 Tobacco plant transformation

The construct plasmids were introduced into wild-type tobacco (Nicotiana tabacum) L.cv Samsun using *Agrobacterium tumefaciens* LBA 4404 via-disc transformation (Horsch et al., 1989). Freshly transformed Agrobacterium plate was used to start a 10 ml culture and grown overnight at 28°C. The next day, 2-4 ml of the overnight culture was again used to start a 150ml culture (with antibiotics incorporated) and grown at 28° C for approximately 24h. Following this, the cells were harvested by dividing cultures into 50 ml sterile falcons and centrifuged at 3000g for 15-20 min (room temperature). Cells were suspended in same volume of liquid MS. Explants from leave tissue of 6-8 weeks old tobacco plantlets were used. Leaves explants were incubated with the Agrobacterium (10-30 min) and placed upside down (abaxial face up) onto plates (no antibiotics) after which the plates were put in growth chamber (22-14°C, 16h light) for 48 h. Leaf explants were transferred unto fresh media plates with antibiotics (50 ug ml^{-1} BASTA to select the transformed cells, and 400 ug ml^{-1} Cefotaxime to control the Agrobacterium), BAP (10mg/ml) and NAA (10mg/ml) of hormones. Explants were maintained in the growth chamber and media refreshed every 7-10 days until shoots develop. After 14-20 days, a second change of media was changed to BAP (10mg/ml) and IAA (10mg/ml) in order to facilitate growth if necessary. Once shoots have started to differentiate they were moved into tall plates (magenta pots) containing MS media plus BASTA. After the plants have developed roots, they were transferred into soil indiviodually..

2.21 Fluorescence microscopy to assess cell specific expression.

Several of the constructs were designed with a YPF cassette included. To check cell specific (guard cell specific) expression of the construct, leaf tissue from T0/T1 were subjected to high resolution chlorophyll fluorescence and confocal microscopy to detect YFP. Small (about 1/2cm) leaf samples were cut from the leaf and mounted on a slide and covered with a # 1.5 cover slip being taking care to avoid damaging the tissue. For live image acquisition, a high resolution microscopy and Nikon A1si inverted confocal microscope equipped with filters for YFP analysis were used. YFP images were acquired by exiting at 515 nm LEDs and emission collected with a band pass filter (530 ± 20 nm) for the high resolution microscope while YFP images for Nikon Alsi were acquired by exiting at 488nm with lasers and its emission collected at 530nm. Chlorophyll auto fluorescence was exited at 480 nm with emission collected at 685 nm which allowed to distinguish between the two signals. A 4X and 40X objective were used with a numerical aperture (N.A.) of 1.4.

2.22 Chlorophyll Fluorescence imaging

Chlorophyll fluorescence measurements were performed on 3-7 weeks-old of Arabidopsis plants seedlings grown in a controlled environment chamber at 130 μmol mol^{-2} s^{-1} and ambient (400 μmol mol–1) [CO_2]. Images of chlorophyll *a* fluorescence were obtained by using a CF Imager (Technologica Ltd., Colchester, UK) described by Barbagallo et al. (2003). Plants were dark adapted for 30 min before a minimal fluorescence (*F*o) measurement was obtained using a weak measuring pulse. After which a 800 ms saturating pules of 5800 μmol photons m^2 s^1 was used to capture maximal fluorescence (*F*m) and the two images used to determine the maximum quantum efficiency of PSII photochemistry (Fv/Fm = Fm-Fo/Fm). Plants were then exposed to an

actinic light of 500 μmol photons m^{-2} s^{-1} for 35 min and steady-state *F*' was continuously monitored, and a saturating pulse applied at 2 min intervals to measure maximum fluorescence in the light (*F*m'). These images were used to determine the operating efficiency of PSII (*F*q'/*F*m'= [*F*m'- *F'*] /*F*m') over time and the induction of steady state photosynthesis after which a light response curve protocol was established using the following light levels 0, 50, 100, 200, 300, 500, 750, 900, 1000,1600,2000 with Fq'/Fm' captured after 2 min at each light level. Relaxation kinetics were determined after the light response curve by turning off the light and monitoring Fv/Fm every 2 minutes until the original value of Fv/Fm had been restored.

2.23 Leaf and rosette area calculations

Chlorophyll fluorescence imaging was used to calculate the leaf areas also at the time of analysis and pictures were taken at weeks 3, 4, 5 and 7. Rosette areas were calculated by the imager.

Gas exchange analysis

2.24. A/C_i curve

The response of assimilation rate of CO_2 (*A*) to intercellular CO_2 concentration (C*i*) was determined at saturating light level (1500 μmol photons m^2 s^1) and a leaf temperature of 25 ± 1.5 °C, using a portable gas exchange system (LI-COR 6400; LI-COR, Lincoln, NE). Photosynthetic carbon fixation rates were measured at a range of CO_2 concentrations (from 0 to 1500 μmol mol for Arabidopsis). Measurements were started at ambient CO_2 concentration (*C*a; 400 μmol mol^1, at which the plants had grown) after which *C*a was decreased in four steps to 50 μmol mol^1 (400, 300, 200, 100 and 50 μmol mol^1) and then returned to near ambient levels to confirm the original rate could be

regained (again in four steps, 150, 250, 350 and 450 μmol mol^{1}). After this, the *C*a was increased step wise to 1500 μmol mol^{1} for completion of the curve in five steps (550, 700, 900, 1100, 1500 and 2000 μmol mol^{1}). The data obtained from these measurements was used to calculate the maximum carboxylation rate (Vc_{max}) and maximum electron transport flow (J_{max}) using the equations of von Caemmerer and Farquhar (1981). These values were then used to estimate Vc_{max} and J_{max} (Sharkey et al., 2007).

2.25. Dynamic and diurnal response to light of photosynthesis

The temporal response of leaf photosynthesis (*A*) and stomatal conductance (g_s) were measured to a single step change in light using plants previously adapted to dark (either predawn or 30 min dark adaptation). Leaves were first equilibrated at a PPFD of 100 μmol m^{-2} s^{-1} until both *A* and g_s reached steady state, once steady state was achieved, PPFD was increased to 1000 μmol m^{-2} s^{-1} for 1 hour and then returned to 100μmol m^{-2} s^{-1} for 30. *A* and g_s were recorded every 1min. The leaf cuvette was maintained at 400 μmol mol m^{-1} CO_2 concentration (Ca), a leaf temperature of 20ºC (±2ºC) and a VPD of 1 0. ±05 kPa.

2.26 Statistical analysis

The significance of data obtained from the image were statistically tested by one way ANOVA followed by a Post Hoc-Turkey alpha (0.05). Differences between means were also analysed using the student t-Test: sample for means where only two groups were compared (Excel 2013).

CHAPTER THREE:

EPIDERMAL-MESOPHYLL TRANSFER EXPERIMENT TO DETERMINE THE INFLUENCE OF MESOPHYLL ON STOMATAL FUNCTION AND BEHAVIOUR.

INTRODUCTION

Stomatal behaviour regulates gas exchange at the leaf atmosphere boundary determining CO_2 uptake for photosynthesis and water loss through transpiration (Willmer and Fricker, 1996) and therefore balance the supply of CO_2 for photosynthesis with transpiration for maintained plant water status and maximum plant growth (Wong, 1979). As mentioned in chapter one, stomatal opening and closing are brought about by changes in turgor pressure within the guard cells as a result of the accumulation or loss of potassium (K^+) ions and organic solutes such as malate or sucrose. Guard cells also contain chloroplasts capable of performing electron transport (Lawson et al., 2002, Lawson et al., 2003b) which could provide a source of energy (ATP) to drive stomata open or use this energy for CO_2 fixation leading to the production of sucrose as an osmotica for stomatal movements. Alternatively it has been suggested that guard cell chloroplasts could provide a signalling mechanism that enables stomatal behaviour to be co-ordinated with underlying demands of the mesophyll (Muschak et al., 1999, Poffenroth et al., 1992, Reckmann et al., 1990). It is well established that there is a high degree of coordination between the stomatal conductance and mesophyll demand for CO_2 (Wong et al., 1979) but the mechanism for this is not entirely known. The fact that stomatal responses to light intensity and changes in CO_2 concentration in guard cells of detached leaf epidermis to be different from those in the intact leaves (Mott et al., 2008a, Fujita et al., 2013, Lee and Bowling, 1992, Schwartz et al., 1988) suggesting that presence of the mesophyll greatly

influences stomatal behaviour (Mott et al., 2008, Wong, 1979, Lee and Bowling, 1992). As a result, approaches have been made in an effort to unravel the mechanisms coordinating stomatal responses with mesophyll photosynthesis using a variety of approaches.

The epidermal peel-mesophyll transfer (Mott et al., 2013, Mott et al., 2008) is one such approach designed to unravel the influence or signals from the mesophyll that may play a role in coordinating stomatal behaviour with mesophyll demand for CO_2. Epidermal–mesophyll transfer experiment, rely on removing the epidermis from one plant and placing it on mesophyll (with the epidermis removed) of another plant type or that of the same plant type but in which the mesophyll has been subjected to different environmental conditions (Mott et al., 2013, Mott et al., 2008). This novel experimental approach was the basis of the research presented in this chapter, in order to assess stomatal responses in the epidermis (where the under lying mesophyll influence is removed) and comparing it with the epidermis of a plant grafted on top of mesophyll of another plant. The aim was to determine whether the guard cells themselves have a mechanism that co-ordinate stomatal response with that of the mesophyll. In order to determine the extent of mesophyll influence on stomatal behaviour, the epidermal peel-mesophyll transfer approach exploited plants with different photosynthetic pathways which include C3 and CAM. In C3 plants, stomata open with light during the day and close at night or under conditions of high [CO_2], whilst stomata in CAM plants do the reverse; stomata opens at night for CO_2 uptake and closes during the day when the evaporative demand is high (Cockburn et al., 1979). It has often been assumed that day time stomatal closure in CAM plants is due to the high CO_2 concentration inside the leaf when the malate stored overnight is decarboxylated (Cockburn et al., 1979). Therefore using mesophyll from these two different photosynthetic types provides an ideal experimental platform to probe

the influence of the mesophyll on stomatal behaviour. Additionally, the Hartwell Laboratory in Liverpool produced transgenic CAM plants in which the expression of different key enzymes in the CAM photosynthetic pathway had been manipulated. Incorporating these plants into our experimental setup provided an additional tool kit for exploring the influence of mesophyll photosynthesis on stomatal behaviour. Before proceeding, it is important to first briefly explain CAM metabolism.

3.1. CAM metabolism

Crassulacean acid metabolism (CAM) differs from C3 photosynthesis with nocturnal uptake of CO_2 and the fixation by phosphoenolpyruvate carboxylase, PEPc (Osmond, 1978, Dayanandan and Kaufman, 1975, Borland et al., 2014). CO_2 is stored in the vacuole in the form of an organic acid, usually malic acid and decarboxylated during the day time behind closed stomata and fixed by Rubisco in the light (Nobel, 1991). CAM plants are adapted to minimise water loss and thriving in water stressed environment when evaporative demand is high. CAM plants uses water input of only 20% of that required by C_3 or C_4 crops hence are grown in areas where precipitation is typically insufficient to support C_3 or C_4 crops as well as are adapted to marginal lands which are poor naturally (Borland et al., 2011). Thus, exploring the agricultural uses of CAM species could have great potential in marginal lands where global warming continues to reduce suitable arable lands due to limited water resources availability (Borland et al., 2014). Hence, engineering CAM metabolism into C3 might be of great potential towards increasing greater plant water use efficiency in the future (Franco et al., 1999). Since the understanding of the mechanism between CO_2 assimilation rate and stomatal conductance is still a challenge, a high demand to model global CO_2 and water exchange has become a necessity thereby putting CAM species into the light. CAM species can and may

therefore be used as model experimental system to examine stomatal responses through their varying photosynthetic biochemistry (von Caemmerer and Griffiths, 2009a).

The main enzymes used for CO_2 fixation and the pathway of CO_2 fixation differ between C3 and CAM plants. Atmospheric CO_2 fixation in CAM plants occurs at night via phosphoenolpyruvate carboxylase (PEPc) and malate dehydrogenase (MDH), generating malate, which is stored as malic acid in the vacuole. During the day malic acid is released from the vacuole and decarboxylated by decarboxylases enzymes (e.g. NAD- Malic enzyme or phosphoenolpyruvate carboxykinase PCK (Dever et al., 2015). The release of CO_2 behind closed stomata is fixed by Rubisco in the Calvin cycle and the high concentrates CO_2 at the site of Rubisco acts as a temporal concentrating mechanism. Pyruvate orthophosphate dikinase (PPDK) is one of the enzymes that catalyze two key steps during light-period malate decarboxylation that occurs during secondary CO_2 fixation in some Crassulacean acid metabolism (CAM) species. The by product from decarboxylation, pyruvate is recycled by the enzymes pyruvate orthophosphate dikinase (PPDK)(Borland et al., 2009).

CAM photosynthesis can be distinguished by four phases (Osmond, 1978). Phase one is fixation of atmospheric CO_2 by PEPc to form malic acid which is stored in the vacuoles, often referred to as nocturnal acidification. Phase two is the transition phase of CO_2 fixation by PEPc to fixation by Rubisco which can occur in the early mornings if the plant is not too water stressed and the stomata are able to open a little. Malic acid is decarboxylated during the light period to release CO_2 internally for re-fixation by Rubisco during phase three which light driven electron transport provides the energy and reductant for this process. The final phase IV occurs late in the photoperiod when stomata may reopen (depending on plant water status) and C3 photosynthesis by Rubisco can occur (Fig.3.1) (Cushman and Bohnert, 1999).

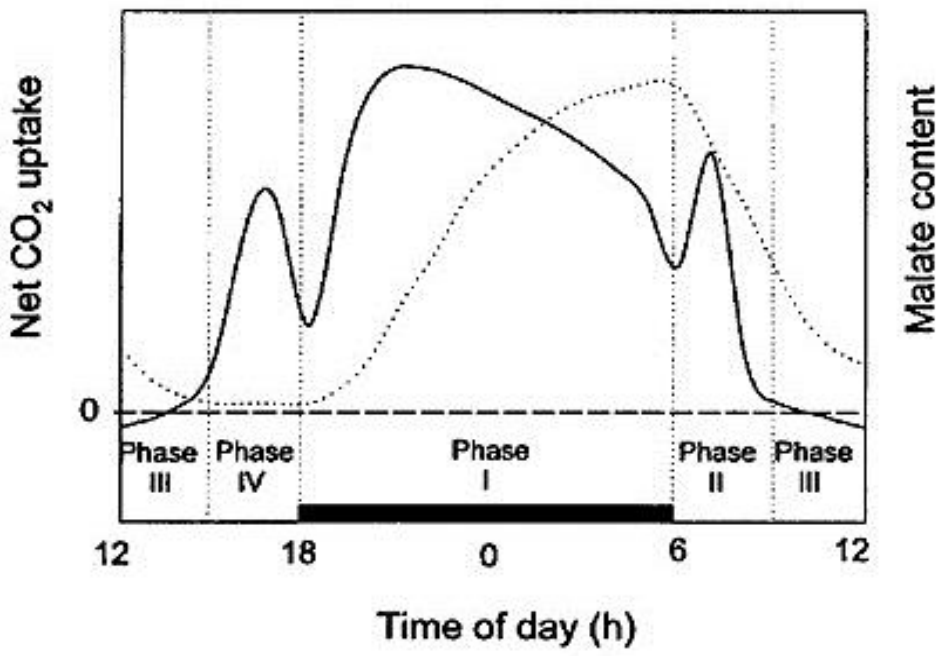

Figure 3. 1. Phases of CAM metabolism showing net CO_2 uptake and malate content. Phase 1 as indicated above occurred during the hours of the night when CO2 is stored in the form of malic acid indicated by dark bar, Phase II occurs early mornings which is the transition from PEPc to Rubisco while phases III occurs in the afternoon when malate is decaboxylated to CO2 and phaselV occurs late evenings when C3 photosynthetic mechanism is displayed. Dotted lines represent malate content and normal line represent CO2 content. Typical CAM metabolism exhibits strictly phases I &III (opening in the night and closure in the light),(copied from Cushman and Burnant, 1999).

Aims

The overall aim of the work in this chapter was to determine the influence and presence of mesophyll on stomatal function and behaviour. The approach used epidermal peels from different plant material either in isolation or grafted onto mesophyll from the same or different plants and subjected these to changes in light intensity and CO_2 and assess stomatal response.

Hypotheses

- Stomatal responses to changes in light intensity and [CO_2] will be different in epidermal peels where the influence of the mesophyll has been removed compared with stomatal responses in intact leaves, suggesting a mesophyll-derived signal.
- Stomatal responses to changes in light and [CO_2] in CAM plants will be different to those in C3 plants with stomata of C3 plants opening in the light and closing in the dark whilst CAM plants close during the light period and open in the dark.
- Altering CAM photosynthesis through transgenic manipulation in the pyruvate orthophosphate dikanase (PPDK) will influence stomatal responses to light and CO_2.

Objectives:

- To characterize stomatal responses in intact leaves and epidermal peels (where the influence of the mesophyll has been removed) of *Vicia faba* and *Kalanchoë fedtschenkoi* to changes in light intensity and CO_2 concentration using a specially designed environment control chamber attached to a microscope.
- Explore the co-ordinated responses between stomatal behaviour and the underlying mesophyll in C3 and CAM plants using epidermal-mesophyll transfer experiment and determine the influence of mesophyll driven signals on stomatal behaviour.
- Use infra-red gas analysis to examine the effect of irradiance and CO_2 concentrations on mesophyll photosynthesis and stomatal conductance in CAM species *Kalanchoë fedtschenkoi*, the C3 species *Vicia faba* and in transgenic CAM species of pyruvate phosphodikanase (PPDK)

3. 2. Materials and Methods

In addition to the general materials and methods chapter and for clarity purposes, this section will have its own separate materials and method.

3.2.1 Plant material and growth conditions

Seeds of broad bean *Vicia faba L*. (long pod) were planted in pots containing commercial potting soil (seed and modular compost plus sand, (Levington F2, Fisons, Ipswich, UK). The compost contained the following nutrient composition N:144; P:73; K:239. Plants of *V. faba* and *Kalanchoë fedtschenkoi* were grown in a controlled growth chamber (F1-totron PG660, Sanyo Gallenkamp Plc) at 64% humidity and temperature 23-24°C under photoperiod of 12hrs PPFD (380-400 µm of light) using halogen quartz iodide lamps (Powerstar HQ1-TS 250 W/NDL, Osram, Munich) and 12 hrs of darkness at 19°C for 1-5 weeks and watered 2-3 times weekly.

Wild type CAM, *Kalanchoë fedtschenkoi* and transgenic PPDK (ortholog of At4g15530) were grown under the same conditions as above but watered once weekly. Wild type *Kalanchoë fedtschenkoi* and transgenic (PPDK) plants were propagated from leaf margin adventitious obtained from the University of Liverpool which were later transferred to soil (same as the compost for *V.faba*). Plants were initially grown in greenhouse environment (16 h photoperiod, 25–30/20 °C day/ night, and natural light supplemented with high-pressure sodium light bulbs, giving between 200–350 µmol m^{-2} s^{-1} (low light), 600–1 400 µmol m^{-2} s^{-1} (high light) respectively). Prior to all experiments, plants were transferred and remained for 14 days in a climate-controlled plant growth cabinet as described above for the *Vicia* in order to acclimate.

Two growth chambers were used for growing the plants. One chamber was programmed for the lights to come on at 9 am and switched off at 9 pm and from here on, this will be referred to as light/standard chamber, whilst the second chamber was programmed with

lights coming on at 9 pm and going off at 9 am and from here on will be referred to as the dark/reverse chamber. Using both these chambers enable plant material to be selected from the complete diel period.

3.2.2 Peeling method of plant material and incubation medium

Fully expanded leaves were excised from the plant and placed on a glass slide and cut with a razor blade into lamina strips (between the major veins on the leaf in order to avoid the peels being contaminated by mesophyll). A tab was made on the lamina by cutting through the upper epidermis without damaging the lower epidermis. The leaf section was turned over and the epidermal strips were peeled manually from the lower surface (abaxial) using the tab of the leaf according to the method of Weyers and Travis, 1981. For measurements on isolated epidermal peels the peel were placed directly in incubation buffer. The incubation medium of 50mM KCL+10mM PIPES-KOH (pH 6.8) was prepared freshly each day (Weyers and Meidner, 1990). For epidermal-mesophyll experiments, peels were removed from the mesophylls and placed back onto mesophyll with the epidermis removed from a leaf of the same species or a different species or mutant. Control leaf segments were prepared from intact detached leaves cut into 1 x 1 cm square and the abaxial side viewed directly. All plant materials were kept hydrated with incubation medium and inside the chamber.

3.2.3 Experimental setup of the novel epidermal-mesophyll transfer

The sample chamber consisted of two aluminium blocks mounted on a purpose built microscope stage. An aperture on the top of the chamber was allowed entry of the long-distance objective (x40, Leica Ltd). A condom with the tip removed was mounted around the circumference of the aperture and attached to the objective to gas seal the chamber. Gas conditions in the chamber were controlled using a setup that consisted of two large cylinders (CO_2-free air) and (10% CO_2 air) passed through a mass flow controller (EL-

flow, Bronkhorst high tech, New Market UK) used to provide air containing the selected CO_2 concentration at a flow rate of 200 ml min^{-1}. Licor (L1-820, Licor Biosciences, Lincoln, Nebraska) was used to monitor the concentrations of CO_2 inside the incubation chamber as well. Chamber temperature was controlled by a circulated cooler that maintained the temperature at 23°C. The plant material was placed in the chamber and subjected to different light intensity of either 0 µmol $m^{-2}s^{-1}$ and 400 µmol $m^{-2}s^{-1}$ and CO_2 concentration was maintained at either (120 µmol mol^{-1} and 650 µmol mol^{-1}). The protocol used were as follows : light intensity of PPFD (400 µmol m^{-2} s^{-1}) + [CO_2] (120 µmol mol^{-1}) were first applied for a period of 1 hour with continuous monitoring and recording of stomatal sizes (after 5-10 mins) after which it was changed to darkness + [CO_2] of 120 µmol mol^{-1} for another 1 hour, and then returned back to the initial conditions of PPFD (400 µmol m^{-2} s^{-1}) + (120 µmol $mol^{-1)}$ for an hour. Again light intensity of PPFD (400 µmol m^{-2} s^{-1}) + high [CO_2] of 650 µmol mol^{-1} were applied for another hour then finally, PPFD (400 µmol m^{-2} s^{-1}) + [CO_2] of 120 µmol mol^{-1}were applied for the last hour.

Stomatal apertures were measured using a (Leica DMRX Leitz 567030 Wetzler Germany) with a long focal objective lens (50X). The epidermal peels were kept from drying out by placing a tube connected to a syringe and inserted into the chamber and buffer dropped into the system at a rate of 1 drop per min. Digitalised photo images of stomata were obtained using image-analysis hardware and software (Bresser Microcam 5.0MP GmbH & Co Gutenberger Rhede-Germany) connected to a computer where the measurements were recorded every 5-10 min over the 5-7 h measuring period. Below, Fig. 3.2 is a schematic diagram of the experimental set up.

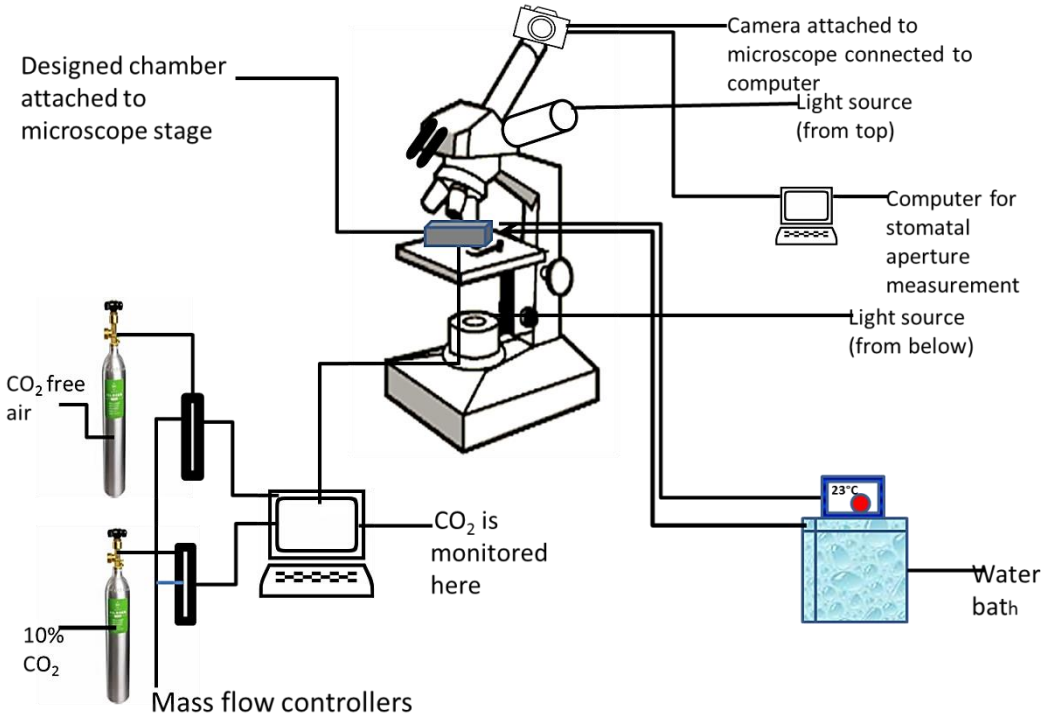

Figure 3.2. Experimental setup of the novel epidermal-mesophyll transfer. A schematic diagram illustrating the set up consisting of aluminium chamber mounted on a microscope stage. Gas conditions consisting of two large cylinders (CO_2-free air) and (10% CO_2 air) passed through a mass flow controller. A computer system installed with the mass flow controllers software or Licor was used to monitor the concentrations of CO_2 inside the incubation chamber. Chamber temperature was controlled by a circulated cooler that maintained the temperature at 23°C. Digitalised photo images of stomata were obtained using image-analysis hardware and software connected to a computer. Top and bottom light sources used to give light at desired intensity.

3.2.4 Gas exchange experiments

Attached leaves from whole plants of *Vicia faba* and *Kalanchoë fedtschenkoi* (wild type and transgenic) were used to measure carbon assimilation (*A*) and stomatal conductance (g_s) in response to change in light and CO_2 concentrations following a similar protocol used for the epidermal peel transfer experiments. Measurement were made using a portable gas exchange system (CIRAS 2, PP systems, Hitchin, Hertsfordshire,UK) and recorded every 1 min for 5 h using the same protocol as the one in the experimental set up.

3.2.5 Statistical Analysis

The data are shown as means of ± SE of five independent experiments and differences between means were analysed using the student t-Test: sample for means.

RESULTS

3.3. Diel stomatal responses in isolated epidermis and whole leaves.

Diel stomatal behaviour were assessed in both isolated epidermal peels incubated in buffer and whole attached plant leaves using gas exchange in both the C3 plant (*Vicia faba*) and wild CAM as well as the transgenic CAM manipulated in levels of PPDK with 5% of the wild-type.

3.3.1 Diel stoma behaviour in C3 and CAM (WT and PPDK) plants

The diel stomatal response in C3 and CAM epidermal peels isolated from the mesophyll were determined by measuring the aperture of individual stoma (taken from new peel at each measurement over the course of a day. The stomatal response in *Vicia faba* over the diel period (Fig.3.3) displayed a typical and expected pattern of stomatal behaviour, consistent with previous observations in many C3 plants. Stomata opened in the light during the diurnal period and closed in the dark. Stomatal aperture increased through the diurnal light period and reached a maximum aperture of around 20.8 µm after 6 hours at 300 µmol m^{-2} s^{-1} PFPD. When light was switch off at the end of the diel period stomatal aperture reduced rapidly reaching a minimum value of 7.6 µm almost immediately which was generally maintained through the nocturnal period albeit with some fluctuation in the aperture.

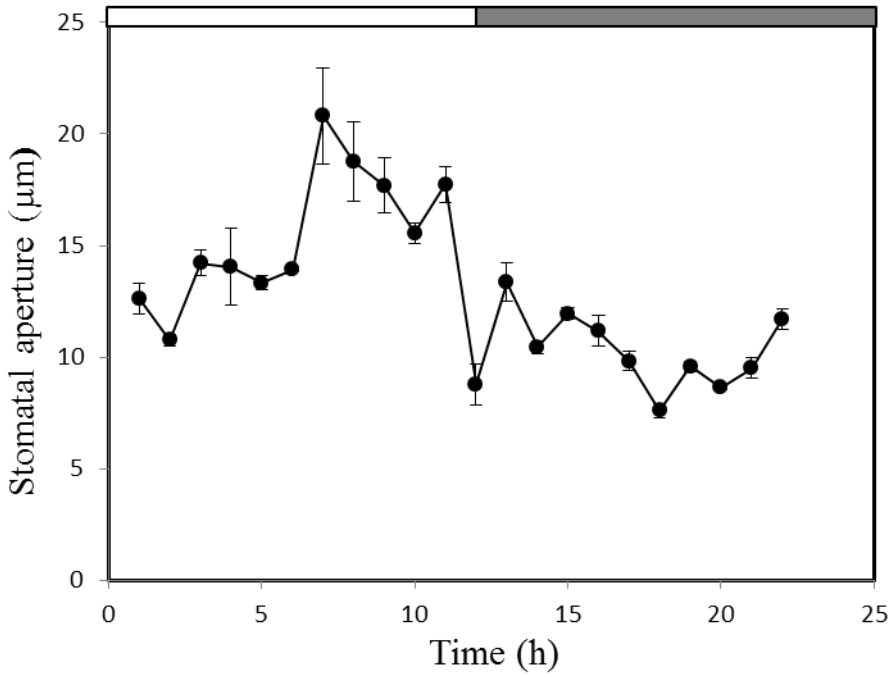

Figure 3. 3. Diel stomatal aperture in *Vicia faba.* Measurements were taken from individual stoma of a leaf segment of biological replicates. The leaf sections placed in a specially designed gas chamber to control the conditions during measurements. Chamber conditions maintained at [CO_2] of 400 µmol mol^{-1} and photosynthetic photon flux density (PPFD) of 400 $\mu mol^{-2}s^{-1}$. Stomatal measurement were taken every hour. White and black boxes represent light and dark respectively. Values are means of five replicates (± SE).

Wild CAM (*Kalonchoe fedtchenkoi*) also displayed a typical pattern for CAM plants, with opposite responses to those observed in the C3 plant. Stomatal opening during the nocturnal phase of the diel period, and closed in the light over the diurnal period. The greatest stomatal aperture of 5.6 µm was recorded after 4h into the dark period, whilst the lowest stomatal aperture of 3.0 µm was observed after 3 hrs in the light period. It was also observed in general that stomatal apertures in *Vicia faba* were greater than those observed in *Kalanchoë fedtschenkoi* (Fig 3.4a).

However, the stomatal behaviour in the transgenic CAM plants manipulated in pyruvate phosphodikanase (PPDK) on Fig 3.4b displayed a more varied and somewhat different pattern compared with the WT CAM plants with similar apertures observed in both the nocturnal and diurnal periods. Stomata opened during both periods with the highest stoma

aperture of 4.3 µm recorded after 4h into the dark period and of 4.5 µm in the light respectively, whilst the lowest stomatal aperture of 1.7 µm was observed after 3 hrs in the dark period and 2.7 in the light period.

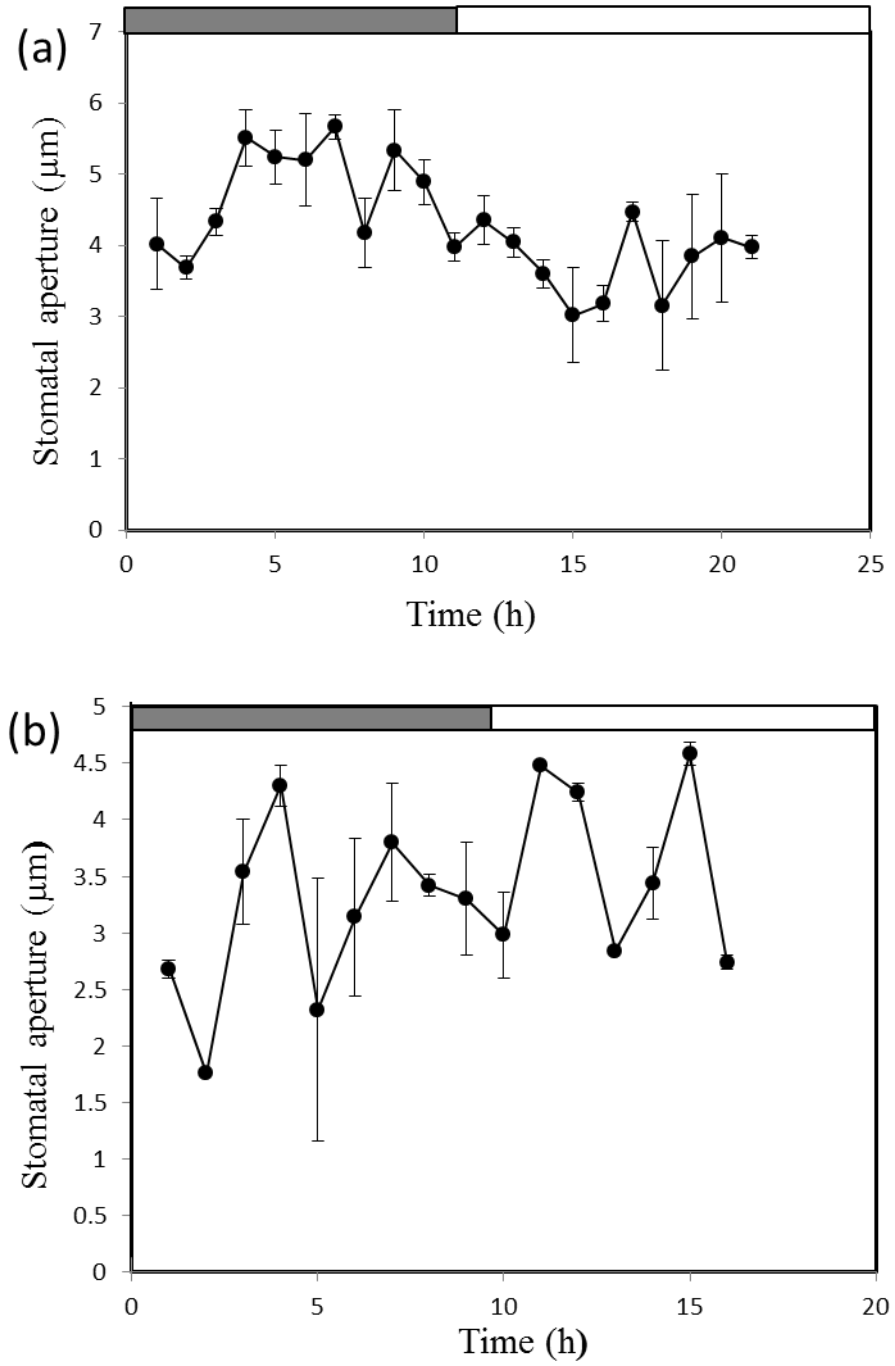

Figure 3. 4. Diel stomatal aperture in (a) WT CAM and (b) CAM pyruvate orthophosphate dikinase (PPDK). Measurements were taken from individual of leaf segments of biological replicates. The leaf sections were placed in a specially designed gas chamber to control the conditions during measurements and conditions maintained at [CO_2] of 400 µmol mol^{-1} and photosynthetic photon flux density (PPFD) of 400 $\mu mol^{-2}s^{-1}$. Stomatal measurement were taken every hour. White and black boxes represent light and dark respectively. Values are means of five replicates (± SE).

3.3.2 Diel whole leaf gas exchange in C3 and CAM (WT and PPDK) plants

The diel whole leaf gas exchange measurements enabled both CO_2 assimilation rate (*A*) and stomatal conductance (g_s) to be determined in *Vicia faba* (C3), wild type CAM and transgenic CAM, (PPDK).

In *Vicia faba* (C3) (Fig. 3.5), photosynthetic carbon fixation rate increased during the diurnal period reaching values of *Ca.* 8 and 12 µmol m^{-2} s^{-1} in the reverse and standard illumination cabinet respectively. In the dark/reverse cabinet, this rate was maintained for the majority of the diurnal period, however *A* in the light/standard illumination cabinet initially was greater than that of the dark/reverse growth cabinet and decreased half way through the diurnal period dropping to a value similar to the dark/reverse cabinet around 8 µmol m^{-2} s^{-1}. Stomatal conductance follows a similar pattern, increasing the light to a maximum value of about 300-400 mmol m^{-2} s^{-1} at the start of the light period before gradually decreasing over the course of the diurnal period (Fig 3.5b &d). However, in the dark, as expected no photosynthetic activity took place and stomatal conductance remained relatively low with an average nigh-time stomatal conductance of 40 mmol m^{-2} s^{-1}. Similar patterns of g_s and *A* were observed in plant grown in either the standard or reverse light cabinets illustrating that the different cabinet did not affect the growth of the plants or the diel pattern of gas exchange which also showed the coordination between *A* and g_s.

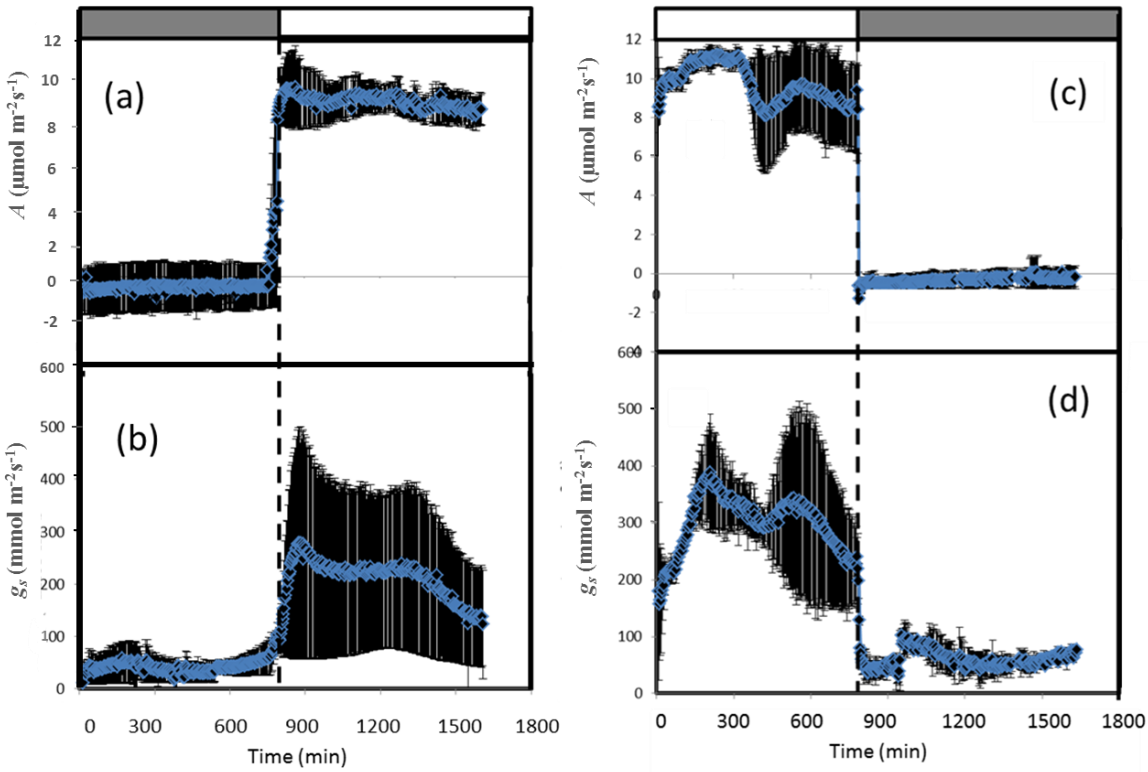

Figure 3. 5. Diel whole leaf gas exchange measurements of *Vicia Faba* (a) photosynthetic carbon assimilation rates and **(b)** stomatal conductance in reverse cabinet and **(c)** Photosynthetic carbon assimilation rates and **(d)** stomatal conductance in standard cabinet of *Vicia faba* plants. The chamber conditions maintained [CO_2] of 400 µmol mol^{-1} and photosynthetic photon flux density (PPFD) of 400 $\mu mol^{-2}s^{-1}$. White boxes represent light (400 µmol $m^{-2}s^{-1}$) while grey boxes represent darkness. Dotted lines separate light and dark period. Data are means of five replicates (± SE).

However, the diel measurements of gas exchange in *Kalonchoe fedtschenkoi* (CAM) were completely different to those of the C3 plants (Fig 3.6). Photosynthetic carbon fixation rate increased during the nocturnal period reaching values of 3.8 and 5.2µmol m^{-2} s^{-1} in the light/standard and dark/reverse illumination cabinet respectively. Following the peak *A* decreased for the remainder of nocturnal period reaching zero µmol m^{-2} s^{-1} in both cabinets by the end of the dark period. However there was a slight increase in *A* observed in some part of the diurnal period reaching a value of 1.8 and 1.6 µmol m^{-2} s^{-1} in the standard and reverse cabinets respectively. Stomatal conductance follows a similar pattern, increasing to a maximum value of about 25-35 mmol m^{-2} s^{-1} in the dark period before gradually decreasing over the course of the diurnal period (Fig 3.6b &d).

However, in the light as stomatal conductance remained relatively low with an average day-time stomatal conductance of 10-15 mmol m^{-2} s^{-1}. Similar patterns of g_s and A were observed in plant grown in either the standard or reverse light cabinets illustrating also that the different cabinet did not affect the growth of the plants or the diel pattern of gas exchange. Rates of A and g_s were much lower than those observed in the C3 plants.

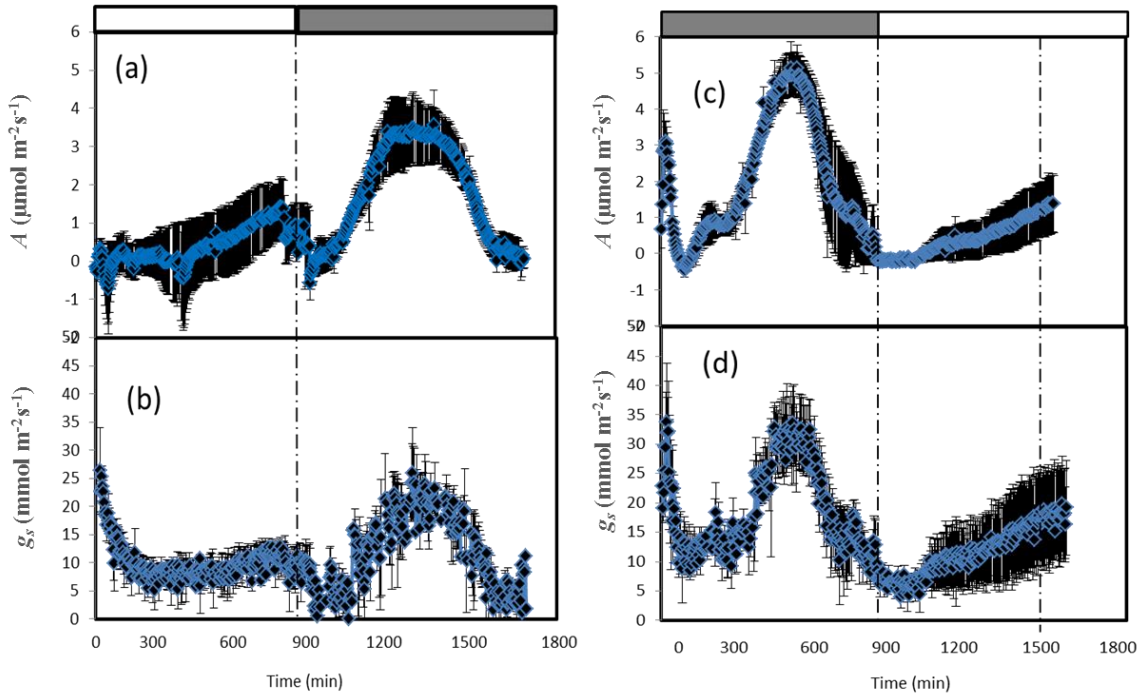

Figure 3. 6. Diel whole leaf gas exchange measurements of WT CAM (a) Photosynthetic carbon assimilation rates and **(b)** stomatal conductance in standard cabinet and **(c)** Photosynthetic carbon assimilation rates and **(d)** stomatal conductance in reverse cabinet of wt CAM plants. The chamber conditions maintained [CO_2] of 400 µmol mol^{-1} and photosynthetic photon flux density (PPFD) of 400 µmol $^{-2}s^{-1}$. White boxes represent light (400 µmol $m^{-2}s^{-1}$) while grey boxes represent darkness. Data are means of five replicates (± SE).

However, the effect of diel CO_2 concentration of 400 µmol mol^{-1} and photosynthetic photon flux density (PPFD) of 400 µmol $^{-2}s^{-1}$ on stomatal responses in the transgenic PPDK did not utilize the same core WT CAM diel response over either in the nocturnal or diurnal period (Fig 3.7).

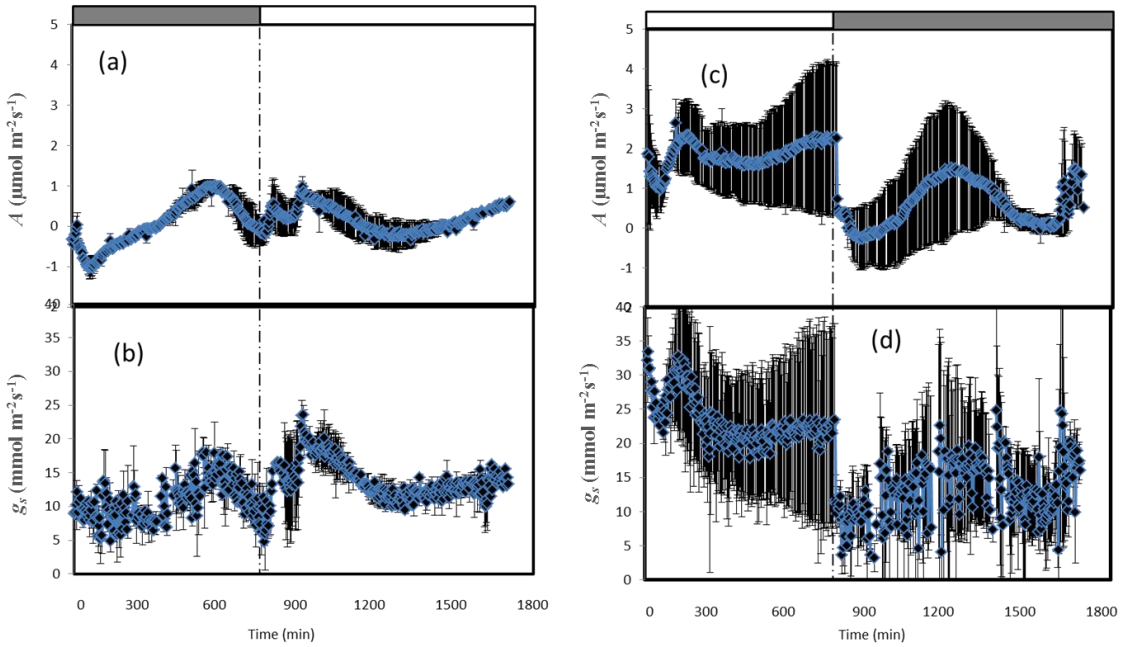

Figure 3. 7. Diel whole leaf gas exchange measurements of pyruvate orthophosphate dikinase (PPDK). (a) Photosynthetic carbon assimilation rates and **(b)** stomatal conductance in reverse cabinet and **(c)** photosynthetic carbon assimilation rates and **(d)** stomatal conductance in standard cabinet of PPDK CAM (*Kalonchoe fedschenkoi*) plants. The chamber conditions maintained [CO_2] of 400 µmol mol^{-1} and photosynthetic photon flux density (PPFD) of 400 µmol $^{-2}s^{-1}$. White boxes represent light (400 µmol $m^{-2}s^{-1}$) while grey boxes represent darkness. Dotted lines separate light and dark period and data are means of five replicates (± SE).

The photosynthetic carbon fixation rate displayed a somewhat different pattern from the typical CAM wild type plants and similar responses were observed in both the nocturnal and daytime periods. Stomata opened during both periods with the greatest stoma aperture of 1.0µmol m^{-2} s^{-1} recorded in the reverse cabinet whilst the lowest stomatal aperture of -0.5µmol m^{-2} s^{-1} was observed. In the standard cabinet, stomata also opened during both periods with the greatest stoma aperture of 2.5 µmol m^{-2} s^{-1} recorded whilst the lowest stomatal aperture of 0.0µmol m^{-2} s^{-1} was observed. Rates of stomatal conductance mirrored the pattern of *A* although the values of g_s were much lower than those observed in CAM wild type.

3.4. Functional stomatal responses to changes in light and [CO2] in isolated epidermal peel, epidermal-mesophyll transfer, detached and whole leaf gas exchange

Despite the fact that guard cells can photosynthesize on their own, the accumulation of mesophyll-derived metabolites act as signals which contribute to the regulation of stomatal movement (Lee and Bowling, 1993, Mott et al., 2013, Mott et al., 2008a, Daloso et al., 2017). It has long been hypothesized that the breakdown of starch, sucrose and lipids is an important mechanism during stomatal opening, which may aid in the production of ATP through glycolysis. Accumulation of osmolytes such as sugars and malate have been suggested to acts as signalling components that connect mesophyll photosynthesis with stomata or guard cell behaviour (Gotow et al., 1988a, Poffenroth et al., 1992a, Wong et al., 1979).

3.4.1. Funtional stoma response in epidermal peel, epidermal-mesophyll transfer and detached leaf in Vicia faba, WT CAM and PPDK

In this section, stomatal function in responses to light and [CO_2] were examined in epidermal peels in which the influence of the mesophyll has been removed and in material in which peels have been grafted onto mesophyll tissue from either the same plant or a different species (Fig 3.8).

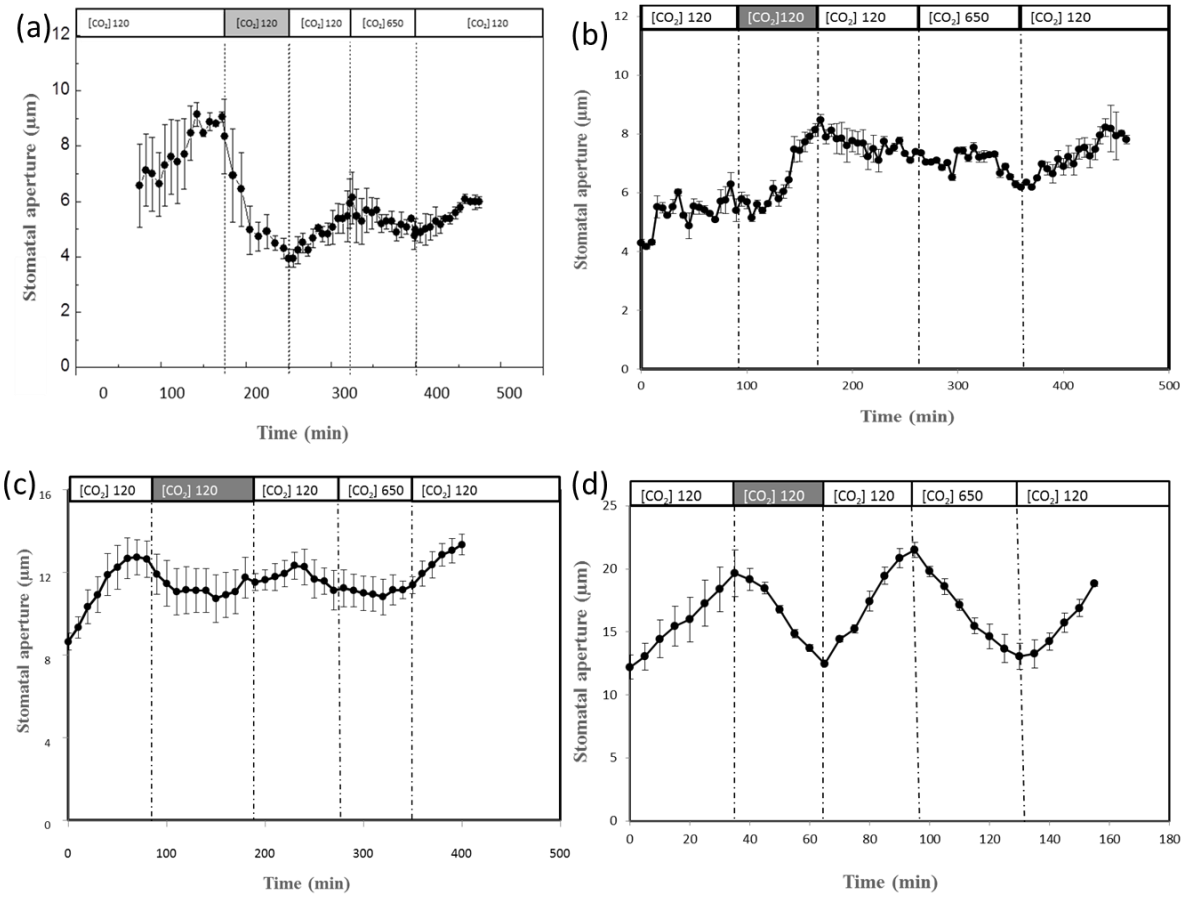

Figure 3. 8. Stomatal response to change in PPFD and CO_2 concentration in C3 and CAM (a) epidermal peel of *Vicia faba;* **(b)** epidermal peels of *Kalonchoe fedschenkoi***;(c)** epidermal-mesophyll experiment of *Vicia faba* strip grafted on CAM mesophyll and (d) whole detached leaf of *Vicia faba*. Stomata responded significantly to all conditions as indicated in the graph **(d).** The chamber conditions were maintained at the following: light/ [CO_2] of 120 µmol mol $^{-1}$: Dark/[CO_2] of 120 µmol mol $^{-1}$ light/ [CO_2] of 120 µmol mol $^{-1}$: light/[CO_2] of 650 µmol mol^{-1} and light/ [CO_2] of 120 µmol mol^{-1}. White and dark boxes represent light (400 µmol $m^{-2}s^{-1}$) and dark respectively. Dotted lines represent change from one light level/[CO_2] to another. Data are means of five replicates (± SE).

Fig. 3.8a shows the result of an isolated epidermal peel of *Vicia faba.* Stoma opened with 400 µmol $m^{-2}s^{-1}$ light and a [CO_2] of 120 µmol mol^{-1} reaching a maximum aperture of about 9.0µm. When light was turned off aperture decreased significantly to 3.9 µm by the end of the dark period. Stomatal aperture was restored to about 6. 0 µm when light turn

back on. When [CO_2] was increased a small decrease in aperture was observed which increased when CO_2 was returned to the low concentration of 120 µmol mol^{-1}.

Stomata in CAM epidermal peels responded to light by opening aperture reaching a maximum aperture of 8.4 µm by the end of the dark period (Fig. 3.8b). When the light was turned off stomata closed a little reducing aperture to 7.2 um, and this decrease in aperture continued when CO_2 concentration was increase to 650 µmol mol^{-1}. However, when the CO_2 concentration of the air being bubbled into the buffer was decreased from 650 µmol $mol^{-1}$to 120 µmol mol^{-1} , stomata responded by increasing aperture.

When the epidermal peel from *Vicia faba* was grafted on to the mesophyll from a CAM plant (Fig. 3.8c), stomata opened during the first hour of the experiment in the light with aperture reaching 12.6µm. When light was removed stomatal aperture decreased slightly to about 10µm. However no significant changes in aperture were apparent when CO_2 concentration was increased although an increase in aperture from 10.8µm to 13.0 µm was observed when [CO_2] was changed from high CO_2 concentration of 650 µmol mol^{-1} to low CO_2 concentration of 120 µmol mol^{-1}.

The stomatal behaviour in a detached leaf of *Vicia faba* (Fig.3.8d,) clearly demonstrates large stomatal responses to all the conditions of light and darkness, low and high CO_2 concentrations. Stomata within two and a half hours demonstrated the pattern shown in Fig.3.8d due to the rapid response to change in light and CO_2 concentrations (opening and closing respectively). Within 30-35 min, stomata reached a significant aperture of 19.6µm and responded to darkness by reducing significantly aperture to 12.4µm. When the light was resumed, stomata opened reaching an aperture of 21.4 µm after 90 min. When [CO_2] was increased to 650 µmol mol^{-1} stomatal aperture decreased to 13.0 µm. Changing [CO_2] back to the original level of 120 µmol mol^{-1} resulted in a rise in aperture significantly to 18.8 µm.

Fig. 3.9 below shows the stomatal movement during the detached leaf experiment.

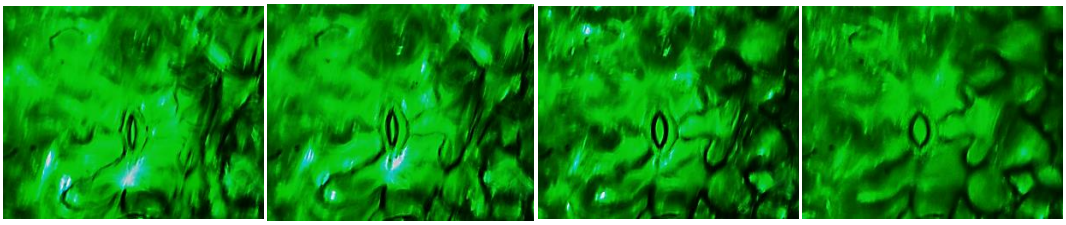

Figure 3. 9. Influence of mesophyll to individual stoma opening. Slides of increasing stoma opening in the detached leaf of *Vicia Faba* after every 5 mins (refer to Fig 3.7d above) in controlled environment chamber. Condition were maintained at PPFD of 400 µmol $m^{-2}s^{-1}$ and [CO_2] of 120 µmol mol^{-1}.

3.4.2 Stomatal and photosynthetic responses in Vicia faba, WT CAM and transgenic CAM (PPDK) plants in response to changes in light and CO_2 concentrations.

Functional whole leaf plant gas exchange analysis was performed on the same plants used above in the epidermal peel-mesophyll experiment in order to assess if g_s responded in a similar manner as individual stoma. Carbon assimilation (*A*) in the light/standard cabinet (Fig. 3.9a) where plants were subjected to 12 h of dark prior to the gas exchange measurements ranged between 3.5-3.9 µmol CO_2 $m^{-2}s^{-1}$ (highest value) at [CO_2] of 120 µmol mol^{-1} $m^{-2}s^{-1}$ and in the light while lowest value was around -1.8 µmol CO_2 $m^{-2}s^{-1}$ in the dark. However, when [CO_2] was increased to 650 µmol mol^{-1} $m^{-2}s^{-1}$, as expected *A* increased, reaching about 16.6 µmol CO_2 $m^{-2}s^{-1}$.

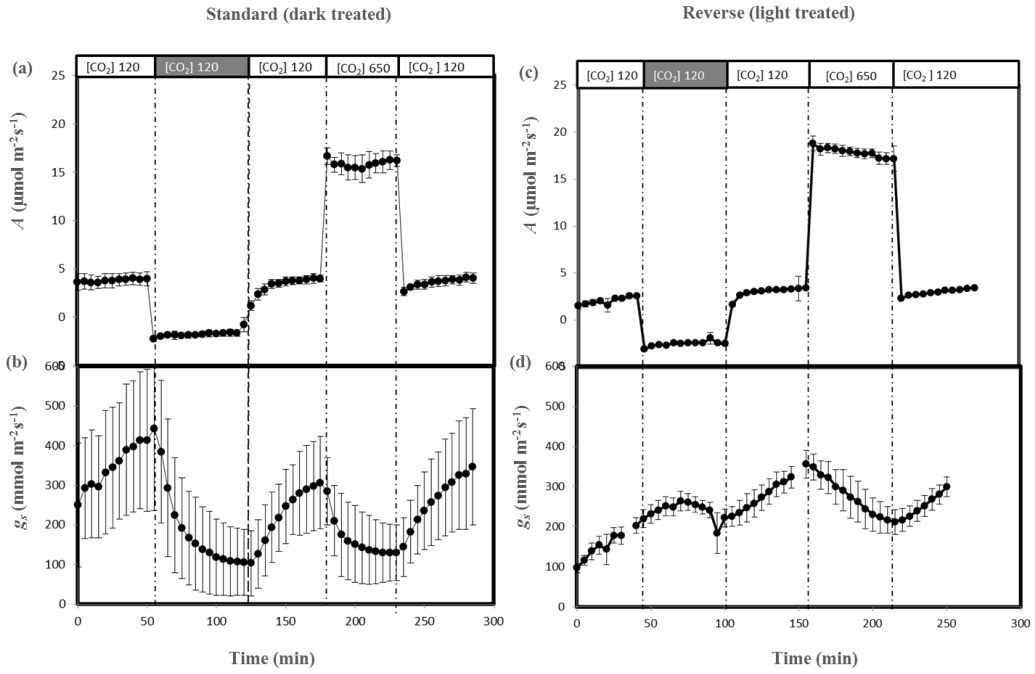

Figure 3. 10. Gas exchange measurements in *Vicia faba* (a) Photosynthetic carbon assimilation rates and **(b)** stomatal conductance of *Vicia faba* subjected to 12 hr darkness prior to experiment from the standard cabinet while **(c)** carbon assimilation and **(d)** stomatal conductance subjected to 12 hr light from the reverse cabinet in response to changes in Photon flux density (PPFD) and [CO_2] as indicated. The chamber conditions were maintained at light/ [CO_2] of 120 µmol mol $^{-1}$: Dark/[CO_2] of 120 µmol mol $^{-1}$: light/ [CO_2] of 120 µmol mol $^{-1}$: light/[CO_2] of 650 µmol mol^{-1} and light/ [CO_2] of 120 µmol mol^{-1}. White and dark boxes represent light (400 µmol m^{-2}s^{-1}) and dark respectively. Dotted lines represent change from one light level/[CO_2] to another. Data are means of five replicates (± SE).

Similarly, in the dark/reverse cabinet where plants were subjected to 12 h of light prior to the gas exchange measurements. *A* ranged between 2.5-3.3 µmol (highest value) at [CO_2] of 120 µmol mol^{-1} m^{-2}s^{-1} and in the light while lowest value was around to -2.4 µmol CO_2 m^{-2}s^{-1} in the dark. Increasing [CO_2] to 650 µmol mol^{-1} increased *A* to 18.7 µmol m^{-2}s^{-} (Fig 3.9c). Stomatal conductance (g_s) in both cabinets responded very similar and mirrored the pattern of *A*. Although the pattern in behaviour are similar, there are situation where it is obvious that g_s responded to changes in light intensity and [CO_2] more slowly or with lags that resulted in a non-coordinated response. For example the increase in g_s in the first phase (initial 50 min at the beginning) of the response in Fig. 3.10 b, whilst *A* remains

stable (Fig. 3.10 a), had reached its steady state, g_s was still increasing showing that the diel correlation between A and g_s can be perturbed by modulation of the length of light or dark phases as experienced in the short term (Hennessey and Field, 1991). It is also interesting to note that g_s continued to increase even while in the dark (Fig. 3.10d).

Similar experiment performed on the CAM plants from the two different cabinets showed the effect of nocturnal and diurnal period on both A and g_s (Fig. 3.11). The gas exchange result of carbon assimilation and stomatal conductance in response to change in light intensity and [CO_2] in the wild CAM showed a distinct difference between the plants grown in the two different cabinet in which they were subjected to either 12 h of darkness in the light/ standard cabinet prior to experiment or 12 h light in the dark/ reverse cabinet prior to the analyses.

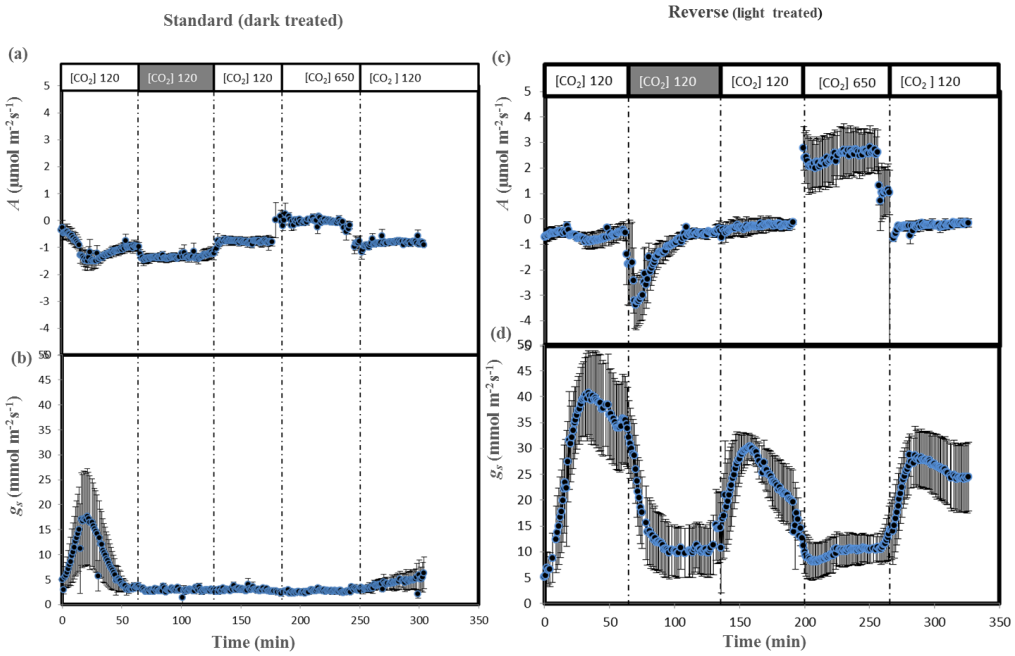

Figure 3. 11 Gas exchange measurements of WT CAM (a) photosynthetic carbon assimilation rates and **(b)** stomatal conductance of plants grown in the standard cabinet subjected to 12 h darkness prior to experiment while **(c)** carbon assimilation and **(d)** stomatal conductance from WT CAM from the reverse cabinet subjected to 12 h of light prior to measurements. The chamber conditions were maintained at the following: light/ [CO_2] of 120 µmol mol $^{-1}$: Dark/[CO_2] of 120 µmol mol $^{-1}$ light/ [CO_2] of 120 µmol mol $^{-1}$: light/[CO_2] of 650 µmol mol^{-1} and light/ [CO_2] of 120 µmol mol^{-1}. White and dark boxes represent light (400 µmol m^{-2}s^{-1}) and dark respectively. Dotted lines represent change from one light level/[CO_2] to another. Data are means of five replicates (± SE).

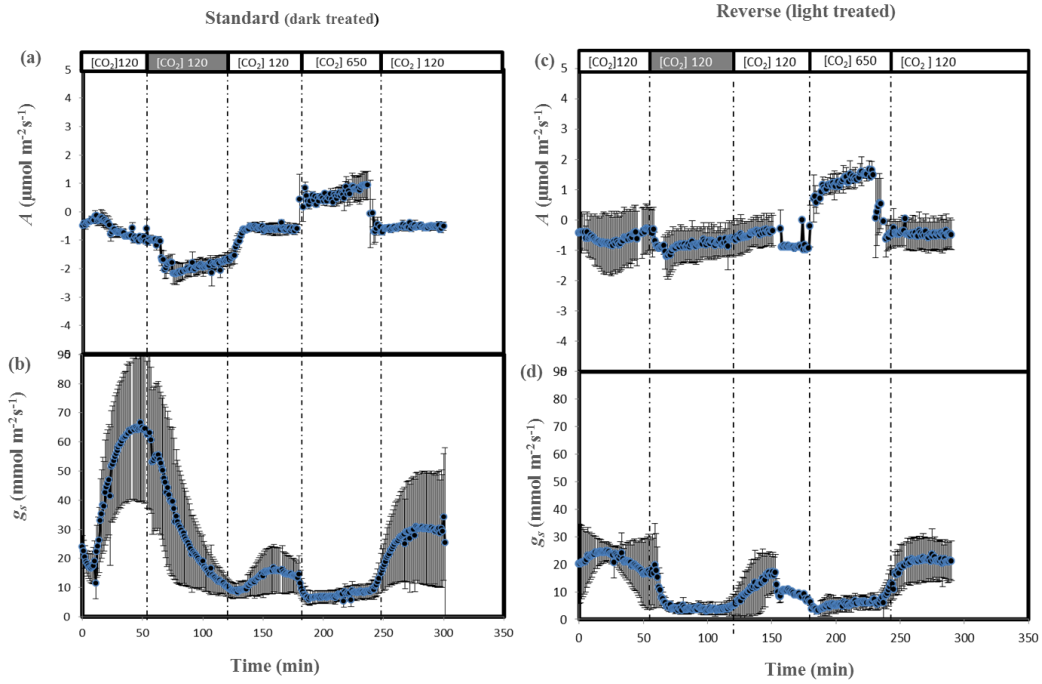

Figure 3. 12. Gas exchange measurements of pyruvate orthophosphate dikinase (PPDK) transgenic CAM (a) Photosynthetic carbon assimilation rates and **(b)** stomatal

conductance of transgenic grown in the standard cabinet and subjected to 12 h darkness prior to experiment while **(c)** carbon assimilation and **(d)** stomatal conductance from the reverse cabinet subjected to 12 h of light prior to measurements.The chamber conditions were maintained at the following: light/ [CO_2] of 120 µmol mol $^{-1}$: Dark/[CO_2] of 120 µmol mol $^{-1}$ light/ [CO_2] of 120 µmol mol $^{-1}$: light/[CO_2] of 650 µmol mol^{-1} and light/ [CO_2] of 120 µmol mol^{-1}. White and dark boxes represent light (400 µmol $m^{-2}s^{-1}$) and dark respectively. Dotted lines represent change from one light level/[CO_2] to another. Data are means of five replicates (± SE).

In plant grown in the dark/reverse cabinet that had been subjected to 12 h light prior to the measurements. Assimilation rate ranged between -0.3 to -0.8µmol CO_2 $m^{-2}s^{-1}$ (highest value) at [CO_2] of 120 µmol mol^{-1} $m^{-2}s^{-1}$ and in the light. However, when light was removed, assimilation decreased to -3.8 µmol CO_2 $m^{-2}s^{-1}$ in the dark. When [CO_2] was increased to 650 µmol mol^{-1} $m^{-2}s^{-1}$, as expected *A* increased, reaching about 2.5 µmol CO_2 $m^{-2}s^{-1}$.

Stomatal conductance was also much more sensitive in plant measured from the dark/reverse cabinet previously been subjected to 12 h light compared with the plants from the light/standard cabinet which had experienced 12h darkness preceding the experiment showing little or no response at all (Figs. 3.11a & b).

Similar, gas exchange experiment was performed on PPDK plants from the two different cabinet showed the effect of nocturnal and diurnal period on both *A* and g_s (Fig 3.12). Results in Fig.3.12c showed plant grown in the dark/reverse cabinet that had been subjected to 12 h light prior to the measurements. Assimilation rate ranged between -0.3 to -0.6µmol CO_2 $m^{-2}s^{-1}$ (highest value) at [CO_2] of 120 µmol mol^{-1} $m^{-2}s^{-1}$ and in the light however, when light was removed, assimilation decreased to -0.8 µmol CO_2 $m^{-2}s^{-1}$. When [CO_2] was increased to 650 µmol mol^{-1} $m^{-2}s^{-1}$, as expected *A* increased, reaching about 1.5 µmol CO_2 $m^{-2}s^{-1}$.

Measurements taken from the standard chamber (Fig.3.12a) shows carbon assimilation similar in pattern to the measurement from the reverse chamber even though to a lesser degree. Stomatal conductance ($g_{s)}$ increased under light and low [CO_2] and decreased under darkness and high [CO_2] as illustrated in Fig 3.12b & d respectively. Again, stomata from the light were more sensitive than those from the dark as in the wild CAM.

DISCUSSION

The coordination between stomatal conductance and mesophyll photosynthesis is important to help maximise WUE and plant productivity (Lawson et al., 2014b). It is well known that stomatal conductance correlates with photosynthesis (Wong, 1979) which balances CO_2 uptake for photosynthesis (*A*) and stomatal conductance (*gs*) to meet the plant's need to remain fully hydrated for optimal growth whilst maintaining sufficient CO_2 for mesophyll photosynthesis (Cowan and Troughton, 1971, Wong et al., 1979). Stomata have complex signal transduction networks which qualifies them for rapid changes in guard cell turgor in response to endogenous and environmental signals which promotes opening and closing of the stomatal pore within time scales of seconds to hours (Assmann and Wang, 2001). However, what is not clear is the mechanism(s) that co-ordinate g_s and *A* and the influence of the mesophyll on stomatal behaviour in this co-ordination. To date it has been assumed that the concentration of CO_2 inside the leaf (C_i) is maintained at a constant ratio between the concentration of CO_2 inside the leaf and that of the surrounding atmosphere C_i:C_a ratio; (Ball and berry, 1982, Mott et al., 1988) and this drives a co-ordinated response of g_s with *A*. However, several studies have suggested that stomatal responses to C_i are too small to account for the large changes in g_s that have been observed in response to light (Raschke, 1975, Farquhar and Raschke, 1978, Sharkey and Raschke, 1981, Farquhar and Sharkey, 1982). Additionally several studies have reported stomatal response to changing light intensity even when C_i is held constant (Messinger et al., 2006, Lawson et al., 2008b, Wang and Song, 2008). Further evidence against a C_i mechanism that co-ordinates g_s with *A* is from studies that have examined stomatal behaviour in transgenic plants with reduced levels of photosynthesis and shown stomatal responses to changing light despite high C_i values (Baroli et al., 2008a, von Caemmerer et al., 2004, Lawson et al., 2008b). Take together all of these studies suggest

that C_i cannot be the only signal that co-ordinates g_s with A. Several reports have suggested a mesophyll driven signal is responsible for the co-ordination between A and g_s. Chloroplastic ATP, NADPH and RuBP have all been proposed to be the possible candidates for the mesophyll signal (Lee and Bowling, 1992, Wong et al., 1979, Zeiger and Zhu, 1998, Tominaga et al., 2001). Other possibilities include malate and sugars transported from the mesophyll which will be discussed later in this section.

In this study, a comparison between stomatal responses to changing light intensity and [CO_2] were examined in epidermal peels and intact leaves in two plant species with different photosynthetic pathways, C3 (*Vicia faba*) which opens in the light and closes stomata in the dark and CAM (*Kalanchoë fedtschenkoi*) which closes stomata in the light and opens in the dark. Following the protocols developed by Mott et al., (2008) epidermal-mesophyll transfer experiments were undertaken to determine if different types of photosynthetic pathways influenced stomatal responses. As it is well-established that circadian rhythms influence stomatal behaviour (Dodd et al., 2005) diurnal measurements of stomatal aperture from epidermal peels (Fig. 3.3 & 3.4 and gas exchange measurements of g_s (Fig. 3.5 - 3.7) from both plant types showed that there were diel patterns of behaviour in stomatal behaviour. However, stomatal aperture changed little during the initial 6h of the diurnal period in both *Vicia faba* and *Kalanchoe fedtschenkoi* which means that there would be little influence on circadian driven changes in stomatal aperture in the subsequent epidermal mesophyll transfer experiments. The similar diel patterns of behaviour between peels and intact plants confirm that the protocol used for isolating and measuring the epidermal peels was appropriate and stomata responded similar to intact leaves. The observed whole leaf diel response of stomata in CAM plants in which levels of PPDK were greatly reduced (Dever et al., 2015) showed a close coordination between A and g_s but displayed stomatal opening and closing both in the

light and dark periods (Fig.3.7). This could be due to the plastic nature of CAM metabolism in these plants, or the reduced levels of PPDK removed the CAM dependency and facilitating more C3 carbon uptake processes (Dever et al., 2015).

Differences in stomatal responses to various environmental stimuli (including light intensity and CO_2 concentration) in epidermal strips and intact leaf have been reported previously in literature (Willmer and Dittrich, 1974, Travis and Mansfield, 1979, Lee and Bowling, 1995). For instance Schwartz et al. (1988) and Travis and Mansfield (1979) demonstrated that although stomata in epidermal peels were able to open in response to light intensity and low [CO_2] the change in stomatal aperture was much less than that observed in intact leaves. However, others have argued that stomata in isolated epidermal peels do not respond to light and [CO_2] in the guard cell (Mott et al., 2008a, Lee and Bowling, 1992, Fujita et al., 2013b), suggesting an important role of the mesophyll in stomatal response.

In response to changes in light intensity and [CO_2], stomata in epidermal peels of *Vicia faba* (Fig.3.8a), responded, albeit with lesser magnitude of change and reduced sensitivity, as expected and similar to the intact leaf (Fig. 3.8d), agreeing with reports that stomata respond and function when in isolation, (Meidner and Mansfield, 1968, Outlaw et al., 1981, Webb et al., 1996, Willmer and Fricker, 1996), but showed different responses than in intact leaves and the magnitude and/or speed of the stomatal responses are not the same as when the mesophyll is present (Schwartz et al. (1988) Travis and Mansfield (1979). Wang et al., (2014) found lower guard cell ATP levels in isolated epidermis compared with intact leaves, which they accredited to the weaker stomatal opening response to white light in the epidermis. Their results provide evidence that both guard cell chloroplasts and mesophyll contribute to the ATP source for H^+ extrusion by guard cells for osmoregulation.

The fact that stomata opened in darkness in the CAM plants is in agreement with what is known about stomatal behaviour in CAM, that due to the different photosynthetic pathway stomata generally open at night and fix CO_2 into organic acids which are stored and released through the day when stomata are closed. Stomatal closure through the day has often been attributed to diel changes in C_i, with stomata opening at night as PEPc starts to draw down CO_2 during the dark assimilation of internal CO_2 (Cockburn et al., 1979). However, what is intriguing is an opening response to darkness was also observed in the stomata in epidermal peels, when the influence of the mesophyll is removed (Fig 3.8b). This suggests that darkness is sensed directly in the guard cells which has not previously been reported. The dampened stomatal response to changing in [CO_2] in the epidermal peels (in both *Vicia* and *Kalenchoe*) compared with the intact leaves points to a role of C_i in these responses and signalling pathways (Mott 1988). The fact that stomata in *Vicia* epidermal peels placed on CAM mesophyll (Fig. 3.8c) behaved more like C3 stomata than CAM (i.e. the fact that the stomata opened with light) questions the mesophyll role in stomatal responses. Having said this, the fact that the stomata remained open and did not close when light was reduced and an increase in aperture was observed when CO_2 concentration was decreased at the end of the measurement period, along with the fact that in general, the stomatal apertures were all great than in the isolate peel (Fig. 3.8a) does point to a role for mesophyll driven consumption of CO_2. Rubisco fixation of CO_2 would be expected in CAM plants in the light, particular when the mesophyll is removed and the temporal CO_2 concentrating mechanism has been removed (von Caemmerer and Griffiths, 2009). These finding from the epidermal peel transfer experiment do not entirely agree with those of Mott et al, (2008) who found that when stomata in isolated epidermis of *T. pallida* and *P.sativum* when placed on an exposed mesophyll from a leaf of the same species or a different species, they regained

responsiveness to light and CO_2. The stomatal responses reported here are less evident, however, it should be noted that the the work of Mott et al., (2008) did not include CAM mesophyll which behaves very different to C3.

The measurements (Fig 3.8d) on the detached whole leaf clearly demonstrated an excellent responses between g_s and A as well as rapid responses unlike those recorded on the isolated epidermis or the peels grafted onto mesophyll. These finding indicate that stomata are influenced by the underlying mesophyll, however this could simply be due to mesophyll photosynthetic consumption of CO_2 altering C_i leading to stomatal opening and closing in response to changes in light and $[CO_2]$ or it could be that sucrose produced in the meosphyll plays a key role in stomatal osmoregulation (Kelly et al., 2013) synchronising stomata with mesophyll. It is also worthy to mention here that the response in the intact detached leaf aside from being very rapid in response to light and CO_2 changes, stomata failed to respond to either light nor $[CO_2]$ at a certain point in the experiment (result not shown) which could possibly be due to an effort to balance or coordinate A and gs in order to check excess transpiration. This could probably be (in addition to C_i) due to accumulation of sucrose in the walls of the guard cells that were not translocated to other parts of the plant (since the plant was a detached one) hence the shutdown of the stomatal walls. This is an interesting finding in this experiment which seemed to be in line with the many hypothesised theories of a mesophyll-derived signal(s). Recalling again, several studies have argued that changes in C_i are often too small to account for the large changes that occurs in stomatal aperture which has even been demonstrated by stomatal responses to PPFD even when C_i is held constant (Lawson et al., 2008; Messinger et al., 2006; Wang et al., 2008). von Caemmerer and Griffiths (2009b) has also demonstrated that high intercellular CO_2 is not the sole cause for stomatal closure during phase lll of CAM.

Sucrose has been hypothesised as a metabolite connecting stomatal behaviour with mesophyll demands for CO_2 and important for co-ordinating response in the two. For a long time it was initially thought that K^+ and its counter ions were the universal osmoticum for osmoregulatory stomatal opening(Fischer, 1968a), however when several studies (MacRobbie & Lettau, 1980) showed that potassium-malate fluxes could not account for all the osmotic required for stomatal opening a role for sucrose was revisited. Tallman and Zeiger (1988) suggested that K^+ and its counter ions including malate were important for early morning stomatal opening but that sucrose was the dominant osmotic for maintaining stomatal conductance late in the afternoon. Apoplastic sucrose has also been proposed to co-ordinate mesophyll photosynthesis with stomatal behaviour (Kang et al., 2007a). Lu et al. (1997a) implied the presence of multiple sucrose pools in mesophyll cells which are a localized mesophyll-apoplast region that exchanges with phloem and stomata, and mesophyll-derived sucrose in guard-cell walls which excess of it is able to diminish stomatal opening. Fujita et al, (2013) also suggested that stomata close as a result of high apoplastic sucrose concentration when mesophyll sucrose efflux exceeds translocation. When photosynthesis is high and sucrose production, exceed the capacity of the phloem to translocate the sucrose, the apoplast sucrose content increases and travels in the apoplast to the guard cells were the sucrose acts as an osmotic and reduces stomatal aperture (Kang et al., 2007a) see review by Lawson et al, (2014). The role of apoplastic sugar concentration have also been linked to hexokinase (HXK) a sugar-phosphorylating enyzmes in guard cells by Kelly et al, (2013) who found an increased expression of hexokinase (HXK) accelerated stomatal closure.

Fig 3.10 and Fig. 3.11 illustrate stomatal and photosynthetic responses to the step changes in light intensity and [CO_2] in *Vicia* (Fig. 3.10) and *Kalenchoe* (Fig. 3.11) grown in either the light/standard cabinet or the dark/reverse cabinet. The identical

photosynthetic responses in *Vicia* illustrate that the different 12h pre-treatment did affect the potential photosynthetic rates. However what was interesting was the fact that stomatal conductance was clearly co-ordinated with *A* in the plants grown in the light standard cabinet (with some indication of slow stomatal response limiting assimilation rates (Lawson & Blatt, 2014). Although g_s and *A* were also well co-ordinated in the dark/reverse cabinet grown plants in the end period of the measurements, g_s increase in with light but unexpectedly continued to increase even when the light was turned off suggesting that g_s could respond to darkness as well.

The considerable differences in both *A* and g_s responses to light intensity and [CO_2] in the CAM plants grown in the two different cabinet illustrate the considerable diel impact of CAM pathway on physiology (Borland et al., 2014). The plants taken from the light/standard cabinets (Figs.3.11a& b) which have prior to the experiment been subjected to 12h of darkness, had stomata that were mostly unresponsive. As seen in (Fig 3.11 c & d) it is obvious that the response of CAM that was subjected to 12 hours of light prior to gas analysis were more responsive than the CAM from the dark. An possible explanation for this is that decarboxylation of malate in the proceeding 12h has left the plants without any carbon stores left and that because these plants are well watered, carbon fixation can occur via Rubisco and therefore stomata respond similar to those in a C3 plant (Franco et al., 1999). High light would reduce C_i to which stomata would respond, as well as responding to light directly through both the blue and red light pathways (Shimazaki et al 2007).This is supported by the similarity in the response of *A* with g_s suggesting stomatal limitation of CO_2 diffusion and *A*. These data strongly suggest that the mesophyll photosynthetic behaviour plays a key role in stomatal behaviour but indicates a C_i driven responses rather than a mesophyll specific metabolite signal.

The observed whole leaf diel response of stomata in CAM plants in which levels of PPDK were greatly reduced (Dever et al. 2016) and had a 5% that of wild type showed a close coordination between A and g_s but displayed stomatal opening and closing both in the light and dark periods (Fig.3.11 below). These finding are similar to those of von Caemmerer and Griffiths (2009a) who investigated the diurnal variation of stomatal sensitivity to [CO_2] and light in two CAM *Kalanchoe* species (with different degrees of CAM) and found that stomata opened in *K. pinnata* in response to a reduced [CO_2] in the dark and in the latter half of the light period while in *K. daigremontiana* which is more succulent and considered welded to the CAM metabolism phases, stomata did not respond to a decreased CO_2 in the light when stomata were closed, even when the supply of internal CO_2 was experimentally reduced. They concluded that stomatal closure and the variability in the responsiveness of stomata to CO_2 could be explained by the existence of a CO_2 sensor which interacts with other signalling pathways (von Caemmerer & Griffiths, 2009).

CHAPTER FOUR:

DESIGN AND DEVELOPMENT OF GOLDEN GATE CONSTRUCTS TO MANIPULATE EXPRESSION OF CYTOCHROME B_6F (RIESKE) AND SEDOHEPTULOSE-1,7-BISPHOSPHATASE (SBPASE) IN *ARABIDOPSIS THALIANA* AND *NICOTIANA TOBACCUM* PLANTS.

INTRODUCTION

The manipulation of photosynthetic enzymes in carbon metabolism have resulted in a great impact on the photosynthetic rates in plant (Lawson et al., 2008b, Lawson et al., 2002, Lefebvre et al., 2005, Raines, 2011, Simkin et al., 2017a, Simkin et al., 2015, von Caemmerer and Furbank, 2016). Quite a number of studies have been carried out on the regulation of carbohydrate metabolism in photosynthetic CO_2 fixation in plants and these have led to several reports of improved photosynthetic capacity leading to increased crop productivity and yield (Raines, 2011, Raines, 2006, Ding et al., 2016, Lefebvre et al., 2005, Long et al., 2006, von Caemmerer and Evans, 2010).

An electron transport chain is a series of complex reactions that transfers electrons from electron donors to electron acceptors alongside the transfer of protons H^+ ions across a membrane. The cytochrome b_6f complex also known as the plastoquinol-plastocyanin reductase is an enzyme found in the electron transport chain on the thylakoid membrane (Berg et al, 2007). In photosynthesis, the cytochrome b_6f complex catalyze the transfer of electrons between the two photosynthetic reaction center Photosystems II and Photosystem I, while at the same time, transferring protons across the thylakoid used to synthesize ATP from ADP for the Calvin Cycle (Stroebel et al., 2003, Yamashita et al., 2007). Rieske is an iron-sulphur protein of the Cytochrome b_6f complex (Rieske et al., 1964) and it is a clustered 2Fe-2S found in plants, animals, and

bacteria.The cytochrome b_6f despite its genetic and structural complexity, has been manipulated through the antisense expression of the RieskeFeS protein which showed reduction in electron transport chain. Additionally, the use of cytochrome b_6f complex inhibitors have suggested that the RieskeFeS protein is important for the successful assembly and optimal function of the cytochrome b_6f complex and electron transport (Price et al., 1998, Kirchhoff et al., 2000, Kirchhoff et al., 2017). Recently overexpression of the Rieske FeS protein in Arabidopsis resulted in substantial improvements of quantum efficiency of PSI and PSII and electron transport which lead to significant impacts on plant yield (Simkin et al., 2017b) .

The Calvin cycle is a pathway primarily for carbon fixation in chloroplasts of C3 plants. This process has three stages, where carboxylation which is the first stage is a process of accepting CO_2 by an acceptor molecule, ribulose-1,5-bisphosphate (RuBP) and is aided by the enzyme ribulose-1,5-bisphosphate carboxylase/ oxygenase (Rubisco). The second stage is the reduction phase that produces triose phosphate by consuming ATP and NADPH produced by the ETC. The third and final stage is the regenerative phase, in which triose phosphates are used to produce back RuBP. In the cycle, the triose phosphates are key intermediates, and they are also available for allocation to either the starch or sucrose biosynthetic pathway (Geiger and Servaites, 1994, Woodrow and Berry, 1988). Balance within the cycle is therefore very important in order to avoid exhaustion of these phosphates hence, the catalytic activities of certain enzymes within the cycle are highly regulated (Raines et al., 1999). In particular, the activity of sedoheptulose-1,7-bisphosphatase (SBPase) is regulated by the redox potential via the ferredoxin/ thioredoxin system, which modulates the enzyme activities in response to light/dark conditions (Buchanan, 1991). In the regenerative phase of the Calvin cycle, SBPase is part of the enzyme that catalyze irreversible reactions (Koßmann et al., 1994). SBPase

catalyses the dephosphorylation of sedoheptulose-1,7-bisphosphate in the regenerative phase of the Calvin cycle to sedoheptulose-7-bisphosphate.

Transgenic approaches have demonstrated striking results of the manipulation of the Calvin cycle where energy conversion led to increasing yield potential (Long et al., 2006, Raines, 2003, Raines, 2006, Raines, 2011, Zhu et al., 2007). Additionally, others have also revealed and shown the importance of SBPase by demonstrating that minimal reductions or the disruption of SBPase and some certain genes has shown to impact negatively on carbon assimilation and growth, thereby demonstrating the enzyme's control over photosynthetic efficiency (Ding et al., 2016, Harrison et al., 1998, Lawson et al., 2006, Raines et al., 1999, Raines and Paul, 2006, Koßmann et al., 1994).

No doubt therefore these studies imply that improvements in photosynthesis may be achieved through overexpressing the activity of individual enzymes. Already, evidences supporting this hypothesis from single manipulations have been demonstrated from transgenic tobacco plants over-expressing SBPase (Lefebvre et al., 2005) and also the combined multigene approach of over-expressing SBPase and FBPA (Simkin et al 2015). These photosynthetic manipulations resulted in increased carbon assimilation, enhanced growth and increased cumulative biomass hence the genetic potentials that lies thereby. It is therefore obvious that number of sense and antisense plants with increased and reduced levels of SBPase and Rieske have varying photosynthetic capacity and have altered carbohydrate status at the whole leaf level thus, leading to modifications in growth and development.

This influence of manipulated electron transport and Calvin cycle on stomatal responses to CO_2 concentration and photon flux density can be determined physiologically in the guard cells specifically as well as how stomatal responses contribute to the capacity of guard cell function (Lawson, 2009, Lawson and Blatt, 2014a, Lawson et al., 2014a).

This chapter describes the design and construction of eleven sense and antisence constructs of these enzymes for use in both *Arabidopsis thaliana* and *Nicotiana tobaccum* specifically in the guard cells. Expression vectors from the cloning strategy 'Golden gate' where used to generate these constructs with guard cell specific promotors. Constructs were designed to alter expression of the SBPase and Rieske genes in a cell specific manner driven by the KST1 and MYB60 promoters. YFP tags were also included in several construct to demonstrate cell specificity.

4.1 Golden-gate Modular cloning technology.

The ability to assemble multiple or complex DNA molecules containing large number of genetic elements is key and an essential part of genetic engineering. Golden gate cloning technique also known as the Moclo or modular cloning allows highly efficient directional assembly of multiple DNA fragments in a single reaction (Engler et al, 2009, Weber et al.,2011). The principle of Golden gate cloning makes it possible for constructs or multiple desired genes assembled seamlessly by using the type lls restriction enzyme in a one-pot one-step cloning reaction (Weber et al, 2011). Type IIs restriction enzyme which is the basis of this cloning strategy cut outside of recognition site and fragments ligated easily into a product lacking the original restriction site allowing any DNA fragment of interest from an entry clone to be transferred into an expression vector without any unwanted sequences in the final construct (Engler et al., 2008). However, as previously explain in materials and methods chapter, fusion sites overlapping with coding sequences are carefully chosen so as to minimize changes to encoded proteins. The figure below (Fig.4.1) illustrates the standardized assembly of this unique cloning system.

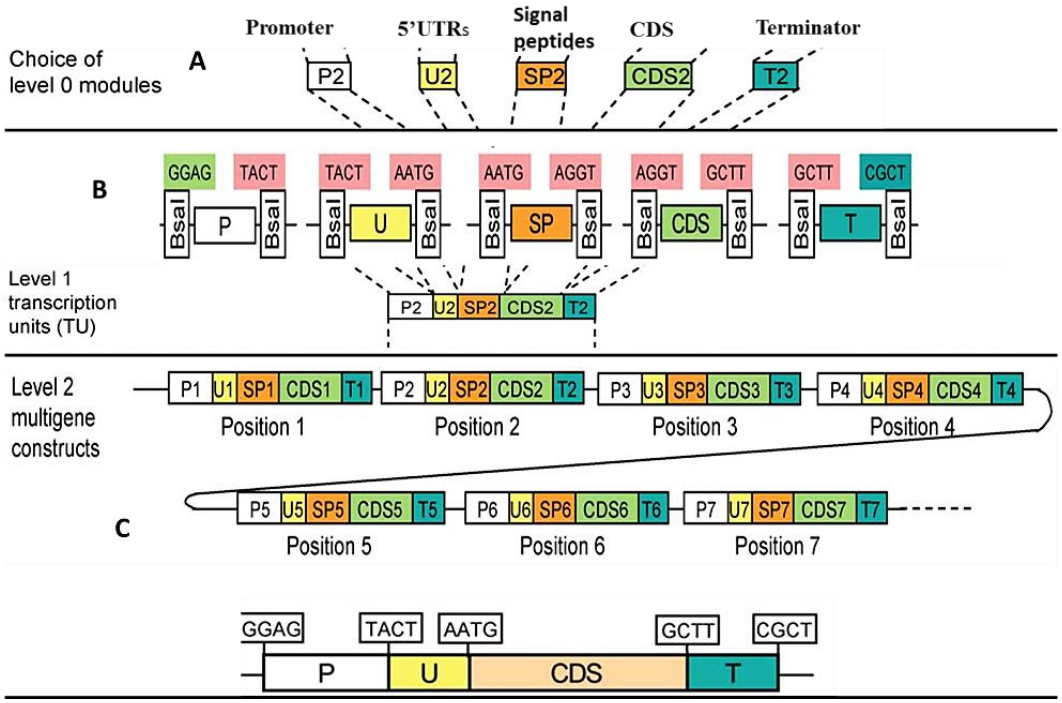

Figure 4. 1. General assemblage of standardized modular cloning system. (A) level 0 modules of cloned or sequenced genetic elements such as promoters (P), 5' untranslated regions (U), signal peptides (SP), coding sequences (CDS) and terminators (T). **(B)** level 1 transcription units assembled from level 0 modules using a one-pot one-step cloning reaction. Level one (1) flanked by compatible fusion sites consisting of 4 nucleotides of choice (boxed) flanked by a type IIS enzyme Bsa1. **(C)** Multigene constructs assembled in a second cloning step from the transcription units. The transcription unit for the cytolic protein was assembled from 4 modules rather than 5, using a CDS module cloned between fusion sites AATG and GCTT. Diagram modified from Weber et al, 2011.

The modular cloning strategy allows systematic assembly of complete transcription units and of multigene constructs from basic standardized modules as exemplified above. Various levels and components are described below.

4.1.1 Level 0 modules

All level 0 destination vectors are based on a pUC19 backbone which confer a spectinomycin resistance (Sp^R). Our genes of interest (SBPase and Rieske) consisted of eight (8) level 0 fragments in the SC position of the destination vectors; pL0M-SC-NtRieske, pL0M-SC-ASNtRieske, pL0M-SC-NtSBPase, pL0M-SC-ASNtSBPase, pL0M-SC-AtRieske, pL0M-SC-AS-AtRieske, pL0M-SC-AtSBPase and pL0M-SC–AtSBPase. While promoters KST1 (pL0M-PU-KST1) and AtMYB60 (pL0M-PU-AtMYB60) in the PU position of destination vectors and terminator, pL0M-T-HSP. The positions in the destination vectors were created to allow the possibility of creating or cloning two or more genetic standardized element as a single module (PU instead P, U, and SC instead of S,C). All level zero (0) were synthesized but cloning of level 0 modules were done by the PCR-amplification of the designated sequences. Additional level 0 construct were designed to determine guard cell specific expression, with YFP (pICSL80014). These were all systematically assembled into level 1 constructs with the incorporated guard cell specific promoters. Below is a table of the constructs at the level 0 modules.

Table 4. 1. List of level 0 standardised modules.

ID/CODE name	Standard name	Full Name
EC23044a	pL0M-SC-AtSBPase	EC23044a pL0M-SC-AtSBPase
EC23045a	pL0M-SC-AtRieske	EC23045a pL0M-SC-AtRieske
EC23149	pL0M-PU-KST1	EC23149 pL0M-PU-KST1
EC23151	pL0M-PU-AtMYB60	EC23151 pL0M-PU-AtMYB60
TL0015	pL0M-SC-NtRieske	TL0015 pL0M-SC-NtRieske
TL0001	pL0M-SC-ASNtRieske	TL0001 pL0M-SC-ASNtRieske
TL0002	pL0M-SC-ASNtSBPase	TL0002 pL0M-SC-ASNtSBPase
pICSL80014	pL0M-SC-YFP	pICSL80014 pL0M-SC-YFP
EC15320	EC15320 (pL0M-T-HSP)	EC15320 (pL0M-T-HSP)

Level 0 standardized modules were synthesized.

RESULTS

4.2. Level 1 modules

Level one (1) modules were created by the assembly of compatible sets of sequenced level 0 above which were assembled into a level 1 destination vector with Golden gate reaction using the enzyme BsaI. These consisted of the backbones, promoters, coding sequences and terminators. The backbone for level 1 modules confer an ampicillin resistance with fusion sites compatible from one vector to the next so that multiple level 1 modules were directionally cloned together and into a level 2 destination vector. Table 4.2 shows how the transcriptional units of all level 1 were assembled into level one backbones. A bioinformatic software called geneious was used in designing the constructs or plasmid maps and also to determine the exact fragment sizes in base pairs of

all the constructs. Fig. 4.3 and 4.4 were used as examples for the level one (1) construct. All the level one constructs were also sequenced and the expected inserts confirmed for all with the correct sequences at the cloning junctions Fig. 4.3b. See appendix for sequencing result.

Table 4. 2. Summary of level one constructs. White background consisting of level 1 construct of genetic element of promoters (red background), coding sequences (orange background) and terminators (blue background) assembled into level one backbone (yellow background).

Full Name	Backbone	P U	S C	T
TL0022 pL1M-R2-pKST1-YFP-tHSP	EC47811 (pL1V-R2)	EC23149 pL0M-PU-KST1	pICSL80014 pL0M-SC-YFP	EC15320 (pL0M-T-HSP)
TL0023 pL1M-R3-pKST1-YFP-tHSP	EC47822 (pL1V-R3)	EC23149 pL0M-PU-KST1	pICSL80014 pL0M-SC-YFP	EC15320 (pL0M-T-HSP)
TL0024 pL1M-R4-pKST1-YFP-tHSP	EC47831 (pL1V-R4)	EC23149 pL0M-PU-KST1	pICSL80014 pL0M-SC-YFP	EC15320 (pL0M-T-HSP)
TL0025 pL1M-R2-pKST1-ASNtSBPase-tHSP	EC47811 (pL1V-R2)	EC23149 pL0M-PU-KST1	TL0002 pL0M-SC-ASNtSBPase	EC15320 (pL0M-T-HSP)
TL0026 pL1M-R3-pKST1-ASNtSBPase-tHSP	EC47822 (pL1V-R3)	EC23149 pL0M-PU-KST1	TL0002 pL0M-SC-ASNtSBPase	EC15320 (pL0M-T-HSP)
TL0027 pL1M-R4-pKST1-ASNtSBPase-tHSP	EC47831 (pL1V-R4)	EC23149 pL0M-PU-KST1	TL0002 pL0M-SC-ASNtSBPase	EC15320 (pL0M-T-HSP)
TL0031 pL1M-R2-pKST1-AtRieske-tHSP	EC47811 (pL1V-R2)	EC23149 pL0M-PU-KST1	EC23045a pL0M-SC-AtRieske	EC15320 (pL0M-T-HSP)
TL0032 pL1M-R3-pKST1-AtRieske-tHSP	EC47822 (pL1V-R3)	EC23149 pL0M-PU-KST1	EC23045a pL0M-SC-AtRieske	EC15320 (pL0M-T-HSP)
TL0033 pL1M-R4-pKST1-AtRieske-tHSP	EC47831 (pL1V-R4)	EC23149 pL0M-PU-KST1	EC23045a pL0M-SC-AtRieske	EC15320 (pL0M-T-HSP)
TL0034 pL1M-R2-pKST1-ASNtRieske-tHSP	EC47811 (pL1V-R2)	EC23149 pL0M-PU-KST1	TL0001 pL0M-SC-ASNtRieske	EC15320 (pL0M-T-HSP)
TL0035 pL1M-R3-pKST1-ASNtRieske-tHSP	EC47822 (pL1V-R3)	EC23149 pL0M-PU-KST1	TL0001 pL0M-SC-ASNtRieske	EC15320 (pL0M-T-HSP)
TL0036 pL1M-R4-pKST1-ASNtRieske-tHSP	EC47831 (pL1V-R4)	EC23149 pL0M-PU-KST1	TL0001 pL0M-SC-ASNtRieske	EC15320 (pL0M-T-HSP)
TL0037 pL1M-R2-pKST1-AtSBPase-tHSP	EC47811 (pL1V-R2)	EC23149 pL0M-PU-KST1	EC23044a (pL0M-SC-AtSBPase)	EC15320 (pL0M-T-HSP)
TL0038 pL1M-R3-pKST1-AtSBPase-tHSP	EC47822 (pL1V-R3)	EC23149 pL0M-PU-KST1	EC23044a (pL0M-SC-AtSBPase)	EC15320 (pL0M-T-HSP)
TL0039 pL1M-R4-pKST1-AtSBPase-tHSP	EC47831 (pL1V-R4)	EC23149 pL0M-PU-KST1	EC23044a (pL0M-SC-AtSBPase)	EC15320 (pL0M-T-HSP)

Fig. 4.2 below Illustrates the specific fusion sites used here in ligating the promoters, coding sequences and the terminators towards building or assembling all the level 1 constructs (as shown above) seamlessly. The KST1 promoter which is a partial segment of the potato (*Solanum tuberosum*) is specifically used to drive expression in the guard cells of potato, tomato (*Solanum lycopersicum*), citrus (*C. sinensis* and *Poncirus trifoliata*) and Arabidopsis (*Arabidopsis thaliana*).

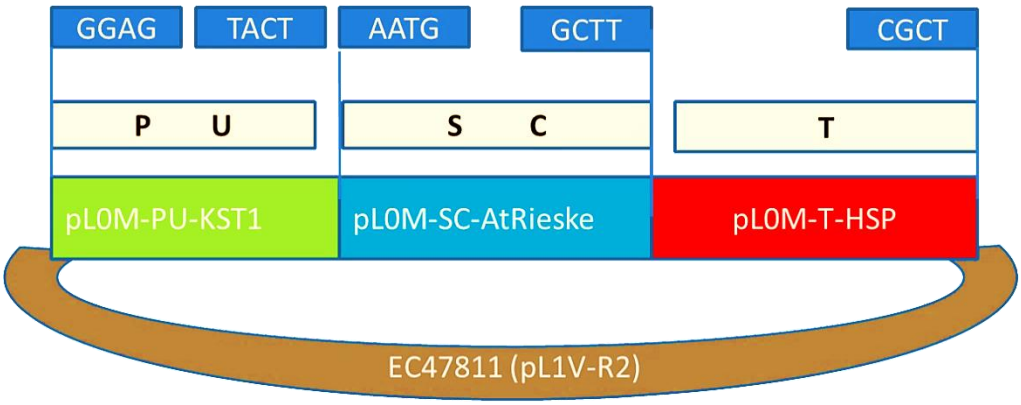

Figure 4. 2. Illustration of level one transcription unit assembly. Level 0 standardized modules of promoter (pL0M-PU-KST1), coding sequence (pL0M-SC-AtRieske) and terminator (pL0M-T-HSP) into a level one backbone (EC47811, pL1V-R2). Destination vectors for the 3 standard elements (pL0-PU, pL0-SC and pL0-T) were made possible by cloning two genetic elements as a single module, for example promoter and 5' untranslated region were cloned as a single module using destination vector pL0-PU while coding sequence cloned in a vector pL0-SC rather than in vector pL0-C. The modules are flanked by standard compatible sequence overhangs known as fusion sites composed of 4 nucleotide sequences (boxed).

Additional level 1 constructs were designed to determine guard cell specific expression, with YFP (pICSL80014 pL0M-SC-YFP). Figures 4.2 and 4.3 below are construct plasmids of pL1M-R2-pKST1-AtSBPase-tHSP and pL1M-R2-pKST1-AtRieske-tHSP.

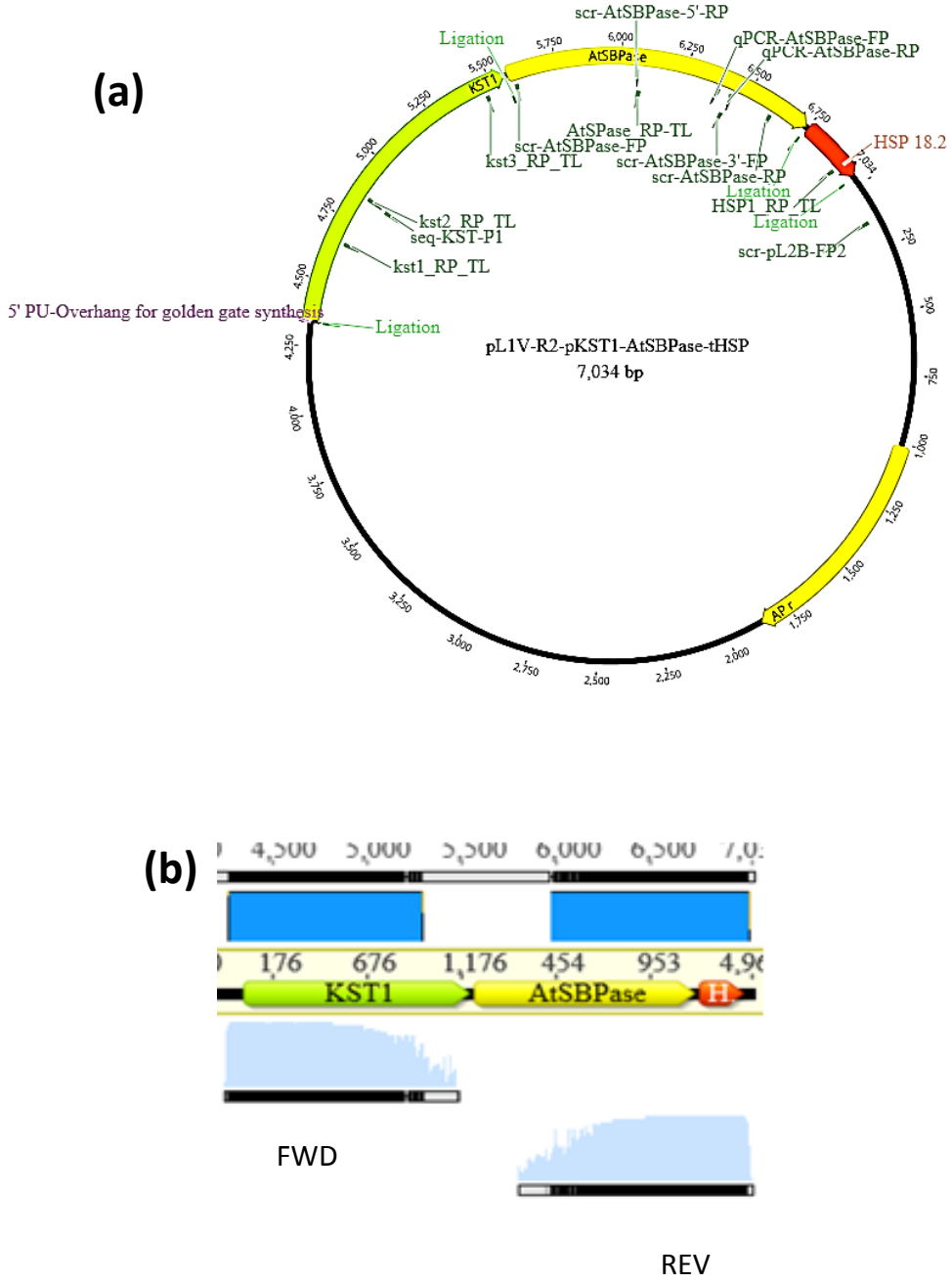

Figure 4. 3. Construct map for level one plasmid pL1M-R2-pKST1-AtSBPase-tHSP for over-expression of SBPase in plants. (a) Standardized modules of promoter (pL0M-PU-KST1), coding sequence (pL0M-SC-AtSBPase and terminator (pL0M-T-HSP) assembled into a level one backbone EC47811 (pL1V-R2). Plasmid consists of 5' PU overhang for golden gate synthesis fusion sites with 4 nucleotide sequences (as indicated in Fig 4.2). Primers for synthesis annealed to specific sites for efficient cloning**. (b)** Sequencing alignment of the gene of interest (thick black bar with forward and reverse primers used) within the DNA fragment of interest. Multiple alignments was performed using Clustal omega (http://www.ebi.ac.uk/Tools/msa/clustalo/) and geneious software www.geneious.com. See appendix for sequence result.

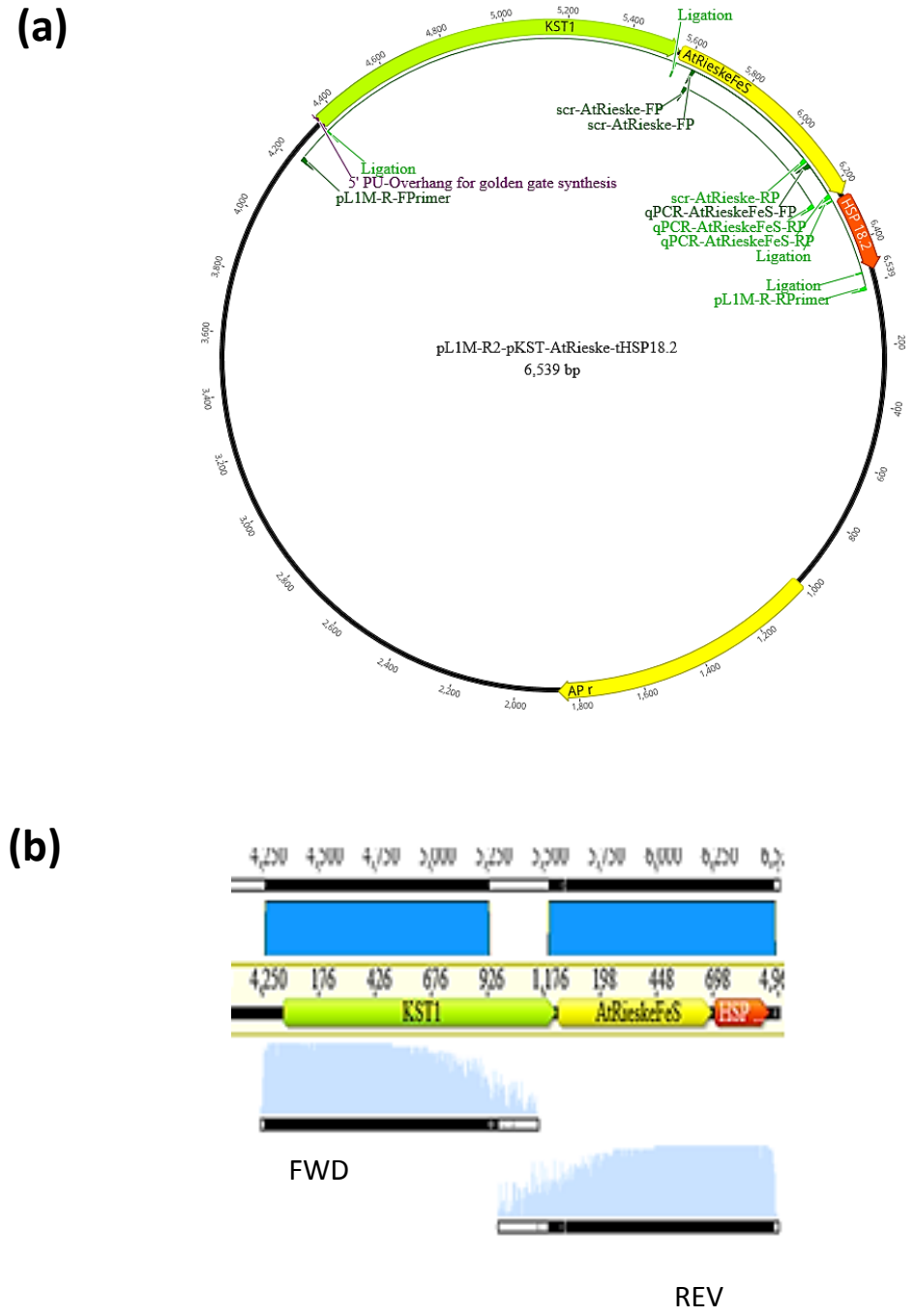

Figure 4. 4. Construct map for level one plasmid pL1M-R2-pKST1-AtRieske-tHSP for over-expression of Rieske in plants. (a) Standardized modules of promoter (pL0M-PU-KST1), coding sequence (pL0M-SC-AtRieske and terminator (pL0M-T-HSP) assembled into a level one backbone EC47811 (pL1V-R2). Plasmid consists of 5' PU overhang for golden gate synthesis fusion sites with 4 nucleotide sequences (as indicated in Fig 4.2). Primers for synthesis annealed to specific sites for efficient cloning**. (b)** Sequencing alignment of the gene of interest (thick black unexpanded bar with forward and reverse primers used) within the DNA fragment of interest. Multiple alignments was performed using Clustal omega **(**http://www.ebi.ac.uk/Tools/msa/clustalo/) and geneious software www.geneious.com. See appendix for sequence result.

4.3 Multigene constructs or level two

In the same way level 1 modules were cloned from standardized modules, multiple transcriptional units of level 1 modules were directionally cloned into a level 2 destination vector. Level 2 constructs were designed in such a way that the upstream fusion sites are compatible with the upstream fusion site of a corresponding level 1 module. This reduces the need for re-cloning of the same transcription unit for different positions (Weber et al, 2011). However, the downstream fusion site is unique to level 2 destination vectors (GGGA) because of the addition of end-linkers (pELE-n) which connect the GGGA fusion site with the fusion site of the last assembled transcription unit in the DNA fragment. All level 2 constructs confer a kanamycin resistance and encode a red colour selectable marker. The end linkers plasmid however, confer an ampicillin resistance like the level 1 constructs but flanked by BpiI sites. Therefore, multigene level 2 constructs are assembled with BpiI from the chosen level 1 modules, a matching end-linker and a level 2 destination vector. Two steps of digestion and ligation can therefore be replaced by a single restriction-ligation step (Weber et al, 2011).

The table 4.3 below summarises the level 2 constructs assembled from level one transcription units, backbones and end-linkers. The last four rows are the list of primers used, together with the expected and exact sizes assessed. The geneious software as previously used in level 1 was as well used to design and assess the final level 2 construct. Due to the large sizes of the fragments of interest, PCR reactions were divided into two (first and second reaction). Forward primers for each reaction are at the top of the columns.

Table 4. 3. Reaction summary (PCR) of all the level two constructs being assembled (white columns). The last four columns (orange and blue) indicates the primers used for the first and second reaction with their expected sizes respectively to be transformed in both *Arabidopsis thaliana* and *Nicotiana tobaccum* plants. The column in green indicates constructs tagged with the YFP in addition for cell specificity.

	ID/Code	Standard name	Backbone	Basta	R2 (Level 1)	R3	pELE-n	Scr-BAR-3'-FP (1st reaction)	Fragment sizes	pL1m-R-Fprimer & Seq- YFP-FP (2nd reaction)	Fragment sizes
1	**TL0040**	pL2B-BAR-(pMYB60)-ASNtSBPase	**pAGM4723** (pL2B backbone)	**EC15324** pL1M-R1-pNOS-BAR-tNOS	**TL0028** pL1M-R2-pMYB60-ASNtSBPase-HSP		**EC41744** (pL1M-ELE-2)	**qPCR-NtSBPase-RP2**	**805**	**qPCR-NtSBPase-FP2**	**2240**
2	**TL0042**	pL2B-BAR-(pKST)ASNtSBPase			**TL0025** pL1M-R2-pKST1-ASNtSBPase-tHSP			**qPCR-NtSBPase-RP2**	**854**	**qPCR-NtSBPase-FP2**	**2132**
3	**TL0043**	pL2B-BAR-(pKST)AtSBPase			**TL0037** pL1M-R2-pKST1-AtSBPase-tHSP			**Scr-AtSBPase-3'-FP**	**682**	**Scr-AtSBPase-RP**	**2429**
4	**TL0044**	pL2B-BAR-(pKST)AtRieske			**TL0031** pL1M-R2-pKST1-AtRieske-tHSP			**qPCR-AtRieske-FP**	**512**	**Scr-AtRieske-RP**	**1718**
5	**TL0045**	pL2B-BAR-(pKST)ASNtRieske			**TL0034** pL1M-R2-pKST1-ASNtRieske-tHSP			**qPCR-NtRieske-RP1**	**1033**	**qPCR-NtRieske-FP2**	**1699**
6	**TL0046**	pL2B-BAR-(pKST)YFP			**TL0022** pL1M-R2-pKST1-YFP-tHSP			**Seq-YFP-FP**	**1039**		
7	**TL0041**	pL2B-BAR-(pMYB60)-ASNtSBPase-(pMYB60)YFP	**pAGM4723** (pL2B backbone)	**EC15324** pL1M-R1-pNOS-BAR-tNOS	**TL0028** pL1M-R2-pMYB60-ASNtSBPase-HSP	**TL0010** pL1M-R3-pMYB60-YFP-HSP	**EC41766** pL1M-ELE-3	**qPCR-NtSBPase-RP1**	**1320**	**qPCR-NtSBPase-FP2**	**3034**
8	**TL0047**	pL2B-BAR-(pKST)ASNtSBPase-(pKST)YFP			**TL0025** pL1M-R2-pKST1-ASNtSBPase-tHSP	**TL0023** pL1M-R3-pKST1-YFP-tHSP		**qPCR-NtSBPase-RP1**	**1329**	**qPCR-NtSBPase-FP2**	**2933**
9	**TL0048**	pL2B-BAR-(pKST)AtSBPase-(pKST)YFP			**TL0037** pL1M-R2-pKST1-AtSBPase-tHSP			**Scr-AtSBPase-3'-FP**	**687**	**Scr-AtSBPase-5'-RP**	**2681**
10	**TL0049**	pL2B-BAR-(pKST)AtRieske-(pKST)YFP			**TL0031** pL1M-R2-pKST1-AtRieske-tHSP			**qPCR-AtRieske-FP**	**513**	**Scr-AtRieske-RP**	**2698**
11	**TL0050**	pL2B-BAR-(pKST)ASNtRieske-(pKST)YFP			**TL0034** pL1M-R2-pKST1-ASNtRieske-tHSP			**qPCR-NtRieske-RP2**	**868**	**qPCR-NtRieske-FP2**	**2506**

Figs. 4.5-4.7 show some examples of the plasmid maps (out of the eleven constructs) constructed by the geneious for level 2 constructs. The construction by the geneious determines the exact fragment sizes to be expected in base pairs of all the constructs (This information was used to check using PCR and the gels).

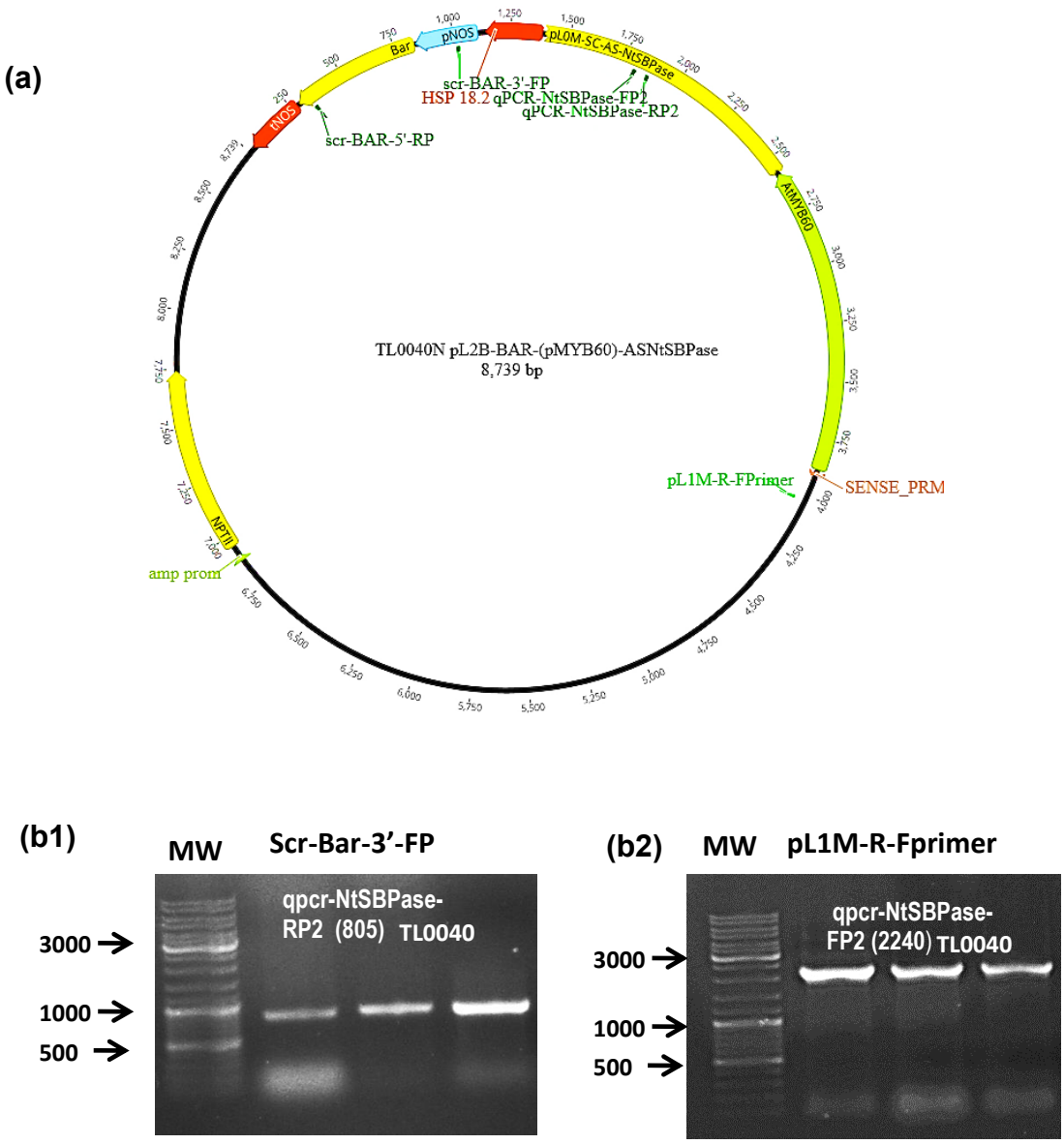

Figure 4. 5 .Construct map for level two plasmid (pL2B-BAR-(pMYB60-ASNtSBPase-tHSP) for expression of SBPase in plants. **(a)** Plasmid contains the genetic modules of level one assembled together with MYB60 promoter, ASNtSBPase coding sequences and terminator.The expression vector produced also carries the NPTII genes for kanamycin selection in bacteria and the BAR gene as a selective marker for herbicide selection in plants. **(b1)** first reaction with Scr-Bar-3'-FP as the forward primer and qpcr-NtSBPase-RP2 as the reverse primer yielding 805bp as expected of the construct. **(b2)** second reaction using pL1M-R-Fprimer and qpcr-NtSBPase-FP2 as forward and reverse primers respectively yielding exact DNA fragment size of 2240bp. Construct designed by geneious www.geneious.com.

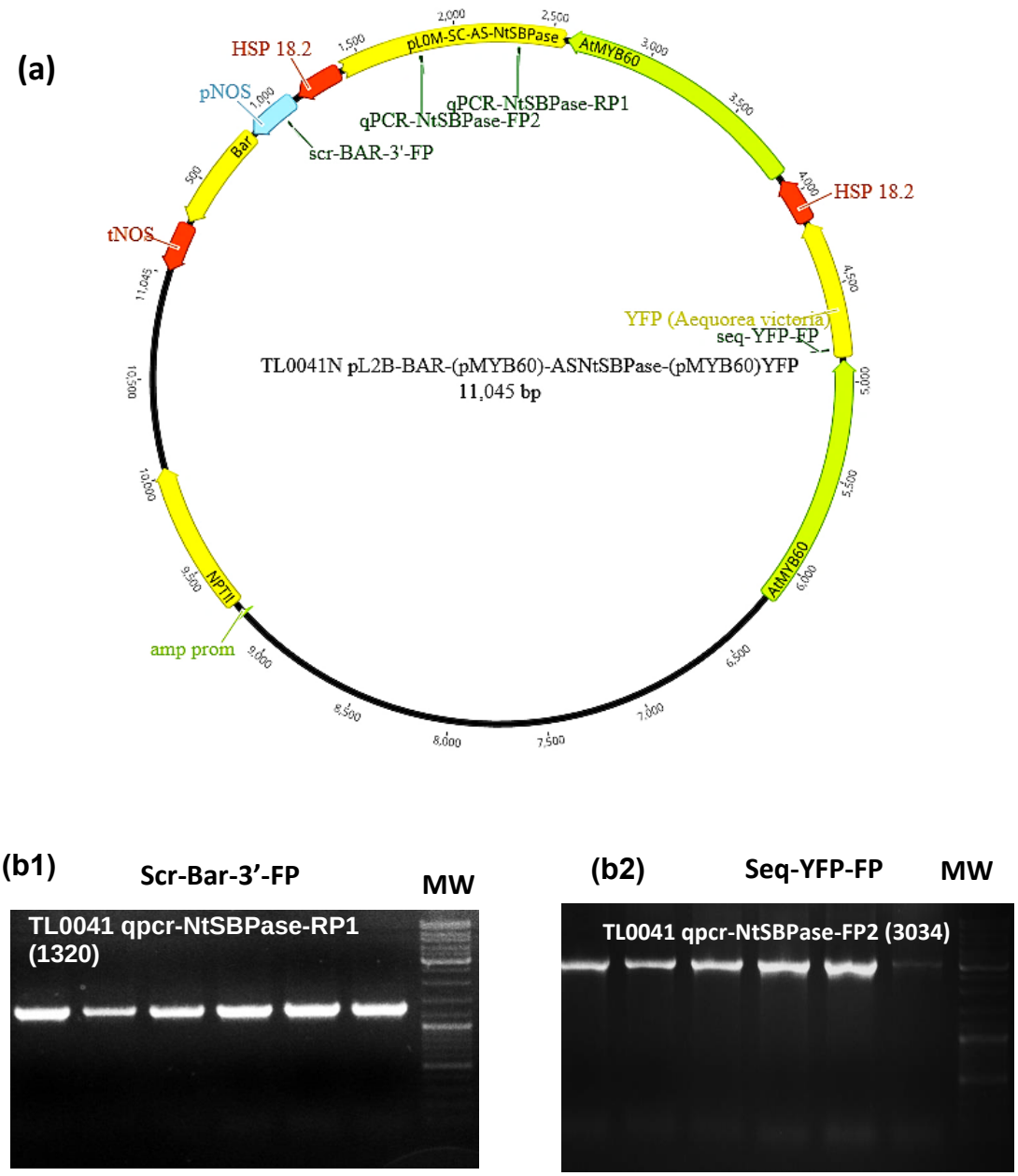

Figure 4. 6. Construct map for level two plasmid (pL2B-BAR-(pMYB60)-ASNtSBPase-(pMYB60)YFP) for expression of SBPase in plants. **(a)** Plasmid contains the genetic modules of level one assembled together of MYB60 promoter, ASNtSBPase coding sequences, bar gene with its respective promoter and terminator for herbicide selection and the YFP together with its promoter and terminator for the yellow fluorescence protein expression in guard cells. **(b1)** First reaction with Scr-Bar-3'-FP as the forward primer and qpcr-NtSBPase-RP1 as the reverse primer yielding 1320bp as expected of the construct. **(b2),** second reaction using Seq-YFP-FP and qpcr-NtSBPase-FP2 for forward and reverse primers respectively yielding exact DNA fragment size of 3034bp. The expression vector produced also carries the NPTII genes for kanamycin selection in bacteria. Construct designed by geneious www.geneious.com

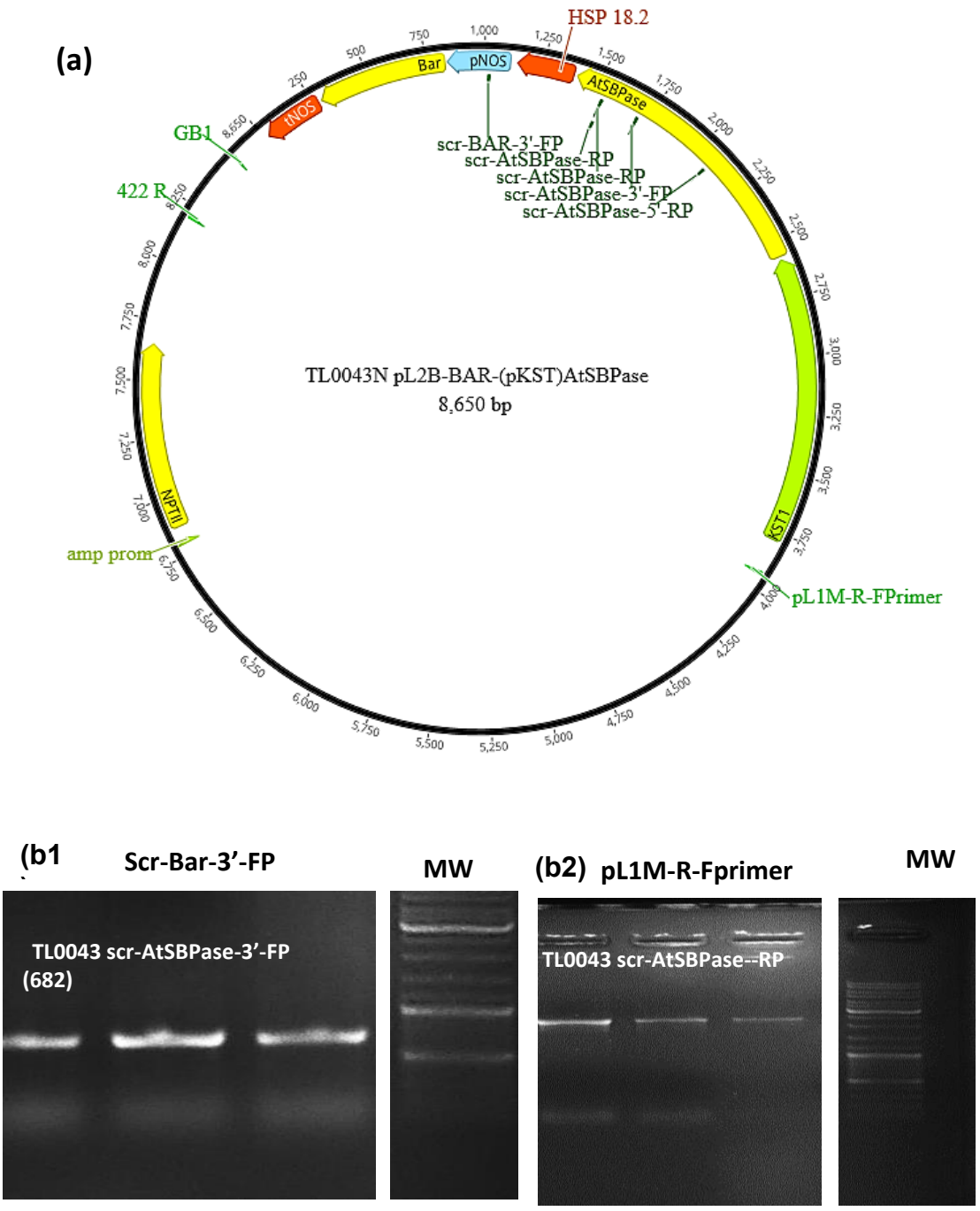

Figure 4. 7. Construct map for level two plasmid (pL2B-BAR-(pKST1)-AtSBPase) for over-expression of SBPase in plants. (a) Plasmid contains the genetic modules of level one assembled together of KST1 promoter followed by AtSBPase coding sequences and terminator. The expression vector produced also carries the NPTII genes for kanamycin selection in bacteria and the BAR gene as a selective marker for Basta herbicide selection in plants. **(b1)** First reaction with Scr-Bar-3'-FP as the forward primer and Scr-AtSBPase-3'-FP as the reverse primer yielding 682bp as expected of the construct. **(b2)** Second reaction using and pL1M-R-Fprimer and scr-AtSBPase--RP for forward and reverse primers respectively yielding exact DNA fragment size of 2429bp. The expression vector produced also carries the NPTII genes for kanamycin selection in bacteria. Construct designed by geneious www.geneious.com**.**

All constructs were used as templates in order to amplify the desired fragment which were transformed in TOP 10 competent E.*coli*. The construction of all level two (table 4.3) were successfully transformed in TOP 10 competent E.*coli*. Evidence for all constructs are shown on Figs 4.9 and 4.10 in colony PCR/gel respectively.

4.4 Transformed *E.coli* colony selection

The efficiency of golden gate cloning technique was demonstrated by the positive growth of transformed *E.coli* colonies in (Fig 4.8). Growth yielded more of white colonies than orange colonies indicating high and efficient transformation. Furthermore, all white colonies picked and tested by PCR showed positive which affirmed successful transformation. Fig 4.8 below shows the transformation efficiency indicated by colour selection. Few orange colonies indicates nontransformed construct.

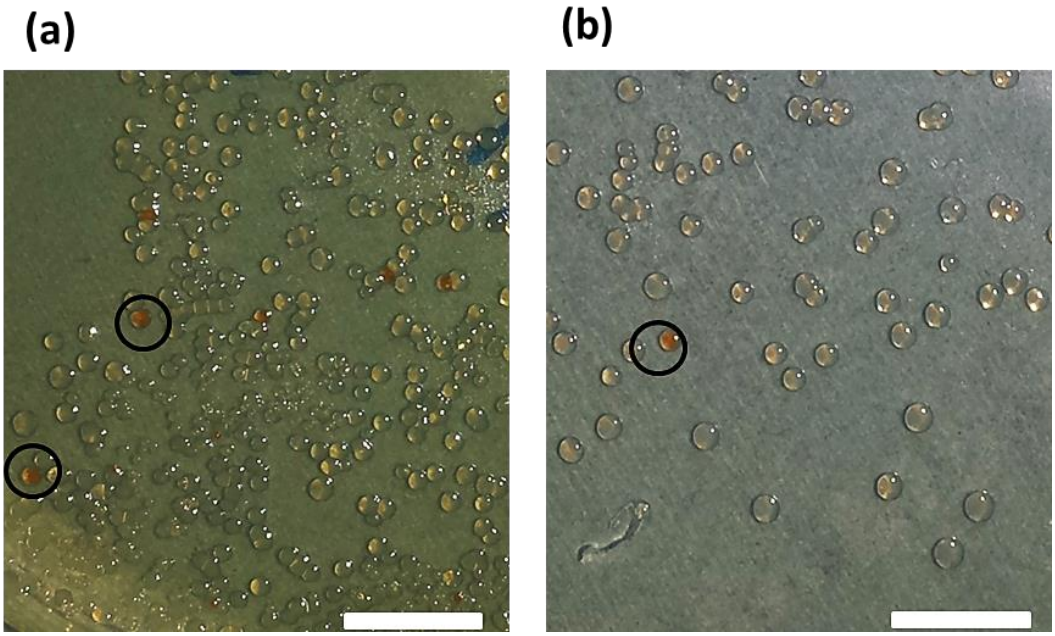

Figure 4. 8. Selection on plates showing cloning efficiency of level two constructs (a) pL2B-BAR-(pKST)AtRieske and (b) pL2B-BAR-(pKST)AtSBPase-(pKST)YFP of an overnight luxuriant growth of transformed *E .coli* cells. Majority of colonies (white) indicates transformed cells while few (orange colonies) indicates untransformed cells. The selection of colonies were performed on plate incorporated with kanamycin (50 µg/mL) and grown overnight at 37°C. Scale bar 2cm.

4.4.1 Selection and determination of fragment sizes in E .coli colonies

The colony PCR results showing exact fragment sizes transformed and analyzed by gel electrophoresis for the first and second reaction are presented below on Fig. 4.9 and 4.10. The codes represents the construct as listed on table 4.3. All three and in some cases six colonies selected per construct showed positive**.** The fragments of interest were amplified using DNA Polymerase and bands of interest yielded exact base pairs as expected.

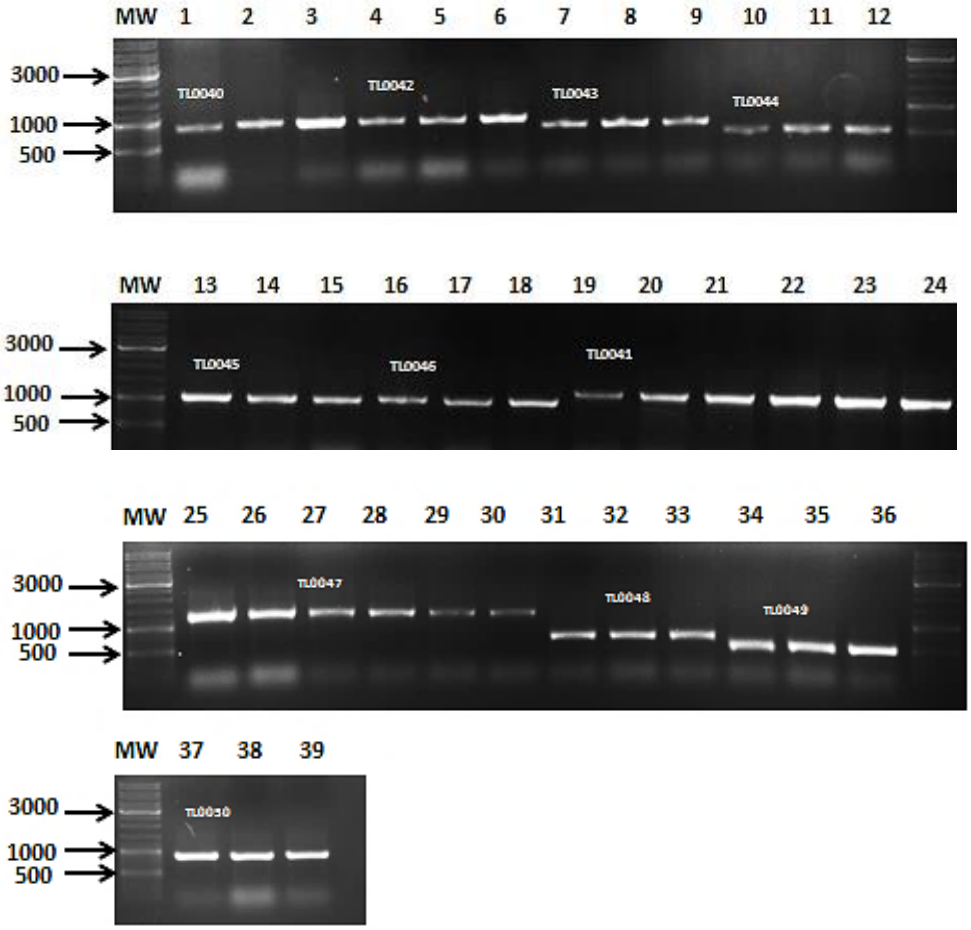

Figure 4. 9. Colony-PCR (first reaction) of the eleven constructs analysed by gel electrophoresis. The presence of the fragments of interest were cloned and checked using the forward primer Sc-Bar-3'-FP and reverse primers (see table 4.3 above) for complete list of reverse primers used for amplification of each construct fragments.The fragments of interest yielded bands as expected in all the colonies selected per construct (denoted here by their codes). TL0040 **(1-3)** 805bp, TL0042 **(4-6)** 854bp, TL0043 **(7-9)** 682bp, TL0044 (10-12) 512bp, TL0045 **(13-15)** 1033bp, TL0046 (16-18)1039bp,TL0041 **(19-24)**1320bp, TL0047 **(25-30)** 1329bp, TL0048 **(31-33)** 687bp, TL0049 **(34-36)** 513bp and TL0050 **(37-39)** 868bp. Samples run alongside a molecular weight marker DNA generular ladder mix from thermos scientific MW in base pairs.

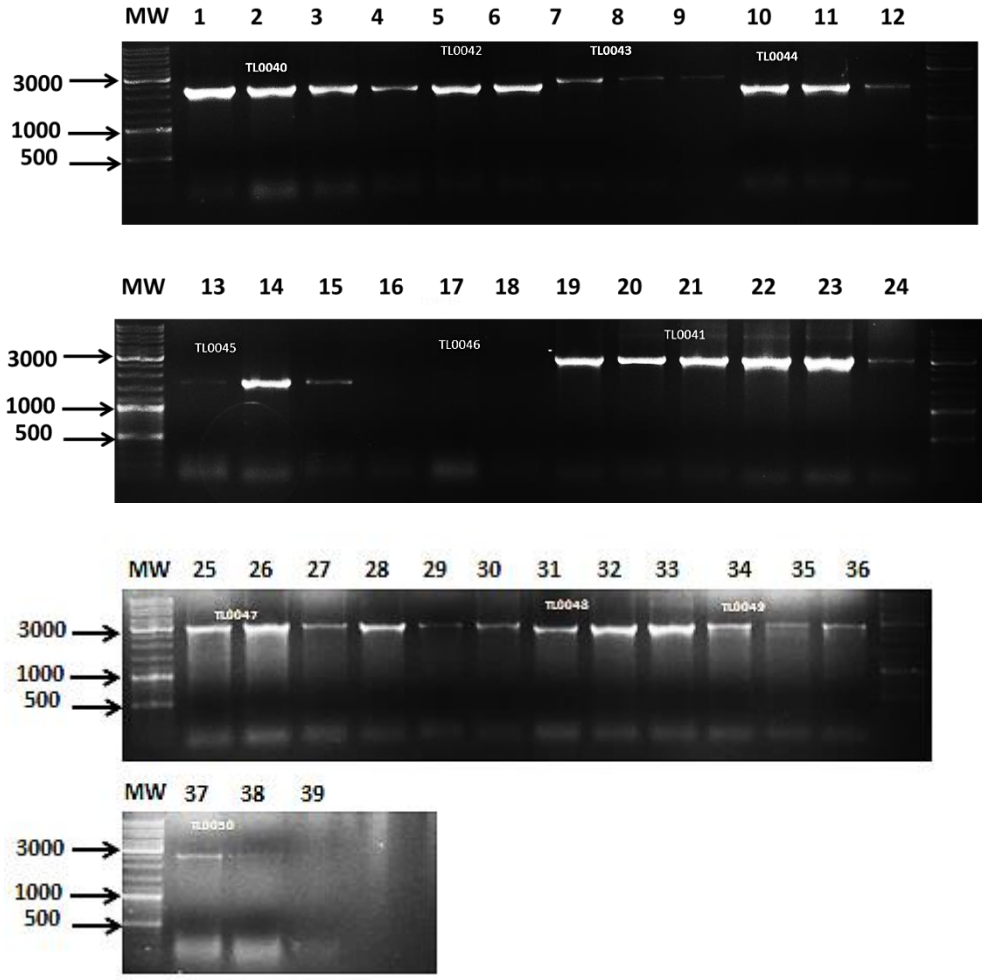

Figure 4. 10. Colony-PCR (second reaction) of the eleven constructs analyzed by gel. The presence of the fragments of interest were cloned and checked using the forward primer pL1M R-Fprimer and Seq-YFP-FP and reverse primers (see table 4.3 complete list of primers for amplification of such fragments. The fragments of interest yielded bands as expected in all the colonies selected per construct. TL0040 **(1-3)** 2240bp, TL0042 **(4-6)** 2132bp, TL0043 **(7-9)** 2429bp TL0044 **(10-12)** 1718bp, TL0045 **(13-15)** 1699bp, TL0046 **(16-18)** negative control,TL0041 **(19-24)** 3034, TL0047 **(25-30)** 2933bp,TL0048 **(31-33)** 2681bp, TL0049 **(34-36)** 2698bp and TL0050 **(37-39)** 2501bp. Samples run alongside a molecular weight marker (DNA generular ladder mix from thermos scientific) MW in base pairs.

4.5. Selection and determination of fragment sizes in *Agrobacterium* colonies

The transformation of *Agrobacterium tumefaciens* strains LBA 4404 for tobacco and GV3101 for Arabidopsis by electroporation were carried out for final transfer of the constructs into plants. Figs. 4.11 (in Arabidopsis plants) and 4.12 (in tobacco plants) show the final confirmation of the presence of the constructs to be transferred into the plants. These yielded the same desired fragments sizes as the *E.coli* plasmids that were sequenced. Agrobacterium colonies carrying desired constructs of interest were screened by PCR and DNA polymerase amplified expected sizes of fragments.

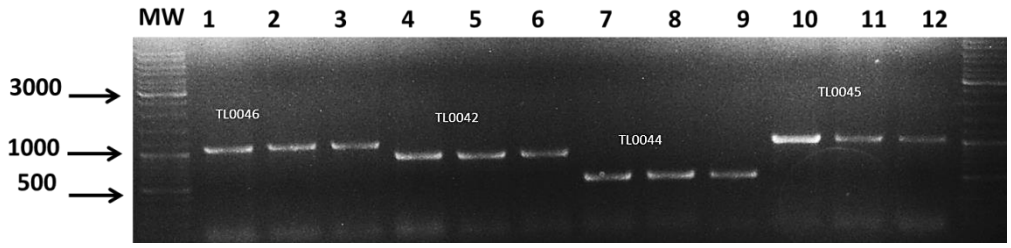

Figure 4. 11.Colony PCR analysis of *Agrobacterium* in Arabidopsis constructs. The presence of the fragments of interest were checked using the same primers used for the E. coli transformation, forward primer Sc-Bar-3'-FP and reverse primers for amplification of such fragments. The fragments of interes (in four constructs above) yielded bands as expected in all the colonies selected per construct. TL0046 **(1-3)**1039bp, TL0042 **(4-6)** 854bp, TL0044 **(7-9)** 682bp and TL0045 **(10-12)** 1033bp. PCR products run alongside molecular weight markers (DNA generular ladder mix from thermoscientific) MW in base pairs

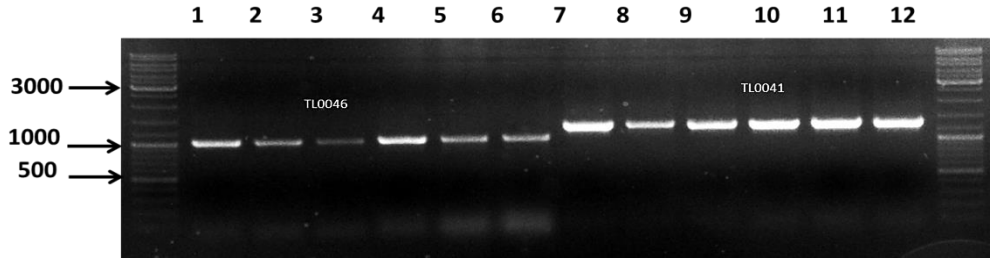

Figure 4. 12. Colony PCR analysis of Agrobacterium in tobacco constructs. The presence of the fragments of interest were cloned and checked using the forward primer Sc-Bar-3'-FP and reverse primers for amplification of such fragments. The fragments of interest (in two constructs above) yielded bands as expected in all the colonies selected per construct. TL0046 (1-6)1039bp and TL0041 (7-12) 1320bp. PCR products run alongside molecular weight markers (DNA generular ladder mix from thermoscientific) MW in base pairs.

DISCUSSION

Desired phenotypes are generated by multiple combinations of various coding sequences. This however, does not necessarily need to operate at genome level but methods that allow generation of constructs containing enough genes for pathway engineering (Weber at al, 2011).

This chapter has utilized optimal efficiency of constructing raw pieces of DNA that allowed the assembly of its discrete functional genetic materials as evidently shown. The Golden gate technique has also simplified the assemblage of these constructs coupled with minimal number of cloning steps and times required.

The construct design which was based on the principles of having a set of compatible overhangs or fusion sites, specific colour selection indicating presence of successful transformation and specific antibiotic selection markers have all been demonstrated in this chapter thereby yielding successful transformation. These have all yielded the desired results as shown on Figs 4.3 and 4.4 used as examples for the level one constructs indicated by the assembling of the modules into transcription units of the level one. The assemblage of level one modules into level two (Fig 4.5-4.7) and Fig 4.9 showing the efficiency of the cloning where white successful colonies dominated the untransformed ones agreeing with Engler et al (2008) confirming the high efficiency of this technique.

Overall, Fig 4.11 and 4.12 showing the colony PCR of all the constructs indicated the DNA fragment sizes as expected. The presence and size of the bands of all the constructs have further confirmed the functionality of these constructs in the plant system that will be shown in the subsequent chapter.

The following chapter therefore describes the production of transgenic homozygous Arabidopsis and tobacco plants coupled with its characterization of these plants using the

constructs presented in this chapter. These will also present the potential these plants will have for the future advances exploiting guard cell functions.

CHAPTER FIVE

PRODUCTION AND CHARACTERISATION OF TRANSGENIC (*ARABIDOPSIS THALIANA* AND *NICOTIANA TOBACCUM)* PLANTS MANIPULATED WITH EXPRESSION OF CYTOCHROME B_6F (RIESKE) AND SEDOHEPTULOSE-1,7-BISPHOSPHATASE (SBPASE).

INTRODUCTION

Stomata play a vital role in photosynthesis by serving as a medium for gas exchange. Improving photosynthesis has shown and can contribute toward greater food security in the coming decades as a result of climate change and world population increase. Hence, increasing photosynthesis will mean improving stomatal functions towards achieving greater WUE and plant productivity. Lawson and Blatt (2014) highlighted of an importance of having greater knowledge and understanding of the physiological and molecular mechanisms that mediates the speed of stomata and coordination with mesophyll demands for CO_2 towards achieving this crucial goal. Genetic mutants especially in Arabidopsis have already begun to reveal the mechanisms that mediate regulation of stomatal conductance (Kelly et al., 2013, Azoulay-Shemer et al., 2015, Wang et al., 2014a).

Transgenic plants with guard cells specific manipulation are therefore important for identification and characterisation of the signal transduction mechanisms that mediate such regulation of stomatal conductance. It is thus obvious that the statement made by Lawson, (2009) cannot be emphasised enough that the understanding of mechanisms coordinating A and g_s demands cell to cell basis of molecular analysis. Therefore, guard

cell photosynthesis demands genetic analyses by guard cell-specific manipulation of photosynthesis. Multiple targets have been identified and could be manipulated to aid more understanding to maximize crop production. Some of these targets are the SBPase and Rieske enzymes which have demonstrated of their significance in controlling photosynthetic processes.

This chapter describes the process of generation or production and characterisation of these transgenic homozygous plants from the constructs presented in the previous chapter. Full-length tobacco and Arabidopsis SBPase (AT3655800) and Rieske (AT 4G03280) were used to generate expression constructs described and subsequent transformation by Agrobacterium carrying these desired constructs were transformed into our Arabidopsis and tobacco genome plant. All homozygous lines were compared to the wild type (Col-0) in the Arabidopsis plants while tobacco transgenic plants compared to both nontransformed azygous controls recovered from the segregating population verified by iDNA (Bartlett et al., 2008). Three to five independent lines were identified for each construct from both Arabidopsis and tobacco plants.

For order and clarity purposes, these will be presented separately starting with the Arabidopsis plant.

RESULTS

AS5.1 Selection of Arabidopsis transformants

Transformed floral plants in the Arabidopsis plants were allowed to mature to seed. Seeds were collected and planted for the screening of the T1 generation and selection of positive transformants achieved. Selection of positive transformants was identified by the

application of BASTA watered on the soil in which the T1 germinated seedlings as transformants were resistant to the herbicide. Image below on Fig 5.1.

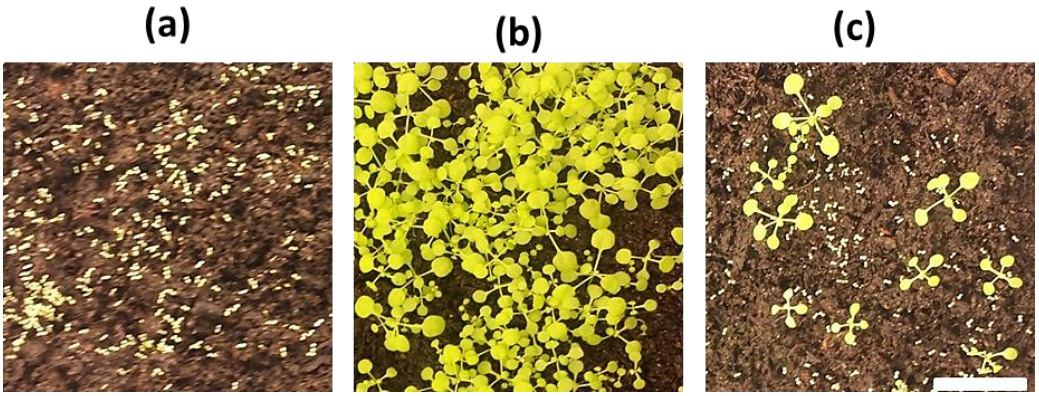

.

Figure 5. 1. Hebicide (BASTA) selection of transformed Arabidopsis plants. Resistant transformants were selected by growing on soil and spraying with BASTA (presence of bar gene confers resistance to the glofusinate ammonium herbicide BASTA). (a) WT control showing complete death of cotyledons grown on BASTA, (b) WT control grown without BASTA and (c) selection of resistant transformants grown on soil watered with BASTA. Plants growth conditions maintained under controlled-environment growth room with (22°C, 8 h light, 16 h dark cycle). White scale bar represents 1cm.

.

The resulting successful transgenic plants (T1 generation) were selected on the herbicide glofusinate ammonium (BASTA) and subsequent screening for homozygous lines began by PCR followed by confirmation by iDNA technology.

5.2 DNA analysis of T1 generation plants.

The result (selected transformed T1 plants) from Fig 5.1 above and tissues from individual plants were check for the presence of the transgene by PCR analysis. The result of the DNA analysis produced PCR fragment sizes exactly as the gene of interest in all the lines screened. The constructs pL2-BAR-(pKST1)-AtRieske-tHSP (512bp) and pL2B-BAR-(pKST1)-AtSBPase-YFP-tHSP (687bp) presented below (Fig.5. 2) used as

examples of all constructs have shown all ten lines selected positive for the presence of the transgene.

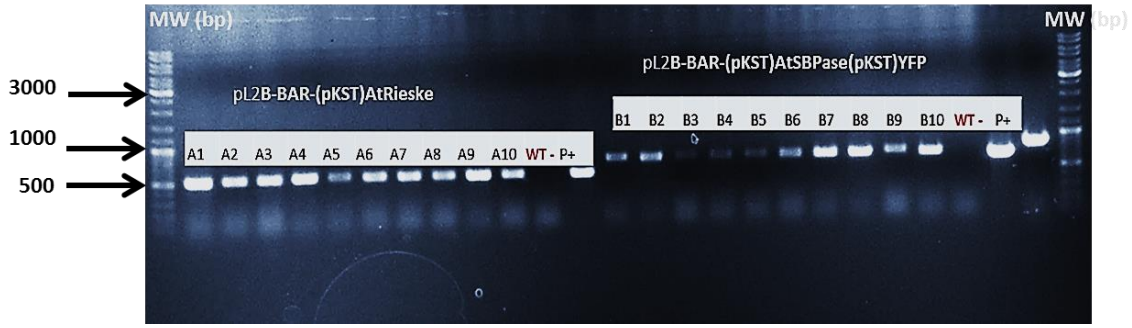

Figure 5. 2. Genomic DNA PCR screening of transformants for presence of the transgene. The presence of transgenes were checked by PCR analysis of genomic DNA of T1 plants pL2-BAR-(pKST1)-AtRieske-tHSP(512bp) and pL2B-BAR-(pKST1)-AtSBPase-YFP-tHSP (687bp).Ten lines were screened per construct. WT DNA (WT+red) and plasmid DNA containing the gene of interest (P+) were used as negative and positive controls respectively. PCR products were run alongside molecular weight marker (DNA generuler ladder mix from thermoscientific) in base pairs.

5.3. Identification and assessment of copy numbers in *Arabidopsis thaliana* Rieske vand SBPase plants.

iDNA technology was used to determine Arabidopsis T-DNA insertion copy numbers. All constructs were confirmed to have T-DNA and constructs with lesser copy numbers or inserts (1 at most) from first generation were carried forward for the next generation selection. See result in appendix.

5.3.1 Fluorescence Microscopy to detect YFP expression in guard cells

SBPase and Rieske YFP mutants T1 plants were rapidly screened for the presence and localization of the yellow fluorescence protein (YFP) specifically in guard cells using high resolution chlorophyll fluorescence microscope. Constructs fused to the yellow fluorescence protein confirmed that expressions driven by the cells specific promoters were confined to the guard cells. In total, all 83 plants analysed were found with

detectable levels of YFP expression. Constructs tagged with either the MYB60 promoter or KST1 promoter revealed the guard cells with the YFP in them while wild type control had no signal. The Fig 5.3 below shows this.

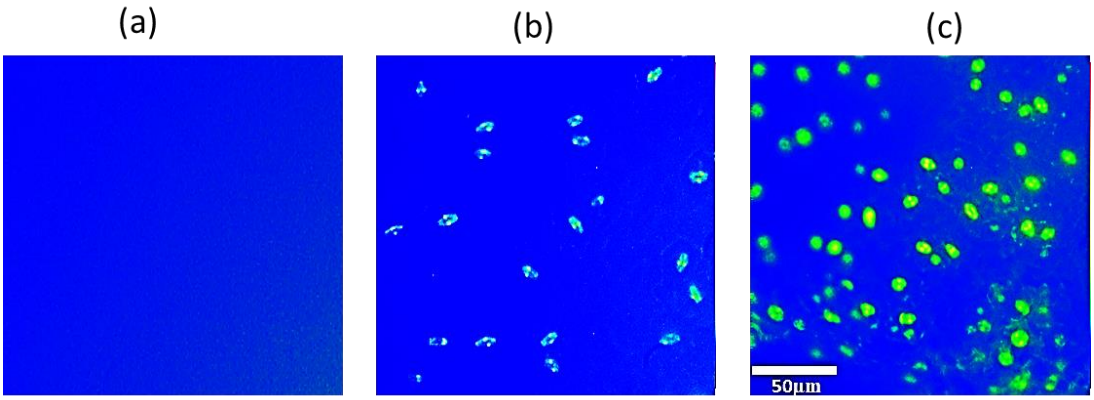

Figure 5. 3. Specific YFP expression in the guard cell of T1 generation. Localization of the YFP in the chloroplasts of guard cells of Arabidopsis transformants**. (a)** Wild type (Col-0) tissue showing no signal while **(b)** Expression of the constructs tagged with YFP and driven by the MYB60 promoter in (pL2B-BAR-(pMYB60)-ASNtSBPase-(pMYB60)YFP)-tHSP and **(c)** KST1 promoter in pL2B-BAR-(pKST1)-AtSBPase-(pKST1)YFP-tHSP in leaf tissue were checked using the High resolution microscope. Images acquired by exiting with 515 nm LEDs and emission collected with a band pass filter 530 ± 20).

Table 5.1 below combines both the successful outcome of plants selected for screening with PCR and the high resolution microscope. This also illustrates the efficiency of the guard cell specific promoters KST1 and MYB60. All the plants of T1 generation selected for both processes were found positive.

Table 5. 1. Number of transformants and positive lines expressing YFP in the guard cells of a leaf tissue under the guard cells specific promoters MYB60 and KST1.

Constructs	No of transformed plants selected on Basta	PCR screened and positive plants		YFP Microscopy screened and positive plants	
		No of screened plants	No of positive plants	No of screened plants	No of positive plants
pL2B-BAR-(pKST)YFP	17	10	10	17	17
pL2B-BAR-(pMYB60)-ASNtSBPase-(pMYB60)YFP	9	9	8	8	8
pL2B-BAR-(pKST)ASNtSBPase-(pKST)YFP	20	10	10	20	20
pL2B-BAR-(pKST)AtRieske-(pKST)YFP	13	10	10	13	13
pL2B-BAR-(pKST)ASNtRieske-(pKST)YFP	15	10	10	15	15
pL2B-BAR-(pKST)AtSBPase-(pKST)YFP	16	10	10	16	16

Combined PCR and YFP analysis of T1 generation of Arabidopsis plants. DNA analysis of Transformed plants of T1 generation yielded all positive results as indicated above and the YFP microscopy also yielded all positive outcome of the selected transformed plants. 9-17 independent lines were screened.

The selection of large number of independent lines makes possible repeatable analysis of the results. Independent lines are designed to minimize the effects of single independent variable which increases the reliability of the results, often through a comparison between lines.

Furthermore, confocal microscope was also used to gain high resolution images of the cell specific expression in T2 generation plants. A Nikon A1si inverted confocal microscope was used to visualize cell specific expression. Expression of the YFP in the guard cells specifically can be clearly seen in this Fig .5.4 below. The lack of signal in the

control plants further proves the specificity of the YFP signal only in the chloroplasts of the guard cells (Fig 5.4).

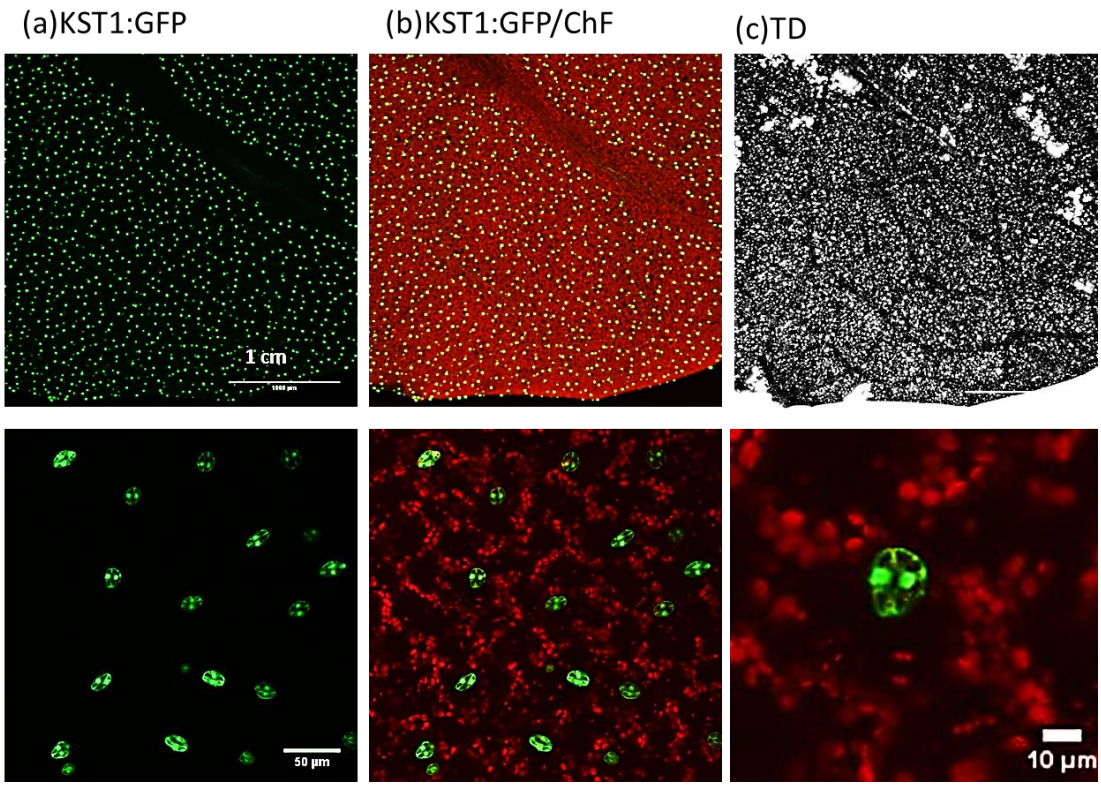

Figure 5. 4. Specific YFP expression in the guard cell of T2 generation. Localization of the YFP in the chloroplasts of guard cells in T2 generation of Arabidopsis transformants (pL2B-BAR-(pKST1)-AtRieske-(pKST1)YFP **(a)** YFP flourescense, **(b)** YFP/Chlorophyll flourescense merged **(c)** bright field (up Expression of the constructs tagged with YFP and driven by the KST1 promoter in leaf tissue were checked using Nikon A1si inverted confocal microscope. YFP images were acquired by exiting at 488nm with lasers and emission collected at 530nm. Chlorophyll auto fluorescence exited at 480 nm with emission collected at 685 nm.

Having confirmed the presence of the constructs in the guard cells of the plants, homozygous T3 plants were further carried forward for physiological analysis. The following plants with the constructs 4-(pL2B-BAR-(pKST1)-AtRieske-tHSP, 6-(pL2B-BAR-(pKST1)-AtSBPase-tHSP, 9-(pL2- BAR- (pKST1)-AtRieske-tHSP-YFP-tHSP) and

11-(pL2B-BAR-(pKST1)-AtSBPase-YFP-tHSP) were selected for characterisation in the Arabidopsis plants. The numbers 4, 6, 9 and 11 attached to the construct represents constructs names in short form. For instance 4 means construct pL2B-BAR-(pKST1)-AtRieske-tHSP which is also written as 4-(pL2B-BAR-(pKST1)-AtRieske-tHSP. Subsequent numbers that followed represent independent lines e. g 4.3.1.

5.4 Physiological analysis

5.4. 1 Photosystem ll operating efficiency and growth analysis

The first obvious thing observed in the transgenic lines was the clear evidence of phenotypes in all the four constructs selected for further analysis.

Observations revealed developmental phenotypes in the early stage of plants growth between the WT and transgenic lines. Fig 5.5-5.8 below shows the phenotype evident between the WT and the mutant within each construct of four weeks old plants. The total rosettes or leaf area of the transgenic plant of the lines within the construct 4-pL2B-BAR-(pKST1)-AtRieske-tHSP evidently showed larger leaf area.

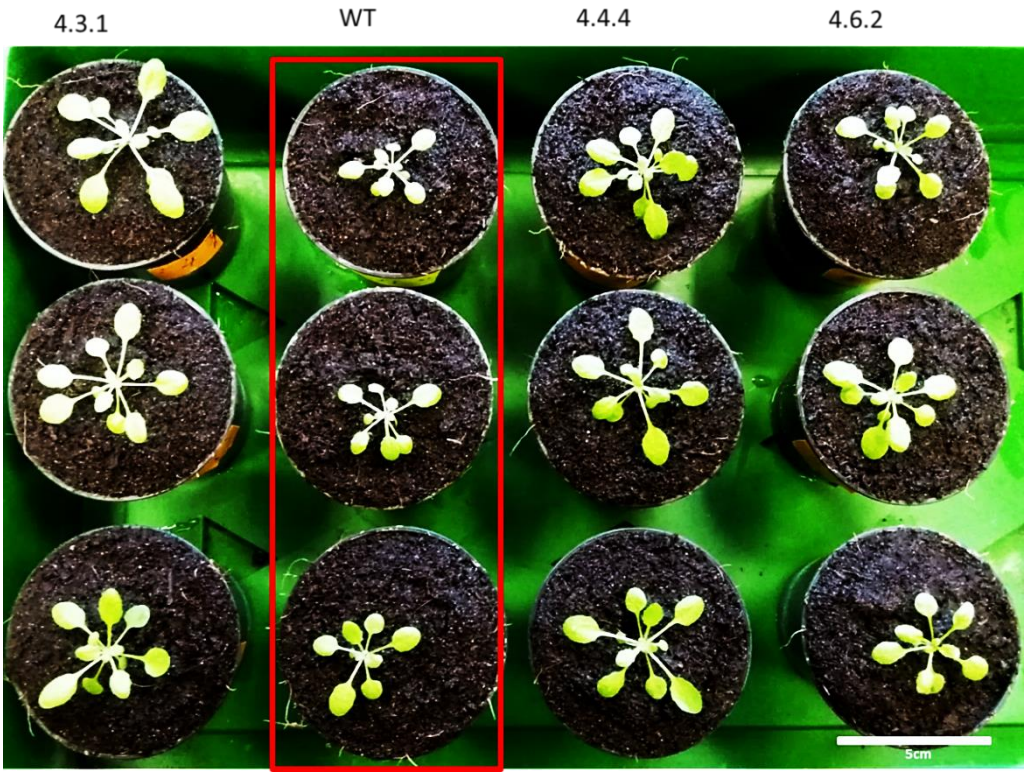

Figure 5. 5. Growth phenotype of WT and homozygous mutant lines of construct 4-(pL2B-BAR-(pKST1)-AtRieske-tHSP plants grown on Soil.4–weeks old plants were germinated and grown for 14 days on soil before picked out and transferred individually to pots. Plants were grown under identical conditions in a controlled-environment growth room with (22°C, 8 h light, 16h dark cycle). *Arabidopsis thaliana* (Col-0) WT and mutant lines are shown. White scale bar represents 5 cm.

The following phenotype observed in the construct 6 which is the same as 6-(pL2B-BAR-(pKST1)-AtSBPase-tHSP below shows the phenotype evident between the WT and the mutant lines within the construct. The construct 6-(pL2B-BAR-(pKST1)-AtSBPase-tHSP evidently showed larger leaf area as shown below (Fig. 5. 6).

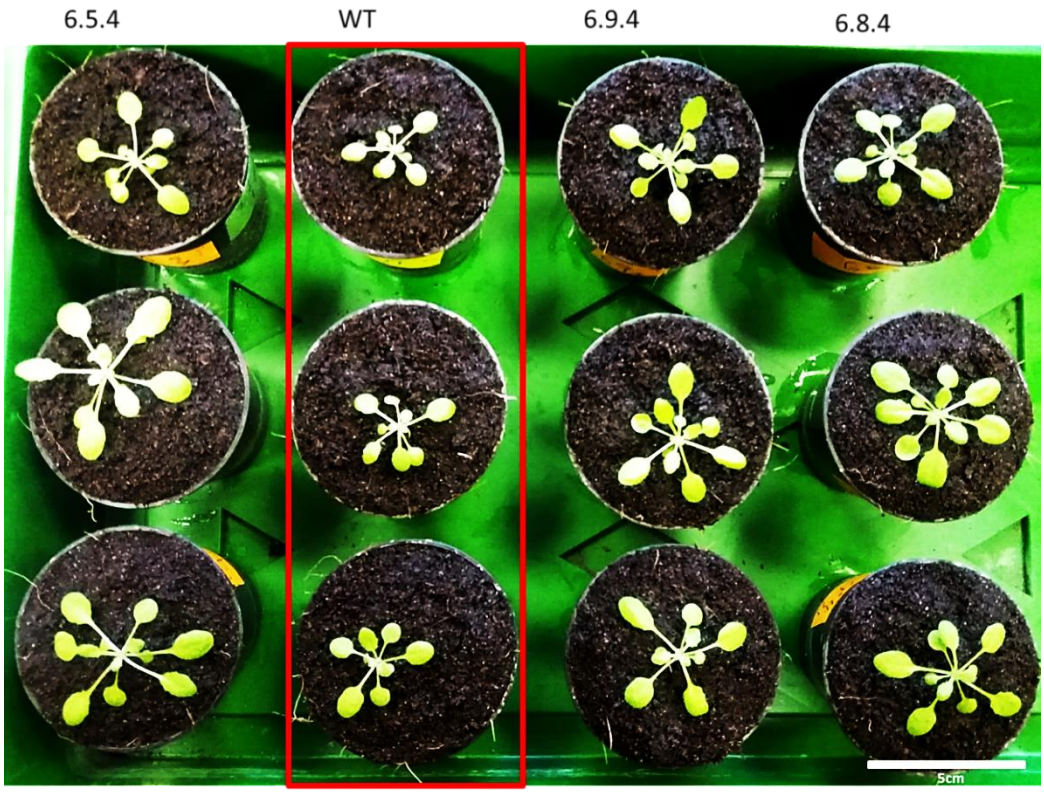

Figure 5. 6. Growth phenotype of WT and homozygous mutant lines of construct 6-(pL2B-BAR-(pKST1)-AtSBPase-tHSP plants grown on Soil. 4–weeks old plants were germinated and grown for 14 days on soil before picked out and transferred to soil. Plants were grown under identical conditions in a controlled-environment growth room with (22°C, 8 h light,16h dark cycle). *Arabidopsis thaliana* (Col-0) WT and mutant lines are shown. White scale bar represents 5 cm.

The construct (Fig 5.7) below which is a Rieske construct but tagged with the YFP 9-pL2-pKST1-AtRieske-tHSP-YFP-tHSP also exhibited a remarkable difference between the WT and transgenic lines as those above. Transgenic lines evidently showed larger leaf area.

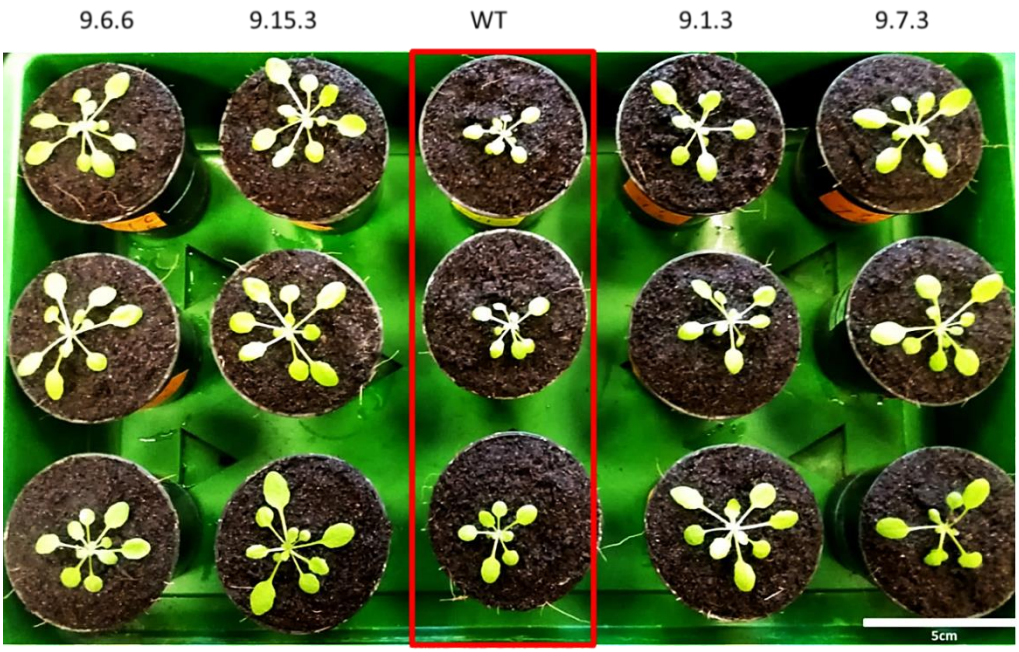

Figure 5. 7. Growth phenotype of WT and homozygous mutant lines of construct 9-(pL2-pKST1-AtRieske-tHSP-YFP-tHSP) plants grown on Soil. 4–weeks old plants were germinated and grown for 10–14 days on soil before picked out and transferred to soil. Plants were grown under identical conditions in a controlled-environment growth room with (22°C, 8 h light, 16 h dark cycle). *Arabidopsis thaliana* (Col-0) WT and mutants lines are shown. White scale bar represents 5 cm.

Finally, the construct 11-(pL2B-BAR-(pKST1)-AtSBPase-YFP-tHSP), an SBPase construct tagged with YFP also showed a remarkable phenotype between the WT and transgenic lines as all the constructs. Transgenic lines evidently showed larger leaf areas (Fig 5.8) below.

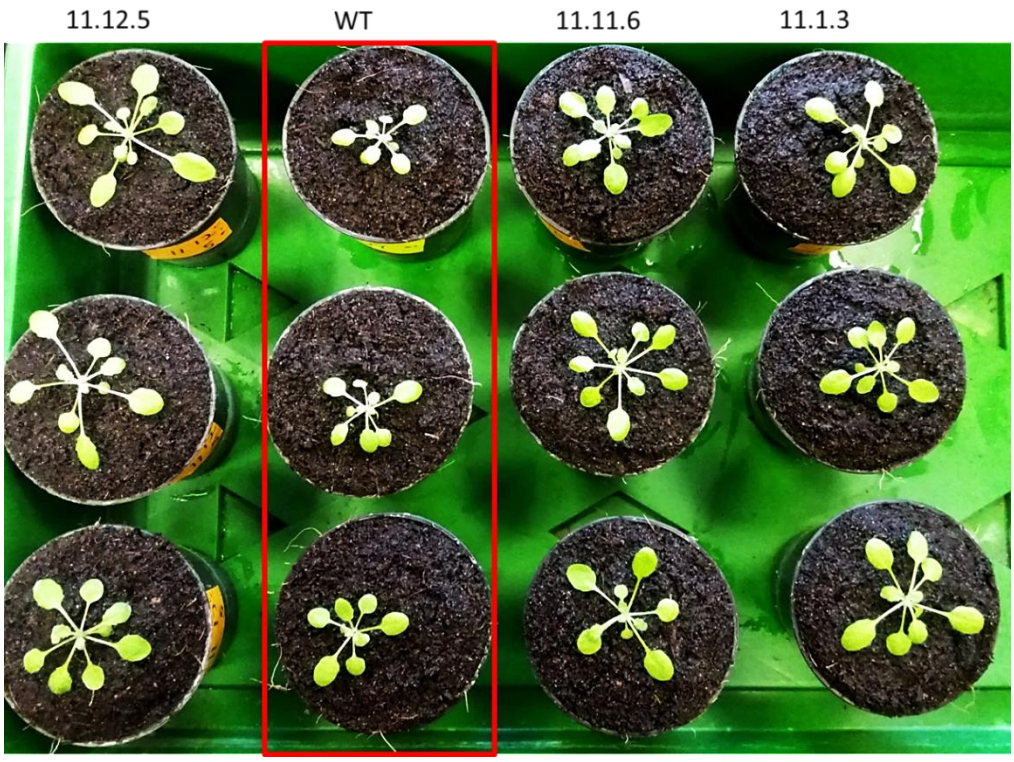

Figure 5. 8. Growth phenotype of WT and homozygous mutant lines of construct 11- (pL2B-BAR-(pKST1)-AtSBPase-YFP-tHSP) grown on soil..4–weeks old plants were germinated and grown for 14 days on soil before picked out and transferred to soil. Plants were grown under identical conditions in a controlled-environment growth room with (22°C, 8 h light, 16 h dark cycle). *Arabidopsis thaliana* (Col-0) WT and mutants lines are shown. White scale bar represents 5 cm.

Chlorophyll fluorescence imaging was also performed on the plants and the operating efficiecny of PSII photochemistry (*Fq'/Fm'*) determined. Chlorophyll fluorescence imaging of WT and mutant lines of construct 4-(pL2B-BAR-(pKST1)-AtRieske-tHSP (Fig. 5.9) to changes in light intensity subjected to 150 µmol m $^{-2}s^{-1}$ and 600 µmol m $^{-2}s^{-1}$ showed significant differences between the wild type and mutants in the first 3 and 4 weeks of recording confirming also the phenotype found in the images observed above. However, as the plants advanced in the next 2-3 weeks, the reductions in *Fq'/Fm'* of the wild type seemed to catch up with the transgenic lines in all constructs suggesting that the expression of these genes might be most critical in their early stages of development.

There were no significant differences found in the later weeks of the experiment between the wild type and the transgenics.

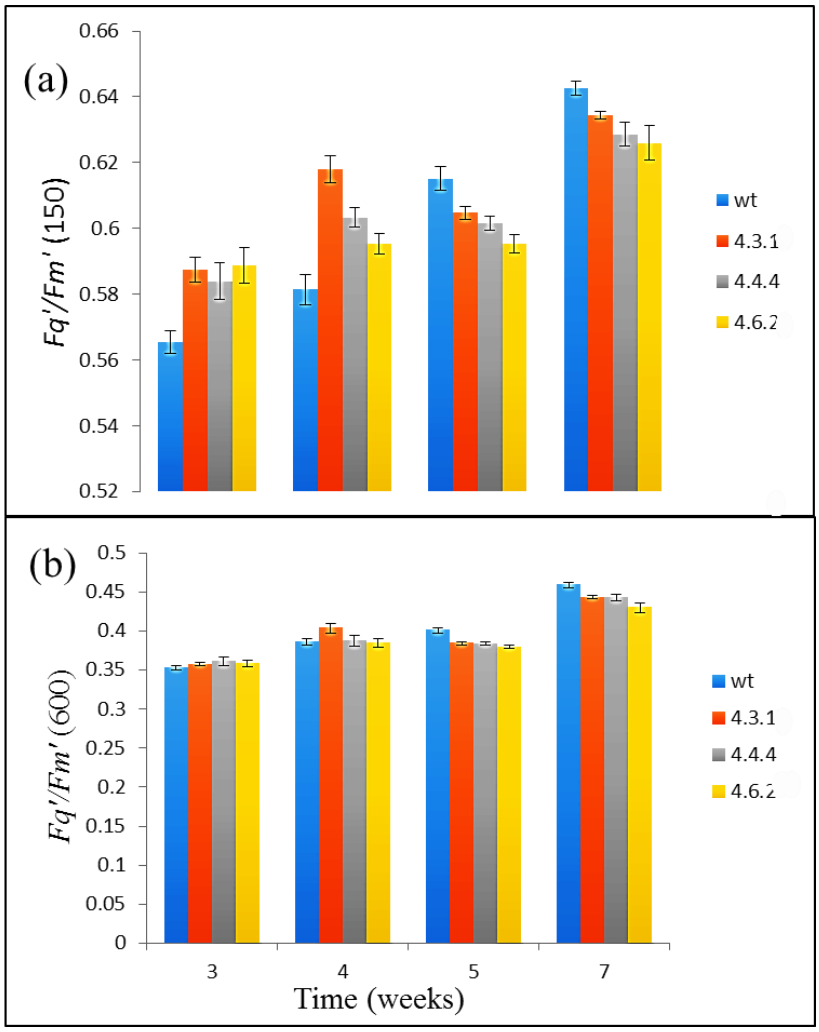

Figure 5. 9. Chlorophyll fluorescence imaging comparison of WT and mutant lines of construct 4-(pL2B-BAR-(pKST1)-AtRieske-tHSP to changes in light intensity. The maximum PSII operating efficiency (Fq'/Fm') values of the whole plant subjected to (a)150 µmol m -2s-1 and (b) 600 µmol m -2s-1 were measured. Plants were germinated and grown for 14 days on soil before picked out and transferred to individual pot on soil. These were grown for additional 5 weeks under identical conditions in a controlled environment growth room (22°C, 8 h light,16 h dark cycle). Arabidopsis thaliana (Col-0) WT and mutants individual lines of the construct 4-(pL2B-BAR-(pKST1)-AtRieske-tHSP measured. Data were obtained using 10-15 individual plants from 3 independent transgenic lines and are derived from weeks 3, 4, 5 and 7. Columns represent mean values, and standard errors are displayed respectively. Significant differences between WT and lines (P< 0.05) at weeks 3 and 4 at 150 µmol m -2s-. Each line was significantly different from wild type WT. At higher light level of 600 µmol m -2s-.1 no difference between the wild type and transgenic found in all the lines.

Similarly, chlorophyll fluorescence imaging of WT and mutant lines of construct 6-pL2B-BAR-(pKST1)-AtSBPase-tHSP to changes in light intensity subjected to 150 µmol $m^{-2}s^{-1}$ and 600 µmol $m^{-2}s^{-1}$ showed significant differences between the wild type and mutants in the first 3 and 4 weeks of recording (Fig.5.10).

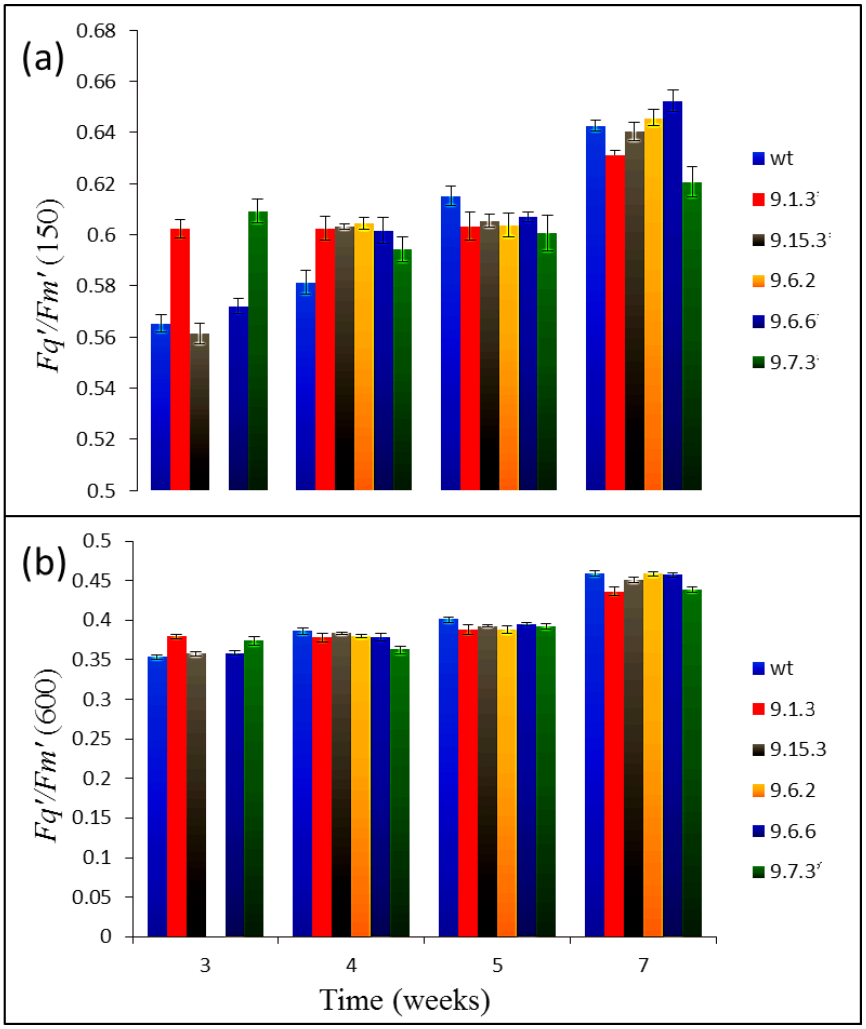

Figure 5. 10. Chlorophyll fluorescence imaging comparison of WT and mutant lines of pL2-BAR--KST1-AtRieske-tHSP-YFP-tHSP construct to changes in light intensity. The maximum PSII operating efficiency (Fq'/Fm') values of the whole plant subjected to (a)150 µmol m $^{-2}s^{-1}$ and (b) 600 µmol m $^{-2}s^{-1}$ were measured. Plants were germinated and grown for 14 days on soil before picked out and transferred to individual pot on soil. These were grown for additional 5 weeks under identical conditions in a controlled environment growth room (22°C, 8 h light, 16 h dark cycle). *Arabidopsis thaliana* (Col-0) WT and mutants lines of the construct 9-pL2-BAR--KST1-AtRieske-tHSP-YFP-tHSP measured in weeks. Data were obtained using 10-15 individual plants from 5 independent transgenic lines and are derived from weeks 3, 4, 5 and 7. Columns represent mean values, and standard errors are displayed respectively. Significant differences between WT and transgenic lines($P < 0.05$) at weeks 3 (9.1.3 and 9.7.3) and week 4 (all lines) at 150 µmol m $^{-2}s^{-1}$ of light intensity. Each line was significantly different from wild type WT. At higher light level of 600 µmol m $^{-2}s^{-1}$ however, there was no difference found between the wild type and transgenic in all the lines.

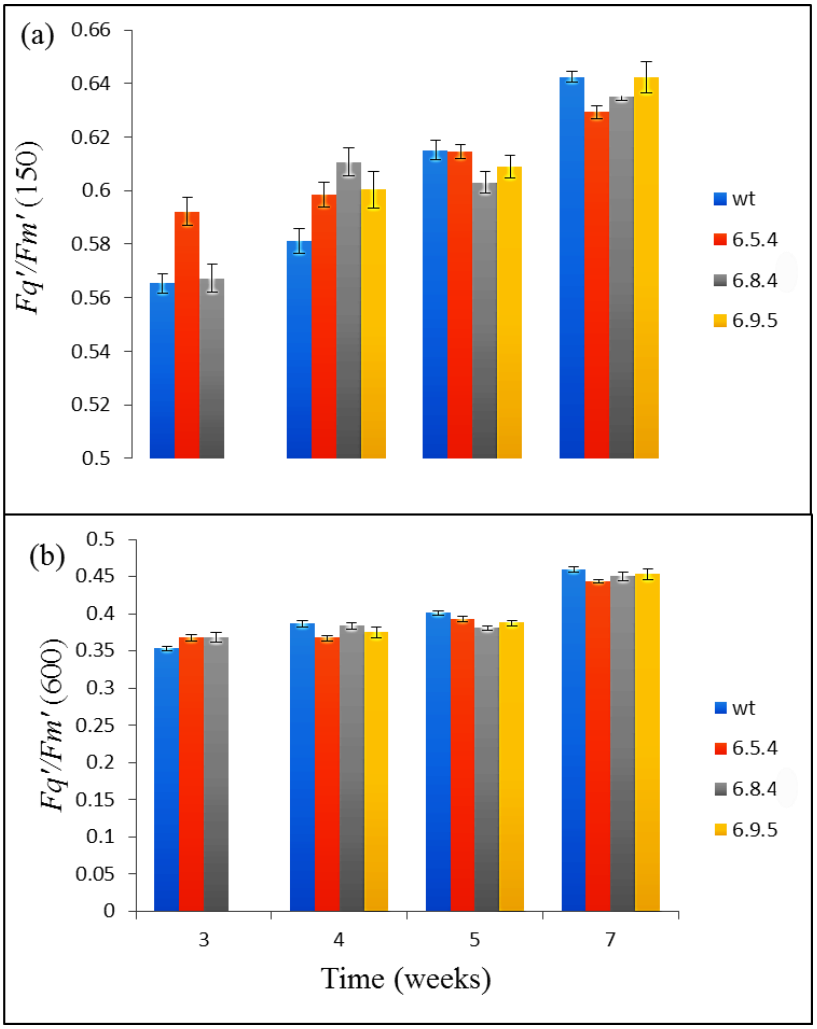

Figure 5. 11 Chlorophyll fluorescence imaging comparison of WT and mutant lines of pL2B-BAR-(pKST1)-AtSBPase-tHSP construct to changes in light intensity. The maximum PSII operating efficiency (Fq'/Fm') values of the whole plant subjected to (a)150 µmol m $^{-2}$s^{-1} and (b) 600 µmol m $^{-2}$s^{-1} were measured. Plants were germinated and grown for 14 days on soil before picked out and transferred to individual pot on soil. These were grown for additional 5 weeks under identical conditions in a controlled environment growth room (22°C, 8 h light, 16 h dark cycle). *Arabidopsis thaliana* (Col-0) WT and mutants representing individual lines of the construct 6- (pL2B-BAR-(pKST1)-AtSBPase-tHSP measured in weeks. Data were obtained using 10-15 individual plants from 3 independent transgenic lines and are derived from weeks 3, 4, 5 and 7. Columns represent mean values, and standard errors are displayed respectively. Significant differences ($P < 0.05$) between WT and transgenic lines at weeks 3 (6.5.4 line) and week 4 (Each line was significantly different from wild type WT) at 150 µmol m $^{-2}$s$^{-.}$ of light. At higher light level of 600 µmol m $^{-2}$s$^{-.1}$ no difference found between the wild type and transgenic in all the lines.

Similarly, operating efficiecny of PSII photochemistry (*Fq'/Fm'*) of WT and mutant lines of construct 9-pL2-BAR--KST1-AtRieske-tHSP-YFP-tHSP to changes in light intensity

subjected to 150 µmol m $^{-2}s^{-1}$ and 600 µmol m $^{-2}s^{-1}$ showed significant differences between the wild type and mutants in the first 3 and 4 weeks of recording (Fig.5.11) below

Similarly, operating efficiecny of PSII photochemistry (*Fq'/Fm'*) of WT and mutant lines of construct 11-pL2B-BAR-(pKST1)-AtSBPase-YFP-tHSP to changes in light intensity subjected to 150 µmol m $^{-2}s^{-1}$ and 600 µmol m $^{-2}s^{-1}$ showed significant differences between the wild type and mutants in the first 3 and 4 weeks of recording (Fig.5.12) below.

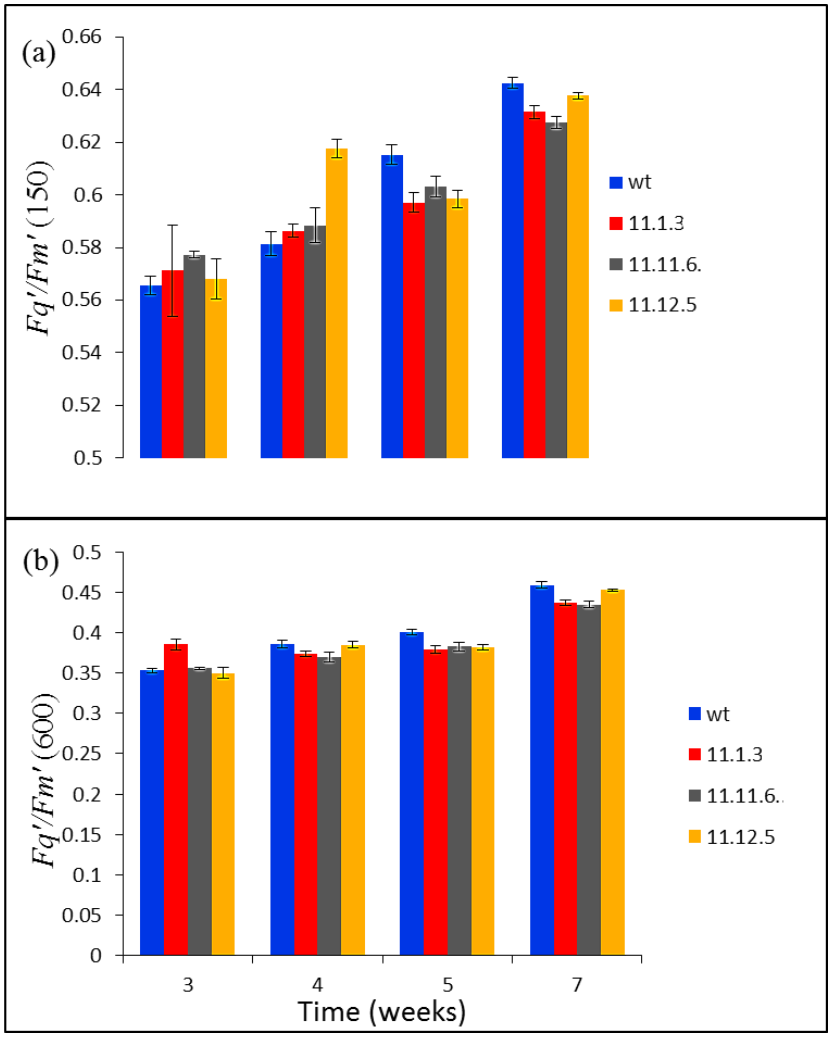

Figure 5. 12. Chlorophyll fluorescence imaging comparison of WT and mutant lines of pL2B-BAR-(pKST1)-AtSBPase-YFP-tHSP construct to changes in light intensity.The maximum PSII operating efficiency (Fq'/Fm') values of the whole plant subjected to (a)150 µmol m $^{-2}s^{-1}$ and (b) 600 µmol m $^{-2}s^{-1}$ were measured. Plants were germinated and grown for 14 days on soil before picked out and transferred to individual pot on soil. These were grown for additional 5 weeks under identical conditions in a controlled environment growth room (22°C, 8 h light, 16 h dark cycle). *Arabidopsis thaliana*(Col-0) WT and mutants lines of the construct 11-(pL2B-BAR-(pKST1)-AtSBPase-YFP-tHSP) measured in weeks. Data were obtained using 10-15 individual plants from 3 independent transgenic lines and are derived from weeks 3, 4, 5 and 7. Columns represent mean values, and standard errors are displayed respectively. Significant differences between WT and transgenic lines ($P< 0.05$) at weeks 3 (line11.11.6) and week 4 (line 11.12.5) at 150 µmol m $^{-2}s^{-1}$. At higher light level of 600 µmol m $^{-2}s^{-.1}$ however, there was no difference found between the wild type and transgenic in all the lines.

Chlorophyll fluorescence imaging used to determine the maximum PSII operating efficiency of photosynthesis (*Fq'/Fm'*) values of the whole plant was also used to capture images at the time of analysis (Fig. 5.13). These images further tells more of the PSII efficiency differences indicated by colours from the scale which ranges from green (lowest value) to orange (highest value). The more the value, the more efficient is the PSII efficiency. Images likewise show the growth differences which were evident between the wild type and transgenic lines. The PSll photosynthetic differences of all the four constructs at week 3 is shown in the figure below which clearly showed a faster growth phenotype with larger rosettes in the transgenic lines than the wild type.

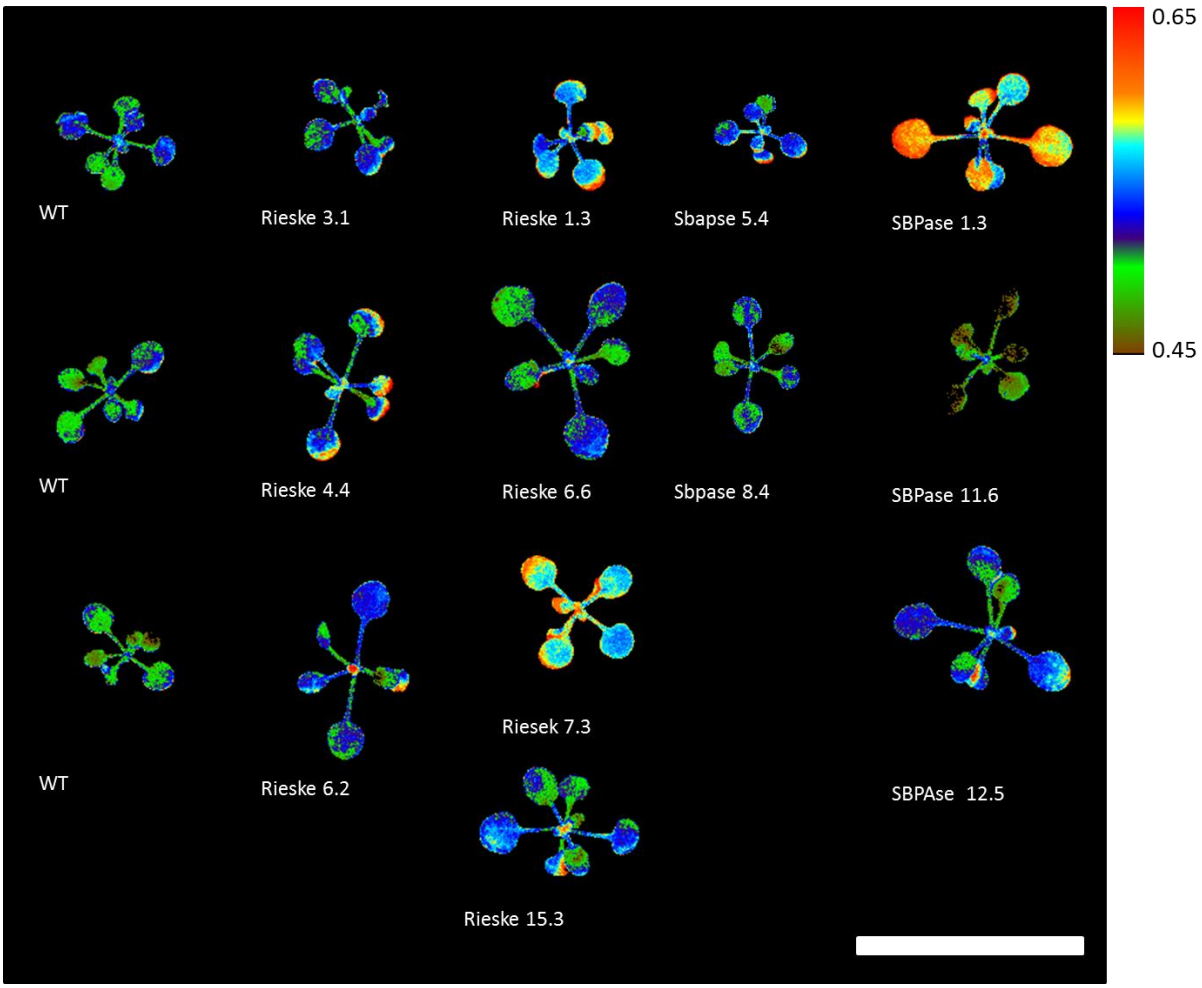

Figure 5. 13. Photosynthetic efficiency of PSll operating systems of images captured of WT and homozygous mutant Arabidopsis plants. 3–weeks old plants were germinated and grown for 14 days on soil before picked out and transferred to individual pots on soil. Plants were grown under identical conditions in a controlled-environment growth room with (22°C, 8 h light, 16 h dark cycle). *Arabidopsis thaliana* (Col-0) WT and mutants are shown. 4-(pL2B- BAR-pKST1-AtRieske) 6- (pL2B-BAR-(pKST1)-AtSBPase), 9-(pL2-pKST1-AtRieske-tHSP-YFP) and 11- (pL2B-BAR-(pKST1)-AtSBPase-YFP) with their respective lines in the third generation. Scale bars represent 5cm and *Fq'/Fm'* values represented by colours as indicated.

Likewise, the photosynthetic efficiency of PSll operating systems of 5 weeks old plants are shown below and values of *Fq'/Fm' exhibited* (Fig 5.14) shown on the scale. At this point of week five, the growth phenotype was clearly evident,as well with rosettes area of the transgenic larger than those of the wild type (Figure 5.14).

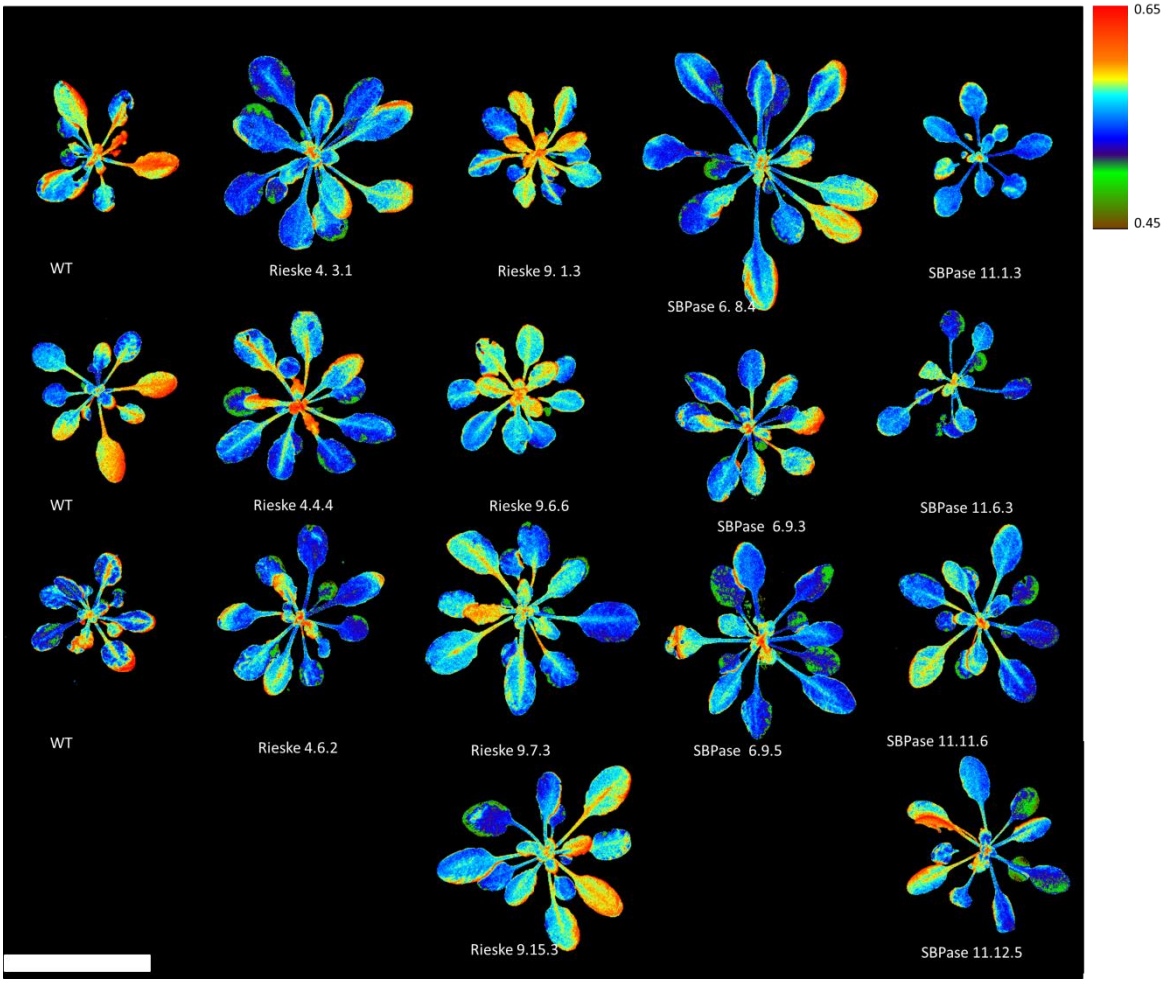

Figure 5. 14. Photosynthetic efficiency of PSll operating systems of images captured of WT and homozygous mutant Arabidopsis plants. 5-weeks old plants were germinated and grown for 14 days on soil before picked out and transferred to soil. Plants were grown under identical conditions in a controlled-environment growth room with (22°C, 8 h light, 16 h dark cycle). *Arabidopsis thaliana* (Col-0) WT and mutants are shown. 4-(pL2B- BAR-pKST1-AtRieske) 6- (pL2B-BAR-(pKST1)-AtSBPase), 9-(pL2-pKST1-AtRieske-tHSP-YFP) 11-(pL2B-BAR-(pKST1)-AtSBPase-YFP) with their respective lines in the third generation. Scale bars represent 5cm and *Fq'/Fm'* values represented by colours as indicated.

Evaluation of the impact of the growth of the transgenic lines on plant development compared to wild type Col-0 were also carried out using the Chlorophyll fluorescence imager to determine the rosettes area from the images. Chlorophyll fluorescence imaging used to determine the maximum PSII operating efficiency of photosynthesis (*Fq'/Fm'*) values of the whole plant was also used to calculate the leaf area at the time of analysis.

Growth was slower in the wild type in the early stages as seen above (Fig 5.13 and 5.14). However, as the plants advanced (week 7), the reductions in rosette area of the wild type seemed to catch up with the transgenic lines which might again be implying that the expression of these two genes might be more active in early developmental stages. This impact on plant growth can be seen clearly on Fig. 5.15 below.

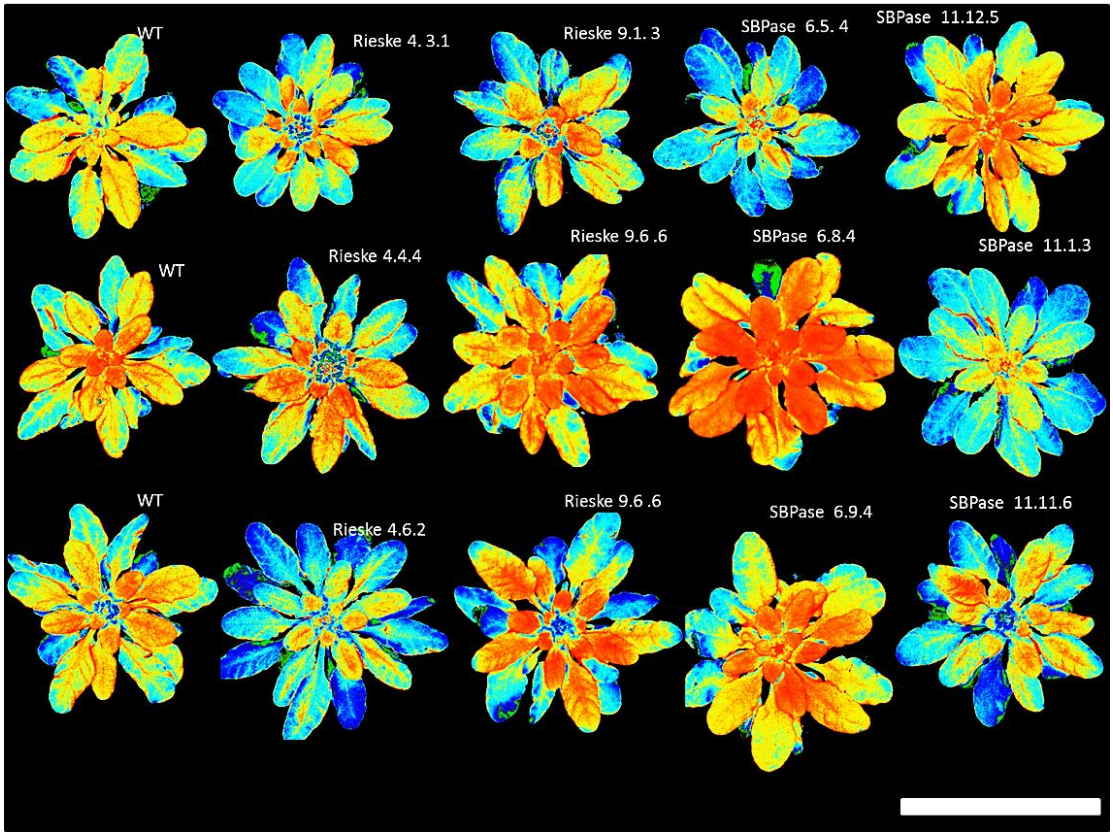

Figure 5. 15. Growth comparism of WT and homozygous mutant plants grown on soil. 7–weeks old plants were germinated and grown for 14 days on soil before picked out and transferred to soil. Wild type leaf area quickly catches up with the transgenic plants in the later weeks of growth. Plants were grown under identical conditions in a controlled-environment growth room with (22°C, 8 h light, 16 h dark cycle). *Arabidopsis thaliana* (Col-0) WT and mutants are shown. 4-(pL2B- BAR-pKST1-AtRieske) 6-(pL2B-BAR-(pKST1)-AtSBPase), 9-(pL2-pKST1-AtRieske-tHSP-YFP) 11- (pL2B-BAR-(pKST1)-AtSBPase-YFP) with their respective lines in the third generation. Scale bar represent 5cm.

Figures 5.16 and 5.17 displays and summarises the comparison of the growth rates of WT and homozygous mutant lines grown for the whole periods of 7 weeks. Each graph displays the lines within a construct compared to the WT. The growth resulted in significant differences ($P< 0.05$) between the wild type and mutants in the first 1 to 5 weeks of recording confirming also the phenotype found, however later on in the weeks again, the reduction in rosettes area of the wild type plants in the initial weeks were compensated leading to minimal differences in leaf areas of all plants (see Fig. 5.16) above. There were no significant differences found in the later weeks unlike the initial weeks of the experiment.

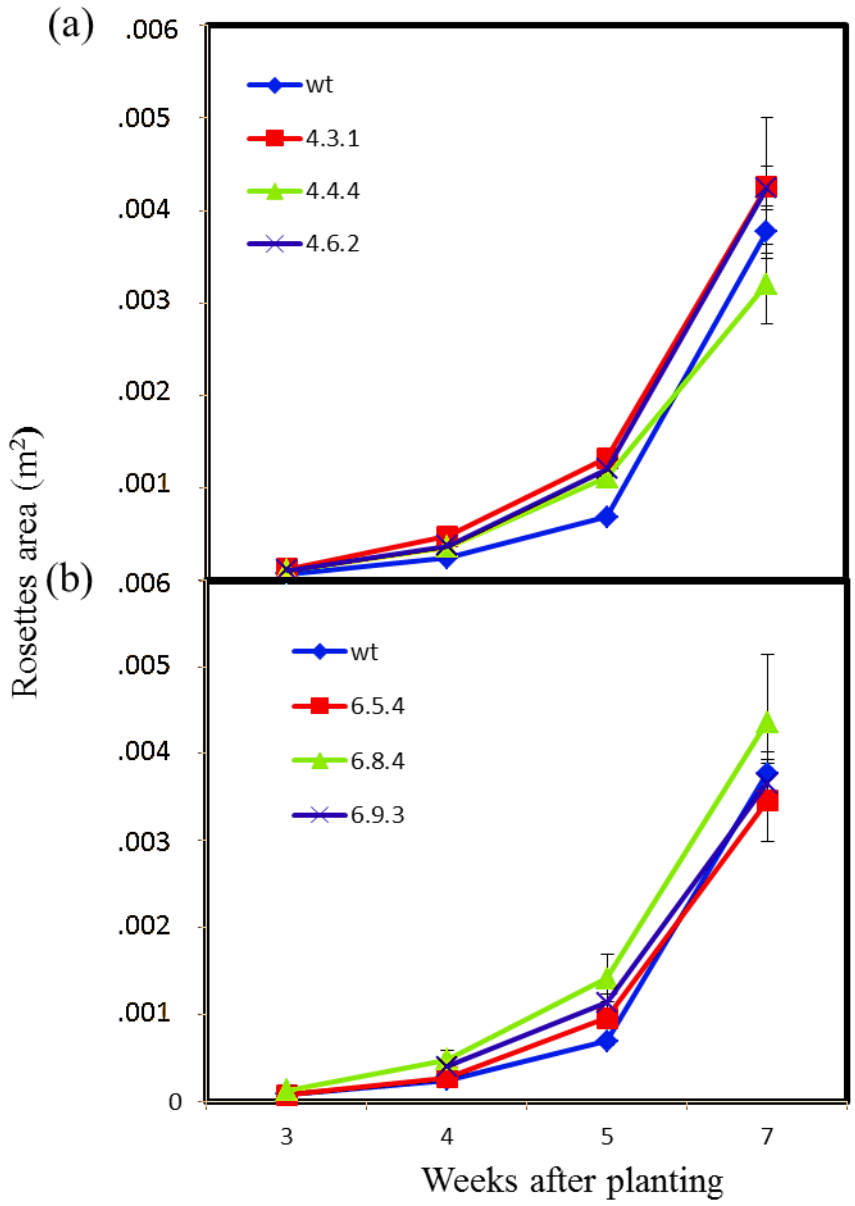

Figure 5. 16. Comparison of the growth rates of WT and homozygous mutant plants grown on soil. Plants were germinated and grown for 14 days on soil before picked out and transferred to individual pots on soil. Plants' growth conditions were maintained at 22°C, 8 h light, 16 h dark cycle. *Arabidopsis thaliana* (Col-0) WT and mutants are shown. Chlorophyll fluorescence imaging was used to calculate the leaf areas at the time of analysis and pictures taken at weeks 3, 4, 5 and 7 and rosettes area calculated from these. (a) WT and construct 4-.(pL2B-BAR-(pKST1)-AtRieske- tHSP-YFP) while (b) WT and construct 6- (pL2B-BAR-(pKST1)-AtSBPase-tHSP-YFP), with their respective lines. Error bars represent SE n=10–15 replicates per line.

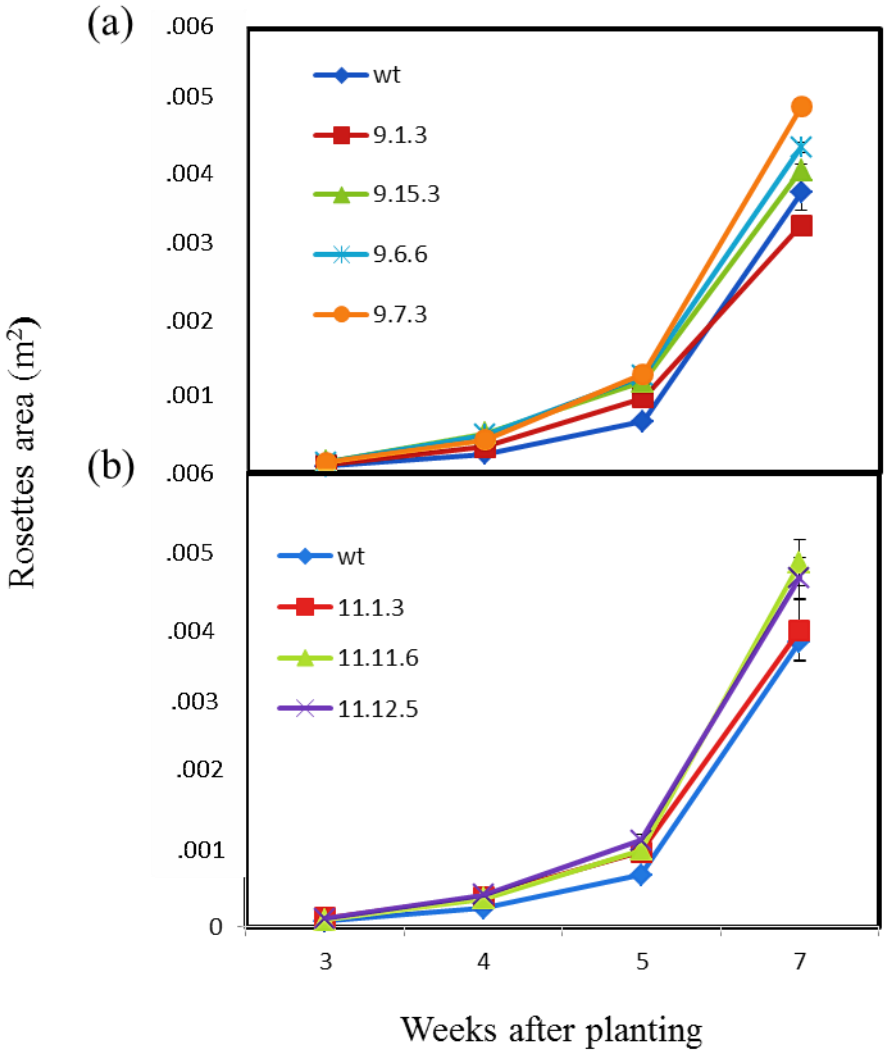

Figure 5. 17. Comparison of the growth rates of WT and homozygous mutant plants grown on soil. Plants were germinated and grown for 14 days on soil before picked out and transferred to individual pots on soil. Plants' condition were maintained at 22°C, 8 h light, 16 h dark cycle). *Arabidopsis thaliana* (Col-0) WT and mutants are shown. Chlorophyll fluorescence imaging was used to calculate the leaf areas at the time of analysis. Pictures were taken at weeks 3, 4, 5 and 7 and rosette areas calculated from these. (a) WT and 9-(pL2B-BAR-(pKST1)-AtRieske-tHSP-YFP) while (b) WT and 11-(pL2B-BAR-(pKST1)-AtSBPase-tHSP-YFP) with their respective lines. Error bars represent SE n=10–15 replicates per line.

5.4.2 Physiological studies of mutant lines revealed no reductions in photosynthetic capacity

In order to assess the impact of the expression of the SBPase and Rieske in the guard cells of matured plants, assimilation rates (*A*) as a function of intercellular [CO_2] or substomatal CO_2 concentration (C_i) was determined for all lines and WT. (Figure 5.18 &5.19**).**

The maximum assimilation rate of wild type was 15.82 μmol $m^{-2}s^{-1}$ achieved at a C_i value of 800 μmol $m^{-2}s^{-1}$ which was also the saturation point. This maximum *A* value was maintained albeit slight variation with increasing C_i. Similarly, the range between the Rieske construct (b) were similar among all the lines with the highest value in line B_6f4.6 with 17.24 μmol $m^{-2}s^{-1}$ of assimilation rate. Result revealed that even though there seem to be differences between the wild type and Rieske, lines B_6f 4.6, there was no significant difference when analysed.

Similarly, the lines within construct SBPase (c) had values similar to the Rieske with a line (SBPase 6.8) having highest assimilation rate value of 17.18 μmol $m^{-2}s^{-1}$ which seemed higher than the wild type but again, there was no significant difference when analysed. These results suggests that at the leaf level photosynthesis, there was no differences or phenotype observed simply because manipulation was carried out at the cellular level which yielded no significant difference compared to the whole leaf.

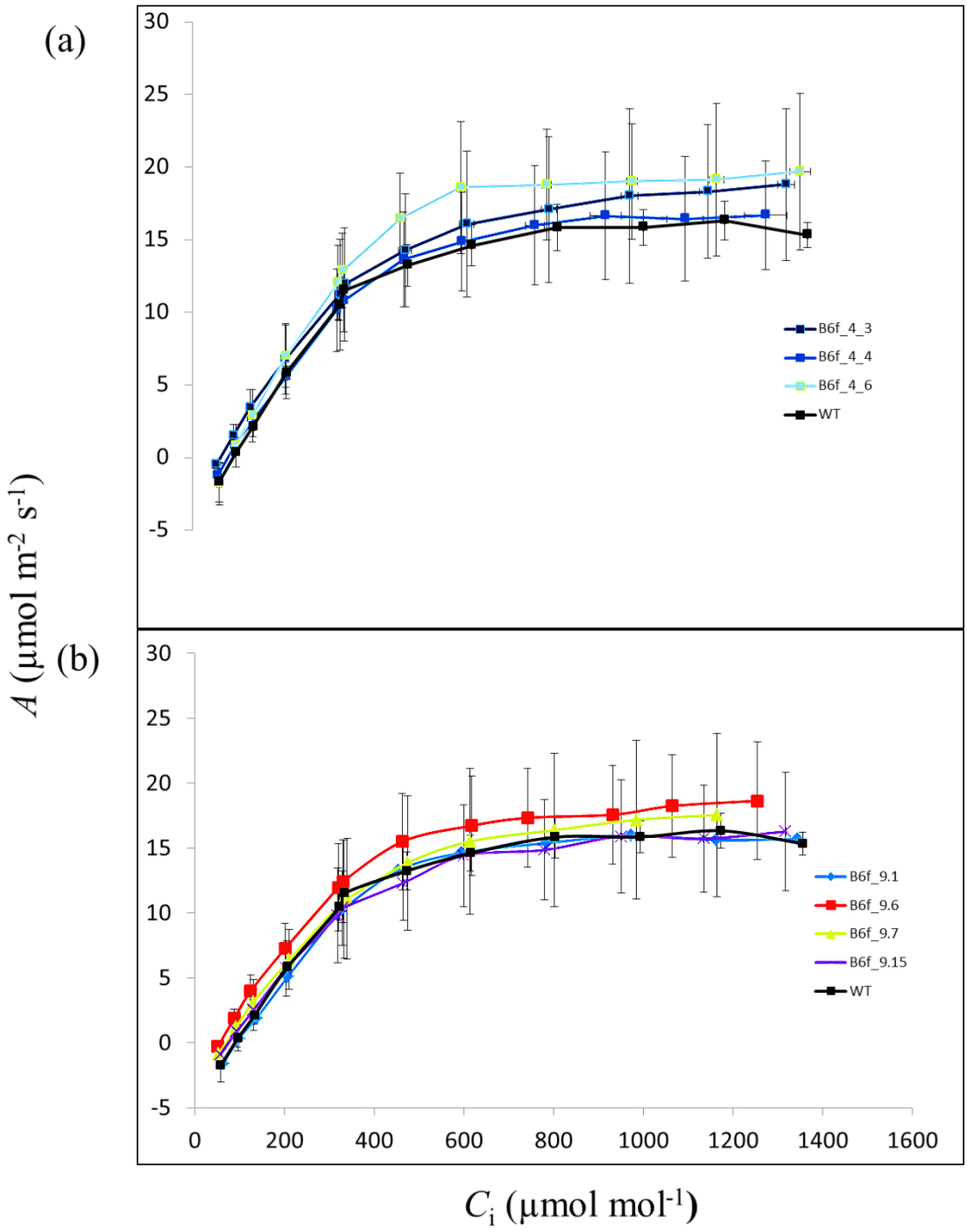

Figure 5. 18. Photosynthetic carbon assimilation rates at different CO_2 concentrations (A/C_i) in (a) b_6f (Rieske) and wild type plants construct 4-(pL2B-BAR-pKST1-AtRieske-tHSP) and (b) b_6f (Rieske) and wild type plants construct 9-(pL2-pKST1-AtRieske-tHSP-YFP). Wild-type (WT) and transgenic plants grown in controlled-environment conditions with a light intensity 130 mmol m^{-2} s^{-1} under an 8h light/16h dark cycle at 22°C for 7 weeks at saturating light levels of (1,000 mmol m^{-2} s^{-1}). Error bars represent ±SD n=6–8 replicate per line.

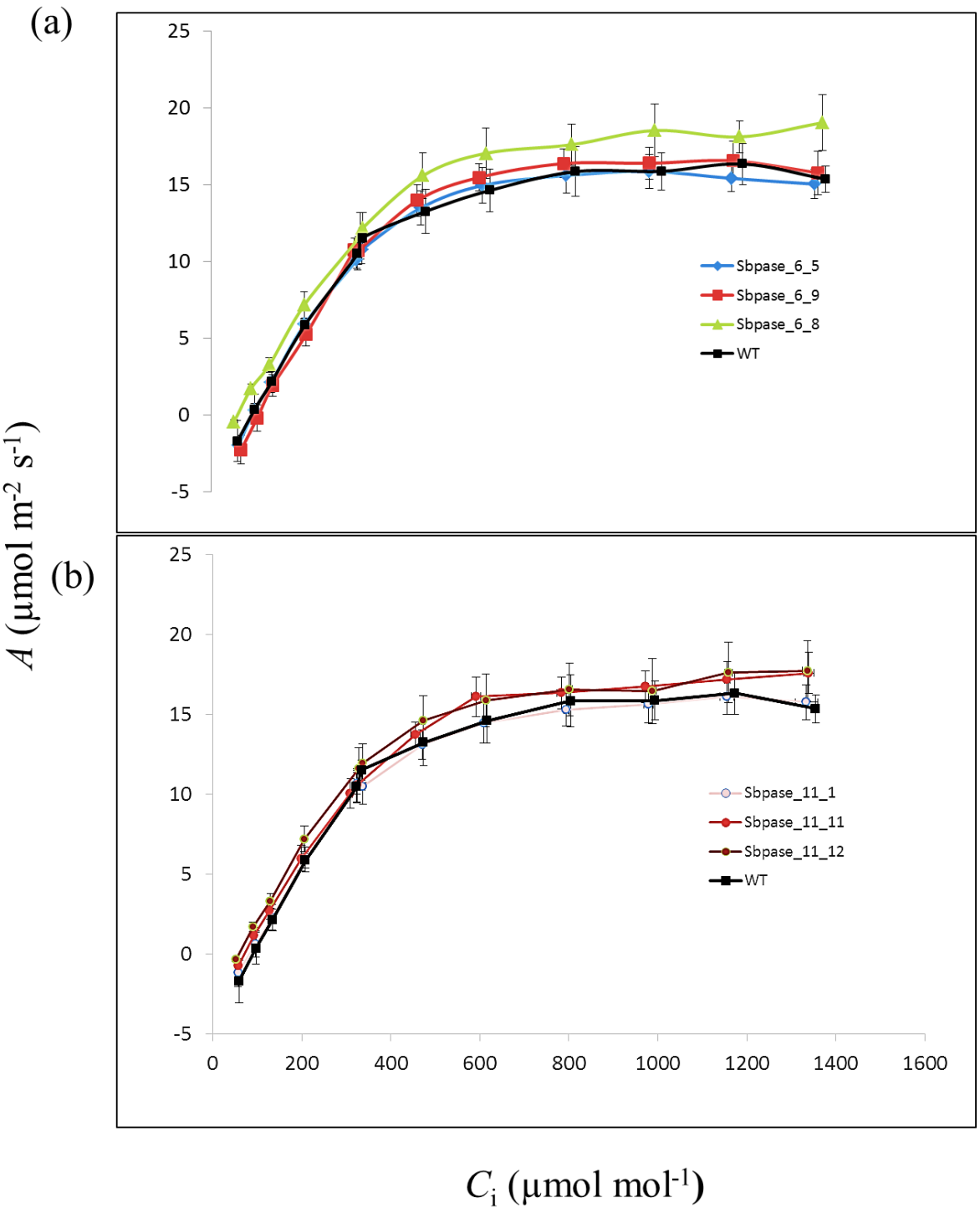

Figure 5.19. Photosynthetic carbon assimilation rates at different CO_2 concentrations (A/C_i) in SBPase plants. (a) SBPase and wild type constructs 6-(pL2B-BAR-(pKST1)-AtSBPase-tHSP-) and (b) SBPaseand wild type construct 11-(pL2B-BAR-(pKST1)-AtSBPase-tHSP-YFP). Wild-type (WT) and transgenic plants grown in controlled-environment conditions with a light intensity 130 mmol m^{-2} s-^{1} under an 8h light/16h dark cycle at 22°C for 7 weeks at saturating light levels of (1,000 mmol m^{-2} s^{-1}). Error bars represent ±SD n=6–8 replicate per line.

From these response curves, the maximum light-saturated rate of photosynthesis (*Asat*) of transgenic were shown to be not significantly different when compared to WT plants (Fig 5. 20).

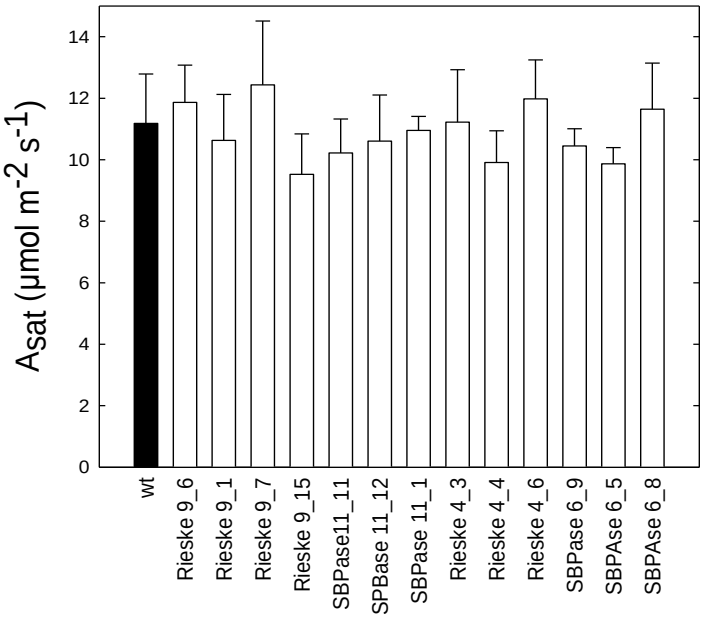

Figure 5.20. Maximum light-saturated rate of photosynthesis (A_{sat}) of WT and transgenics. Data derived from the A/C_i response curves using the equations by von Caemmerer and Farquhar (1981). Values represent 5-8 plants from 3–4 individual lines for each construct set. Lines over-expressing SBPase and Rieske are represented. Error bars SD n=6–8 replicates per line.

The physiological parameters V_{cmax} and J_{max}, which describe the maximum velocity of Rubisco and the regeneration of RuBP respectively were also estimated (Fig 5.21). The capacity for regeneration of the CO_2 acceptor molecule RuBP as shown from the analysis of the A/C_i response curves also yielded no difference between the WT and the transgenic lines (SBPase and Rieske). Interestingly, in all of the lines, J_{max} was also found to have no difference between the wild type and transgenics.

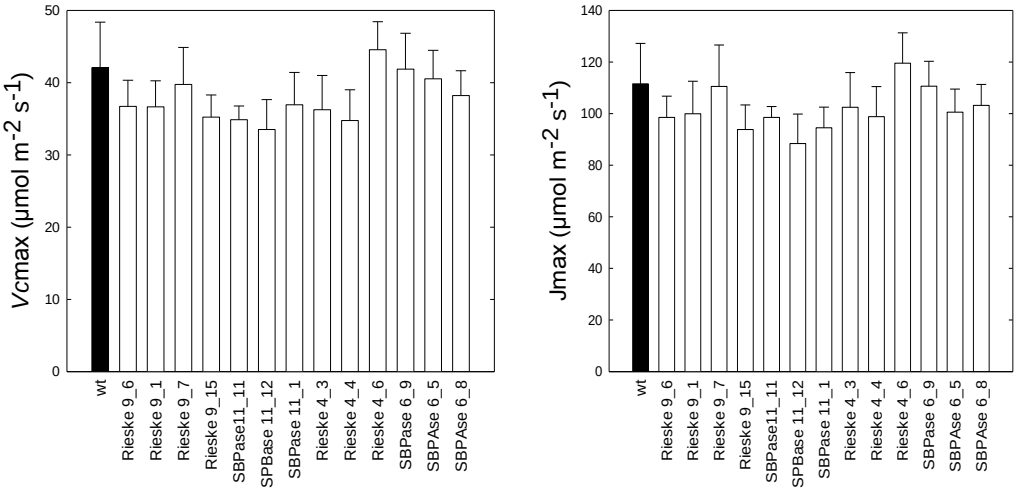

Figure 5. 21. V_{cmax} (Rubisco activity) and J_{max} (electron transport activity) of WT and trangenics. Data derived from the A/C_i response curves using the equations by von Caemmerer and Farquhar (1981). Values represent 5-8 plants from 3–4 individual lines for each construct. Lines over-expressing SBPase and Rieske are represented. Error bars +SD n=6–8 replicates per line.

The result of the operating efficiency of PSII photochemistry *F*q'/*F*m' of matured of 6-7 weeks old plant overtime which ran a simultaneous protocol comprising of the induction to steady state, light response curve and relaxation response of the transgenic lines and wild type were analysed. All results exhibited closely related values as shown on the figures 5.22-5.24 below. An induction to steady state of photosynthesis is shown below (Fig.22).

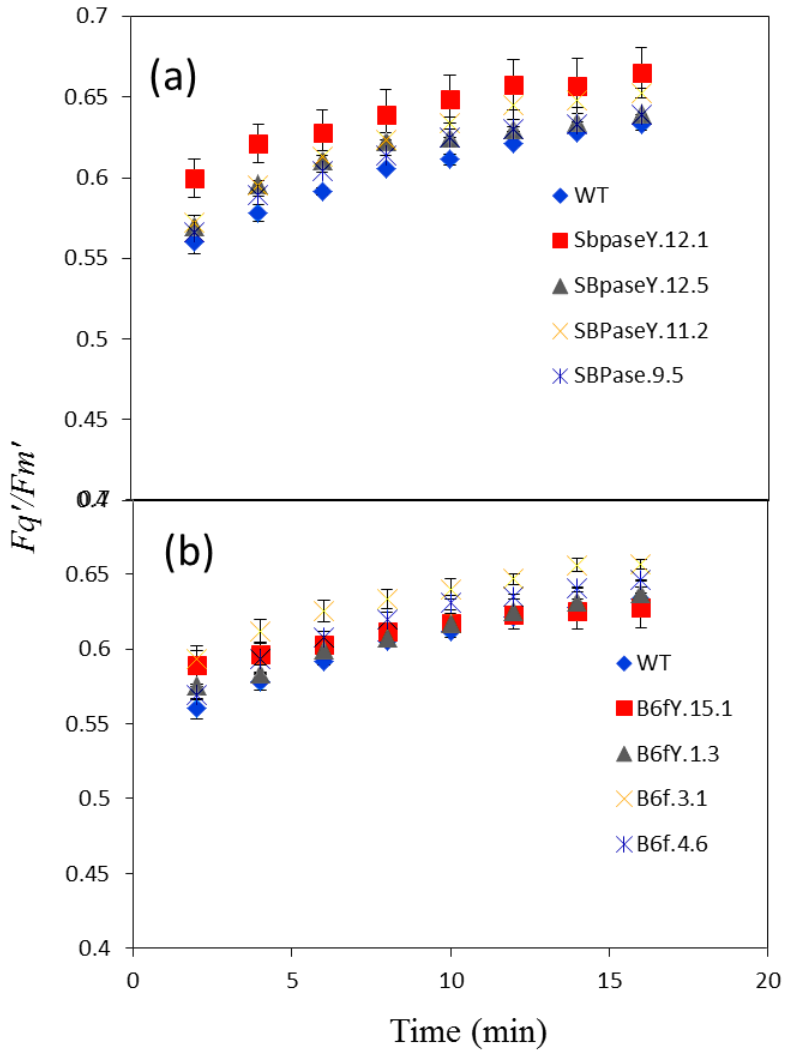

Figure 5.22. Chlorophyll fluorescence imaging of the induction of steady state photosynthesis of mature plant (6–7weeks) to determine the operating efficiency of PSII photochemistry (*Fq'/Fm'*) from a minimal fluorescence (*F*o) and maximal fluorescence (*F*m). Plants were dark adapted for 30 min followed by 500 µmol m^{-2} s^{-1} light. Data are derived from images of F' and Fm' taken from WT and transgenic lines of **(a)** SBPase construct and **(b)** Rieske constructs. Error bars represent ±SD 3-5 replicates per line.

The light response curves also yielded no significant difference between the wild type and the transgenic lines below (Fig 5.23).

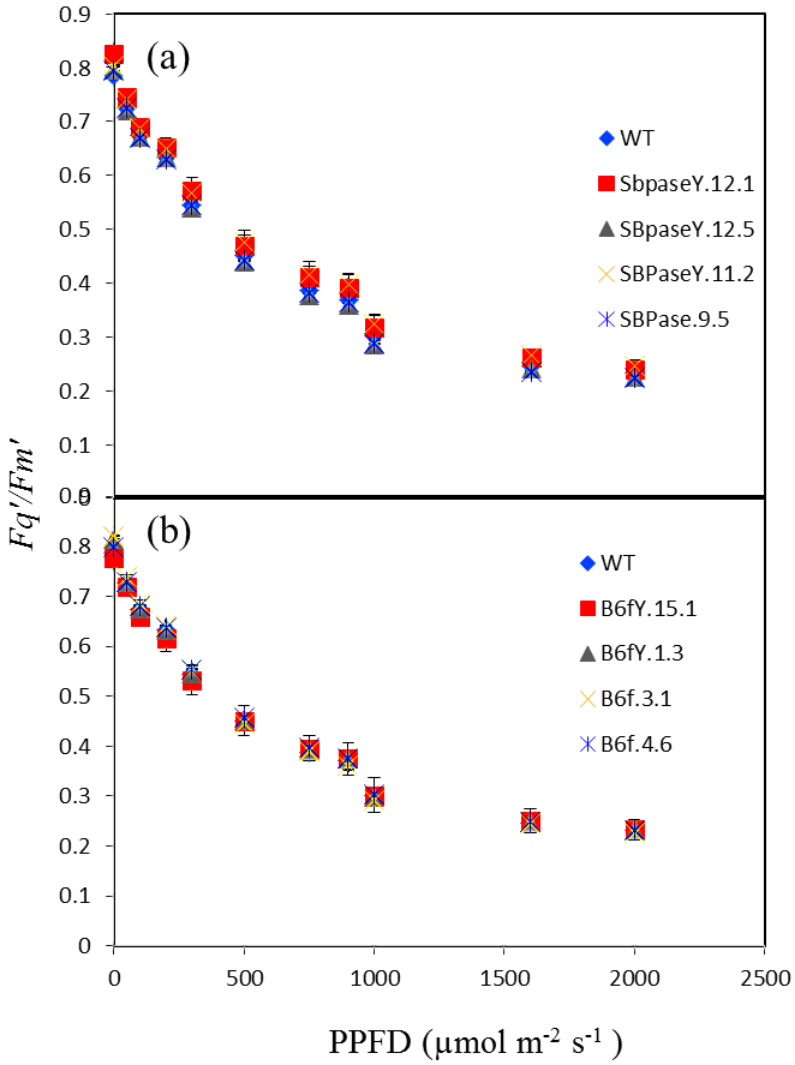

Figure 5. 23. Chlorophyll fluorescence imaging of the light response curves of mature plants (6–7weeks) to determine the operating efficiency of PSII photochemistry (*Fq'/Fm'*). Reading taken from plants dark adapted for 30 min followed by light levels of 0, 50, 100, 200, 300, 500, 750, 900, 1000,1600, 2000. Data were derived from images of F' and Fm' taken from WT and transgenic lines of **(a)** SBPase construct and **(b)** Rieske constructs. Error bars represent ±SD 3-5 replicates per line.

The relaxation kinetics determined after the light response curve by turning off the light in order to regain back to original value of Fv/Fm yielded similarly. No significant differences were observed between the wild type and transgenics responses (Fig. 5.24).

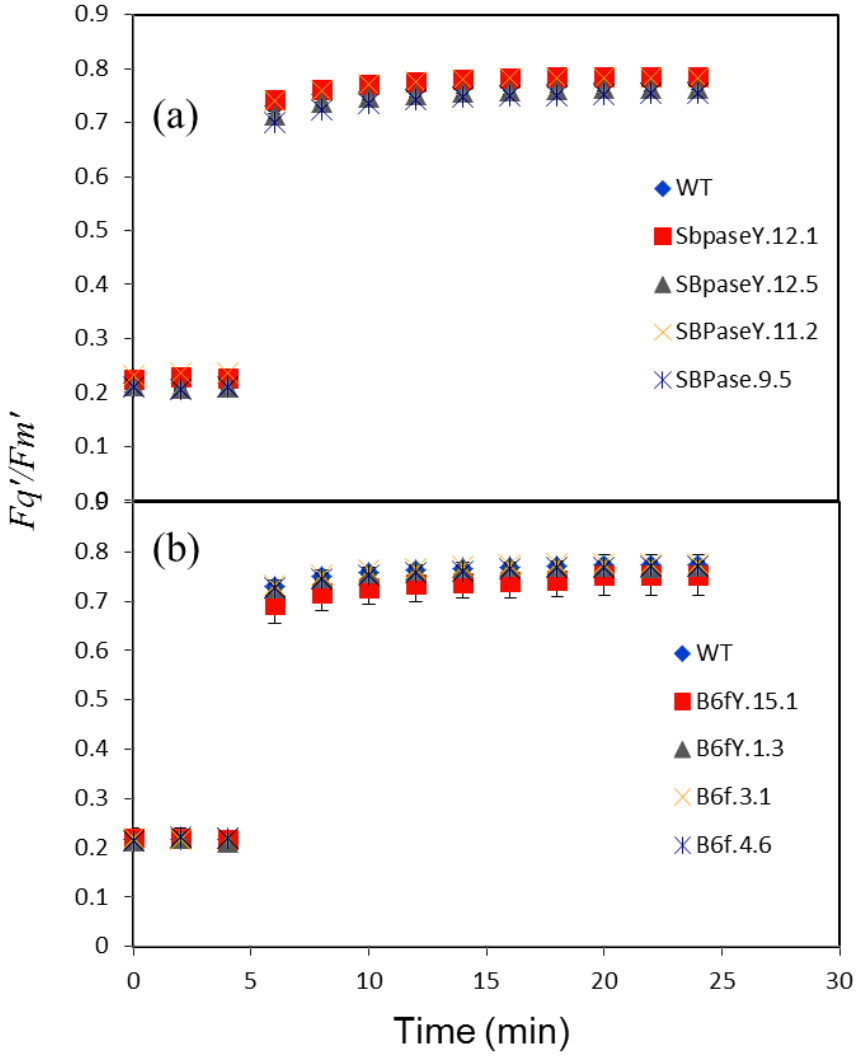

Figure 5. 24. Chlorophyll fluorescence imaging of relaxation kinetics of mature plants (6–7weeks) to determine the operating efficiency of PSII photochemistry (*Fq'/Fm'*). Reading taken from plants dark adapted for 30 min and monitoring Fv/Fm every 2 minutes until the original value of Fv/Fm restored.Data were derived from images of F' and Fm' taken from WT and transgenic lines of **(a)** SBPase construct and **(b)** Rieske constructs. Error bars represent ±SD 3-5 replicates per line.

5.4.3 An investigation into dynamic response of A and g_s to step changes in light

Light is a dynamic variable and considered most important environmental factor influencing both stomatal behaviour and photosynthetic rate. To investigate the temporal variation responses in *A* and g_s to light change, the speed of stomatal responses and magnitude of change in coordination with *A* was determined. It is a well-established fact that slow stomatal responses limits *A* hence resulting in substantial loss in photosynthetic rates in the long run (Lawson and Blatt, 2014). However, McAusland et al., (2016)

illustrated that short-term improvements in *A* could be gained by enhancing the rapidity of stomatal responses and coordination with *A*. They further highlighted that close proximity between stomatal conductance and carbon assimilation has the potential to achieve a substantial improvement in WUE.

Based on this, a step change temporal response to light where the coordination between carbon assimilation and stomatal conductance determined in the transgenic lines generated and the wild type plants.

The result of plants exposed at an initial PPFD of 100 μmol m^{-2} s^{-1} and then subjected to a high light intensity of approximately 1000 μmol m-2 s-1 for an hour and finally back to initial 100 μmol $m^{-2}s^{-1}$ of light is shown below (Fig 5.25).

Result showed similar outcome with the wild type and mutant lines except the line 11.11 with a higher assimilation rate and stomatal conductance. Steady-state of *A* and g_s at the initial PPFD of 100 μmol $m^{-2}s^{-1}$ were similar among all the lines including WT. The lowest values recorded for steady-state *A* at the initial PPFD of 100 μmol $m^{-2}s^{-1}$ ranged from -2 to -3 μmol $m^{-2}s^{-1}$ while the highest recorded steady state value at PPFD of 1000 μmol $m^{-2}s^{-1}$ ranged from 8.99 to 12.53 μmol $m^{-2}s^{-1}$. Overall, the line 11.11 ranked the highest with assimilation rate of 12.53 which is the construct (pL2B-BAR-(pKST1)-AtSBPase-YFP). Similarly, stomatal conductance, g_s were similar among all the lines including WT with the lowest steady state achieved at the initial PPFD of 100 μmol $m^{-2}s^{-1}$ ranged between 0.11 to 0.17mol $m^{-2}s^{-1}$ while the highest recorded steady state value at PPFD of 1000 μmol $m^{-2}s^{-1}$ ranged from 0.208 to 0.370 mol $m^{-2}s^{-1}$ with line 11.11 topping the list as well. Also, from the curves, it is obvious that an increase in PPFD to 1000 μmol $m^{-2}s^{-1}$ led to an immediate and rapid increase in *A* compared to g_s which showed a modestly slow response for all lines.

All lines and wild type measured achieved steady-state *A* approximately at about 1000 secs after high PPFD whereas g_s was scrawling behind and still increasing as it had not attained the maximum values within this timeframe until at about 1500 secs after high PPFD. Although there were lack of coordination between *A* and g_s the final steady-state values of *A* and g_s in almost all plants (transgenic and wild type) except line 11.11 were significantly correlated. Additionally, all plants showed a faster rate of decrease in *A* (After PPFD was returned to 100 μmol $m^{-2}s^{-1}$) than initial increase (after PPFD was increased from 100 to 1000 μmol $m^{-2}s^{-1}$). Likewise, there was greater rapidity in stomatal closing than opening in all plants.

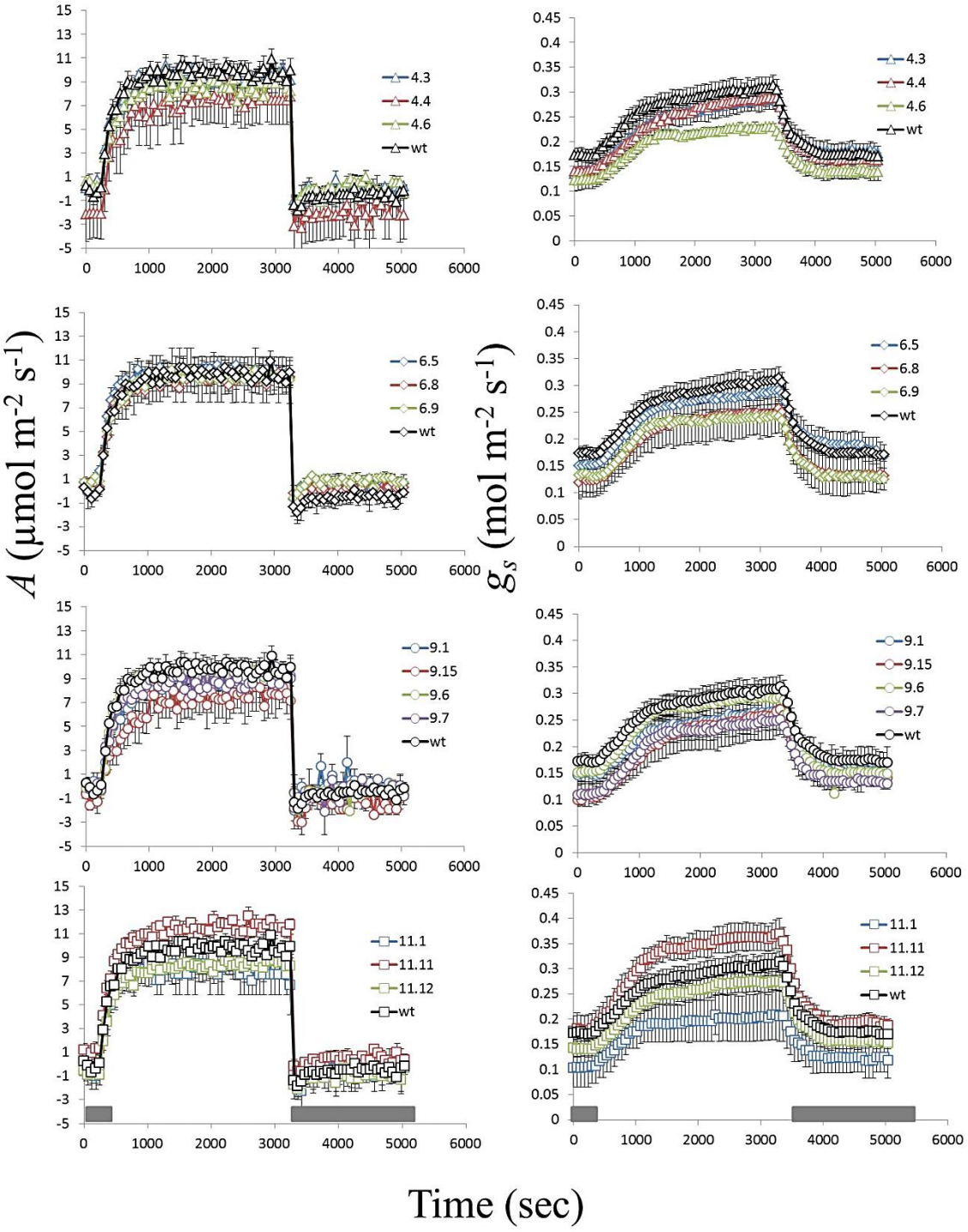

Figure 5. 25. A step change gas exchange measurements of wild type and Arabidopsis mutants. (a) Photosynthetic carbon assimilation rates and **(b)** stomatal conductance to an increase in irradiance from 100 µmol $m^{-2}s^{-1}$ (shaded area) followed by 1000 µmol $m^{-2}s^{-1}$ with time. 4-(pL2- BAR-pKST1-AtRieske-tHSP), 6-(pL2B-BAR-(pKST1)-AtSBPase-tHSP), 9-(pL2- BAR-pKST1-AtRieske-tHSP-YFP) and 11-(pL2B-BAR-(pKST1)-AtSBPase-YFP). Data are the means of 5–8 replicates (±SD). Single factor differences were analysed using a one-way ANOVA $P< 0.05$.

DISCUSSION

Transgenic studies have provided numerous evidences that manipulation of certain enzymes are potential route for the improvement of plant productivity (Lawson et al., 2008b, Lawson et al., 2002, Lefebvre et al., 2005, Raines, 2011, Simkin et al., 2017a, Simkin et al., 2015, von Caemmerer and Furbank, 2016). Light and CO_2 are two important environmental factor and are considered most important factors influencing both stomatal behaviour and photosynthetic rate. Iinvestigation to determine temporal variation in A and g_s by determining the speed of stomatal responses and magnitude of change in coordination with A have been reported (McAusland et al., 2016). Therefore improving the rapidity of stomatal responses will therefore greatly improve productivity and WUE but achieving this require greater knowledge of the physiological and molecular mechanisms that determine the speed of stomata and coordination with mesophyll demands for CO_2 (Lawson and Blatt, 2014).

In this chapter, we generated transgenic Arabidopsis (*Arabidopsis thaliana*) plants overexpressing the Rieske and SBPase and characterised photosynthetic and stomatal responses. SBPase and Rieske mutant lines with altered manipulation were identified in *Arabidopsis thaliana*. The analysis carried out such as the DNA and herbicides screening plus the localization of the YFP have all revealed that these genes are present in the guard cells of the transgenic plants.

Phenotypes observed (Figs.5.5-5.8) suggested that the transformed plants exhibited significant faster initial growth rates evidenced by larger leaf area and faster rosette increases which may suggests that SBPase and Rieske might be of importance for stomatal behaviour and enhanced plant growth. Studies have reported of increase yield in plant productivity by overexpressing these genes in the whole plants (Lefebvre et al,

2005, Raines, 2011, Simkin et al, 2017), however it is interesting that we have observed similar enhancement of growth despite expression being limited to guard cells. The quantum efficiency of PSII photochemistry in the transgenic lines was also significantly higher in early development. These data imply that the photosynthetic efficiency of young plants may have a greater impact on plant development. These finding are consistent with earlier studies which reported that the stimulatory effects of increased levels of SBPase occurred earlier in development (Lefebvre et al., 2005) which may also demonstrate the different limitations witnessed on photosynthesis between developing and fully expanded leaves (Ölçer et al., 2001).

It is important also to keep in mind that little changes in photosynthetic capacity counts and can have a great impact on plant development (Lefebvre et al.,2005).Therefore, these results suggest that altered expression (assumed due to the expression of the construct) of *SB*pase and Reiske in guard cells alone in plants seem to improve the overall plant photosynthetic efficiency and growth in these plants compared with the wild type suggesting that genes manipulation in the guard cells may be playing roles in plant development even when not necessarily linked to photosynthesis. This has been shown by previous work on transgenic plants that the environmental conditions under which the plants are grown can influences the impact in enzyme activity hence the relative importance of any individual enzyme over carbon fixation or photosynthesis is not constant but can vary depending on growth condition and development (Stitt and Schulze, 1994; Raines, 2003).

The CO_2 assimilation rate A versus calculated internal CO_2 concentration C_i (A/C_i) response curves showed some changes in the A/C_i curves, but there was no significant difference between the transgenic lines and the wild type (Fig. 5.18 &5.19). The Asat,

Vcmax and Jmax drived from the (A/Ci) curves yielded no significant differences as well. These results however is envisaged as the mesophyll photosynthetic have not been manipulated. This agrees with the findings where transgenic guard cells chlorophyll-deficient Arabidopsis plants had stomatal size, index, and whole-leaf photosynthetic rates comparable to wild-type plants (Azoulay-Shemer et al., 2015).

The dynamic responses of *A* and g_s to step change in light (Fig 5.25) showed non-coordination between *A* and *gs*, with *A* exhibiting a faster and more varied response than g_s in both wild type and transgenic lines. Such cumulative responses could have significant implications for carbon assimilation and negative impact on water use efficiency in dynamic environmental conditions that are prevalent today. Lawson and Blatt (2014) modelled and synchronised *gs* and *A* and calculated a theoretical 20% increase in water use efficiency if g_s matched mesophyll demands for CO_2 in response to PPFD. However, both *A* and g_s attained similar steady state in all the plants.

The line 11.11 (pL2B-BAR-(pKST1)-AtSBPase-YFP) had both combination of rapid responses and higher steady-state values of both *A* and g_s which is quite striking. This line may imply that the reduction of CO_2 diffusional limitations of *A* is experienced as a result of faster and speedy stomatal response, g_s. Nonetheless, it is apparent that stomatal limitation of *A* was experienced in all plants as it took a longer time for g_s to reach steady state than *A*.

Since (C_i) has long been put forward as an indicator that mediates close correlation between g_s and *A* (Wong et al., 1979, Mansfield et al., 1990, Buckley and Mott, 2013), it is expected that there will be no further increases in g_s once steady-state has been established or reached in *A*. However as it is the case here, results in the step changes do not support this conclusion but rather seems to agree with findings from work on

transgenic plants which showed increasing *gs* with light despite maintaining high C_i ((von Caemmerer et al., 2004, Baroli et al., 2008b, Lawson et al., 2008b). This also points to additional findings by von Caemmerer and Griffiths (2009a) who working with CAM demonstrated that intercellular CO_2 is not the only factor causing stomatal closure during phase III of CAM.

In conclusion numerous studies have shown that photosynthetic enzymes in carbon metabolism have yielded increased photosynthetic rates in plant at the whole leaf level (Driever et al., 2017a, Miyagawa et al., 2001, Driever et al., 2017b, Uematsu et al., 2012, Long et al., 2006, von Caemmerer and Furbank, 2016, Raines, 2011, Simkin et al., 2017a). The same genes overexpressed (SBPase and Rieske FeS) have resulted in increased yield in Arabidopsis plants at the whole leaf level (Simkin et al., 2017c). Similar outcomes have been demonstrated in this chapter but the actual levels of expression in the guard cells needs to be assessed, although is a difficult procedure that needs further work to develop the protocols. Although the tobacco has not been mentioned here again as intended due to time (even though we have already generated our third generation T3 homozygous plants), we expect similar results outcome. However, the characterisation of these transgenic generated lines in both antisense and sense will soon be carried out

Plants have adaptive features that allow them to cope with many external changes, subjecting these mutants to different environmental conditions may therefore yield yet novel phenotypes different from those observed here.

CHAPTER SIX: GENERAL DISCUSSION

This research was based on elucidating the role of guard cells chloroplasts in stomatal regulation and the role these cells could play in coordinating stomatal function with the underlying mesophyll. Coordination between stomata and mesophyll has often been reported (Wong et al., 1979; Buckley et al., 2003) but the mechanisms coordinating such responses have not been fully understood. A comprehensive understanding of the signals or metabolites synchronising stomatal conductance and carbon assimilation are therefore paramount towards successful manipulations of stomatal behaviour for enhancing water use efficiency and sustainable inputs in agriculture land.

Here two approaches (physiological and molecular) have been used to elucidate mesophyll-derived signals that coordinate mesophyll CO_2 demands with stomatal behaviour towards improving WUE and crop yield (Lawson et al, 2014). The findings from both approaches are summarised;

6.1 Epidermal-mesophyll approach

In order to examine the relationship between stomatal behaviour and mesophyll photosynthesis a novel epidermal mesophyll transfer approach was used on plants with different photosynthetic pathways (C3 and CAM). We used the obligate crassulacean acid metabolism (CAM) plant *Kalanchoë fedtschenkoi* plant in which stomata open at night and close during the day to study stomatal dynamics in response to changes in light and CO_2 concentration at different period of the diurnal CAM cycle. These species were also used in the epidermal peel transfer experiment in which the epidermis from the C3 plant *Vicia faba* was placed on the mesophyll from *Kalanchoë fedtschenkoi* and vice versa. The main findings from these studies were:

***C_i* driven signal:** This was illustrated by the dampened stomatal responses to changes in [CO_2] and light in the isolated epidermal peels in *Vicia faba* compared to the detached whole leaf experiment in *Vicia* faba plants. This is also in agreement with findings in literature that reported stomata respond and function differently when in isolation or different degrees in stomatal responses to various environmental stimuli in epidermal strips and intact leaves (Willmer and Dittrich, 1974, Travis and Mansfield, 1979, Lee and Bowling, 1995), which has often been attributed to a role of C_i in these responses and signalling pathways (Mott 1988). Plants have demonstrated faster responses of g_s to A as a result of CO_2 consumption for mesophyll photosynthesis unlike those of the isolated epidermis or the peels grafted onto mesophyll which again points to the role of the C_i mediating A and g_s. These finding indicate that stomata are influenced by the underlying mesophyll to changes in light and [CO_2]. However, Wang et al., (2014) found that stomata in the epidermal peels function to a lesser degree than when the mesophyll is present. These authors proposed that the amounts of ATP required for the proton pumps for guard cell osmoregulation were lower in isolated epidermis which resulted in a decreased stomatal opening in response to white light, suggesting that both guard cell chloroplasts and mesophyll contributed to the required ATP for osmoregulation.

Darkness initiate stomatal opening in CAM. Stomatal opening in darkness in CAM is a known phenomenon and an expected occurrence due to the drawdown of CO_2 during the dark assimilation phase of internal CO_2 (Borland, 2009). However, the finding that stomata opening response to darkness in CAM epidermal peels, when the influence of the mesophyll has been removed is interesting and has not previously reported. These results suggest the guard cells of CAM plants sense and response to darkness and that the signal receptor or signal transduction pathway may reside within the guard cells themselves

and/or that guard cell photosynthesis may play a role. It is clear that the responses are not entirely driven by mesophyll demands for CO_2 (von Caemmerer & Griffiths, 2009).

CAM plasticity; a potential tool for maximizing carbon gain and water use efficiency: Stomatal and photosynthetic responses to a step change in light intensity and [CO_2] in intact leaves of *Kalanchoë* grown in either the light/standard cabinet or the dark/reverse cabinet have illustrated different responses that impact of CAM physiology (Borland et al., 2014). Stomata in plants pre-treated with 12h dark (phase 1 of CAM) were mostly unresponsive to changes in light and [CO_2].Whereas stomata in plants pre-treated with 12h light (phase 3) demonstrated C3 type behaviour. In these plants, decarboxylation of the stored nocturnal malate would have already taken place and these plants would be expected to have low malate levels and also low C_i levels subjecting them to stomatal opening in the light hence exhibiting C3 photosynthesis (Borland & Griffith, 2009). Malate is imported from the mesophyll or synthesized internally in the guard cells themselves from starch degradation or guard cell CO_2 fixation (Roelfsema and Hedrich, 2005, Horrer et al., 2016, Lawson et al. 2014, Vavasseur and Raghavendra, 2005, Lawson, 2009). These data also indicate the influence of the mesophyll indicating a C_i driven responses in stomatal behaviour or that malate level were low in the guard cells and play a role in guard cell metabolism and osmoregulation. These data have also shown the capability or plasticity of the *Kalonchoe fedshenkoi* switching from CAM to C3 and back to CAM suggesting that there are no metabolic incompatibilities between C3 photosynthesis and the CAM adaptation (Borlard et al, 2014). Thus, the CAM pathway can be engineered into a C3 crops as a means of enhancing water-use efficiency or increasing carbon balance.

Defection in PPDK in CAM results in C3-like stomatal response: The response of the stomata in CAM plants manipulated with 5% lower than the wild type in pyruvate

orthophosphate dikinase, PPDK (Figs 3.4 and 3.12) had clearly shown the disruption of the mesophyll circadian clock in the activity of the regenerative enzyme hence the plant showed lesser commitment to CAM by opening both in the light and dark. (Dever et al. 2015). Similarly, Borland et al., (1999) has demonstrated that reducing the capacity of CAM leaves to synthesize malic acid at night had shown associated reductions in metabolite concentrations which could override circadian control of PEPC kinase.

6.2 Molecular approach manipulation of photosynthetic enzymes; impacts on stomatal function

Efforts to comprehend the involvement of guard cell photosynthesis in stomatal function requires manipulating photosynthesis specifically in guard cells (Lawson 2014). As outlined in chapters one and five, recent studies have shown a role for mesophyll regulation of stomatal aperture either by importing organic acids from the mesophyll for osmotic adjustments or used for the production of ATP required for the proton pumps involved in guard cell osmoregulation. Therefore, the genetic manipulation of metabolites involved in metabolism and photosynthetic enzymes in the guard cells themselves could also lead to changes in stomatal behaviour and potentially improve photosynthesis and water use efficiency in plants (Santelia and Lawson, 2016).

It was in line with this that the second approach was employed and we demonstrated the potential of generated transgenic plants with altered guard cell metabolism. We particularly have demonstrated specificity of the KST promotor and shown that expression was only in the guard cells. This has also shown the potential of this promotor for manipulating guard cell specific metabolism. This agrees with the earlier work of Muller-Rober et al., (1998) as well as the work by Kelly et al. (2013 & 2017). The rationale for choosing these two targets were two-fold. First it is still not known if guard

cell electron transport and/or guard cell Calvin cycle activity directly impacts on stomatal responses (see Lawson 2009; Lawson et al., 2014); secondly, it has been hypothesized that guard cell photosynthesis could provide the mechanisms that co-ordinates stomatal responses with those of the underlying mesophyll (Lawson et al., 2002; 2003).

Our findings from using this approach is summarised below

Significant impact on growth development: These manipulations in increased SBPase and Rieske genes in the guard cells resulted in substantial and significant impacts on early plant development shown by early phenotype. These results are consistent with studies demonstrating the control of the manipulation of these genes (Price et al., 1998;Ruuska et al., 2000; Yamori et al., 2011b) which suggest that overexpression of the Rieske FeS protein maybe a possible means to increasing photosynthesis and yield, however in these studies Rieske FeS was manipulated in the mesophyll and not in the guard cells. In addition to increased rates of photosynthetic efficiency, a substantial and significant increase in the growth of the rosette area were observed in both the SBPase and Rieske FeS plants in the early vegetative phase, suggesting that improvements in biomass could be due to increased light and photosynthesis as a result of greater leaf area achieved in the transgenics (Lefebvre et al., 2005).

Greater rate of A and g_s in response to a step change in light intensity: Our results from the transgenic plants also demonstrated that manipulating photosynthetic enzymes in the guard cells can impact on stomatal responses and carbon assimilation. Both the rapidity of stomatal responses as well as the magnitude of change was altered in the transgenic plants. This was particularly evident in the SBPase lines. However, as no knowledge of the expression levels was possible it was difficult to assess the exact role of SBPase in stomatal responses. . These data shown both an

increase in g_s and *A* suggesting the reduction of CO_2 diffusional limitations of *A* based on the stomatal model designed towards enhancing assimilation rate and possibly WUE (McAusland et al., (2016).

The results obtained from these approaches has shown the potentials in manipulating guard cells towards plant productivity. Based on our findings, the following can further be exploited in order to elucidate mesophyll-stomatal interactions and subsequent impacts on WUE and plant productivity

Future work.

- Further investigation of the mechanisms and sensory and signalling pathways in stomatal opening to darkness in CAM plants. These results suggests that guard cells of CAM plants sense and response to darkness and responses may not be entirely driven by mesophyll demands for CO_2.
- The regulation of the activity of sugar transporters which move sugars into and out of the guard cells or vacuole will greatly assist in identifying the role of sucrose in stomatal function and the feasibility of enhancing plant WUE through the manipulation of guard cell sucrose metabolism and how this links to Calvin cycle activity in the guard cells in terms of sucrose production.
- Other manipulated enzymes of CAM metabolism in *Kalanchoe fedshenkoi* could be used to determine the role ofthese enzymes in stomatal regulations and the possible effect of these manipulated enzymes on the driving force of CAM; the circadian clock.
- The possible extension of a CAM phase (by taking advantage of CAM plasticity). In order to overcome the perceive constraints of CO_2 acquisition in CAM by using

enzymes machinery in the decarboxylation phase. For instance, the possible extension of phase 1 to balance the CO_2 uptake by extending the activity of PEPC through PPCK (knocking out).

- An ultimate goal for engineering CAM is the ability to install a complete, obligate CAM pathway as in C3 plants to maximize WUE. However, intermediate steps in CAM as shown in the results can be beneficial as some CAM-cycling or facultative CAM exhibiting partial commitment to CAM and probable maintenance of carbon balance. Strategies to engineer a CAM pathway might provide benefit to C3 plants (Kebeish et al.2012). However, bearing in mind the cost of using the enzymes' mechaninary required for such processes.
- Single or multigene combined constructs of the enzymes used or other enzymes expressed in the guard cells: Exploitation of other single or individual enzymes in guard cells or multiple or combined enzymes in electron transport and Calvin cycle transformations could lead to changes in stomatal behaviour by demonstrating the role of other enzymes in electron transport chain or Calvin cycle which could potentially improve photosynthesis and water use efficiency in plants.
- Assessment of intrinsic water use efficiency (iWUE): It will be interesting to see the effect on WUE by using the model designed by Vialet-Chabrand et al., (2016) for use in the transgenic lines Models are now available to assess temporal relationship between A and g_s and McAusland et al., (2016) have shown that short-term improvements in A could be gained by enhancing the rapidity of stomatal responses and coordination with A.

- Quantification of level of transcripts abundance in guard cells: Guard cell specific quantification in the transgenic and wild types from subsequent generations

would be required to determine the impact of enzyme manipulation on functional processes and determine the mechanisms and pathways these contribute to stomatal behaviour..

Having said all the above, guard cells metabolism is a fast-paced area of research and more opportunities still awaits its exploitation to bring to an unequivocal view of its metabolism. The findings highlighted using this approach can therefore be further exploited as researchers are continuously adopting multicity of approaches in order to shed more lights towards plants WUE and productivity.

REFERENCES

ALLAWAY, W. & MILTHORPE, F. 2012. STRUCTURE AND FUNCTIONING 0F STOMATA. *Soil Water Measurement, Plant Responses, and Breeding for Drought Resistance,* **4,** 57.

ALLAWAY, W. G. 1973. Accumulation of malate in guard cells of Vicia faba during stomatal opening. *Planta,* **110,** 63-70.

ALLEN, C. D., MACALADY, A. K., CHENCHOUNI, H., BACHELET, D., MCDOWELL, N., VENNETIER, M., KITZBERGER, T., RIGLING, A., BRESHEARS, D. D., HOGG, E. H., GONZALEZ, P., FENSHAM, R., ZHANG, Z., CASTRO, J., DEMIDOVA, N., LIM, J.-H., ALLARD, G., RUNNING, S. W., SEMERCI, A. & COBB, N. 2010. A global overview of drought and heat-induced tree mortality reveals emerging climate change risks for forests. *Forest Ecology and Management,* **259,** 660-684.

ANDEREGG, L. D., ANDEREGG, W. R., ABATZOGLOU, J., HAUSLADEN, A. M. & BERRY, J. A. 2013. Drought characteristics' role in widespread aspen forest mortality across Colorado, USA. *Glob Change in Biology,* **19,** 1526-37.

ANDEREGG, W. R. L., KANE, J. M. & ANDEREGG, L. D. L. 2012. Consequences of widespread tree mortality triggered by drought and temperature stress. *Nature Climate Change,* **3,** 30.

ANDRES, Z., PEREZ-HORMAECHE, J., LEIDI, E. O., SCHLUCKING, K., STEINHORST, L., MCLACHLAN, D. H., SCHUMACHER, K., HETHERINGTON, A. M., KUDLA, J., CUBERO, B. & PARDO, J. M. 2014. Control of vacuolar dynamics and regulation of stomatal aperture by tonoplast potassium uptake. *Proc National Academy of Science U S A,* **111,** E1806-14.

ANTUNES, W. C., PROVART, N. J., WILLIAMS, T. C. & LOUREIRO, M. E. 2012a. Changes in stomatal function and water use efficiency in potato plants with altered sucrolytic activity. *Plant Cell and Environment,* **35,** 747-59.

ANTUNES, W. C., PROVART, N. J., WILLIAMS, T. C. & LOUREIRO, M. E. 2012b. Changes in stomatal function and water use efficiency in potato plants with altered sucrolytic activity. *Plant, cell & environment,* **35,** 747-759.

ARONSSON, H. & JARVIS, P. 2002. A simple method for isolating import-competent Arabidopsis chloroplasts. *FEBS Lett,* **529,** 215-20.

ARONSSON, H. & JARVIS, R. P. 2011. Rapid isolation of Arabidopsis chloroplasts and their use for in vitro protein import assays. *Methods Mol Biol,* **774,** 281-305.

ASSMANN, S. M. & JEGLA, T. 2016. Guard cell sensory systems: recent insights on stomatal responses to light, abscisic acid, and CO2. *Current Opininion in Plant Biology,* **33,** 157-167.

ASSMANN, S. M. & SHIMAZAKI, K. 1999. The multisensory guard cell. Stomatal responses to blue light and abscisic acid. *Plant Physiol,* **119,** 809-16.

ASSMANN, S. M. & WANG, X. Q. 2001. From milliseconds to millions of years: guard cells and environmental responses. *Curr Opin Plant Biol,* **4,** 421-8.

AUBRY, S., ARESHEVA, O., REYNA-LLORENS, I., SMITH-UNNA, R. D., HIBBERD, J. M. & GENTY, B. 2016. A Specific Transcriptome Signature for Guard Cells from the C4 Plant Gynandropsis gynandra. *Plant Physiol,* **170,** 1345-57.

AZOULAY-SHEMER, T., PALOMARES, A., BAGHERI, A., ISRAELSSON-NORDSTROM, M., ENGINEER, C. B., BARGMANN, B. O. R., STEPHAN, A. B. & SCHROEDER, J. I. 2015. Guard cell photosynthesis is critical for stomatal

turgor production, yet does not directly mediate CO(2)- and ABA-induced stomatal closing. *The Plant journal : for cell and molecular biology,* **83,** 567-581.

BAKER, N. R., OXBOROUGH, K., LAWSON, T. & MORISON, J. I. 2001. High resolution imaging of photosynthetic activities of tissues, cells and chloroplasts in leaves. *Journal of Experimental Botany,* **52,** 615-621.

BARBAGALLO, R. P., OXBOROUGH, K., PALLETT, K. E. & BAKER, N. R. 2003. Rapid, noninvasive screening for perturbations of metabolism and plant growth using chlorophyll fluorescence imaging. *Plant Physiology,* **132,** 485-493.

BAROLI, I., PRICE, G. D., BADGER, M. R. & VON CAEMMERER, S. 2008b. The contribution of photosynthesis to the red light response of stomatal conductance. *Plant Physiology,* **146,** 737-47.

BARRADAS, V. L. & JONES, H. G. 1996. Responses of CO2 assimilation to changes in irradiance: laboratory and field data and a model for beans (Phaseolus vulgaris L.). *Journal of Experimental Botany,* **47,** 639-645.

BARTLETT, J. G., ALVES, S. C., SMEDLEY, M., SNAPE, J. W. & HARWOOD, W. A. 2008. High-throughput Agrobacterium-mediated barley transformation. *Plant Methods,* **4,** 22.

BERGMANN, D. C. & SACK, F. D. 2007. Stomatal development. *Annual Review in Plant Biology.,* **58,** 163-181.

BERRY, J. A., BEERLING, D. J. & FRANKS, P. J. 2010. Stomata: key players in the earth system, past and present. *Current Opinion in Plant Biology,* **13,** 233-40.

BORLAND, A. M., BARRERA ZAMBRANO, V. A., CEUSTERS, J. & SHORROCK, K. 2011. The photosynthetic plasticity of crassulacean acid metabolism: an evolutionary innovation for sustainable productivity in a changing world. *New Phytology,* **191,** 619-33.

BORLAND, A. M., GRIFFITHS, H., HARTWELL, J. & SMITH, J. A. 2009. Exploiting the potential of plants with crassulacean acid metabolism for bioenergy production on marginal lands. *Journal of Experimental Botany,* **60,** 2879-96.

BORLAND, A. M., HARTWELL, J., WESTON, D. J., SCHLAUCH, K. A., TSCHAPLINSKI, T. J., TUSKAN, G. A., YANG, X. & CUSHMAN, J. C. 2014. Engineering crassulacean acid metabolism to improve water-use efficiency. *Trends in Plant Science,* **19,** 327-38.

BOYER, J. S. 1982. Plant productivity and environment. *Science,* 218**,** 443-8.

BROWNLEE, C. 2001. The long and the short of stomatal density signals. *Trends in Plant Science,* **6,** 441-442.

BUCHANAN, B. B. 1991. Regulation of CO2 assimilation in oxygenic photosynthesis: the ferredoxin/thioredoxin system. Perspective on its discovery, present status, and future development. *Arch ive in Biochemistry and Biophysics,* **288,** 1-9.

BUCKLEY, T. N. 2005. The control of stomata by water balance. *New Phytologist,* **168,** 275-292.

BUCKLEY, T. N. & MOTT, K. A. 2013. Modeling Stomatal Conductance in Response to Environmental Factors. *Plant, cell & environment*.

CALCAGNO, P.L (2013) Analysis of insertion mutants and construction of transgenic plants for the investigation of the CP12 protein family in Arabidopsis thaliana. Doctoral Dissertation. University of Essex, Department of Biological Sciences, Colchester. United Kingdom.

CARDON, Z. G. & BERRY, J. 1992. Effects of O2 and CO2 Concentration on the Steady-State Fluorescence Yield of Single Guard Cell Pairs in Intact Leaf Discs of Tradescantia albiflora Evidence for Rubisco-Mediated CO2 Fixation and Photorespiration in Guard Cells. *Plant Physiology,* **99,** 1238-1244.

CHEN, C., XIAO, Y. G., LI, X. & NI, M. 2012. Light-regulated stomatal aperture in Arabidopsis. *Mole cular Plant,* **5,** 566-72.

CIAIS, P., REICHSTEIN, M., VIOVY, N., GRANIER, A., OGÉE, J., ALLARD, V., AUBINET, M., BUCHMANN, N., BERNHOFER, C., CARRARA, A., CHEVALLIER, F., DE NOBLET, N., FRIEND, A. D., FRIEDLINGSTEIN, P., GRÜNWALD, T., HEINESCH, B., KERONEN, P., KNOHL, A., KRINNER, G., LOUSTAU, D., MANCA, G., MATTEUCCI, G., MIGLIETTA, F., OURCIVAL, J. M., PAPALE, D., PILEGAARD, K., RAMBAL, S., SEUFERT, G., SOUSSANA, J. F., SANZ, M. J., SCHULZE, E. D., VESALA, T. & VALENTINI, R. 2005. Europe-wide reduction in primary productivity caused by the heat and drought in 2003. *Nature,* **437,** 529.

CLOUGH STEVEN, J. & BENT ANDREW, F. 2008. Floral dip: a simplified method for Agrobacterium -mediated transformation of Arabidopsis thaliana. *The Plant Journal,* **16,** 735-743.

COCKBURN, W., TING, I. P. & STERNBERG, L. O. 1979. Relationships between stomatal behavior and internal carbon dioxide concentration in Crassulacean acid metabolism plants. *Plant Physiology,* **63,** 1029-1032.

COMINELLI, E., GALBIATI, M., VAVASSEUR, A., CONTI, L., SALA, T., VUYLSTEKE, M., LEONHARDT, N., DELLAPORTA, S. L. & TONELLI, C. 2005. A guard-cell-specific MYB transcription factor regulates stomatal movements and plant drought tolerance. *Current Biology,* **15,** 1196-1200.

COUSINS, A. B., BAROLI, I., BADGER, M. R., IVAKOV, A., LEA, P. J., LEEGOOD, R. C. & VON CAEMMERER, S. 2007. The role of phosphoenolpyruvate carboxylase during C4 photosynthetic isotope exchange and stomatal conductance. *Plant Physiology,* **145,** 1006-1017.

COWAN, I. & TROUGHTON, J. 1971. The relative role of stomata in transpiration and assimilation. *Planta,* **97,** 325-336.

CUSHMAN, J. C. & BOHNERT, H. J. 1999. Crassulacean acid metabolism: molecular genetics. *Annual review of plant biology,* **50,** 305-332.

DALOSO, D. M., ANJOS, L. & FERNIE, A. R. 2016a. Roles of sucrose in guard cell regulation. *New Phytologist*.

DALOSO, D. M., MEDEIROS, D. B., ANJOS, L., YOSHIDA, T., ARAÚJO, W. L. & FERNIE, A. R. 2017. Metabolism within the specialized guard cells of plants. *New Phytologist,* **216,** 1018-1033.

DALOSO, D. M., WILLIAMS, T. C., ANTUNES, W. C., PINHEIRO, D. P., MULLER, C., LOUREIRO, M. E. & FERNIE, A. R. 2016b. Guard cell-specific upregulation of sucrose synthase 3 reveals that the role of sucrose in stomatal function is primarily energetic. *New Phytologist*, **209,** 1470-83.

DALOSO, D. M., WILLIAMS, T. C., ANTUNES, W. C., PINHEIRO, D. P., MÜLLER, C., LOUREIRO, M. E. & FERNIE, A. R. 2015. Guard cell-specific upregulation of sucrose synthase 3 reveals that the role of sucrose in stomatal function is primarily energetic. *New Phytologist*. **38**, 2353-71

DAYANANDAN, P. & KAUFMAN, P. B. 1975. Stomatal movements associated with potassium fluxes. *American Journal of Botany***,** 221-231.

DEVER, L. V., BOXALL, S. F., KNEROVA, J. & HARTWELL, J. 2015. Transgenic perturbation of the decarboxylation phase of Crassulacean acid metabolism alters physiology and metabolism but has only a small effect on growth. *Plant Physiology*, **167,** 44-59.

DING, F., WANG, M., ZHANG, S. & AI, X. 2016. Changes in SBPase activity influence photosynthetic capacity, growth, and tolerance to chilling stress in transgenic tomato plants. *Science Report,* **6,** 32741.

DODD, A. N., SALATHIA, N., HALL, A., KÉVEI, E., TÓTH, R., NAGY, F., HIBBERD, J. M., MILLAR, A. J. & WEBB, A. A. 2005. Plant circadian clocks increase photosynthesis, growth, survival, and competitive advantage. *Science,* **309,** 630-633.

DOI, M., KITAGAWA, Y. & SHIMAZAKI, K.-I. 2015. Stomatal blue light response is present in early vascular plants. *Plant Physiology,* **169,** 1205-1213.

DOI, M., WADA, M. & SHIMAZAKI, K.-I. 2006. The fern Adiantum capillus-veneris lacks stomatal responses to blue light. *Plant and cell physiology,* **47,** 748-755.

DRIEVER, S. M., SIMKIN, A. J., ALOTAIBI, S., FISK, S. J., MADGWICK, P. J., SPARKS, C. A., JONES, H. D., LAWSON, T., PARRY, M. A. J. & RAINES, C. A. 2017b. Increased SBPase activity improves photosynthesis and grain yield in wheat grown in greenhouse conditions. *Philosophical Transactions of the Royal Society B-Biological Sciences,* 372.

EASTMOND, P. J., ASTLEY, H. M., PARSLEY, K., AUBRY, S., WILLIAMS, B. P., MENARD, G. N., CRADDOCK, C. P., NUNES-NESI, A., FERNIE, A. R. & HIBBERD, J. M. 2015. Arabidopsis uses two gluconeogenic gateways for organic acids to fuel seedling establishment. *Nature communications,* **6,** 6659.

EDWARDS, D., KERP, H. & HASS, H. 1998. Stomata in early land plants: an anatomical and ecophysiological approach. *Journal of Experimental Botany,* **49,** 255-278.

EISENACH, C., CHEN, Z. H., GREFEN, C. & BLATT, M. R. 2012. The trafficking protein SYP121 of Arabidopsis connects programmed stomatal closure and K+ channel activity with vegetative growth. *The Plant Journal,* **69,** 241-251.

ENGLER, C., KANDZIA, R. & MARILLONNET, S. 2008. A one pot, one step, precision cloning method with high throughput capability. *PloS one,* **3,** e3647.

FARQUHAR, G. D., DUBBE, D. R. & RASCHKE, K. 1978. Gain of the feedback loop involving carbon dioxide and stomata: theory and measurement. *Plant Physiology,* **62,** 406-12.

FARQUHAR, G. D. & RASCHKE, K. 1978. On the resistance to transpiration of the sites of evaporation within the leaf. *Plant Physiology,* **61,** 1000-1005.

FARQUHAR, G. D. & SHARKEY, T. D. 1982. Stomatal conductance and photosynthesis. *Annual review of plant physiology,* **33,** 317-345.

FISCHER, R. 1968a. Stomatal opening: role of potassium uptake by guard cells. *Science,* **160,** 784-785.

FISCHER, R. & HSIAO, T. C. 1968. Stomatal opening in isolated epidermal strips of Vicia faba. II. Responses to KCl concentration and the role of potassium absorption. *Plant Physiology,* **43,** 1953-1958.

FISCHER, R. A. 1968b. Stomatal opening: role of potassium uptake by guard cells. *Science,* **160,** 784-5.

FRANCO, A. C., HERZOG, B., HUBNER, C., DE MATTOS, E. A., SCARANO, F. R., BALL, E. & LUTTGE, U. 1999. Diurnal changes in chlorophyll a fluorescence, CO(2)-exchange and organic acid decarboxylation in the tropical CAM tree Clusia hilariana. *Tree Physiology,* **19,** 635-644.

FRANKS, P. J. & FARQUHAR, G. D. 2007. The mechanical diversity of stomata and its significance in gas-exchange control. *Plant Physiology,* **143,** 78-87.

FRECHILLA, S., TALBOTT, L. D. & ZEIGER, E. 2004. The blue light-specific response of Vicia faba stomata acclimates to growth environment. *Plant Cell Physiology,* **45,** 1709-14.

FUJITA, T., NOGUCHI, K. & TERASHIMA, I. 2013a. Apoplastic mesophyll signals induce rapid stomatal responses to CO2 in Commelina communis. *New Phytology,* **199,** 395-406.

FUJITA, T., NOGUCHI, K. & TERASHIMA, I. 2013b. Apoplastic mesophyll signals induce rapid stomatal responses to CO2 in Commelina communis. *New Phytologist,* **199,** 395-406.

GAGO, J., DALOSO DDE, M., FIGUEROA, C. M., FLEXAS, J., FERNIE, A. R. & NIKOLOSKI, Z. 2016. Relationships of Leaf Net Photosynthesis, Stomatal Conductance, and Mesophyll Conductance to Primary Metabolism: A Multispecies Meta-Analysis Approach. *Plant Physiology,* **171,** 265-79.

GALBIATI, M., SIMONI, L., PAVESI, G., COMINELLI, E., FRANCIA, P., VAVASSEUR, A., NELSON, T., BEVAN, M. & TONELLI, C. 2008. Gene trap lines identify Arabidopsis genes expressed in stomatal guard cells. *The Plant Journal,* **53,** 750-762.

GAO, J. J., DAI, Z. J., MEI, X. F., GE, Z. P., WEI, W., XIE, H. L. & LI, S. S. 2015. Interference of natural and anthropogenic forcings on variations in continental freshwater discharge from the Red River (Vietnam) to sea. *Quaternary International,* **380,** 133-142.

GEHLEN, J., PANSTRUGA, R., SMETS, H., MERKELBACH, S., KLEINES, M., PORSCH, P., FLADUNG, M., BECKER, I., RADEMACHER, T., HAUSLER, R. E. & HIRSCH, H. J. 1996. Effects of altered phosphoenolpyruvate carboxylase activities on transgenic C3 plant Solanum tuberosum. *Plant Mol Biol,* **32,** 831-48.

GEIGER, D. R. & SERVAITES, J. C. 1994. Diurnal Regulation of Photosynthetic Carbon Metabolism in C3 Plants. *Annual Review of Plant Physiology and Plant Molecular Biology,* **45,** 235-256.

GOTOW, K., TAYLOR, S. & ZEIGER, E. 1988a. Photosynthetic Carbon Fixation in Guard Cell Protoplasts of Vicia faba L. : Evidence from Radiolabel Experiments. *Plant Physiology,* **86,** 700-5.

GOTOW, K., TAYLOR, S. & ZEIGER, E. 1988b. Photosynthetic carbon fixation in guard cell protoplasts of Vicia faba L. Evidence from radiolabel experiments. *Plant physiology,* **86,** 700-705.

GOTOW, K., TAYLOR, S ZEIGLER, E 1998. Photosynthetic Carbon Fixation in Guard Cell Protoplasts of Vicia faba L.1. *Plant physiology,* **86,** 700-705.

HAMPP, R., OUTLAW, W. H. & TARCZYNSKI, M. C. 1982. Profile of Basic Carbon Pathways in Guard Cells and Other Leaf Cells of Vicia faba L. *Plant Physiology,* **70,** 1582-5.

HARRISON, E. P., WILLINGHAM, N. M., LLOYD, J. C. & RAINES, C. A. 1998. Reduced sedoheptulose-1,7-bisphosphatase levels in transgenic tobacco lead to decreased photosynthetic capacity and altered carbohydrate accumulation. *Planta,* **204,** 27-36.

HENNESSEY, T. L. & FIELD, C. B. 1991. Circadian rhythms in photosynthesis oscillations in carbon assimilation and stomatal conductance under constant conditions. *Plant Physiology,* **96,** 831-836.

HETHERINGTON, A. M. & WOODWARD, F. I. 2003a. The role of stomata in sensing and driving environmental change. *Nature,* **424,** 901-8.

HETHERINGTON, A. M. & WOODWARD, F. I. 2003b. The role of stomata in sensing and driving environmental change. *Nature,* **424,** 901-908.

HIPKINS, M. F., FITZSIMONS, P. J. & WEYERS, J. D. 1983. The primary processes of photosystem II in purified guard-cell protoplasts and mesophyll-cell protoplasts from Commelina communis L. *Planta,* **159,** 554-560.

HIYAMA, A., TAKEMIYA, A., MUNEMASA, S., OKUMA, E., SUGIYAMA, N., TADA, Y., MURATA, Y. & SHIMAZAKI, K. I. 2017. Blue light and CO2 signals converge to regulate light-induced stomatal opening. *Nat Commun,* **8,** 1284.

HORRER, D., FLUTSCH, S., PAZMINO, D., MATTHEWS, J. S., THALMANN, M., NIGRO, A., LEONHARDT, N., LAWSON, T. & SANTELIA, D. 2016. Blue Light Induces a Distinct Starch Degradation Pathway in Guard Cells for Stomatal Opening. *Current Biology,* **26,** 362-70.

HORSCH, R. B., FRY, J., HOFFMANN, N., NEIDERMEYER, J., ROGERS, S. G. & FRALEY, R. T. 1989. Leaf disc transformation. *Plant molecular biology manual.* Springer. 63-79

HUMBLE, G. & RASCHKE, K. 1971. Stomatal opening quantitatively related to potassium transport evidence from electron probe analysis. *Plant Physiology,* **48,** 447-453.

IMAMURA, S. 1943. Untersuchungen über den Mechanismus der Turgorschwankung der Spaltöffnungsschließzellen. *Japan Journal of Botany,* **12,** 251-346.

IPCC. 2013.: Summary for Policymakers. In: Climate Change 2013**:** The Physical Science basis working group I. Contribution to the fifth assessment report of the Intergovernmental Panel on Climate Change**.,** Switzerland.

JAKOBSON, L., VAAHTERA, L., TOLDSEPP, K., NUHKAT, M., WANG, C., WANG, Y. S., HORAK, H., VALK, E., PECHTER, P., SINDAROVSKA, Y., TANG, J., XIAO, C., XU, Y., GERST TALAS, U., GARCIA-SOSA, A. T.,

KANGASJARVI, S., MARAN, U., REMM, M., ROELFSEMA, M. R., HU, H., KANGASJARVI, J., LOOG, M., SCHROEDER, J. I., KOLLIST, H. & BROSCHE, M. 2016. Natural Variation in Arabidopsis Cvi-0 Accession Reveals an Important Role of MPK12 in Guard Cell CO2 Signaling. *PLoScience Biology,* **14,** e2000322.

JEZEK, M. & BLATT, M. R. 2017. The Membrane Transport System of the Guard Cell and Its Integration for Stomatal Dynamics. *Plant Physiology,* **174,** 487-519.

JIA, W. & ZHANG, J. 2008. Stomatal movements and long-distance signaling in plants. *Plant Signal Behaviour,* **3,** 772-777.

JONES, H. G. 1998. Stomatal control of photosynthesis and transpiration. *Journal of Experimental Botany,* 387-398.

KANG, Y., OUTLAW, W. H., FIORE, G. B. & RIDDLE, K. A. 2007a. Guard cell apoplastic photosynthate accumulation corresponds to a phloem-loading mechanism. *Journal of experimental botany,* **58,** 4061-4070.

KEELING, R. E., KORTZINGER, A. & GRUBER, N. 2010. Ocean deoxygenation in a warming world. *Annual Review in Maritime Science,* **2,** 199-229.

KEENAN, T. F., GRAY, J., FRIEDL, M. A., TOOMEY, M., BOHRER, G., HOLLINGER, D. Y., MUNGER, J. W., O'KEEFE, J., SCHMID, H. P., WING, I. S., YANG, B. & RICHARDSON, A. D. 2014. Net carbon uptake has increased through warming-induced changes in temperate forest phenology. *Nature Climate Change,* **4,** 598.

KELLY, G., MOSHELION, M., DAVID-SCHWARTZ, R., HALPERIN, O., WALLACH, R., ATTIA, Z., BELAUSOV, E. & GRANOT, D. 2013. Hexokinase mediates stomatal closure. *The Plant Journal,* **75,** 977-988.

KIM, H.-H., GOINS, G. D., WHEELER, R. M. & SAGER, J. C. 2004. Stomatal conductance of lettuce grown under or exposed to different light qualities. *Annals of Botany*, **94,** 691-697.

KINOSHITA, T., DOI, M., SUETSUGU, N., KAGAWA, T., WADA, M. & SHIMAZAKI, K.-I. 2001. Phot1 and phot2 mediate blue light regulation of stomatal opening. *Nature,* **414,** 656-660.

KINOSHITA, T. & SHIMAZAKI, K.-I. 2002. Biochemical evidence for the requirement of 14-3-3 protein binding in activation of the guard-cell plasma membrane H+-ATPase by blue light. *Plant and Cell Physiology*, **43,** 1359-1365.

KIRCHHOFF, H., HORSTMANN, S. & WEIS, E. 2000. Control of the photosynthetic electron transport by PQ diffusion microdomains in thylakoids of higher plants. *Biochemistry and Biophys ics Acta,* **1459,** 148-68.

KIRCHHOFF, H., LI, M. & PUTHIYAVEETIL, S. 2017. Sublocalization of Cytochrome b6f Complexes in Photosynthetic Membranes. *Trends Plant Sci,* 22**,** 574-582.

KOßMANN, J., SONNEWALD, U. & WILLMITZER, L. 1994. Reduction of the chloroplastic fructose-1, 6-bisphosphatase in transgenic potato plants impairs photosynthesis and plant growth. *The Plant Journal,* **6,** 637-650.

LAKE, J., QUICK, W., BEERLING, D. & WOODWARD, F. 2001. Plant development: signals from mature to new leaves. *Nature*, **411,** 154-154.

LASCEVE, G., LEYMARIE, J. & VAVASSEUR, A. 1997. Alterations in light-induced stomatal opening in a starch-deficient mutant of Arabidopsis thaliana L. deficient in chloroplast phosphoglucomutase activity. *Plant, Cell & Environment,* **20,** 350-358.

LAWSON, T. 2009. Guard cell photosynthesis and stomatal function. *New Phytologist,* **181,** 13-34.

LAWSON, T. & BLATT, M. R. 2014a. Stomatal size, speed, and responsiveness impact on photosynthesis and water use efficiency. *Plant Physiology,* 164**,** 1556-70.

LAWSON, T. & BLATT, M. R. 2014b. Stomatal Size, Speed, and Responsiveness Impact on Photosynthesis and Water Use Efficiency. *Plant Physiology,* **164,** 1556-1570.

LAWSON, T., BRYANT, B., LEFEBVRE, S., LLOYD, J. C. & RAINES, C. A. 2006. Decreased SBPase activity alters growth and development in transgenic tobacco plants. *Plant Cell Environ,* **29,** 48-58.

LAWSON, T., DAVEY, P. A., YATES, S. A., BECHTOLD, U., BAESHEN, M., BAESHEN, N., MUTWAKIL, M. Z., SABIR, J., BAKER, N. R. & MULLINEAUX, P. M. 2014a. C-3 photosynthesis in the desert plant Rhazya stricta is fully functional at high temperatures and light intensities. *New Phytologist,* **201,** 862-873.

LAWSON, T., KRAMER, D. M. & RAINES, C. A. 2012. Improving yield by exploiting mechanisms underlying natural variation of photosynthesis. *Current opinion in biotechnology,* **23,** 215-220.

LAWSON, T., LEFEBVRE, S., BAKER, N. R., MORISON, J. I. & RAINES, C. A. 2008a. Reductions in mesophyll and guard cell photosynthesis impact on the control of stomatal responses to light and CO2. *Journal of Experimental Botany,* **59,** 3609-19.

LAWSON, T., LEFEBVRE, S., BAKER, N. R., MORISON, J. I. & RAINES, C. A. 2008b. Reductions in mesophyll and guard cell photosynthesis impact on the control of stomatal responses to light and CO2. *Journal of experimental botany,* **59,** 3609-3619.

LAWSON, T., OXBOROUGH, K., MORISON, J. & BAKER, N. Evaluating guard cell photosynthesis in intact green leaves using chlorophyll fluorescence imaging. *Science Access,* 3.

LAWSON, T., OXBOROUGH, K., MORISON, J. I. & BAKER, N. R. 2002. Responses of photosynthetic electron transport in stomatal guard cells and mesophyll cells in intact leaves to light, CO2, and humidity. *Plant Physiology,* **128,** 52-62.

LAWSON, T., OXBOROUGH, K., MORISON, J. I. & BAKER, N. R. 2003b. The responses of guard and mesophyll cell photosynthesis to CO2, O2, light, and water stress in a range of species are similar. *Journal of experimental botany,* **54,** 1743-1752.

LAWSON, T., OXBOROUGH, K., MORISON, J. I. L. & BAKER, N. R. 2003c. The responses of guard and mesophyll cell photosynthesis to CO2, O-2, light, and water stress in a range of species are similar. *Journal of Experimental Botany,* **54,** 1743-1752.

LAWSON, T., SIMKIN, A. J., KELLY, G. & GRANOT, D. 2014b. Mesophyll photosynthesis and guard cell metabolism impacts on stomatal behaviour. *New Phytologist,* **203,** 1064-81.

LAWSON, T., SIMKIN, A. J., KELLY, G. & GRANOT, D. 2014c. Mesophyll photosynthesis and guard cell metabolism impacts on stomatal behaviour. *New Phytologist,* **203,** 1064-1081.

LAWSON, T., VON CAEMMERER, S. & BAROLI, I. 2011. Photosynthesis and stomatal behaviour. *Progress in Botany 72.* Springer.

LAWSON, T. & WEYERS, J. 1999. Spatial and temporal variation in gas exchange over the lower surface of Phaseolus vulgaris L. primary leaves. *Journal of Experimental Botany,* **50,** 1381-1391.

LEE, J.-S. & BOWLING, D. 1995. Influence of the mesophyll on stomatal opening. *Functional Plant Biology,* **22,** 357-363.

LEE, J. & BOWLING, D. 1992. Effect of the mesophyll on stomatal opening in Commelina communis. *Journal of experimental botany,* **43,** 951-957.

LEE, J. & BOWLING, D. 1993. The effect of a mesophyll factor on the swelling of guard cell protoplasts of Commelina communis L. *Journal of plant physiology,* **142,** 203-207.

LEFEBVRE, S., LAWSON, T., ZAKHLENIUK, O. V., LLOYD, J. C., RAINES, C. A. & FRYER, M. 2005. Increased sedoheptulose-1,7-bisphosphatase activity in transgenic tobacco plants stimulates photosynthesis and growth from an early stage in development. *Plant Physiology,* **138,** 451-60.

LI, C.-L., WANG, M., MA, X.-Y. & ZHANG, W. 2014. NRGA1, a Putative Mitochondrial Pyruvate Carrier, Mediates ABA Regulation of Guard Cell Ion Channels and Drought Stress Responses in Arabidopsis. *Molecular plant,* ssu061.

LLOYD, F. E. 1908. *The physiology of stomata*, Carnegie Institution of Washington.

LONG, S. P., ZHU, X. G., NAIDU, S. L. & ORT, D. R. 2006. Can improvement in photosynthesis increase crop yields? *Plant, Cell & Environment,* **29,** 315-330.

LU, P., OUTLAW JR, W. H., SMITH, B. G. & FREED, G. A. 1997a. A new mechanism for the regulation of stomatal aperture size in intact leaves (accumulation of mesophyll-derived sucrose in the guard-cell wall of Vicia faba). *Plant Physiology,* **114,** 109-118.

LU, P., OUTLAW JR, W. H., SMITH, B. G. & FREED, G. A. 1997b. A New Mechanism for the Regulation of Stomatal Aperture Size in Intact Leaves (Accumulation of Mesophyll-Derived Sucrose in the Guard-Cell Wall of Vicia faba). *Plant Physiology*, **114,** 109-118.

LU, P., ZHANG, S. Q., OUTLAW, W. H., JR. & RIDDLE, K. A. 1995. Sucrose: a solute that accumulates in the guard-cell apoplast and guard-cell symplast of open stomata. *FEBS Lett,* **362,** 180-4.

LURIE, S. 1977. Photochemical properties of guard cell chloroplasts. *Plant Science Letters,* 10**,** 219-223.

MACROBBIE, E. 1987. Ionic Relations of Guard Cells EAC MacRobbie. *Stomatal function***,** 125.

MADHAVAN, S. & SMITH, B. N. 1982. Localization of ribulose bisphosphate carboxylase in the guard cells by an indirect, immunofluorescence technique. *Plant physiology,* **69,** 273-277.

MANSFIELD, T., HETHERINGTON, A. & ATKINSON, C. 1990. Some current aspects of stomatal physiology. *Annual review of plant biology,* 41**,** 55-75.

MANSFIELD, T. & MAJERNIK, O. 1970. Can stomata play a part in protecting plants against air pollutants? *Environmental Pollution (1970),* **1,** 149-154.

MATROSOVA, A., BOGIREDDI, H., MATEO-PENAS, A., HASHIMOTO-SUGIMOTO, M., IBA, K., SCHROEDER, J. I. & ISRAELSSON-NORDSTROM, M. 2015. The HT1 protein kinase is essential for red light-induced stomatal opening and genetically interacts with OST1 in red light and CO2 -induced stomatal movement responses. *New Phytologist,* **208,** 1126-37.

MCAUSLAND, L., VIALET-CHABRAND, S., DAVEY, P., BAKER, N. R., BRENDEL, O. & LAWSON, T. 2016. Effects of kinetics of light-induced stomatal responses on photosynthesis and water-use efficiency. *New Phytologist,* **211,** 1209-1220.

MEDEIROS, D. B., MARTINS, S. C., CAVALCANTI, J. H., DALOSO, D. M., MARTINOIA, E., NUNES-NESI, A., DAMATTA, F. M., FERNIE, A. R. &

ARAUJO, W. L. 2016. Enhanced Photosynthesis and Growth in atquac1 Knockout Mutants Are Due to Altered Organic Acid Accumulation and an Increase in Both Stomatal and Mesophyll Conductance. *Plant Physiology,* **170,** 86-101.

MEIDNER, H. & MANSFIELD, T. A. 1968. Physiology of stomata. *Physiology of stomata.*

MEIDNER, H. & WILLMER, C. 1993. Circadian rhythm of stomatal movements in epidermal strips. *Journal of experimental botany,* **44,** 1649-1652.

MELIS, A. & ZEIGER, E. 1982a. Chlorophyll a Fluorescence Transients in Mesophyll and Guard Cells : MODULATION OF GUARD CELL PHOTOPHOSPHORYLATION BY CO(2). *Plant Physiology,* **69,** 642-7.

MELIS, A. & ZEIGER, E. 1982b. Chlorophyll a Fluorescence Transients in Mesophyll and Guard Cells MODULATION OF GUARD CELL PHOTOPHOSPHORYLATION BY CO2. *Plant physiology,* **69,** 642-647.

MESSINGER, S. M., BUCKLEY, T. N. & MOTT, K. A. 2006. Evidence for involvement of photosynthetic processes in the stomatal response to CO2. *Plant Physiology,* **140,** 771-778.

MIYAGAWA, Y., TAMOI, M. & SHIGEOKA, S. 2001. Overexpression of a cyanobacterial fructose-1,6-/sedoheptulose-1,7-bisphosphatase in tobacco enhances photosynthesis and growth. *Nature Biotechnology,* **19,** 965-9.

MORISON, J. & JARVIS, P. 1983. Direct and indirect effects of light on stomata. I. In Scots pine and Sitka spruce. *Plant, Cell & Environment,* **6,** 95-101.

MOTT, K. A. 1988. Do Stomata Respond to CO(2) Concentrations Other than Intercellular? *Plant Physiology,* **86,** 200-3.

MOTT, K. A. 2009. Opinion: stomatal responses to light and CO(2) depend on the mesophyll. *Plant Cell Environmrnt,* **32,** 1479-86.

MOTT, K. A., BERG, D. G., HUNT, S. M. & PEAK, D. 2013. Is the signal from the mesophyll to the guard cells a vapour-phase ion? *Plant, cell & environment*.

MOTT, K. A., BERG, D. G., HUNT, S. M. & PEAK, D. 2014. Is the signal from the mesophyll to the guard cells a vapour-phase ion? *Plant Cell Environ,* **37,** 1184-91.

MOTT, K. A., SIBBERNSEN, E. D. & SHOPE, J. C. 2008a. The role of the mesophyll in stomatal responses to light and CO2. *Plant, cell & environment,* **31,** 1299-1306.

MÜLLER-RÖBER, B., ELLENBERG, J., PROVART, N., WILLMITZER, L., BUSCH, H., BECKER, D., DIETRICH, P., HOTH, S. & HEDRICH, R. 1995a. Cloning and electrophysiological analysis of KST1, an inward rectifying K+ channel expressed in potato guard cells. *The EMBO Journal,* **14,** 2409-2416.

MÜLLER-RÖBER, B., ELLENBERG, J., PROVART, N., WILLMITZER, L., BUSCH, H., BECKER, D., DIETRICH, P., HOTH, S. & HEDRICH, R. 1995b. Cloning and electrophysiological analysis of KST1, an inward rectifying K+ channel expressed in potato guard cells. *The EMBO journal,* **14,** 2409.

MUSCHAK, M., WILLMITZER, L. & FISAHN, J. 1999. Gas-exchange analysis of chloroplastic fructose-1, 6-bisphosphatase antisense potatoes at different air humidities and at elevated CO2. *Planta,* **209,** 104-111.

NELSON, S. D. & MAYO, J. M. 1975. The occurrence of functional non-chlorophyllous guard cells in Paphiopedilum spp. *Canadian Journal of Botany,* **53,** 1-7.

NILSON, S. E. & ASSMANN, S. M. 2007. The control of transpiration. Insights from Arabidopsis. *Plant physiology,* **143,** 19-27.

NOBEL, P. S. 1991. Achievable productivities of certain CAM plants: basis for high values compared with C3 and C4 plants. *New Phytologist,* **119,** 183-205.

OGAWA, T., ISHIKAWA, H., SHIMADA, K. & SHIBATA, K. 1978. Synergistic action of red and blue light and action spectra for malate formation in guard cells of Vicia faba L. *Planta,* **142,** 61-65.

OLSEN, R. L., PRATT, R. B., GUMP, P., KEMPER, A. & TALLMAN, G. 2002. Red light activates a chloroplast-dependent ion uptake mechanism for stomatal opening under reduced CO2 concentrations in Vicia spp. *New Phytologist,* **153,** 497-508.

OSMOND, C. 1978. Crassulacean acid metabolism: a curiosity in context. *Annual Review of Plant Physiology,* **29,** 379-414.

OUTLAW, W. H., JR. & DE VLIEGHERE-HE, X. 2001. Transpiration rate. An important factor controlling the sucrose content of the guard cell apoplast of broad bean. *Plant Physiology,* **126,** 1716-24.

OUTLAW, W. H. & LOWRY, O. H. 1977. Organic acid and potassium accumulation in guard cells during stomatal opening. *Proceedings of the National Academy of Sciences,* **74,** 4434-4438.

OUTLAW, W. H. & MANCHESTER, J. 1979. Guard cell starch concentration quantitatively related to stomatal aperture. *Plant Physiology,* 64**,** 79-82.

OUTLAW, W. H., MAYNE, B. C., ZENGER, V. E. & MANCHESTER, J. 1981. Presence of both photosystems in guard cells of Vicia faba L implications for environmental signal processing. *Plant physiology*, **67,** 12-16.

PARK WILLIAMS, A., ALLEN, C. D., MACALADY, A. K., GRIFFIN, D., WOODHOUSE, C. A., MEKO, D. M., SWETNAM, T. W., RAUSCHER, S. A., SEAGER, R., GRISSINO-MAYER, H. D., DEAN, J. S., COOK, E. R., GANGODAGAMAGE, C., CAI, M. & MCDOWELL, N. G. 2012. Temperature

as a potent driver of regional forest drought stress and tree mortality. *Nature Climate Change,* **3,** 292.

PEARCY, R. W. 1990. Sunflecks and photosynthesis in plant canopies. *Annual review of plant biology,* **41,** 421-453.

PEARCY, R. W. & WAY, D. A. 2012. Two decades of sunfleck research: looking back to move forward. *Tree physiology,* **32,** 1059-1061.

PEIRSON, S. N., BUTLER, J. N. & FOSTER, R. G. 2003. Experimental validation of novel and conventional approaches to quantitative real-time PCR data analysis. *Nucleic Acids Research,* **31**, e73.

PFAFFL, M. W., HORGAN, G. W. & DEMPFLE, L. 2002. Relative expression software tool (REST) for group-wise comparison and statistical analysis of relative expression results in real-time PCR. *Nucleic Acids Research*, **30**, e36.

POFFENROTH, M., GREEN, D. B. & TALLMAN, G. 1992a. Sugar Concentrations in Guard Cells of Vicia faba Illuminated with Red or Blue Light : Analysis by High Performance Liquid Chromatography. *Plant Physiology,* **98,** 1460-71.

PRICE, G. D., CAEMMERER, S. V., EVANS, J. R., SIEBKE, K., ANDERSON, J. M. & BADGER, M. R. 1998. Photosynthesis is strongly reduced by antisense suppression of chloroplastic cytochrome complex in transgenic tobacco. *Functional Plant Biology,* **25,** 445-452.

RAINES, C. A. 2003. The Calvin cycle revisited. *Photosynthesis research,* **75,** 1-10.

RAINES, C. A. 2006. Transgenic approaches to manipulate the environmental responses of the C3 carbon fixation cycle. *Plant, cell & environment,* **29,** 331-339.

RAINES, C. A. 2011. Increasing Photosynthetic Carbon Assimilation in C₃ Plants to Improve Crop Yield: Current and Future Strategies. *Plant Physiology,* **155,** 36.

RAINES, C. A., LLOYD, J. C. & DYER, T. A. 1999. New insights into the structure and function of sedoheptulose-1, 7-bisphosphatase; an important but neglected Calvin cycle enzyme. *Journal of experimental botany,* **50,** 1-8.

RAINES, C. A. & PAUL, M. J. 2006. Products of leaf primary carbon metabolism modulate the developmental programme determining plant morphology. *Journal of Experimental Botany,* **57,** 1857-1862.

RAISSIG, M. T., MATOS, J. L., ANLEU GIL, M. X., KORNFELD, A., BETTADAPUR, A., ABRASH, E., ALLISON, H. R., BADGLEY, G., VOGEL, J. P., BERRY, J. A. & BERGMANN, D. C. 2017. Mobile MUTE specifies subsidiary cells to build physiologically improved grass stomata. *Science,* **355,** 1215-1218.

RAO, I. M. & ANDERSON, L. E. 1983. Light and stomatal metabolism II. Effects of sulfite and arsenite on stomatal opening and light modulation of enzymes in epidermis. *Plant physiology,* **71,** 456-459.

RASCHKE, K. 1975. Stomatal action. *Annual Review of Plant Physiology,* 26**,** 309-340.

RASCHKE, K. & DITTRICH, P. 1977. [14C] Carbon-dioxide fixation by isolated leaf epidermes with stomata closed or open. *Planta,* **134,** 69-75.

RASCHKE, K. & SCHNABL, H. 1978. Availability of Chloride Affects the Balance between Potassium Chloride and Potassium Malate in Guard Cells of Vicia faba L. *Plant Physiology,* **62,** 84-7.

RECKMANN, U., SCHEIBE, R. & RASCHKE, K. 1990. Rubisco activity in guard cells compared with the solute requirement for stomatal opening. *Plant physiology,* **92,** 246-253.

REICHSTEIN, M., BAHN, M., CIAIS, P., FRANK, D., MAHECHA, M. D., SENEVIRATNE, S. I., ZSCHEISCHLER, J., BEER, C., BUCHMANN, N.,

FRANK, D. C., PAPALE, D., RAMMIG, A., SMITH, P., THONICKE, K., VAN DER VELDE, M., VICCA, S., WALZ, A. & WATTENBACH, M. 2013. Climate extremes and the carbon cycle. *Nature,* **500,** 287.

RIESKE, J. S., MACLENNAN, D. H. & COLEMAN, R. 1964. Isolation and properties of an iron-protein from the (reduced coenzyme Q)-cytochrome C reductase complex of the respiratory chain. *Biochemical and Biophysical Research Communications,* **15,** 338-344.

ROELFSEMA, M. R. & HEDRICH, R. 2005. In the light of stomatal opening: new insights into 'the Watergate'. *New Phytologist,* **167,** 665-91.

ROELFSEMA, M. R. G., HANSTEIN, S., FELLE, H. H. & HEDRICH, R. 2002. CO2 provides an intermediate link in the red light response of guard cells. *The Plant Journal,* **32,** 65-75.

RUSCONI, F., SIMEONI, F., FRANCIA, P., COMINELLI, E., CONTI, L., RIBONI, M., SIMONI, L., MARTIN, C. R., TONELLI, C. & GALBIATI, M. 2013. The Arabidopsis thaliana MYB60 promoter provides a tool for the spatio-temporal control of gene expression in stomatal guard cells. *Journal of Experimental Botany,* **64,** 3361-3371.

SANTELIA, D. & LAWSON, T. 2016. Rethinking Guard Cell Metabolism. *Plant Physiology,* **172,** 1371-1392.

SCHEIBE, R., RECKMANN, U., HEDRICH, R. & RASCHKE, K. 1990. Malate dehydrogenases in guard cells of Pisum sativum. *Plant physiology,* **93,** 1358-1364.

SCHNABL, H. 1980. CO2 and malate metabolism in starch-containing and starch-lacking guard-cell protoplasts. *Planta,* **149,** 52-8.

SCHNABL, H. 1981. The compartmentation of carboxylating and decarboxylating enzymes in guard cell protoplasts. *Planta,* **152,** 307-313.

SCHROEDER, J. I., ALLEN, G. J., HUGOUVIEUX, V., KWAK, J. M. & WANER, D. 2001. GUARD CELL SIGNAL TRANSDUCTION. *Annual Review in Plant Physiology and Plant Molecular Biology,* **52,** 627-658.

SCHWARTZ, A., ILAN, N. & GRANTZ, D. A. 1988. Calcium effects on stomatal movement in Commelina communis L. Use of EGTA to modulate stomatal response to light, KCl and CO2. *Plant Physiology,* **87,** 583-587.

SCHWARTZ, A. & ZEIGER, E. 1984. Metabolic energy for stomatal opening. Roles of photophosphorylation and oxidative phosphorylation. *Planta,* **161,** 129-136.

SHARKEY, T. D., BERNACCHI, C. J., FARQUHAR, G. D. & SINGSAAS, E. L. 2007. Fitting photosynthetic carbon dioxide response curves for C3 leaves. *Plant, Cell & Environment,* **30,** 1035-1040.

SHARKEY, T. D. & RASCHKE, K. 1981. Effect of light quality on stomatal opening in leaves of Xanthium strumarium L. *Plant Physiology,* **68,** 1170-1174.

SHIMAZAKI, K.-I., GOTOW, K. & KONDO, N. 1982. Photosynthetic properties of guard cell protoplasts from Vicia faba L. *Plant and Cell Physiology,* **23,** 871-879.

SHIMAZAKI, K.-I. & OKAYAMA, S. 1990. Calvin Benson cycle enzymes in guard-cell protoplasts and their role in stomatal movement. *Biochemie und Physiologie der Pflanzen,* **186,** 327-331.

SHIMAZAKI, K.-I. & ZEIGER, E. 1985. Cyclic and noncyclic photophosphorylation in isolated guard cell chloroplasts from Vicia faba L. *Plant physiology,* **78,** 211-214.

SHTEIN, I., SHELEF, Y., MAROM, Z., ZELINGER, E., SCHWARTZ, A., POPPER, Z. A., BAR-ON, B. & HARPAZ-SAAD, S. 2017. Stomatal cell wall composition:

distinctive structural patterns associated with different phylogenetic groups. *Annals of Botany,* **119,** 1021-1033.

SIMKIN, A. J., LOPEZ-CALCAGNO, P. E., DAVEY, P. A., HEADLAND, L. R., LAWSON, T., TIMM, S., BAUWE, H. & RAINES, C. A. 2017a. Simultaneous stimulation of sedoheptulose 1,7-bisphosphatase, fructose 1,6-bisphophate aldolase and the photorespiratory glycine decarboxylase-H protein increases CO2 assimilation, vegetative biomass and seed yield in Arabidopsis. *Plant Biotechnology Journal,* **15,** 805-816.

SIMKIN, A. J., MCAUSLAND, L., HEADLAND, L. R., LAWSON, T. & RAINES, C. A. 2015. Multigene manipulation of photosynthetic carbon assimilation increases CO2 fixation and biomass yield in tobacco. *Journal of Experimental Botany,* **66,** 4075-90.

SIMKIN, A. J., MCAUSLAND, L., LAWSON, T. & RAINES, C. A. 2017b. Overexpression of the RieskeFeS Protein Increases Electron Transport Rates and Biomass Yield. *Plant Physiology,* **175,** 134.

SIMKIN, A. J., MCAUSLAND, L., LAWSON, T. & RAINES, C. A. 2017c. Overexpression of the RieskeFeS Protein Increases Electron Transport Rates and Biomass Yield. *Plant Physiology,* **175,** 134-145.

SMITH, A. M. & STITT, M. 2007. Coordination of carbon supply and plant growth. *Plant and Cell Environment,* **30,** 1126-49.

STEVENS, R. & MARTIN, E. 1978. Structural and functional aspects of stomata. *Planta,* 142**,** 307-316.

STROEBEL, D., CHOQUET, Y., POPOT, J. L. & PICOT, D. 2003. An atypical haem in the cytochrome b(6)f complex. *Nature,* 426**,** 413-8.

SUETSUGU, N., TAKAMI, T., EBISU, Y., WATANABE, H., IIBOSHI, C., DOI, M. & SHIMAZAKI, K.-I. 2014a. Guard Cell Chloroplasts Are Essential for Blue Light-Dependent Stomatal Opening in Arabidopsis. *PloS one,* 9**,** e108374.

SUETSUGU, N., TAKAMI, T., EBISU, Y., WATANABE, H., IIBOSHI, C., DOI, M. & SHIMAZAKI, K. 2014b. Guard cell chloroplasts are essential for blue light-dependent stomatal opening in Arabidopsis. *PLoS One,* 9**,** e108374.

TALBOTT, L. & ZEIGER, E. 1998. The role of sucrose in guard cell osmoregulation. *Journal of Experimental Botany,* **49,** 329-337.

TALBOTT, L. D. & ZEIGER, E. 1993. Sugar and Organic Acid Accumulation in Guard Cells of Vicia faba in Response to Red and Blue Light. *Plant Physiology,* **102,** 1163-1169.

TALBOTT, L. D. & ZEIGER, E. 1996. Central roles for potassium and sucrose in guard-cell osmoregulation. *Plant Physiology,* **111,** 1051-1057.

TALLMAN, G. & ZEIGER, E. 1988a. Light quality and osmoregulation in vicia guard cells : evidence for involvement of three metabolic pathways. *Plant Physiology,* **88,** 887-95.

TALLMAN, G. & ZEIGER, E. 1988b. Light quality and osmoregulation in Vicia guard cells evidence for involvement of three metabolic pathways. *Plant Physiology,* **88,** 887-895.

TANAKA, Y., SUGANO, S. S., SHIMADA, T. & HARA-NISHIMURA, I. 2013. Enhancement of leaf photosynthetic capacity through increased stomatal density in Arabidopsis. *New Phytologist,* **198,** 757-764.

TERASHIMA, I., TANG, Y. & MURAOKA, H. 2016. Spatio-temporal variations in photosynthesis. *Journal of plant research,* **3,** 295-298.

TICHÁ, I. 1982. Photosynthetic characteristics during ontogenesis of leaves. 7. Stomata density and sizes. *Photosynthetica*.

TINOCO-OJANGUREN, C. & PEARCY, R. W. 1993. Stomatal dynamics and its importance to carbon gain in two rainforest Piper species. I. VPD effects on the transient stomatal response to lightflecks. *Oecologia***,** 388-394.

TOMINAGA, M., KINOSHITA, T. & SHIMAZAKI, K.-I. 2001. Guard-cell chloroplasts provide ATP required for H+ pumping in the plasma membrane and stomatal opening. *Plant and Cell Physiology*, **42,** 795-802.

TRAVIS, A. & MANSFIELD, T. 1979. Stomatal responses to light and CO2 are dependent on KCI concentration. *Plant, Cell & Environment,* **2,** 319-323.

TSIONSKY, M., CARDON, Z. G., BARD, A. J. & JACKSON, R. B. 1997. Photosynthetic Electron Transport in Single Guard Cells as Measured by Scanning Electrochemical Microscopy. *Plant Physiology,* **113,** 895-901.

UEMATSU, K., SUZUKI, N., IWAMAE, T., INUI, M. & YUKAWA, H. 2012. Increased fructose 1,6-bisphosphate aldolase in plastids enhances growth and photosynthesis of tobacco plants. *Journal of Experimental Botany,* **63,** 3001-9.

UENO, O. 2001. Ultrastructural localization of photosynthetic and photorespiratory enzymes in epidermal, mesophyll, bundle sheath, and vascular bundle cells of the C4 dicot Amaranthus viridis. *Journal of experimental biology* **52,** 1003-13.

VAVASSEUR, A. & RAGHAVENDRA, A. S. 2005. Guard cell metabolism and CO2 sensing. *New Phytologist,* **165,** 665-82.

VIALET-CHABRAND, S., MATTHEWS, J., BRENDEL, O., BLATT, M., WANG, Y., HILLS, A., GRIFFITHS, H., ROGERS, S. & LAWSON, T. 2016. Modelling water use efficiency in a dynamic environment: An example using Arabidopsis thaliana. *Plant Science,* **251,** 65-74.

VON CAEMMERER, S. & EVANS, J. R. 2010. Enhancing C(3) Photosynthesis. *Plant Physiology,* **154,** 589-592.

VON CAEMMERER, S. & FARQUHAR, G. D. 1981. Some relationships between the biochemistry of photosynthesis and the gas exchange of leaves. *Planta,* **153,** 376-87.

VON CAEMMERER, S. & FURBANK, R. T. 2016. Strategies for improving C4 photosynthesis. *Current Opinion in Plant Biollogy,* **31,** 125-34.

VON CAEMMERER, S. & GRIFFITHS, H. 2009a. Stomatal responses to CO2 during a diel Crassulacean acid metabolism cycle in Kalanchoe daigremontiana and Kalanchoe pinnata. *Plant Cell and Environment,* **32,** 567-76.

VON CAEMMERER, S. & GRIFFITHS, H. 2009b. Stomatal responses to CO2 during a diel Crassulacean acid metabolism cycle in Kalanchoe daigremontiana and Kalanchoe pinnata. *Plant Cell Environ,* **32,** 567-76.

VON CAEMMERER, S., LAWSON, T., OXBOROUGH, K., BAKER, N. R., ANDREWS, T. J. & RAINES, C. A. 2004. Stomatal conductance does not correlate with photosynthetic capacity in transgenic tobacco with reduced amounts of Rubisco. *Journal of Experimental Botany,* **55,** 1157-1166.

WANG, P. & SONG, C. P. 2008. Guard-cell signalling for hydrogen peroxide and abscisic acid. *New Phytologist,* **178,** 703-718.

WANG, S. W., LI, Y., ZHANG, X. L., YANG, H. Q., HAN, X. F., LIU, Z. H., SHANG, Z. L., ASANO, T., YOSHIOKA, Y., ZHANG, C. G. & CHEN, Y. L. 2014a. Lacking chloroplasts in guard cells of crumpled leaf attenuates stomatal opening: both guard cell chloroplasts and mesophyll contribute to guard cell ATP levels. *Plant Cell and Environment,* **37,** 2201-10.

WANG, Y., NOGUCHI, K., ONO, N., INOUE, S.-I., TERASHIMA, I. & KINOSHITA, T. 2014b. Overexpression of plasma membrane H+-ATPase in guard cells promotes light-induced stomatal opening and enhances plant growth. *Proceedings of the National Academy of Sciences,* **111,** 533-538.

WANG, Y., NOGUCHI, K. & TERASHIMA, I. 2008. Distinct light responses of the adaxial and abaxial stomata in intact leaves of Helianthus annuus L. *Plant and Cell Environment,* **31,** 1307-16.

WEBB, A. A., MCAINSH, M. R., MANSFIELD, T. A. & HETHERINGTON, A. M. 1996. Carbon dioxide induces increases in guard cell cytosolic free calcium. *The Plant Journal,* **9,** 297-304.

WEBER, E., ENGLER, C., GRUETZNER, R., WERNER, S. & MARILLONNET, S. 2011. A Modular Cloning System for Standardized Assembly of Multigene Constructs. *PLOS ONE,* **6,** e16765.

WEYERS, J. D. & MEIDNER, H. 1990. Methods in stomatal research.

World Water Organisation 2010: The high-level conference on water and global health at the United Nations. April 8-9, 2010. United Nations Headquarters , New York City.

WILLMER, C. & DITTRICH, P. 1974. Carbon dioxide fixation by epidermal and mesophyll tissues of Tulipa and Commelina. *Planta,* 117**,** 123-132.

WILLMER, C. & FRICKER, M. 1996. *Stomata,* Springer Science & Business Media.

WILMER, C. & FRICKER, M. 1996. Stomata. *Chapmann & Hall, London.*

WONG, S., COWAN, IR, FARQUHAR GD 1979. Stomatal conductance correlates with photosynthetic activity. *Nature,* **282,** 424-426

WOODROW, I. E. & BERRY, J. A. 1988. Enzymatic Regulation of Photosynthetic CO2, Fixation in C3 Plants. *Annual Review of Plant Physiology and Plant Molecular Biology,* **39,** 533-594.

YAMASHITA, E., ZHANG, H. & CRAMER, W. A. 2007. Structure of the Cytochrome b(6)f Complex: Quinone Analogue Inhibitors as Ligands of Heme c(n). *Journal of molecular biology,* **370,** 39-52.

YANG, C.-Y., CHEN, Y.-C., JAUH, G. Y. & WANG, C.-S. 2005. A lily ASR protein involves abscisic acid signaling and confers drought and salt resistance in Arabidopsis. *Plant physiology,* **139,** 836-846.

YOO, C. Y., PENCE, H. E., JIN, J. B., MIURA, K., GOSNEY, M. J., HASEGAWA, P. M. & MICKELBART, M. V. 2010. The Arabidopsis GTL1 transcription factor regulates water use efficiency and drought tolerance by modulating stomatal density via transrepression of SDD1. *The Plant Cell* **22,** 4128-4141.

ZEIGER, E., ARMOND, P. & MELIS, A. 1981. Fluorescence Properties of Guard Cell Chloroplasts EVIDENCE FOR LINEAR ELECTRON TRANSPORT AND LIGHT-HARVESTING PIGMENTS OF PHOTOSYSTEMS I AND II. *Plant Physiology,* **67,** 17-20.

ZEIGER, E., TALBOTT, L. D., FRECHILLA, S., SRIVASTAVA, A. & ZHU, J. 2002. The guard cell chloroplast: a perspective for the twenty-first century. *New Phytologist,* **153,** 415-424.

ZEIGER, E. & ZHU, J. 1998. Role of zeaxanthin in blue light photoreception and the modulation of light-CO2 interactions in guard cells. *Journal of Experimental Botany,* **49,** 433-442.

ZEMEL, E. & GEPSTEIN, S. 1985. Immunological evidence for the presence of ribulose bisphosphate carboxylase in guard cell chloroplasts. *Plant Physiology,* **78,** 586-590.

ZHU, M. & ASSMANN, S. M. 2017. Metabolic Signatures in Response to Abscisic Acid (ABA) Treatment in Brassica napus Guard Cells Revealed by Metabolomics. *Science Report,* **7,** 12875.

ZHU, X.-G., DE STURLER, E. & LONG, S. P. 2007. Optimizing the distribution of resources between enzymes of carbon metabolism can dramatically increase photosynthetic rate: a numerical simulation using an evolutionary algorithm. *Plant Physiology,* **145,** 513-526

APPENDIXES

Appendix 1

1.- (a) Primers used for cloning, construction of vector plasmids, sequencing and screening of mutant plants.

Oligo type	Oligo Name	5' to 3' sequence	length	uses
STD	**scr-pL2B-FP2**	CGAGTGGTGATTTTGTGCCG	20	Primer for screening. It is placed in the vector backbone and is compatible with all other pL2B RP primers.
STD	**scr-BAR-3'-FP**	CTGAGTGGCTCCTTCAACGT	20	Primer for screening constructs containing BAR . It is placed in the pNOS sequence preceding the BAR CDS and is compatible with all other pL2B RP primers.
STD	**scr-BAR-3'-FP2**	ACGGAAGTTGACCGTGCTTG	20	Primer for screening containing BAR . It is placed in the gene's coding sequence and is compatible with all other pL2B RP primers.
STD	**scr-BAR-5'-RP**	TTCTGGCAGCTGGACTTCAG	20	Primer for screening constructs containing BAR . It is placed in the gene's coding sequence and is compatible with all other pL2B RP primers.
STD	**scr-AtSBPase-3'-FP**	TACACACTGCGATACACCGG	20	Primer for screening and cloning . It is placed in the gene's coding sequence and is compatible with all other pL2B RP primers.
STD	**scr-AtSBPase-5'-RP**	CTTCCACTGGACCTCCCATG	20	Primer for screening and cloning . It is placed in the gene's coding sequence and is compatible with all other pL2B RP primers.
STD	**scr-AtRieske-FP**	ACTGGCTACATGCTTGTCCC	20	Primer for screening and cloning . It is placed in the gene's coding sequence and is compatible with all other pL2B RP primers.
STD	**scr-AtRieske-RP**	ATTCCGCTGCAACTACATCG	20	Primer for screening and cloning . It is placed in the gene's coding sequence and is compatible with all other pL2B RP primers.
STD	**seq-YFP-RP**	TCACTTGTACAGCTCGTCCATG	22	Primer designed for YFP sequencing and screening

1. (b) Primers use for cloning, construction of vector plasmids, sequencing and screening of mutant plants.

Oligo type	Oligo Name	5' to 3' sequence	length	uses
STD	**seq-YFP-FP**	CCATCCTGGTCGAGCTGGAC	20	Primer designed for YFP sequencing and screening
	EYFP-seq-RP	GAACTTCAGGGTCAGCTTGC	20	Primers for sequencing and screening YFP.
STD	**qPCR-NtRieske-FP1**	TTTATTTGCCCCTGCCATGGAT	22	Primer for screening and cloning. It is placed in the gene's coding sequence and is compatible with all other pL2B RP primers.
STD	**qPCR-NtRieske-RP1**	AGTCTGTTTCAACCCATGGGAC	22	
STD	**qPCR-NtRieske-FP2**	ATGGCTCAAAACTCATCCACCT	22	Primer for screening and cloning. It is placed in the gene's coding sequence and is compatible with all other pL2B RP primers.
STD	**qPCR-NtRieske-RP2**	AACACAACCAAGGTGAGTACAC	22	
STD	**qPCR-NtSBPase-FP1**	GGAGGAATGGTGCCTGATGTTA	22	Primer for screening and cloning. It is placed in the gene's coding sequence and is compatible with all other pL2B RP primers.
STD	**qPCR-NtSBPase-RP1**	TTGGCAGTTGGAGATGTCACAT	22	
STD	**qPCR-NtSBPase-FP2**	ACAAGTTGCTTTTCGACGCATT	22	Primer for screening and cloning. It is placed in the gene's coding sequence and is compatible with all other pL2B RP primers.
STD	**qPCR-NtSBPase-RP2**	GTCTTGGAGCTCAGGTACTTCC	22	
STD	**qPCR-AtRieske-FP**	AACGCCCAAGGAAGAGTCGT	22	Primer for screening and cloning. It is placed in the gene's coding sequence and is compatible with all other pL2B FP primers.
STD	**qPCR-AtRieske-RP**	ACCACCATGGAGCATCACCA	21	Primer for screening and cloning . It is placed in the gene's coding sequence and is compatible with all other pL2B RP primers.

1.**(c)** Primers used for cloning, construction of vector plasmids, sequencing and screening of mutant plants.

Oligo type	Oligo Name	5' to 3' sequence	length	uses
STD	**qPCR-AtSBPase-FP**	TCGACAACTCCGAATACAGCAAGC	20	Primer for screening and cloning. It is placed in the gene's coding sequence and is compatible with all other pL2B RP primers.
STD	**qPCR-AtSBPase-RP**	AACCATTCCTCCGGTGTATCGC	24	Primer for screening and cloning. It is placed in the gene's coding sequence and is compatible with all other pL2B RP primers.
STD	**AtSPase_RP-TL**	TGGAAGGTGGGTTTAGTGTTGC	22	Primer designed for sequencing and screening. It is placed in the gene's coding sequence and is compatible with all other pL2B RP primers.
STD	**BAR1_RP_TL**	ACCATCGTCAACCACTACATCG	22	Primer for sequencing. It is placed in the gene's coding sequence and is compatible with all other pL2B RP primers.
STD	**HSP1_RP_TL**	TGTTGGATCTCTTCTGCAGC	20	Primer for screening. It is placed in the terminator's sequence and is compatible with all other pL2B RP primers.
STD	**kst1_RP_TL**	ACCCTACCAAATATTTAACGG	21	Primer for screening and sequencing . It is placed in the promoter' s sequence and is compatible with all other pL2B RP primers.
STD	**kst2_RP_TL**	TGGACCCTACACACTATGACG	21	Primer for screening and sequencing. It is placed in the promoter’s sequence and is compatible with all other pL2B RP primers.
STD	**kst3_RP_TL**	TTCTCGTGAGAGTTCACAAGC	21	Primer for screening and sequencing. It is placed in the promoter's sequence and is compatible with all other pL2B RP primers.

Appendix 2

Colony PCR reaction mix .	**Number of reaction**
	1
H2O	11.6
Buffer	1.5
Primer F	0.75
Primer R	0.75
dNTPs	0.2
DreamTaq	0.2
bacteria in tip	
Total	15

qRT-PCR reaction mix	**Number of reaction**
	1
H2O	6.1
SYBR	7.5
Primer mix	0.4
cDNA (1/2 dilution)	**1**
Total	15

The cycling conditions for colony PCR were set as follows: initial denaturation step of 94-98°C for 2-4min to activate the polymerase, followed by 35 cycles of denaturation at 94-98°C for 30 s, annealing at 60°C for 30 s and extension at 72°C for 1min per kb. Then finally with an additional 72°C for 7 min to complete the reaction

Appendix 3.

Sequencing results of pL1M-R2-pKST1-AtRieske-tHSP clone. Primers used for screening were also used for sequencing the fragment produced in the PCRs. Result showing the alignment of the sequences obtained with the AtRieske gene or upstream regions showing the exact position of insertion. Asterisks indicates exact nucleotides alignment. Constructs inserts confirmed for all with correct sequences at the cloning junctions. Multiple alignments was performed using Clustal omega (http://www.ebi.ac.uk/Tools/msa/clustalo/).

pL1M-R2-pKST1-AtSBPase-tHSP

```
AtSBPase      CGCTCTTTTCTCTTAGGTTTACCCGCCAATATATCCTGTCAAACACTGATAGTTTAAACC
Forward       CGCTCTTTTCTCTTAGGTTTACCCGCCAATATATCCTGTCAAACACTGATAGTTTAAACC
              ************************************************************


SBPase        ACTTCGTGCAGAAGACAATAGTGGAGAAGCTTTTAAACATCGATAATTCATCACTTTTAT
Forward       ACTTCGTGCAGAAGACAATAGTGGAGAAGCTTTTAAACATCGATAATTCATCACTTTTAT
              ************************************************************


SBPase        TTTTTGTACTCTTCTTCTTCTTCCTTCCTTTCTTTTTTTTTTTTTTGTGTGAAATTTGATA
Forward       TTTTTGTACTCTTCTTCTTCTTCCTTCCTTTCTTTTTTTTTTTTTTGTGTGAAATTTGATA
              ************************************************************


SBPase        TTTTTTGTCTTAAATGATTAATCTATTGTGTAGAAAATAGATTTTCTTGTTAGTGTATAA
```

```
Forward      TTTTTTGTCTTAAATGATTAATCTATTGTGTAGAAAATAGATTTTCTTGTTAGTGTATAA
             ************************************************************

SBPase       ATTTTATAAAATAAATTTAAAGACCTCTTAATATAATTTTCGCTTAGGCCACGAGATTTG
Forward      ATTTTATAAAATAAATTTAAAGACCTCTTAATATAATTTTCGCTTAGGCCACGAGATTTG
             ************************************************************

SBPase       TTGAGCCGCCCTGATTATCATAAATTATTTGAAGATTTTGGTCTGCAATTGTCAGCTAAT
Forward      TTGAGCCGCCCTGATTATCATAAATTATTTGAAGATTTTGGTCTGCAATTGTCAGCTAAT
             ************************************************************

SBPase       CTCCAACTAAATAATGTCCAACATAATTTGGACCCTACCAAATATTTAACGGGCAAAGAT
Forward      CTCCAACTAAATAATGTCCAACATAATTTGGACCCTACCAAATATTTAACGGGCAAAGAT
             ************************************************************

SBPase       TAATATAACACTATAGTATATAAAATGACATTCATGAGTGTGAAATTGTATATAGTGTTC
Forward      TAATATAACACTATAGTATATAAAATGACATTCATGAGTGTGAAATTGTATATAGTGTTC
             ************************************************************

SBPase       ATGTGCATATTTTACTATTTTCTTGCAAATCATATGGTTCATATACAATAATAACAATGG
Forward      ATGTGCATATTTTACTATTTTCTTGCAAATCATATGGTTCATATACAATAATAACAATGG
             ************************************************************

SBPase       AAAAGACAGGTGTTTGGCCTGTAATGGGTCTATATTGTCCAGATCTTGGTGGACCCTACA
Forward      AAAAGACAGGTGTTTGGCCTGTAATGGGTCTATATTGTCCAGATCTTGGTGGACCCTACA
             ************************************************************

SBPase       CACTATGACGTCTGTCAAATAATCTTGGAAAAATAACTTGTTGCACGACTCTTCGAGTCT
Forward      CACTATGACGTCTGTCAAATAATCTTGGAAAAATAACTTGTTGCACGACTCTTCGAGTCT
             ************************************************************

SBPase       AATTTTCAGTGATTTATTTAATAATGACTAAGTTTTATCGCTTTTATAATGACAAAAAGG
Forward      AATTTTCAGTGATTTATTTAATAATGACTAAGTTTTATCGCTTTTATAATGACAAAAAGG
             ************************************************************
```

```
SBPase      ATTTCTTATTATTACTATCTCTGTTCTATATTAATTGAATCGATGAGCCAATTATATGAA
Forward     ATTTCTTATTATTACTATCTCTGTTCTATATTAATTGAATCGATGAGCCAATTATATGAA
            ************************************************************

SBPase      ATTTTATCAAATATTCATTTTAAATTTTGAACGATAAAAAAAGCCTCATGAGAATTTTAT
Forward     ATTTTATCAAATATTCATTTTAAATTTTGAACGATAAAAAAAGCCTCATGAGAATTTTAT
            ************************************************************

SBPase      CAAAGTAAAATATGAAAAAAATGATTATCAAGTAAAAATGAACAAAGAGAATAATATGAA
Forward     CAAAGTAAAATATGAAAAAAATGATTATCAAGTAAAAATGAACAAAGAGAATAATATGAA
            ************************************************************

SBPase      GGTTTTATCAAACATTCATCTTAAATTTTGAACGATAAAAAA-GCTTCGTAAAGAATATT
Forward     GGTTTTATCAAACATTCATCTTAAATTTTGAACGATAAAAAA-GCTTCGTAAAGAATATT
            ************************************************************

SBPase      TTATCATANTAAAACATGATTATCAAGTAAAAGTGAACAANNGGAGTAATATGAAGATTT
Forward     TTATCATANTAAAACATGATTATCAAGTAAAAGTGAACAANNGGAGTAATATGAAGATTT
            ************************************************************


SBPase      GTGCAAGTATGCTTGCTCTGAAGAAGTACN-GAGCTTCAAGACATGGGAGGNCCAGTGGA
Reverse     GTGCAAGTATGCTTGCTCTGAAGAAGTACN-GAGCTTCAAGACATGGGAGGNCCAGTGGA
            ************************************************************

SBPase      AGGTGGGTTTAGTGTTGCGTTTGANCCATTGGATGGATCAAGCATTGTGGATACAAATTT
Reverse     AGGTGGGTTTAGTGTTGCGTTTGANCCATTGGATGGATCAAGCATTGTGGATACAAATTT
            ************************************************************

SBPase      CACTGTGGGAACCATATTCGGTGTTTGGCCTGGAGACAAGTTAACCGGAATCACTGGAGG
Reverse     CACTGTGGGAACCATATTCGGTGTTTGGCCTGGAGACAAGTTAACCGGAATCACTGGAGG
            ************************************************************
```

```
SBPase      AGATCAAGTGGCTGCAGCCATGGGAATCTACGGTCCACGAACCACTTATGTTTTGGCTGT
Reverse     AGATCAAGTGGCTGCAGCCATGGGAATCTACGGTCCACGAACCACTTATGTTTTGGCTGT
            ************************************************************

SBPase      TAAGGGCTTTCCAGGAACTCATGAGTTCTTGCTTCTTGATGAAGGGAAATGGCAGCATGT
Reverse     TAAGGGCTTTCCAGGAACTCATGAGTTCTTGCTTCTTGATGAAGGGAAATGGCAGCATGT
            ************************************************************

SBPase      AAAGGAGACAACAGAGATCGCAGAAGGGAAAATGTTCTCACCAGGAAACTTAAGAGCCAC
Reverse     AAAGGAGACAACAGAGATCGCAGAAGGGAAAATGTTCTCACCAGGAAACTTAAGAGCCAC
            ************************************************************

SBPase      ATTCGACAACTCCGAATACAGCAAGCTGATTGATTACTACGTGAAAGAGAAATACACACT
Reverse     ATTCGACAACTCCGAATACAGCAAGCTGATTGATTACTACGTGAAAGAGAAATACACACT
            ************************************************************

SBPase      GCGATACACCGGAGGAATGGTTCCTGATGTTAACCAGATTATTGTGAAGGAGAAAGGAAT
Reverse     GCGATACACCGGAGGAATGGTTCCTGATGTTAACCAGATTATTGTGAAGGAGAAAGGAAT
            ************************************************************

SBPase      CTTCACAAATGTGACTTCTCCTACGGCTAAGGCAAAGTTGAGGCTGTTGTTTGAAGTGGC
Reverse     CTTCACAAATGTGACTTCTCCTACGGCTAAGGCAAAGTTGAGGCTGTTGTTTGAAGTGGC
            ************************************************************

SBPase      TCCTCTTGGCCTGCTCATAGAGAATGCTGGTGGATTCAGCAGTGATGGACACAAGTCCGT
Reverse     TCCTCTTGGCCTGCTCATAGAGAATGCTGGTGGATTCAGCAGTGATGGACACAAGTCCGT
            ************************************************************

SBPase      GCTTGACAAGACCATCATCAACCTCGACGATAGAACTCAAGTTGCTTATGGCTCAAAGAA
Reverse     GCTTGACAAGACCATCATCAACCTCGACGATAGAACTCAAGTTGCTTATGGCTCAAAGAA
            ************************************************************

SBPase      CGAGATCATCCGCTTCGAAGAAACCCTTTATGGAACATCAAGACTCAAGAATGTTCCCAT
Reverse     CGAGATCATCCGCTTCGAAGAAACCCTTTATGGAACATCAAGACTCAAGAATGTTCCCAT
```

```
            ************************************************************


SBPase      TGGAGTTACCGCTTAGGCTTATATGAAGATGAAGATGAAATATTTGGTGTGTCAAATAAA
Reverse     TGGAGTTACCGCTTAGGCTTATATGAAGATGAAGATGAAATATTTGGTGTGTCAAATAAA
            ************************************************************


SBPase      AAGCTTGTGTGCTTAAGTTTGTGTTTTTTTCTTGGCTTGTTGTGTTATGAATTTGTGGCT
Reverse     AAGCTTGTGTGCTTAAGTTTGTGTTTTTTTCTTGGCTTGTTGTGTTATGAATTTGTGGCT
            ************************************************************


SBPase      TTTTCTAATATTAAATGAATGTAAGATCTCATTATAATGAATAAACAAATGTTTCTATAA
Reverse     TTTTCTAATATTAAATGAATGTAAGATCTCATTATAATGAATAAACAAATGTTTCTATAA
            ************************************************************


SBPase      TCCATTGTGAATGTTTTGTTGGATCTCTTCTGCAGCATATAACTACTGTATGTGCTATGG
Reverse     TCCATTGTGAATGTTTTGTTGGATCTCTTCTGCAGCATATAACTACTGTATGTGCTATGG
            ************************************************************


SBPase      TATGGACTATGGAATATGATTAAAGATAAGCGCTAAG---------
Reverse     TATGGACTATGGAATATGATTAAAGATAAGCGCTAAGCNGANTCTG
            ***********************************
```

pL1M-R2-pKST1-AtRieske-tHSP

```
Rieske       -CTCTTTTCTCTTAGGTTTACCCGCCAATATATCCTGTCAAACACTGATAGTTTAAACCA
Forward      GCTCTTTTCTCTTAGGTTTACCCGCCAATATATCCTGTCAAACACTGATAGTTTAAACCA
              ************************************************************

Rieske       CTTCGTGCAGAAGACAAGTAAGGAGAAGCTTTTAAACATCGATAATTCATCACTTTTATT
Forward      CTTCGTGCAGAAGACAAGTAAGGAGAAGCTTTTAAACATCGATAATTCATCACTTTTATT
             ************************************************************

Rieske       TTTTGTACTCTTCTTCTTCTTCCTTCCTTTCTTTTTTTTTTTTTTGTGTGAAATTTGATAT
Forward      TTTTGTACTCTTCTTCTTCTTCCTTCCTTTCTTTTTTTTTTTTTTGTGTGAAATTTGATAT
             ************************************************************

Rieske       TTTTTGTCTTAAATGATTAATCTATTGTGTAGAAAATAGATTTTCTTGTTAGTGTATAAA
Forward      TTTTTGTCTTAAATGATTAATCTATTGTGTAGAAAATAGATTTTCTTGTTAGTGTATAAA
             ************************************************************

Rieske       TTTTATAAAATAAATTTAAAGACCTCTTAATATAATTTTCGCTTAGGCCACGAGATTTGT
Forward      TTTTATAAAATAAATTTAAAGACCTCTTAATATAATTTTCGCTTAGGCCACGAGATTTGT
             ************************************************************

Rieske       TGAGCCGCCCTGATTATCATAAATTATTTGAAGATTTTGGTCTGCAATTGTCAGCTAATC
Forward      TGAGCCGCCCTGATTATCATAAATTATTTGAAGATTTTGGTCTGCAATTGTCAGCTAATC
             ************************************************************

Rieske       TCCAACTAAATAATGTCCAACATAATTTGGACCCTACCAAATATTTAACGGGCAAAGATT
Forward      TCCAACTAAATAATGTCCAACATAATTTGGACCCTACCAAATATTTAACGGGCAAAGATT
             ************************************************************

Rieske       AATATAACACTATAGTATATAAAATGACATTCATGAGTGTGAAATTGTATATAGTGTTCA
Forward      AATATAACACTATAGTATATAAAATGACATTCATGAGTGTGAAATTGTATATAGTGTTCA
             ************************************************************
```

```
Rieske       TGTGCATATTTTACTATTTTCTTGCAAATCATATGGTTCATATACAATAATAACAATGGA
Forward      TGTGCATATTTTACTATTTTCTTGCAAATCATATGGTTCATATACAATAATAACAATGGA
             ************************************************************

Rieske       AAAGACAGGTGTTTGGCCTGTAATGGGTCTATATTGTCCAGATCTTGGTGGACCCTACAC
Forward      AAAGACAGGTGTTTGGCCTGTAATGGGTCTATATTGTCCAGATCTTGGTGGACCCTACAC
             ************************************************************

Rieske       ACTATGACGTCTGTCAAATAATCTTGGAAAAATAACTTGTTGCACGACTCTTCGAGTCTA
Forward      ACTATGACGTCTGTCAAATAATCTTGGAAAAATAACTTGTTGCACGACTCTTCGAGTCTA
             ************************************************************

Rieske       ATTTTCAGTGATTTATTTAATAATGACTAAGTTTTATCGCTTTTATAATGACAAAAAGGA
Forward      ATTTTCAGTGATTTATTTAATAATGACTAAGTTTTATCGCTTTTATAATGACAAAAAGGA
             ************************************************************

Rieske       TTTCTTATTATTACTATCTCTGTTCTATATTAATTGAATCGATGAGCCAATTATATGAAA
Forward      TTTCTTATTATTACTATCTCTGTTCTATATTAATTGAATCGATGAGCCAATTATATGAAA
             ************************************************************

Rieske       TTTTATCAAATATTCATTTTAAATTTTGAACGATAAAAAAAGCCTCATGAGAATTTTATC
Forward      TTTTATCAAATATTCATTTTAAATTTTGAACGATAAAAAAAGCCTCATGAGAATTTTATC
             ************************************************************

Rieske       AAAGTAAAATATGAAAAAAATGATTATCAAGTAAAAATGAACAAAGAGAATAATATGAAG
Forward      AAAGTAAAATATGAAAAAAATGATTATCAAGTAAAAATGAACAAAGAGAATAATATGAAG
             ************************************************************

Rieske       GTTTTATCAAACATTCATCTTAAATTTTGAACGATAAAAAAAGCTTCGTAAAGAATATTT
Forward      GTTTTATCAAACATTCATCTTAAATTTTGAACGATAAAAAAAGCTTCGTAAAGAATATTT
             ************************************************************

Rieske       TATCATAGTAAANN-TGATTATCAAGTAAAAGTAACACAACTTCT-GTGATTCACTT-CA
```

```
Forward      TATCATAGTAAANN-TGATTATCAAGTAAAAGTNANCNANNGGAGTANTATNAAGANTTA
             ********************************* *   *          **  *     *
```

```
Rieske       TTCTAGATCAATGGCGTCCTCATCCCTTTCCCN-GCTACTCAGCTTGGTTCTAGCAGAAG
Reverse      TTCTAGATCAATGGCGTCCTCATCCCTTTCCCN-GCTACTCAGCTTGGTTCTAGCAGAAG
             ************************************************************

Rieske       TGCTTTGATGGCGATGTCAAGTGGGTTGTTTGTGAAGCCAACGAAGATGAATCATCAAAT
Reverse      TGCTTTGATGGCGATGTCAAGTGGGTTGTTTGTGAAGCCAACGAAGATGAATCATCAAAT
             ************************************************************

Rieske       GGTTAGAAAAGAGAAGATTGGATTGAGAATTTCTTGTCAAGCGTCGAGTATTCCAGCAGA
Reverse      GGTTAGAAAAGAGAAGATTGGATTGAGAATTTCTTGTCAAGCGTCGAGTATTCCAGCAGA
             ************************************************************

Rieske       CAGAGTTCCAGATATGGAAAAGAGAAAAACTTTGAATCTTCTTCTTCTTGGGGCTCTTTC
Reverse      CAGAGTTCCAGATATGGAAAAGAGAAAAACTTTGAATCTTCTTCTTCTTGGGGCTCTTTC
             ************************************************************

Rieske       TCTACCTACTGGCTACATGCTTGTCCCTTACGCTACCTTCTTTGTTCCTCCTGGAACCGG
Reverse      TCTACCTACTGGCTACATGCTTGTCCCTTACGCTACCTTCTTTGTTCCTCCTGGAACCGG
             ************************************************************

Rieske       AGGTGGAGGTGGTGGTACTCCAGCCAAGGATGCCCTTGGAAACGATGTAGTTGCAGCGGA
Reverse      AGGTGGAGGTGGTGGTACTCCAGCCAAGGATGCCCTTGGAAACGATGTAGTTGCAGCGGA
             ************************************************************

Rieske       ATGGCTTAAGACTCATGGTCCCGGTGACCGAACCTTGACCCAAGGATTAAAGGGAGATCC
Reverse      ATGGCTTAAGACTCATGGTCCCGGTGACCGAACCTTGACCCAAGGATTAAAGGGAGATCC
             ************************************************************
```

```
Rieske      GACTTACCTAGTTGTAGAGAACGACAAGACTCTAGCGACATACGGTATCAACGCAGTGTG
Reverse     GACTTACCTAGTTGTAGAGAACGACAAGACTCTAGCGACATACGGTATCAACGCAGTGTG
            ************************************************************

Rieske      CACTCATCTTGGATGTGTTGTGCCATGGAACAAAGCTGAGAACAAGTTTCTATGTCCTTG
Reverse     CACTCATCTTGGATGTGTTGTGCCATGGAACAAAGCTGAGAACAAGTTTCTATGTCCTTG
            ************************************************************

Rieske      CCATGGATCCCAATACAACGCCCAAGGAAGAGTCGTTAGAGGTCCAGCCCCATTGTCGCT
Reverse     CCATGGATCCCAATACAACGCCCAAGGAAGAGTCGTTAGAGGTCCAGCCCCATTGTCGCT
            ************************************************************

Rieske      AGCGTTGGCTCACGCGGATATAGATGAAGCTGGGAAGGTTCTTTTTGTTCCATGGGTGGA
Reverse     AGCGTTGGCTCACGCGGATATAGATGAAGCTGGGAAGGTTCTTTTTGTTCCATGGGTGGA
            ************************************************************

Rieske      AACTGACTTCAGGACTGGTGATGCTCCATGGTGGTCTTAAGCTTATATGAAGATGAAGAT
Reverse     AACTGACTTCAGGACTGGTGATGCTCCATGGTGGTCTTAAGCTTATATGAAGATGAAGAT
            ************************************************************

Rieske      GAAATATTTGGTGTGTCAAATAAAAAGCTTGTGTGCTTAAGTTTGTGTTTTTTTCTTGGC
Reverse     GAAATATTTGGTGTGTCAAATAAAAAGCTTGTGTGCTTAAGTTTGTGTTTTTTTCTTGGC
            ************************************************************

Rieske      TTGTTGTGTTATGAATTTGTGGCTTTTTCTAATATTAAATGAATGTAAGATCTCATTATA
Reverse     TTGTTGTGTTATGAATTTGTGGCTTTTTCTAATATTAAATGAATGTAAGATCTCATTATA
            ************************************************************

Rieske      ATGAATAAACAAATGTTTCTATAATCCATTGTGAATGTTTTGTTGGATCTCTTCTGCAGC
Reverse     ATGAATAAACAAATGTTTCTATAATCCATTGTGAATGTTTTGTTGGATCTCTTCTGCAGC
            ************************************************************

Rieske      ATATAACTACTGTATGTGCTATGGTATGGACTATGGAATATGATTAAAGATAAGCGCTGA
Reverse     ATATAACTACTGTATGTGCTATGGTATGGACTATGGAATATGATTAAAGATAAGCGCTGA
```

```
             ************************************************************


Rieske       GCTCGA---

Reverse      GCTCGANNC

             ******
```

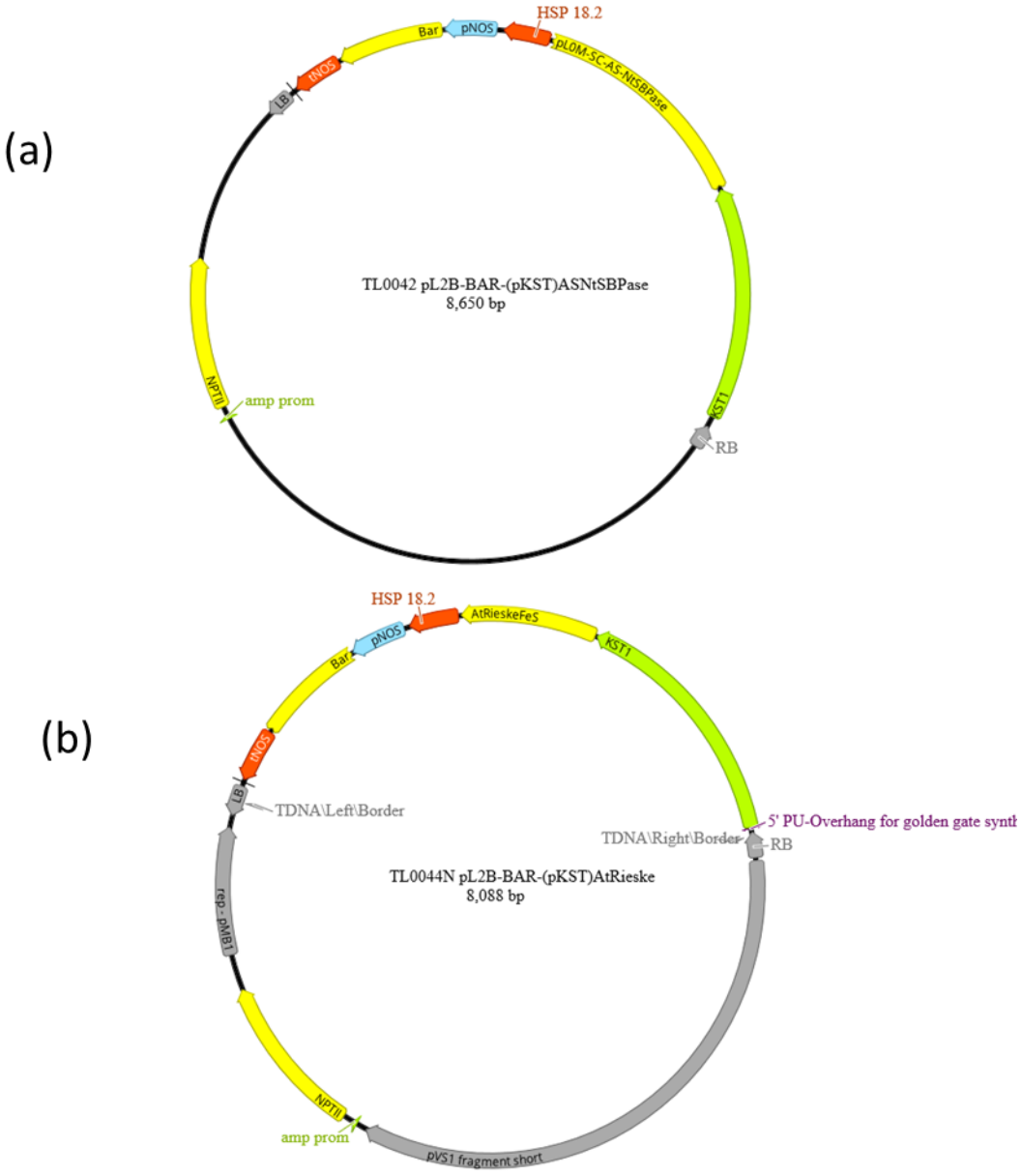

Constructs for plant expression showing structures present between left and right borders sequences. **(a)** Vector for the expression of TL0042 **(pL2B-BAR-(pKST1)ASNtSBPase) (b)** Vector for expression of TL0044 **pL2B-BAR-(pKST1)AtRieske**. constructs made using the pAGM4723 plant transformation backbone which confers resistance to BASTA herbicide in plants and Kn resistance in bacteria. Construct designed by geneious www.geneious.com.

(c)

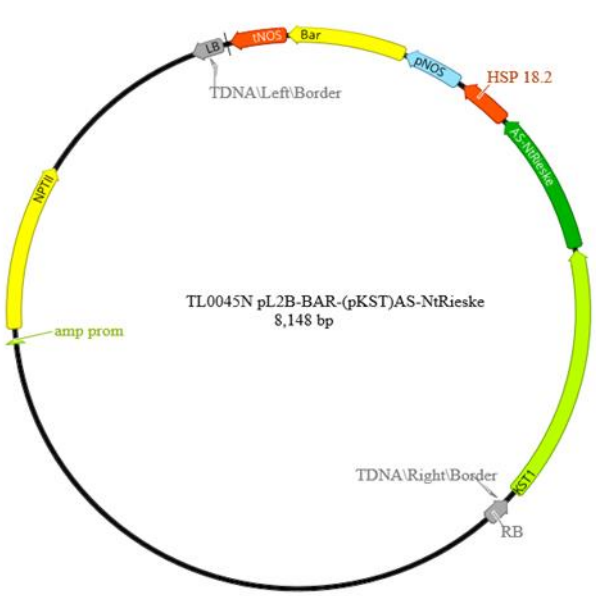

(d)

Constructs for plant expression showing structures present between left and right borders sequences. **(c)** Vector for the expression of TL0045 **(pL2B-BAR-(pKST1)ASNtRieske)** **(d)** Vector for expression of TL0046 **(pL2B-BAR-(pKST1)YFP**. Constructs made using the pAGM4723 plant transformation backbone which confers resistance to BASTA herbicide in plants and Kn resistance in bacteria. Construct designed by geneious www.geneious.com.

(e)

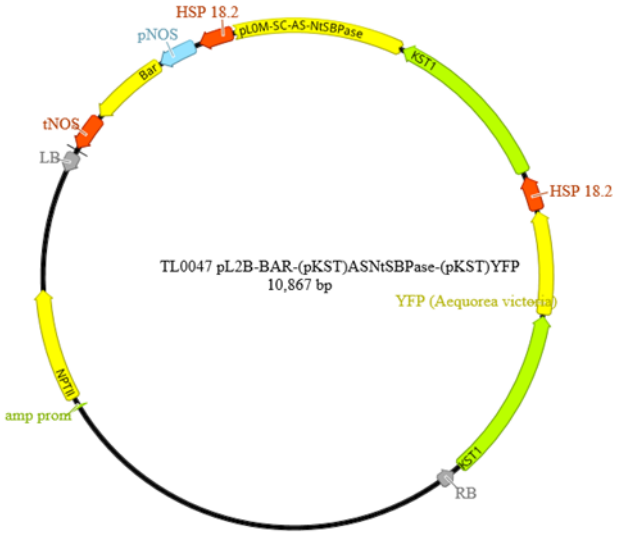

(f)

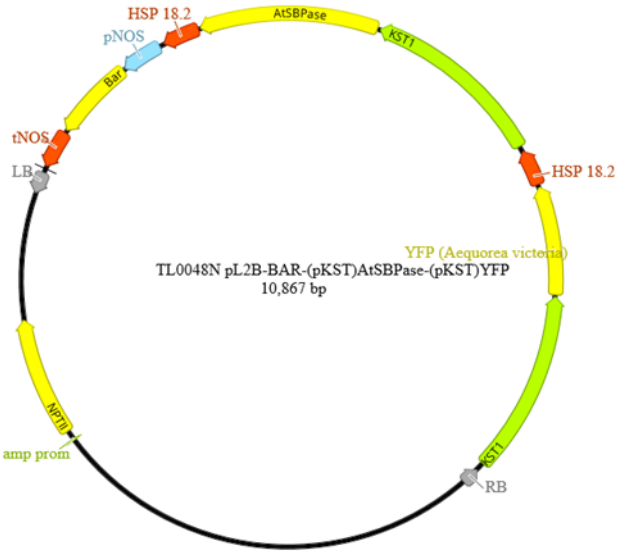

Constructs for plant expression showing structures present between left and right borders sequences. **(e)** Vector for the expression of TL0047 TL0047 **(pL2B-BAR-(pKST1)ASNtSBPase-(pKST)YFP**) **(f)** Vector for expression of TL0048 **(pL2B-BAR-(pKST)AtSBPase-(pKST)YFP)**. Constructs made using the pAGM4723 plant transformation backbone which confers resistance to BASTA herbicide in plants and Kn resistance in bacteria. Construct designed by geneious www.geneious.com.

(g)

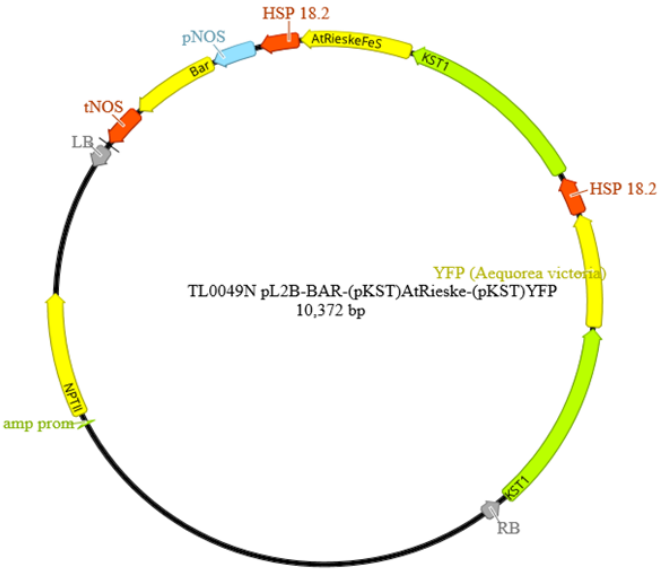

(h)

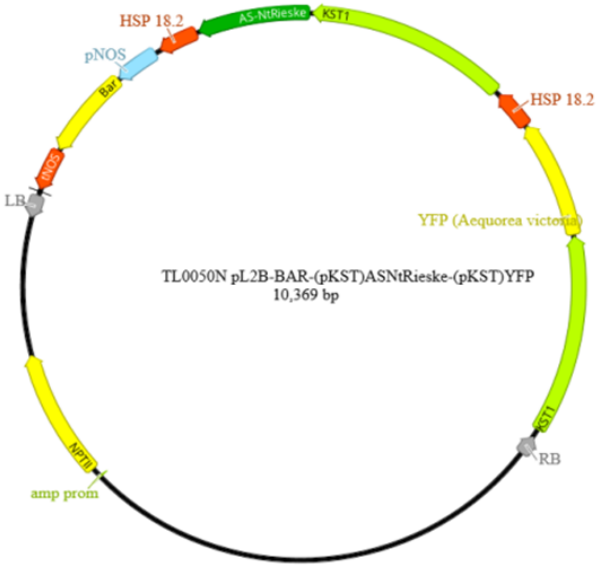

Constructs for plant expression showing structures present between left and right borders sequences. **(e)** Vector for the expression of TL0047 TL0049 **(pL2B-BAR-(pKST)AtRieske-(pKST1)YFP**) **(f)** Vector for expression of TL0050 **(pL2B-BAR-(pKST)ASNtRieske-(pKST)YFP)**. Constructs made using the pAGM4723 plant transformation backbone which confers resistance to BASTA herbicide in plants and Kn resistance in bacteria. Construct designed by geneious www.geneious.com.